HEINRICH HEINE
UNIVERSITÄT DÜSSELDORF

Genetic control of root meristem development in barley (*Hordeum vulgare*)

Inaugural-Dissertation

zur Erlangung des Doktorgrades

der Mathematisch-Naturwissenschaftlichen Fakultät

der Heinrich-Heine-Universität Düsseldorf

vorgelegt von

Gwendolyn Kirschner

aus Bad Kreuznach

Düsseldorf, Juli 2017

aus dem Institut für Entwicklungsgenetik

der Heinrich-Heine-Universität Düsseldorf

Gedruckt mit der Genehmigung der

Mathematisch-Naturwissenschaftlichen Fakultät der

Heinrich-Heine-Universität Düsseldorf

Referent: Professor Dr. Rüdiger Simon

Korreferent: Professor Dr. Maria von Korff Schmising

Tag der mündlichen Prüfung: 11.09.2017

I. Eidesstattliche Erklärung

Eidesstattliche Erklärung zur Dissertation mit dem Titel:

„Genetic control of root meristem development in barley (*Hordeum vulgare*)"

Ich versichere an Eides statt, dass die Dissertation von mir selbständig und ohne unzulässige fremde Hilfe unter Beachtung der „Grundsätze zur Sicherung guter wissenschaftlicher Praxis an der Heinrich-Heine-Universität Düsseldorf" erstellt worden ist.

Außerdem versichere ich, dass ich diese Dissertation nur in diesem und keinem anderen Promotionsverfahren eingereicht habe und dass diesem Promotionsverfahren kein gescheitertes Promotionsverfahren vorausgegangen ist.

_____ _____

Ort, Datum Unterschrift

This work is funded by the Cluster of Excellence on Plant Science (CEPLAS)

“Es sagt viel über die Welt aus, mein Kind,
sagte der Vater zu dem Knaben,
dass die Dummen glücklich sind
und die Schlauen Depressionen haben.”

„Hast du Depressionen?“, fragt das Känguru.
„Nee“, sage ich. „Du?“
„Nee.“

Aus: Marc-Uwe Kling, „Das Känguru-Manifest“

II. Contents

Contents

Contents

III. Aims of this study

The aim of this study is a detailled analysis of the barley (*Hordeum vulgare*) root apical meristem.

Crop plant research mostly focuses on above-ground organs, as these organs are directly connected to yield. Root growth, however, is still often neglected, although root growth contributes to yield by providing the plant's access to water, nutrients and anchorage to the soil. Barley is the fourth most abundant crop plant, and ranks among the most salt-tolerant crop species, which makes it particularly interesting for root research.

Plant growth is enabled by the activity of meristems. Shoot and root meristems harbour stem cells which are controlled by organizing centers. Development and maintenance of a stable stem cell population is enabled by fine-tuned networks of receptors, peptides, transcription factors and phytohormones. Although phytohormone and genetic signalling is well analysed in the main model plants *Arabidopsis thaliana*, rice and maize, hardly anything is known about it in barley.

In this study, the root meristem development of barley, maintenance and related genetic and hormonal factors will be compared to the respective structures in *Arabidopsis*, rice and maize to reveal underlying concepts, but also differences. The study will be extended to the shoot apical meristem, as it was shown that some genes are involved in both shoot and root meristem development and maintenance.

To do this, the root apical meristem will first be characterised in detail. By means of cell wall stainings, the origins of the root cell layers will be examined. Distinct regions of the meristem will be distinguished by monitoring the cell division activity in the root meristem by RNA *in situ* hybridisation and staining for fluorescence microscopy. Moreover, the widely conserved CLE peptide dependent module for root meristem maintenance will be examined by peptide application to barley roots.

Secondly, in order to demonstrate how knowledge from barley can be applied to other plants and what makes the barley root meristem structure special, the root stem cell niches of the major model plants *Arabidopsis*, maize and rice will be compared to the barley stem cell niche on the basis of literature search. As barley is more salt-tolerant than other crop plants, barley as role model for salt resistance will be discussed.

Thirdly, the effect of the phytohormones cytokinin and auxin on barley roots and root meristem growth will be analysed. Furthermore, the cytokinin signalling will be analysed by reporter lines. Homologues of auxin-related genes known from other plants will be identified in barley. Transgenic fluorescent reporter lines will be created that visualize the gene expression and subcellular localisation of these genes. The expression patterns will be confirmed by RNA *in situ* hybridization.

Aims of this study

At last, barley homologues of genes involved in stem cell and QC specification in the root meristem will be identified and their expression pattern will be examined by transgenic fluorescent reporter lines. Expression of genes that are putatively involved in the shoot apical meristem development will moreover be examined in the shoot meristem.

The results of this study will lead to a better understanding of general concepts of meristem development and maintenance.

IV. Unique and Conserved Features of the Barley Root Meristem

The following manuscript was published in Frontiers in Plant Science in July, 2017

Authors:

Gwendolyn K. Kirschner[1], Yvonne Stahl[1], Maria von Korff[2] and Rüdiger Simon[1]

Affiliations:

[1]Institute for Developmental Genetics and Cluster of Excellence on Plant Sciences, Heinrich Heine University, Universitätsstr. 1, D-40225 Düsseldorf, Germany

[2]Institute for Plant Genetics, Heinrich Heine University Düsseldorf, c/o Department of Plant Developmental Biology, Max Planck Institute for Plant Breeding Research, Carl-von-Linné-Weg 10, D-50829 Köln

Contributions:

Gwendolyn K. Kirschner, Yvonne Stahl and Rüdiger Simon conceived the project, Gwendolyn K. Kirschner, Yvonne Stahl. Maria von Korff and Rüdiger Simon planned the experiments, Gwendolyn K. Kirschner performed all experiments, Gwendolyn K. Kirschner and Rüdiger Simon wrote the manuscript, all authors contributed to the final version.

frontiers in Plant Science

ORIGINAL RESEARCH
published: 21 July 2017
doi: 10.3389/fpls.2017.01240

Unique and Conserved Features of the Barley Root Meristem

Gwendolyn K. Kirschner[1,2,3], *Yvonne Stahl*[1], *Maria Von Korff*[2,3,4] *and Rüdiger Simon*[1,3]*

[1] *Institute for Developmental Genetics, Heinrich Heine University, Düsseldorf, Germany,* [2] *Institute for Plant Genetics, Heinrich Heine University, Düsseldorf, Germany,* [3] *Cluster of Excellence on Plant Sciences (CEPLAS), Heinrich Heine University, Düsseldorf, Germany,* [4] *Department of Plant Breeding and Genetics, Max Planck Institute for Plant Breeding Research, Cologne, Germany*

Plant root growth is enabled by root meristems that harbor the stem cell niches as a source of progenitors for the different root tissues. Understanding the root development of diverse plant species is important to be able to control root growth in order to gain better performances of crop plants. In this study, we analyzed the root meristem of the fourth most abundant crop plant, barley (*Hordeum vulgare*). Cell division studies revealed that the barley stem cell niche comprises a Quiescent Center (QC) of around 30 cells with low mitotic activity. The surrounding stem cells contribute to root growth through the production of new cells that are displaced from the meristem, elongate and differentiate into specialized root tissues. The distal stem cells produce the root cap and lateral root cap cells, while cells lateral to the QC generate the epidermis, as it is typical for monocots. Endodermis and inner cortex are derived from one common initial lateral to the QC, while the outer cortex cell layers are derived from a distinct stem cell. In rice and *Arabidopsis*, meristem homeostasis is achieved through feedback signaling from differentiated cells involving peptides of the CLE family. Application of synthetic CLE40 orthologous peptide from barley promotes meristem cell differentiation, similar to rice and *Arabidopsis*. However, in contrast to *Arabidopsis*, the columella stem cells do not respond to the CLE40 peptide, indicating that distinct mechanisms control columella cell fate in monocot and dicot plants.

Keywords: root meristem, stem cell niche, CLE peptide signaling, root architecture, root development, barley

OPEN ACCESS

Edited by:
Kimberly Lynne Gallagher, University of Pennsylvania, United States

Reviewed by:
Raffaele Dello Ioio, Sapienza Università di Roma, Italy
Christophe Perin, Agricultural Research Centre for International Development, France

***Correspondence:**
Rüdiger Simon
ruediger.simon@hhu.de

Specialty section:
This article was submitted to Plant Evolution and Development, a section of the journal Frontiers in Plant Science

Received: *27 April 2017*
Accepted: *30 June 2017*
Published: *21 July 2017*

Citation:
Kirschner GK, Stahl Y, Von Korff M and Simon R (2017) Unique and Conserved Features of the Barley Root Meristem. Front. Plant Sci. 8:1240. doi: 10.3389/fpls.2017.01240

INTRODUCTION

The root system of cereal crops from the family of *Poaceae* like barley, maize and rice is composed of different types of roots formed during consecutive developmental stages. In the embryo, the primary root primordium and the primordia of seminal roots are initiated (Luxová, 1986). The primary root is initiated below the scutellar node, while the seminal roots are formed later above the scutellar node from the mesocotyl. In the subsequent life of the plant, the largest part of the root system is built by shoot-borne post-embryonic nodal roots (reviewed in Orman-Ligeza et al., 2013). Primary root growth depends on cell division and expansion. Meristematic cells at the root tip are small and divide rapidly several times before they are displaced from the meristem. At the transition zone, they enter a phase in which they cease division and start to rapidly elongate and differentiate (elongation-differentiation zone) (reviewed in Ivanov and Dubrovsky, 2013). In *Arabidopsis thaliana*, the number of cells in the meristem increases after germination, until the meristem reaches its final size when the rates of cell division and the rate at which cells exit the meristem into the elongation-differentiation zone are balanced (Dello Ioio et al., 2007).

The meristematic cells are derived from a group of stem cells located in the distal stem cell niche (Dolan et al., 1993). In many plant species, the stem cell niche is organized from a mitotically less active region termed the quiescent center (QC) (Clowes, 1984). In *Arabidopsis thaliana,* the QC is surrounded by a single layer of stem cells which give rise to the different tissues that make up the main body of the root (Dolan et al., 1993). The proximally located stem cells give rise to stele, endodermis and cortex, while the distal cells produce the root cap (columella), epidermis and lateral root cap cells. The QC maintains these stem cells in their undifferentiated state through short-range signaling (van den Berg et al., 1997). One of these signals depends on the homeobox transcription factor WUSCHEL-RELATED HOMEOBOX5 (WOX5) that is expressed in the QC and maintains both the distal stem cells and the size of the proximal meristem, together with other factors (Sarkar et al., 2007). The differentiating cells surrounding the stem cell niche, however, provide feedback-signals that serve to limit the size of the stem cell population. One of these is CLAVATA3/ENDOSPERM SURROUNDING REGION40 (CLE40), a peptide carrying a secretion signal and a conserved 14-amino-acid motif (CLE motif) near its C terminus (Cock and McCormick, 2001). CLE40 is expressed in the stele and in differentiated columella cells (Stahl et al., 2009). CLE40 signaling requires ARABIDOPSIS CRINKLY4, a receptor-like kinase that is expressed in the distal stem cells and in differentiated columella cells (De Smet et al., 2008; Stahl et al., 2009). CLE40 was shown to restrict *WOX5* expression in order to create a feedback regulation that maintains the size of the distal stem cell population (Stahl et al., 2009). A CLE peptide dependent pathway can also serve to promote premature differentiation of the proximal meristem, via an unknown pathway involving CLAVATA2 and CORYNE (Hobe et al., 2003; Fiers et al., 2005; Pallakies and Simon, 2014).

The basic structure of the meristem and the stem cell niche is generally similar between species like *Arabidopsis*, tomato, rice and maize. Their roots consist of the same cell types, which are the columella, lateral root cap, epidermis, cortex, endodermis, and stele. However, the number of cell files, their origin and the size of the stem cell domains differ between species. Firstly, the size of the QC varies considerably between species, ranging from four cells in *Arabidopsis* and rice to 400–900 in maize (Clowes, 1984; Dolan et al., 1993; Jiang et al., 2003; Ni et al., 2014). Secondly, maize and rice roots generate a larger number of cortex cell files than tomatoes (2-3 files) or *Arabidopsis* (1 file) (Lim et al., 2000; Rebouillat et al., 2009; Ron et al., 2013). In *Arabidopsis*, tomato and rice, both cortex and endodermis share an initial cell (Dolan et al., 1993; Ron et al., 2013; Ni et al., 2014). Epidermis and lateral root cap are derived from a common ancestor cell in *Arabidopsis*, whereas the epidermis initial of rice and maize is independent of the lateral root cap (Dolan et al., 1993; Clowes, 1994; Lim et al., 2000; Ni et al., 2014). To identify general mechanisms of root meristem development, more plant species from different evolutionary branches should be compared. Barley (*Hordeum vulgare*) is the fourth most abundant crop plant and of significant agronomic importance (FAO, 2014). The genome sequence of the barley cultivar (cv.) Morex was published in 2012 and serves as basis for molecular genetic studies (Mayer et al., 2012). While the adaptation of the shoot development to many different environments has been well studied, not much is known about the root development and the architecture of the barley root meristem was not previously described in detail (Luxová, 1986). Knowledge on the anatomy of the barley root provides the basis to understand root development and to study its molecular control mechanisms. Here, we have analyzed the root meristem of the barley cv. Morex at a cellular level, determined the size of the QC, the number and origin of the fundamental cell layers and cell division patterns in the stem cell niche. We further show that evolutionary conserved CLE-peptide dependent signaling pathways control meristem differentiation in the proximal meristem in barley, but in contrast to *Arabidopsis*, do not control the maintenance of columella stem cells.

MATERIALS AND METHODS

Plant Growth

Seeds of the barley (*H. vulgare*) cv. Morex were husked and sterilized by washing the seeds in 70% EtOH shortly and in 5% sodium hypochlorite for 30 min on a shaker at 4°C. The seeds were then rinsed with autoclaved dH_2O twice and plated on square plastic plates (120 × 120 mm) containing growth agar (0,5 g MES hydrate, 2,2 g Murashige & Skoog medium per liter, pH 5.7). Per plate, 5 seeds were placed 2 cm from the top of the plate into the agar. The plates were then stored for at least 2 days in darkness at 4°C for stratification and placed in a 16°C phytochamber with 24 h light at a 45° angle to the shelf for growth. *Arabidopsis thaliana* (Col-0) seeds were treated and grown as described in Stahl et al. (2009).

Peptide Treatment

The synthetic peptides were acquired from Thermo Fisher Scientific and Centic Biotec with the following amino acid sequences: HvCLE402p (MLOC_3686.1) REVPTGPDPIHH; AtCLE40p RQVHypTGSDPLHHK (Hyp = hydroxyproline); mCLE40p LPQHPHGRSDVT. The peptides were added to the growth medium at a final concentration of 1 μM and the seeds were grown on these plates as described above for 5 days after germination (DAG).

RNA *In situ* Hybridisations

Probes for the *HISTONE H4* (AK357536) mRNA were prepared from the whole coding sequence. The DNA was cloned into the pGGC000 entry vector of the GreenGate cloning system (Lampropoulos et al., 2013) and amplified including the T7 and SP6 promoter sites by PCR. RNA probes were produced as described in Hejátko et al. (2006). RNA *in situ* hybridisations were performed on roots of plants 8 DAG as described in Jackson (1991), except for the following changes: after fixing the tissue over night at 4°C in 4 % para-formaldehyde, 0.1% tween-20, 0.1% triton-x-100 in PBS, a Leica ASP 300 tissue processor was used for embedding with the following protocol: 1 h 50% Ethanol (EtOH), 1 h 70% EtOH, 1 h 95% EtOH plus Eosin Y, 1 h 100% EtOH plus Eosin Y, 1 h 100% EtOH, 1 h 100%

EtOH, three times 1 h 100% Xylol, 20 min paraplast at 60°C, 10 min paraplast at 60°C. 10 μm sections were made at the microtome.

Staining and Microscopy

Modified pseudo-Schiff propidium iodide (mPS-PI) staining was performed as described for floral stalks in Truernit et al. (2008) on root tips of plants 8 DAG. The staining with Schiff reagent and PI was carried out using vacuum. The samples were examined with either a 25x oil objective with a numeric aperture (NA) of 0.8 using a Zeiss laser scanning microscope (LSM) 510 Meta or a 40x water objective with a NA of 1.20 using a Zeiss LSM 780. PI was excited with a 561 nm Argon laser with emission detection at 566–718 nm.

For cross sections of the root hair zone, roots were embedded in melted 5% agarose and sectioned manually with a sharp razor blade. Endodermis staining with berberine hemisulfate was carried out as described in Lux et al. (2005). The samples were examined with a 40x water objective with a NA of 1.20 using a Zeiss LSM 780. Green fluorescence was excited with a 488 nm Argon laser with emission detection at 490–544 nm. Transmitted light pictures were taken with a transmitted light detector (T-PMT).

EdU staining was performed with the Click-iT EdU Imaging Kit (Invitrogen) and the fluorophor Alexa568 as described in the manufacturer's manual with the following modifications: root tips of plants 8 DAG were covered with 10 μM EdU in dH_2O and placed in the phytochamber for the respective incubation time. Root tips were fixed for 1 h under vacuum and permeabilized for 1 h at room temperature. The Click-iT reaction was carried out for 1 h under vacuum in darkness. DNA-counterstaining was performed with 1 μg/ml DAPI in PBS for 1 h in darkness under vacuum. The samples were cleared for around 14 days at 4°C in clearing solution described in Warner et al. (2014). The roots were examined with a 40x water objective with a NA of 1.20 using the Zeiss LSM 780. DAPI was excited with a 405 nm Diode with emission detection at 410–560 nm, Alexa568 was excited with a 514 nm Argon laser and emission was detected at 545–697 nm in a separate track. The pinhole was set to 2,05 Airy units. Pictures were taken with the tile scan function with 10% overlap, a threshold of 0.70 and automatically stitched by the microscope software.

RNA *in situ* hybridizations were examined with a plan-neofluar 20x objective with a NA of 0.50 or a plan-neofluar 40x objective with a NA of 0.75 using a Zeiss Axioskop light microscope.

Data Analysis

For the alignment of the CLE-motifs, the 12 amino acid CLE-motif of *Arabidopsis* CLE40 (Hobe et al., 2003) was used for a BLAST search of barley CLE homologs. Barley homologs were obtained from http://webblast.ipk-gatersleben.de/barley/ using the default BLAST parameter settings among high and low-confidence genes (Mayer et al., 2012). Alignments were performed using MEGA7 (Molecular Evolutionary Genetics Analysis version 7.0) for bigger datasets and a MUSCLE alignment.

Measurements of the meristem length, counting of the distal stem cells and segmentation of the z-stacks were carried out in Fiji (Schindelin et al., 2012). For meristem length measurements, the border between meristem and elongation zone was defined by the first cell in the outermost cortex cell layer that doubled in cell length compared to its distal neighbor and analysis was carried out qualitatively from direct observation (as described in Dello Ioio et al., 2007). Segmentation of cells in the z-stack of the stem cell niche was performed with the MorphoLibJ plugin and morphological segmentation (Legland et al., 2016). All plots were created in R (R Core Team, 2015). Statistical significances of the meristem length and the distal stem cell differences were determined by a two-tailed Student's *T*-Test with the indicated *p*-value. For image compilation, Adobe Photoshop was used. In the microscope images of the meristems contrast and brightness were changed in parts of the images, as the images were composed of single microscope images.

RESULTS

Adapted mPS-PI Staining Allows Whole Mount Imaging of Barley Root Meristems and Reveals That the Barley Meristem Approximates a Steady Size within 6 DAG

In the first days of seedling development, the seminal roots are the main root type involved in water uptake (Knipfer and Fricke, 2011), so they are of particular importance for development of the plant in water stress conditions. We therefore focused our study on this root type. There is no consensus in the literature on the number of seminal roots and the appearance of a primary root in different barley cultivars (Hackett, 1968; Luxová, 1986). Under our experimental conditions, the root system of the barley cv. Morex consists of 2–6 seminal roots that arise during the course of the first five DAG. Around 10 DAG, adventitious roots arise from the shoot. This is in accordance with the data of Knipfer and Fricke (2011) and Hackett (1969). Luxová (1986) distinguished primary and seminal roots of barley by position in the embryo, however, this was not possible for the cv. Morex without dissecting the embryo. Because we could not detect a phenotypical difference between any of the first roots, we made no distinction between primary and seminal roots. Within the first 16 DAG, the roots grew to an average length of approximately 5 cm in our growth conditions (**Figure 1A**). After germination, the number of cells in the meristem increases, until the meristem reaches its full size when the rates of cell division and cell elongation are balanced. However, problems in visualizing meristem cells in barley result from the thickness and size of the roots which make microscopy impossible without clearing. By adapting the technique of mPS-PI staining (Truernit et al., 2008) which was previously described for Arabidopsis flower stalks to barley, we could stain the root cell walls and starch granules in the root tip for confocal microscopy without previous sectioning. To measure the meristem size, we analyzed the outermost layer of the cortex cells next to the epidermis and defined the transition zone between the meristem and the elongation

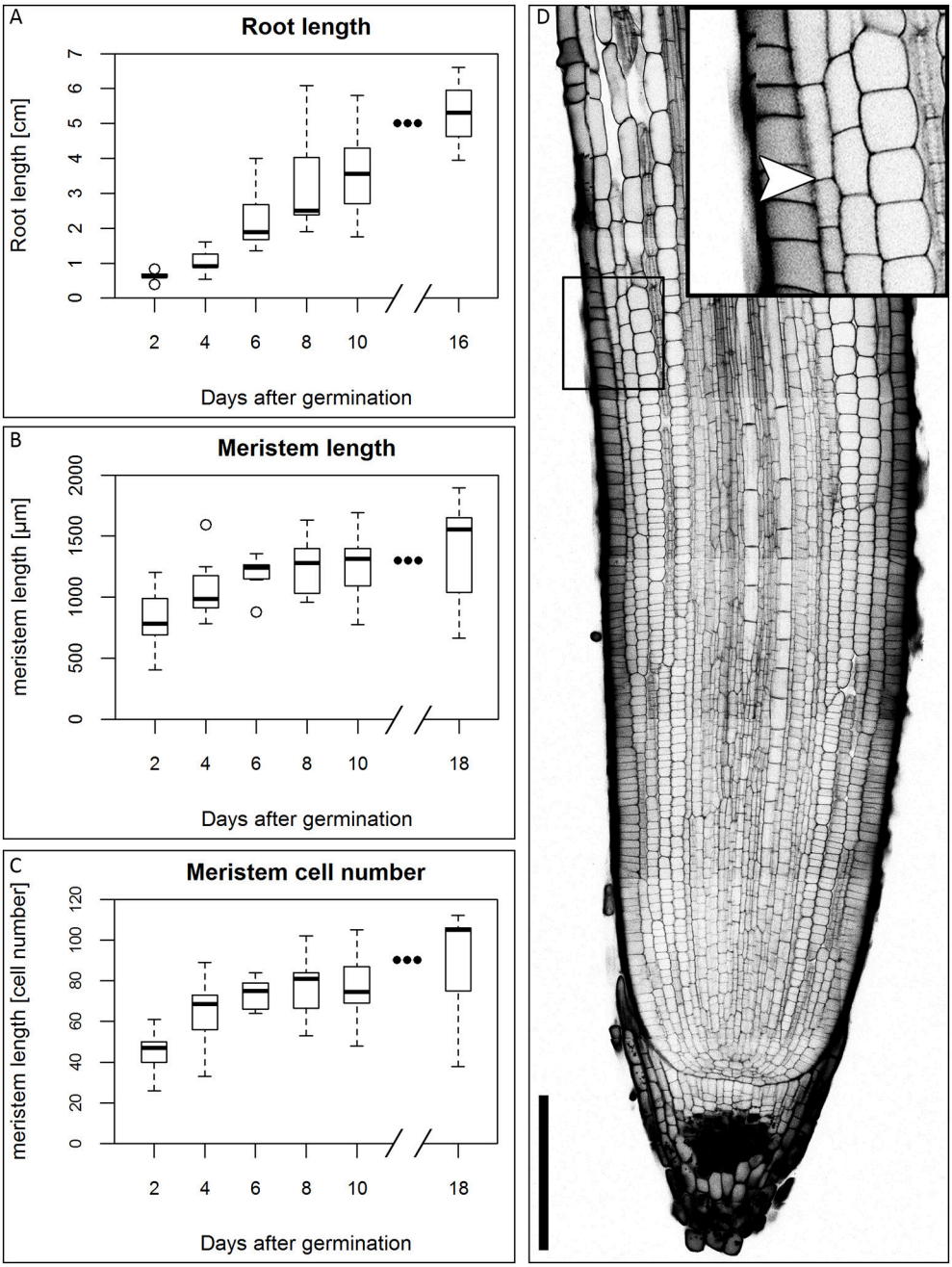

FIGURE 1 | Growth of the barley root and the root meristem. **(A)** Root length of the barley root system at the first DAG; the average length of all roots of single plants was measured, $n = 3$–11 plants per time point, experiment was performed twice. **(B)** Meristem length of barley roots at different DAG in µm; the meristem growth is highest in the first DAG; after 6 DAG most of the meristems approximate a steady size; $n = 9$–17 per time point, experiments were performed twice. **(C)** Meristem cell number at different DAG; also the cell number of the meristem has reached a steady size after 6 DAG; n = 9–17 per time point, experiments were performed twice. **(D)** Representative picture of the root tip 10 DAG, starch and cell walls stained with mPS-PI staining; arrowhead indicates the transition zone; inset shows a magnification of the transition zone; scale bar represents 200 µm.

zone as prior exemplified for *Arabidopsis*. There, the transition between the meristem and the elongation zone is defined as the region where the first cortical cell doubles in size compared to its distal neighbor (Dello Ioio et al., 2007). The observation that the different seminal roots of a single barley seedling emerge over the course of up to 5 days following germination complicates this type of analysis, as the measured roots will differ slightly in age and, accordingly, developmental stage. This is reflected in the variation in root meristem lengths at each time point (**Figures 1B,C**). The meristem continued to

grow, but growth slowed down approximately 6 DAG, while root length steadily increased in the monitored time window (**Figures 1A–C**).

Cell Layers in the Barley Root

We first characterized the number and identity of root cell files. Because cells are not yet differentiated in the root meristem, they cannot be distinguished only on the basis of their morphology. We therefore stained the suberized tissue in a cross section of the differentiated part of the root (root hair zone) with the fluorescent dye berberine hemisulfate (**Figure 2**). In this region of the root, the endodermis, the exodermis and the epidermis have suberized cell walls as diffusion barriers (Nawrath et al., 2013). We found that the barley root consists of one layer of epidermis, one layer of exodermis derived from the cortex, four layers of cortical cells and one endodermal layer. The cortex cells can be categorized into inner cortex (small cells) and outer cortex (larger cells) on the basis of their morphology. The central cylinder of the barley cv. Morex root comprises one large central and eight smaller peripheral metaxylem vessels, confirming similar observations on seminal roots of the cv. Golf by Knipfer and colleagues (Knipfer and Fricke, 2011). As the exodermis only forms in the differentiating zone of the root in a layer of cortical cells beneath the epidermis, it can be considered as cortex cell file in the root meristem (Enstone et al., 2003).

The Barley QC Consists of around 30 Cells

In many plant species analyzed, the QC serves to maintain adjacent stem cells in an undifferentiated state by short range signaling (Dolan et al., 1993; van den Berg et al., 1997; Ni et al., 2014; Kerk and Feldman, 1994). QC and stem cells of maize and *Arabidopsis* are characterized by their slower cell division rate in comparison to the surrounding cells (Clowes, 1984; Dolan et al., 1993). This quiescence could be necessary to protect the QC from DNA damage caused by DNA replication and allows to provide a pool of cells with an error-free genome for renewing the surrounding stem cells (Heyman et al., 2014). To investigate the cell division rate in the barley stem cell niche, we made use of two approaches, EdU staining and RNA *in situ* hybridization to detect expression of Histone H4, which is specifically expressed during S-phase. EdU is a thymidine analog that is incorporated into the DNA during DNA synthesis and hence labels cells in the S-phase of the cell-cycle (Kotogány et al., 2010). In *Arabidopsis,* a 24 h incubation with EdU labeled all cells in the stem cell niche except for the QC cells (Vanstraelen et al., 2009). In the barley root meristem, a 24 h treatment with EdU marked almost all nuclei in the stem cell niche (**Figure 3B**), while after a 12 h incubation with EdU 60 % of the roots (9/15) carried cells lacking EdU label in the putative stem cell niche (**Figure 3A**). Results of a 6 h EdU treatment were even more striking and 70% of all roots (30/44) lacked EdU incorporation at this position (**Figure 4**). Importantly, we could not detect any group of cells that was non-dividing over more than 24 h. To identify the QC cells, we analyzed the cell division rate in different subsets of the stem cell region in roots that were treated with EdU for 6 h (**Figure 4**). Notably, the cell division rates in the subsets revealed that a quiescence gradient in the QC region exists, with the highest quiescence, i.e. the lowest cell division rates in the cell layer adjacent to the root cap (subset 1) and increasing cell division rates in subsets 2, 3 and 4 (**Figures 4B–I**). Subset 3, with the most striking difference in cell division rate in comparison to the other subsets, is displayed in **Figures 4F,G** and includes around 9 cells in longitudinal sections (blue frame). The cell division rate in subset 3 ranged from 0 to 30%, while the cell division rate in the surrounding cells (orange region in **Figure 4F**) was predominantly in a range from 20 to 60% (**Figure 4G**). We therefore suggest that subset 3 cells represent the QC region. However, in 14/40 roots, more than 30% of the QC cells were EdU stained within a 6 h period (**Figure 4G**). To confirm this cell division pattern, we performed RNA *in situ* hybridisation with a probe detecting *Histone H4*. Cell division rates in subset 3 (blue frame in **Figure 5B**) ranged from 0–20 and10–50% in the surrounding region (orange frame in **Figures 5B,C**), supporting the previous identification of the QC in subset 3. Assuming that the QC has a hemispherical shape, we calculated that the entire QC consists of around 30 cells.

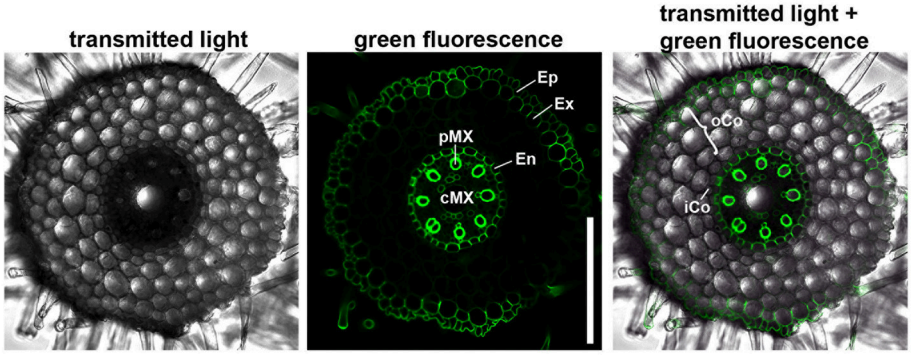

FIGURE 2 | Anatomy of the barley root. Cross section of a root 8 DAG in the root hair zone, suberin stained with berberine hemisulfate; epidermis (Ep), exodermis (Ex), and endodermis (En) have suberized cell walls, while inner (iCo) andouter cortex (oCo) cells except for exodermis have not; eight peripheral meta xylem (pMX) vessels (autofluorescent) surround one central meta xylem (cMX) vessel in the central cylinder; scale bar represents 200 μm; $n = 16$, experiment performed three times.

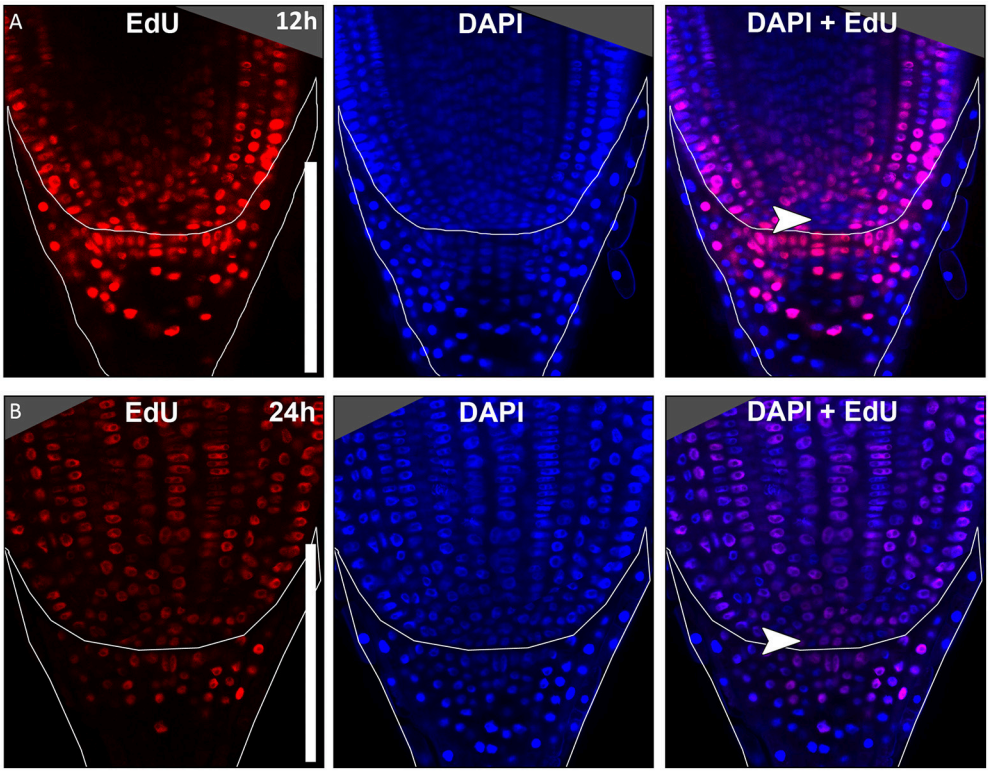

FIGURE 3 | Cell division in the barley root tip. Roots of plants 8 DAG were treated with the cell division marker EdU (red), nuclei counterstained with DAPI (blue), merge image shows an overlay of both stainings. **(A)** Exemplary barley root tip after 12 h treatment with EdU. **(B)** Exemplary barley root tip after 24 h treatment with EdU; no area of low cell division rate is visible; scale bar represents 200 μm; arrow heads point to the putative QC region.

Formation of Epidermis, Cortex, and Endodermis

We studied mPS-PI stained barley roots to identify the clonal origin of the epidermal, the five cortical and the endodermal cell layers. By tracing the outlines of cells, we found that the endodermis and a variable number of cortex cell files share the same founder cell which locates adjacent to the QC (in 17/23 roots at 5–8 DAG). In most cases, a QC abutting inner cortex endodermis initial (ICEI) gave rise to the endodermal cell layer and the inner cortex cell layer, whose descendants remained distinctly smaller than the outer cortex cell layers (see **Figure 2**). However, in contrast to the model organism *Arabidopsis*, cell division patterns are less regular. We often found that cells at a distance to the QC underwent periclinal cell divisions, thereby generating additional cortex cell files (white arrow heads in **Figure 6A**). The outer cortex cell layers derived from a distinct outer cortex initial (OCI) that first generated two cortex cell files by alternating between anticlinal and periclinal divisions. Further periclinal division in descendants give rise to additional cortex layers. Serial optical sections confirm this cell division pattern (**Figure 6B**, Supplementary Movie 1). This pattern of cell layer generation differs from that in rice, where a ground tissue stem cell abutting the QC undergoes four rounds of asymmetric divisions to generate endodermis, cortex, exodermis and sclerenchyma cell layers (Rebouillat et al., 2009; Ni et al., 2014). In maize, the position and cell division pattern of stem cells has not yet been analyzed in detail (Hochholdinger et al., 2004a; Jiang and Feldman, 2005). In barley, the epidermis can be traced back to a dedicated stem cell adjacent to the QC (in 20/26 roots at 5–8 DAG) (**Figure 6A**). The origin of the vascular system and division patterns of vascular stem cells could not be traced back unequivocally by our mPS-PI staining method. Cell division patterns appeared highly variable, and reporter lines marking cell clones would be required to determine number and behavior of vascular initials. However, a single file of metaxylem cells is prominent in all roots, which can be identified at a distance of more than 5 cells from the QC (**Figures 2**, **6A**).

Formation and Structure of the Lateral Root Cap and the Columella

At the root tip, we observed a distinct border that separates the starch-containing columella cells and the undifferentiated columella precursors from the proximal part of the root (**Figure 6A**). Differentiated columella cells contain starch grains that are necessary for gravitropism (Kiss et al., 1996). In rice, maize and *Arabidopsis* all cells of the columella and lateral root cap except for the columella stem cells contain starch grains (**Figure 10**; Dolan et al., 1993; Lim et al., 2000; Wang et al., 2014). In barley cv. Morex, we detected starch granules only in the five to six distal layers of the columella. The lateral root cap and on

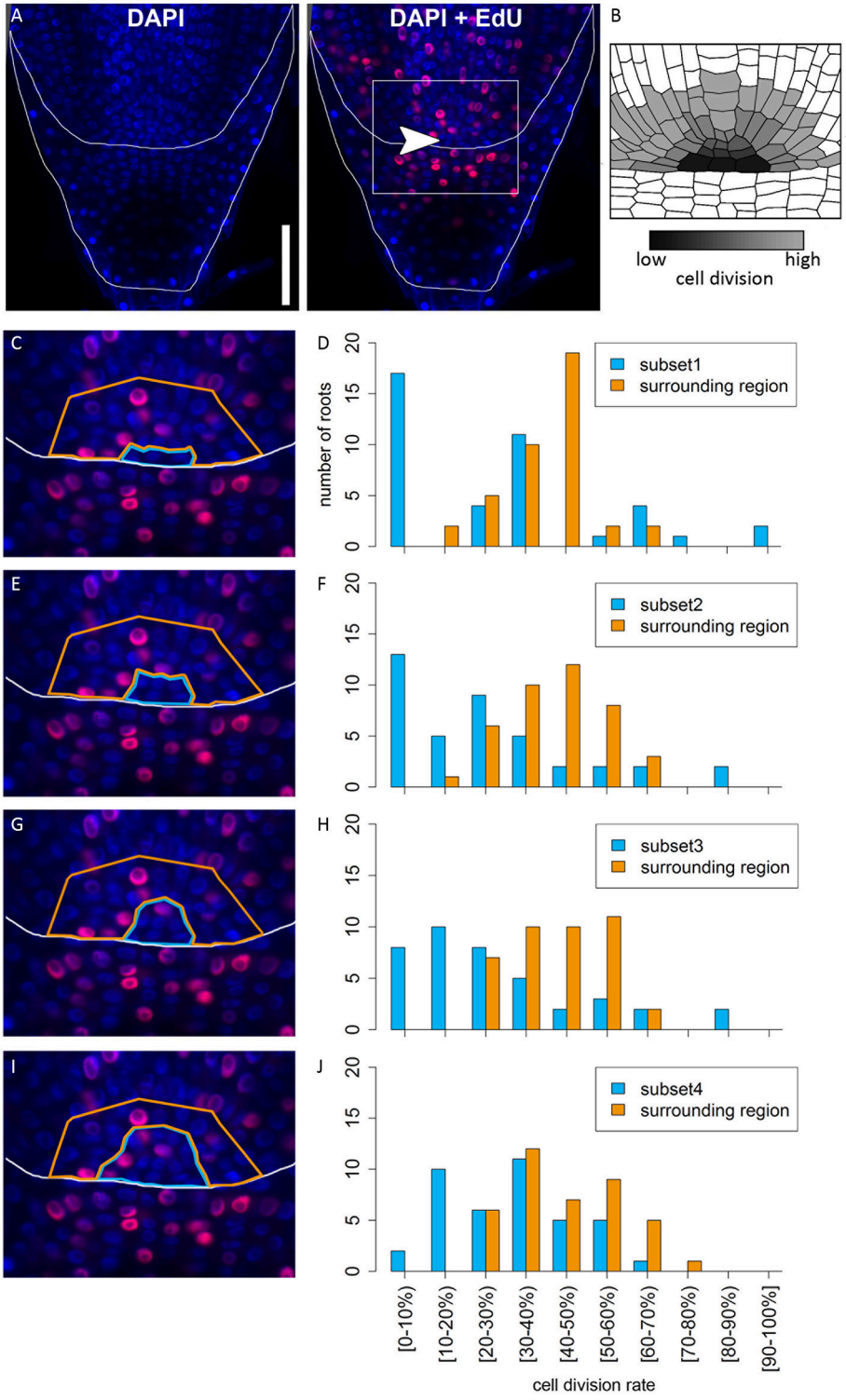

FIGURE 4 | Analysis of cell division rates in different regions of the barley root tip. Roots of plants 8 DAG were treated with the cell division marker EdU (red) for 6 h and counterstained with DAPI as in **Figure 3**. **(A)** Exemplary barley root tip after treatment with EdU; merge image shows an overlay of DAPI and EdU staining; white arrow head points to the putative QC region; scale bar represents 100 μm. **(B)** Schematic view on the stem cell niche with cell division rates; cells with low division activity are marked with dark gray, cells with high division activity with light gray. **(C,E,G,I)** Magnification of the region marked in **(A)**; schematic view of the respective analyzed regions; bright blue marks the putative QC region in the center, orange marks the surrounding reference region. **(D,F,H,J)** Diagrams show the number of

(Continued)

FIGURE 4 | Continued
roots that showed cell division at the rate given on the x-axis in the respective area in the stem cell niche; different areas (bright blue and orange) refer to the areas marked by colors in **(C,E,G,I)**; square brackets for the cell division rates indicate that the following number is included in the column, while round brackets indicate that the numbers are excluded. **(C)** The putative QC includes only the four most central cells of the stem cell niche next to the root cap border (subset 1). **(D)** A large difference in cell division rate can be found between the putative QC region and the surrounding cells. **(E)** The putative QC includes the region from **(C)** plus around four proximal cells (subset 2); here again, there is an obvious difference in cell division rate between the QC and the surrounding cells, indicating that this subset enclosures the QC region **(F)**. **(G)** The putative QC includes the region from **(E)** plus around four proximal cells (subset 3), meaning that the putative QC region here includes 9 cells proximal to the root cap border. **(H)** Again, there is a difference in cell division rates between the putative QC region and the surrounding cells, indicating this subset still enclosures the QC region. **(I)** The putative QC region consists of the region marked in **(G)** plus one additional cell layer surrounding it (subset 4); here, the difference in cell division rate does not appear **(J)**, meaning that this subset probably includes more than only the QC region.

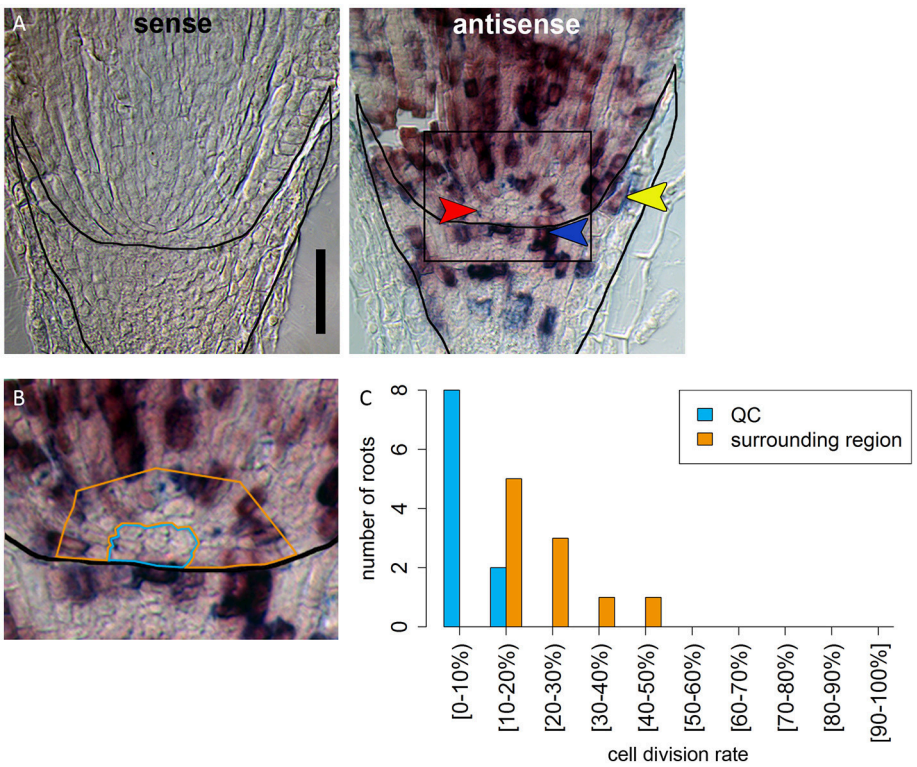

FIGURE 5 | Identification of a region of slowly dividing cells in the barley stem cell niche. **(A)** RNA in *situ* hybridizations with probe against the S-phase marker *H4*; the sense control shows no staining; in the antisense sample, cells in the S-phase expressing *H4* are stained in purple; red arrow head in points to the putative QC region without *H4* expression; orange arrowhead points to cell divisions that form the lateral root cap; blue arrowhead points to cell divisions in the distal stem cells that build the columella; scale bar represents 100 μm. **(B)** Magnification of the region marked in **(A)**; orange and blue frame surround the regions analyzed in **(C)**; frame around the root marks the position of the root cap border. **(C)** Percentage of cells that have express *H4* as cell division marker in the respective area in the stem cell niche illustrated in **(B)**.

average four cell layers proximal to the differentiated root cap cells, however, lacked starch granules (**Figures 1D**, **6A**, **9E**) and might act as columella stem cells. EdU treatment revealed that the first cell layer distal to the QC had a high cell division potential, which declined in the three more distal layers (**Figures 6C,D**). We occasionally also observed cell divisions in differentiated root cap cells (gray arrowhead in **Figure 6C**), which was also noted for columella cells in *Arabidopsis*, but not for rice (Wang et al., 2014; Hong et al., 2015). The lateral root cap originates from periclinal and oblique (in 6/30 roots at 5–8 DAG) cell divisions of lateral columella stem cells (**Figure 6A**, cells framed with orange), and lateral root cap cells maintain high division activity (marked by orange line in **Figure 6C**). Extended EdU staining over 48 h confirmed that most lateral root cap cells divided at least once within this time frame. *Histone H4* expression analysis supported the conclusions drawn from EdU stainings, showing that (1) all cells of the root cap remain division active, and (2) that the columella stem cell layer proximal to the QC maintains the highest divisional activity (blue arrow head in **Figure 5A**). The cell division pattern and cell wall arrangement at the position of the epidermis initial (EPI) indicates that the epidermal cell layer and the lateral root cap of barley are of independent origin, as it is typical for monocot roots (**Figure 6A**; Clowes, 2000; Rebouillat et al., 2009).

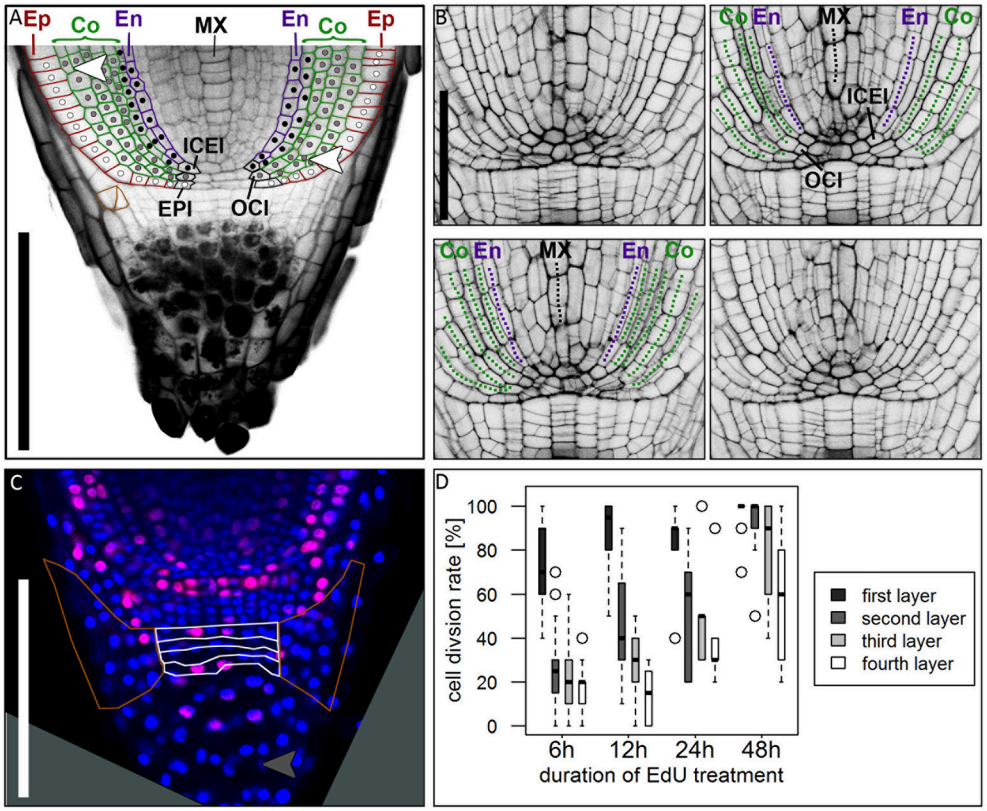

FIGURE 6 | Cell division patterns in the root meristem. **(A)** Root tip stained with mPS-PI staining; colored cell walls mark the epidermal (red), cortical (green) and endodermal (magenta) cell files; white dots mark the cell lineage of the epidermis resulting from the arrangement of cell walls, derived from the epidermis inital (EPI); gray dots mark the cell lineage of the outer cortex cell layers, derived from the outer cortex initial (OCI); black dots mark the cell lineage of the inner cortex cell layers and the endodermis, derived from the inner cortex/endodermis initial (ICEI); white arrowhead points to a periclinal cell division in the cortex; orange cell walls marks an oblique cell division that forms the lateral root cap; Ep, epidermis; Co, cortex; En, endodermis; MX, metaxylem; scale bar represents 200 μm. **(B)** Longitudinal optical sections through the barley stem cell niche from the same z-stack presented in Supplementary Movie 1; Images were acquired at a distance of 5 μm; labels according to **(A)**, dotted lines follow the cell files in the respective colors; ICEI and OCI are visible in the center of the root, marked by appearance of the metaxylem and confirmed by tracing the cells in Supplementary Movie 1; scale bar represents 100 μm. **(C)** Root tip treated with EdU for 6 h; white borders mark the layers of undifferentiated cells distal to the root cap border, orange borders mark the lateral root cap; gray arrow head points to a cell division in the differentiated part of the root cap; root age 8 DAG; scale bars represent 200 μm. **(D)** Diagram showing the cell division rates of the layers of undifferentiated cells distal to the QC marked with white borders in **(B)** visualized by different EdU treatment times, 6, 12, 24, and 48 h (black = first layer distal to QC, dark-gray = second layer, light-gray = third layer, white = fourth layer); cell division rate is highest in the first layer distal to the QC, but increasing in the other layers after prolonged EdU treatment; $n = 44$ (6 h), 12 (12 h), 5 (24 h), and 14 (48 h); experiment was performed twice.

The Barley Meristem Is Consumed upon CLE40 Peptide Treatment While the Distal Stem Cells Are Unaffected

In *Arabidopsis*, a constant population of columella stem cells is maintained through a negative feedback regulation, involving the differentiated columella cells and the QC. The QC promotes columella stem cell fate in adjacent cells due to a non-cell autonomous function of the mobile transcription factor WOX5 (Pi et al., 2015). Differentiated columella cells, which are the descendants of the columella stem cells, express the secreted peptide CLE40 which acts via receptor kinases to confine *WOX5* expression (Stahl et al., 2009, 2013). An excess of CLE40 causes a rapid differentiation of stem cells toward columella cell fate. Additionally, CLE40 also regulates the size of the proximal meristem: here, increased levels of CLE40 can induce stem cell differentiation and loss of meristem activity (Hobe et al., 2003; Fiers et al., 2005). We now asked if a similar mechanism is acting in barley, and identified 21 CLE family peptides encoded in the available barley genome (Mayer et al., 2012). In *Arabidopsis*, CLE peptides are involved in a variety of developmental processes, but only two of them, CLE40 and CLAVATA3 (CLV3), act in meristem maintenance pathways. In rice, FLORAL ORGAN NUMBER2 (FON2) and FON2-LIKE CLE PROTEIN1 (FCP1) encode highly homologous CLE peptides, and of all CLE genes analyzed, only FCP1, FON2, CLV3, and CLE40 carry two introns, reflecting a common evolutionary origin (Fletcher et al., 1999; Hobe et al., 2003; Chu et al., 2006; Suzaki et al., 2006, 2008). Our search for CLE genes in the barley genome uncovered MLOC_3686 (named now HvCLE402) (Mayer et al., 2012), which carries two introns and encodes a CLE peptide highly related to FCP1 (**Figures 7**, **8**). Treating barley plants with 1 μM synthetic HvCLE402 peptide consisting of the 12 amino

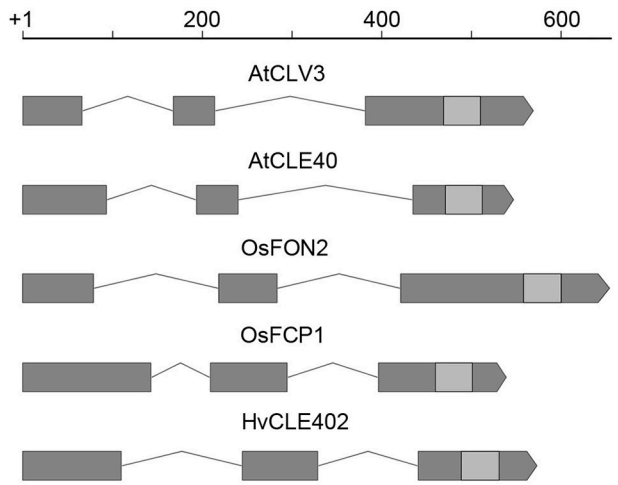

FIGURE 7 | *CLE* gene structure in *Arabidopsis*, rice and barley. Gene structure of *CLV3*, *CLE40* (*Arabidopsis*) (Fletcher et al., 1999; Hobe et al., 2003), *FON2*, *FCP1* (rice) (Suzaki et al., 2006, 2008), and *HvCLE402* (barley); all of these *CLE* genes consist of three exons (gray boxes), two introns (lines connecting the boxes) and the sequence coding for the CLE-motif (light gray boxes); scale bar in bp.

HvCLE402	**R**	**E**	**V**	**P**	**T**	**G**	**P**	**D**	**P**	**I**	**H**	**H**
OsFCP1	**R**	**E**	**V**	**P**	**T**	**G**	**P**	**D**	**P**	**I**	**H**	**H**
OsFCP2	**R**	**E**	**V**	**P**	**S**	**G**	**P**	**D**	**P**	**I**	**H**	**H**
OsFON2	**R**	**S**	**V**	**P**	**A**	**G**	**P**	**D**	**P**	**M**	**H**	**H**
AtCLV3	**R**	**T**	**V**	**P**	**S**	**G**	**P**	**D**	**P**	**L**	**H**	**H**
AtCLE40	**R**	**Q**	**V**	**P**	**T**	**G**	**S**	**D**	**P**	**L**	**H**	**H**

FIGURE 8 | Sequences of the CLE-motifs of selected CLE genes from rice, *Arabidopsis* and barley. CLE-motifs of FCP1, FCP2, and FON2 from rice, CLV3 and CLE40 from *Arabidopsis* and CLE402 from barley (Suzaki et al., 2008). The CLE-motif from barley completely matches the one from FCP1.

acid CLE motif (HvCLE402p) or the *Arabidopsis* AtCLE40 peptide led to a significantly reduced root meristem length in comparison to untreated or mock treated plants (**Figures 9A,B**). We found that the number of proximal meristem cells was severely reduced (**Figure 9C**), indicating that the reduction of meristem size is likely caused by premature differentiation of proximal meristematic cells. This is consistent with observations made for the response of rice or Brachypodium to increased CLE peptide levels (Kinoshita et al., 2007; Czyzewicz et al., 2015). In the distal root meristem, 4 layers of columella stem cells give rise to the starch granule containing columella cells. In *Arabidopsis*, columella stem cell fate and number is negatively feedback regulated by CLE40 peptide, which is generated by differentiated columella cells. We asked if a similar regulation takes place in barley, and counted columella stem cell layers in peptide treated and untreated roots. Treatment with high levels of HvCLE402 or AtCLE40 peptides caused a minor, albeit statistically significant reduction of stem cell number, indicating that regulation of stem cell fate cannot depend solely on HvCLE402 (**Figures 9D,E**). Furthermore, we found that the HvCLE402 peptide can trigger both differentiation of columella stem cells and the proximal meristem cells in *Arabidopsis*, like the AtCLE40 peptide (**Figure 10**, Stahl et al., 2009), indicating that the CLE40 pathway controlling proximal meristem maintenance is highly conserved between monocots and dicots, while the distal meristem is only partially regulated through a CLE40 pathway.

DISCUSSION

To understand the fundamental concepts of root growth, it is important to compare the differences in operating mechanisms between higher plants from the two major groups, monocots and dicots. Here, primary root growth is enabled by root meristems at the tip of the roots, which harbor the stem cell niche that provides the precursors for the various root tissues. Root stem cell niches of different plants share a similar architecture, but the sizes of the stem cell niches, the number of stem cells, the origin of differentiating root cell types and the signaling systems that control cell fates differ significantly. While the principle frameworks governing root meristem functions in the model dicot *Arabidopsis* have been established and are basically understood, far less is known about root meristem functions in monocot species. Analysis of grass root meristems has focussed on maize and rice, and to a lesser extent on Brachypodium (Hardtke and Pacheco-Villalobos, 2015), which all represent examples of closed meristems with discrete initials that, in most cases, give rise to individual cell files. The stem cell niches differ vastly in size between these species, with 4–6 QC cells in rice, but 800–1,200 QC cells in maize (**Figure 11**; Jiang et al., 2003; Ni et al., 2014). For rice, the origins of cortex and endodermis have been studied in more detail. Here, a stem cell abutting the QC gives rise to several cortex layers and the endodermis via a series of ordered anticlinal and periclinal divisions, resembling the scenario in *Arabidopsis*, with 4 QC cells and a shared initial giving rise to a single cortex cell layer and the endodermis (Dolan et al., 1993; Ni et al., 2014). Similarly, a shared initial generates the lateral root cap and the epidermal cell file, while a single layer of stem cells distal to the QC forms the columella in *Arabidopsis* (Dolan et al., 1993). The overall architecture combined with clonal analysis revealed that lateral root caps and epidermis can be traced back to different stem cells in rice and maize (Hochholdinger et al., 2004b; Wang et al., 2014). Our overall understanding on gene functions regulating the root stem cell niches in monocot species is still very limited, and mostly based on comparative analysis with *Arabidopsis*. Here, we have analyzed for the first time the root meristem architecture of *H. vulgare* (barley), as one of the most important crop species, with the aim to identify commonalities and characteristic features of monocot stem cell systems. We found that, regarding size and general architecture, the barley root meristem occupies an intermediate position between those of maize and rice. Our combined EdU staining and analysis of *HISTONE H4* expression patterns identified approximately 30 slowly dividing cells at the QC position (**Figures 4**, **5**). Unlike in *Arabidopsis* we could not find a clearly defined cell region with complete quiescence, but rather an area displaying a gradual quiescence, with the highest quiescence in the cell layer adjacent to the root cap (**Figure 4**).

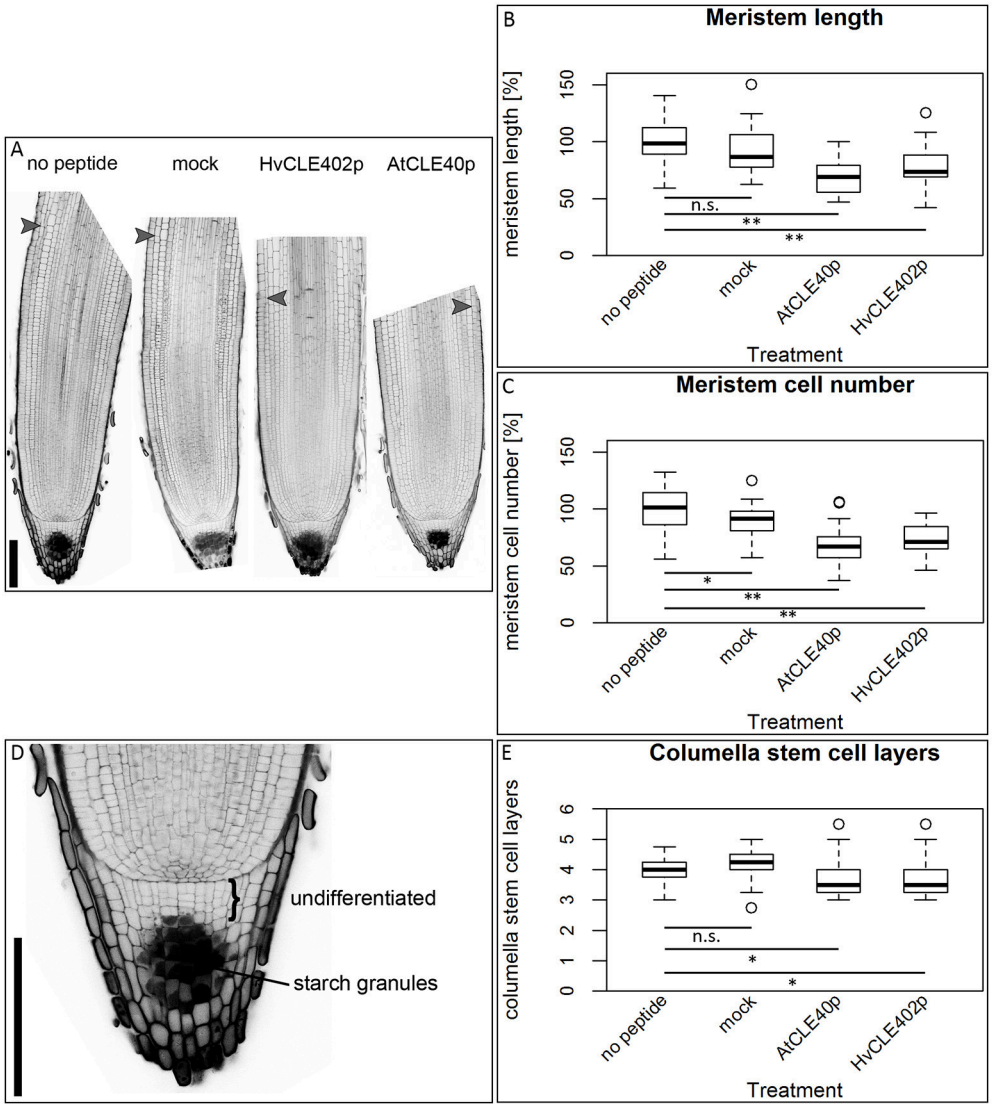

FIGURE 9 | The barley root meristem and distal stem cell niche upon CLE40 peptide treatment. **(A)** The proximal meristem cells of the barley root differentiate prematurely when grown on medium containing either 1 μM HvCLE402p or 1 μM AtCLE40p compared to medium containing no peptide or 1 μM mock peptide (mCLE40p) for five DAG; arrowheads mark the transition zone between meristematic and elongation zone. **(B)** Meristem length measured in μm normalized to untreated plants (no peptide). **(C)** Meristem cell number normalized to untreated plants; asterisks indicate a significant difference between the respective treatments; n.s. = not significant; * = $p < 0.05$, ** = $p < 0.001$; experiment performed 5 times; $n = 17$–54. **(D)** Exemplary distal root meristem with brackets marking the columella stem cells. **(E)** The number of distal stem cell layers is unaltered by peptide treatment; per root, four vertical columns were analyzed and the average is displayed in the diagram; experiments were performed 4 times; $n = 14$–31, scale bar 200 μm.

This resembles the situation in maize, where quiescence and size of the QC are highly variable. The barley QC is thus considerably larger than that of rice, where each QC cell neighbors dedicated initials (**Figure 11**; Ni et al., 2014). There, rare asymmetric divisions of QC cells serve to replace adjacent stem cells, while QC cell divisions in barley may also serve to expand the QC size. Although we identified the barley QC based on a lower cell division rate, all QC cells were found to divide within a 24 h time window (**Figure 3**). This is in stark contrast to the QCs of rice or maize, where no cell divisions in the QC were observed even within a 48 h window (Ni et al., 2014; Jiang et al., 2003). In *Arabidopsis*, less than 20% of all QC cells divided within a 24 h period (Vanstraelen et al., 2009; Cruz-Ramírez et al., 2013). Rarely dividing QC cells have been implicated to be protected from DNA damage and act as a genetic "cache" to replace damaged stem cells. However, for this purpose alone, rather modest differences in cell cycle frequency between QC and surrounding stem cells might be sufficient (Cruz-Ramírez et al., 2013). Importantly, barley generates several seminal roots which might be competing for resource allocation, explaining the wide range of cell divison rates and resulting meristem lengths that we noted earlier (**Figures 1B,C**). A lower quiescence of the barley QC might thus reflect the physiological state during rapid growth phases. An earlier study by Clowes (1984) found a correlation

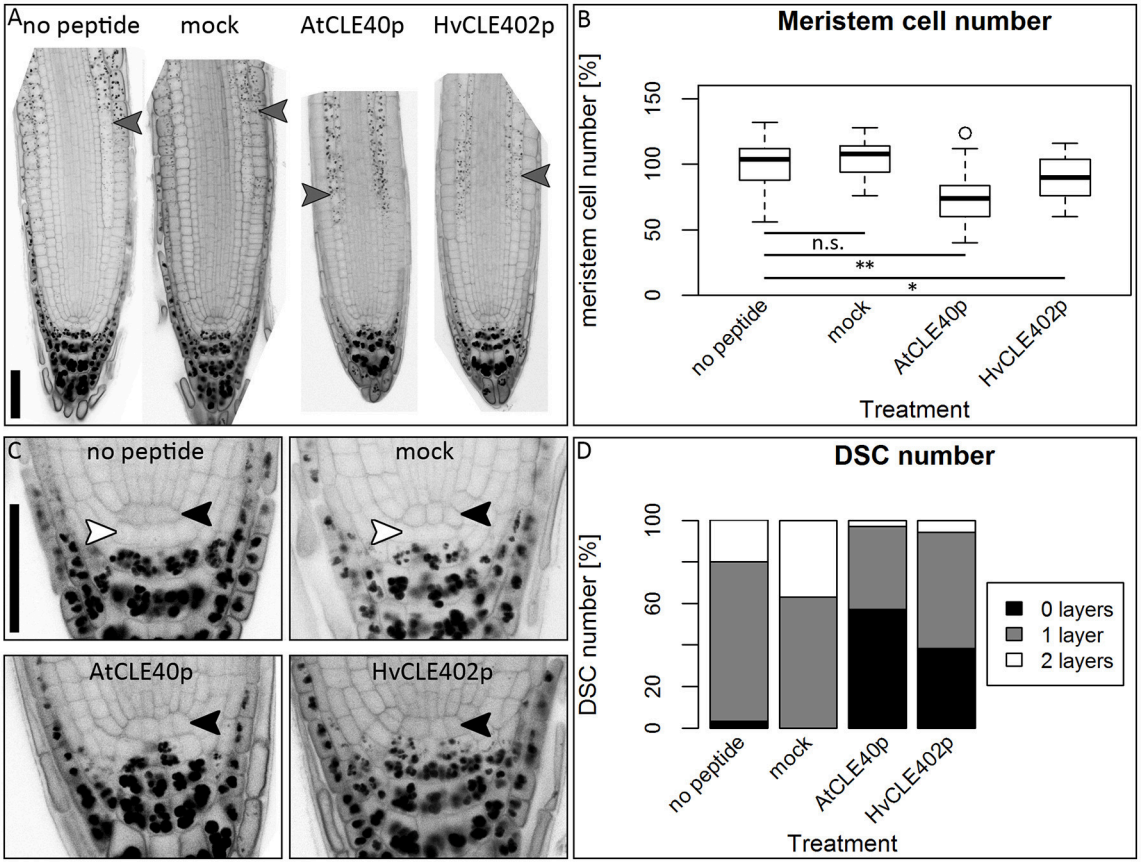

FIGURE 10 | The *Arabidopsis* root meristem and the distal stem cell niche upon CLE40 peptide treatment. **(A)** Exemplary meristems of *Arabidopsis* roots upon 1 μM HvCLE402p, 1 μM AtCLE40p or mock treatment for five DAG; gray arrowheads mark the transition zone between meristematic and elongation zone. **(B)** In comparison to untreated or mock (mCLE40p) treated plants, growth on AtCLE40p or HvCLE402p leads to a reduced meristem size; meristem size was counted in cell number and normalized to untreated (no peptide) plants; asterisks indicate a significant difference between the respective treatments; n.s. = not significant; * = $p < 0.05$, ** = $p < 0.001$. **(C)** Exemplary pictures of *Arabidopsis* distal stem cell niches upon HvCLE402p, AtCLE40p or mock treatment; black arrow heads mark the QC position, white arrow heads mark distal stem cells without starch; treatment with both AtCLE40p and HvCLE402p leads to a differentiation of the distal stem cells, visible by accumulation of starch granules. **(D)** Percentage of roots with no undifferentiated distal stem cells (DSCs) (black bars), one layer (gray bars), or two layers (white layers); experiment performed once; $n = 27–34$; scale bars 50 μm.

between the number of cells in the QC and the root diameter, suggesting that bigger roots might need a larger QC, either as a source of DNA-damage protected cells, or as provider of short-range signals for surrounding stem cells (van den Berg et al., 1997; Cruz-Ramírez et al., 2013).

The origin of endodermis and cortex and the regulation of their formation is well researched in *Arabidopsis* and, to a more limited extend, also in rice. In *Arabidopsis*, the cortex cell layer and the endodermis originate from a common initial (Dolan et al., 1993). Because there are more cortex cell layers in rice than in *Arabidopsis* (5 cortex cells layers, one layer of sclerenchyma, and one layer of exodermis, Rebouillat et al., 2009), the sequence of initial divisions is more complex. Rebouillat and colleagues summarize that first an anticlinal cell division near the QC generates the epidermis-endodermis initial, followed by eight successive asymmetric periclinal cell divisions that generate the endodermis, sclerenchyma layer, exodermis and five cortex layers (Rebouillat et al., 2009). A later study confirms this cell division pattern in regard to the endodermis and cortex, but states that the epidermis is not derived from the same stem cell (Ni et al., 2014). For barley, our studies of the cell wall arrangement by mPS-PI staining suggest that the endodermis and a variable number, 1–3, of inner cortex cell layers are derived from a common ancestor, the ICEI, while 2–4 outer cortex cell layers originate from a different precursor (OCI) (**Figure 6**, Supplementary Movie 1). Notably, formative cell divisions that generated new cortex cell layers occurred at a distance to the QC, indicating that they are either not controlled by the QC itself, or that longer range signals are operating that act over several cell diameters. In *Arabidopsis*, a so-called middle cortex layer is initiated by periclinal cell divisions at a short distance to the QC, which were dependent on the SCARECROW (SCR) transcription factor function, and repressed by gibberellic acid (GA) signaling (Paquette and Benfey, 2005). The independent and distinct origin of inner and outer cortex cells in barley could be reflected in physiological differences between these cell

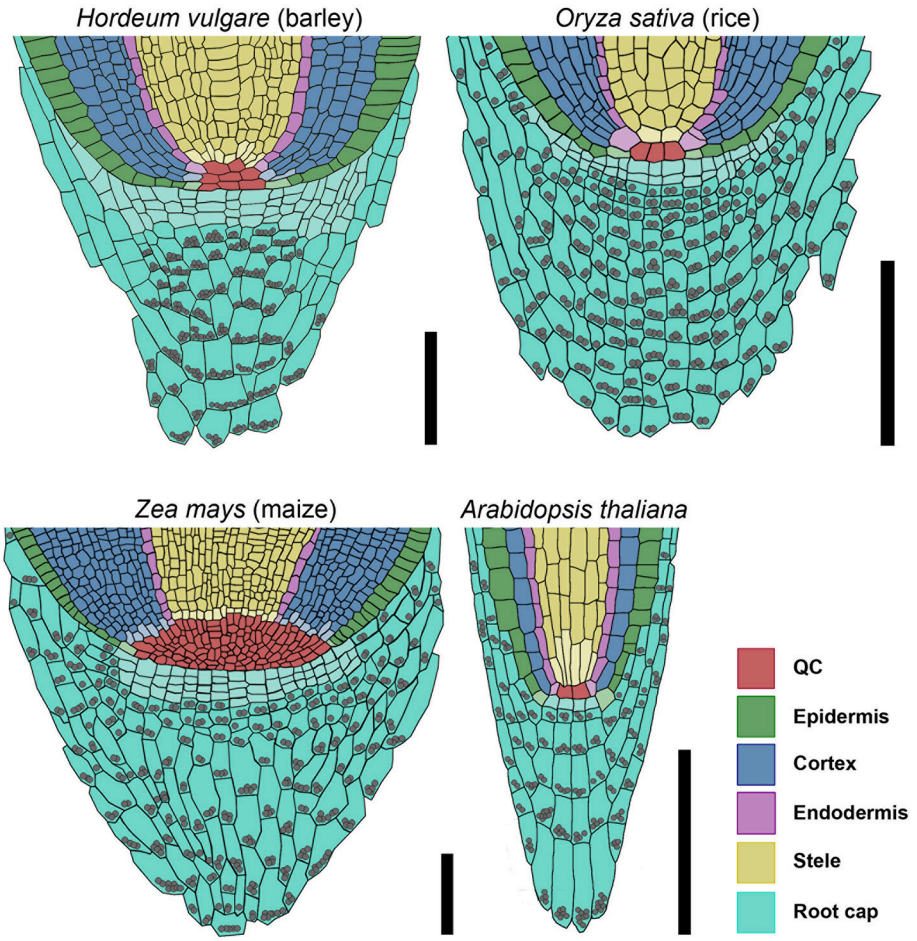

FIGURE 11 | Models of barley, rice, maize, and *Arabidopsis* root stem cell niches. Cell types are marked by color code according to the legend, stem cells that give rise to different tissues are depicted in the respective light colors; gray spheres represent starch granules in the root; the rice stem cell niche was created according to Ni et al. (2014) and Wang et al. (2014); the maize stem cell niche was created according to Kerk and Feldman (1994), Jiang and Feldman (2005) and Jiang et al. (2010); scale bar 100 μm.

types. In rice, inner and outer cortex cells differ significantly in their cell wall composition and morphology, and in their relative contribution to the ground tissue mass and aerenchyma (Henry et al., 2016). Reporter lines for genes expressed in certain root tissues and marker lines to trace back the cell divisions are not yet available in barley, but would further contribute to increasing our knowledge about the cell lineages in the root.

The barley columella consists of 4 stem cell layers, capped with about 10 layers of differentiated columella cells carrying starch granules, similar to the columella systems of rice or maize (Jiang et al., 2010; Wang et al., 2014). The stem cells in the layer proximal to the QC divide more rapidly than distal ones, indicating that divisional activity is promoted by the QC. In *Arabidopsis*, the columella stem cells are maintained by a CLE40 dependent feedback regulation between QC and differentiated cells (Stahl et al., 2009). We identified 21 genes encoding putative CLE-family peptides in the available barley genome data (Mayer et al., 2012). Alignments with CLE peptide sequences from rice and *Arabidopsis* resulted in the identification of one predicted peptide with the same amino acid sequence in the CLE motif as FCP1. In rice and barley, treatment with the FCP1 or HvCLE402 peptide induced premature differentiation of the proximal root meristem, similar to the observations made for *Arabidopsis* roots (**Figure 9**). However, in contrast to *Arabidopsis*, the barley distal root meristem displayed no differentiation of columella stem cells (**Figure 9**). Interestingly, the HvCLE402 peptide triggered differentiation of *Arabidopsis* columella stem cells (**Figure 10**), which suggests that the receptors perceiving the CLE40 peptides from different species are closely related, but that the mechanisms maintaining distal stem cell populations in barley act independently of the CLE40-dosage.

We have here provided a first framework for a more detailed analysis of root development and stem cell niches in the major crop plant barley. We uncovered commonalities with other monocot species, but also significant functional differences that highlight the importance of a comparative approach in plant developmental studies.

AUTHOR CONTRIBUTIONS

GK, YS, and RS conceived the project, GK, YS, MV, and RS planned the experiments, GK performed all experiments, GK and RS wrote the manuscript, all authors contributed to the final version.

FUNDING

Funding to GK, MV, and RS is acknowledged from the Deutsche Forschungsgemeinschaft through the Cluster of Excellence on Plant Sciences [CEPLAS, EXC1028].

ACKNOWLEDGMENTS

We are grateful to Marc Somssich and Wilma van Esse for valuable discussions, Carin Theres for technical assistance, Ikram Blilou for help with the RNA *in situ* hybridizations and Solomon H. Orse for support throughout the run of this project.

SUPPLEMENTARY MATERIAL

The Supplementary Material for this article can be found online at: http://journal.frontiersin.org/article/10.3389/fpls.2017.01240/full#supplementary-material

REFERENCES

Chu, H., Qian, Q., Liang, W., Yin, C., Tan, H., Yao, X., et al. (2006). The FLORAL ORGAN Number4 gene encoding a putative ortholog of arabidopsis CLAVATA3 regulates apical meristem size in rice. *Plant Physiol.* 142, 1039–1052. doi: 10.1104/pp.106.086736

Clowes, F. A. L. (1984). Size and activity of quiescent centres of roots. *New Phytol.* 96, 13–21. doi: 10.1111/j.1469-8137.1984.tb03538.x

Clowes, F. A. L. (1994). Origin of the epidermis in root meristems. *New Phytol.* 127, 335–347. doi: 10.1111/j.1469-8137.1994.tb04284.x

Clowes, F. A. L. (2000). Pattern in root meristem development in angiosperms. *New Phytol.* 146, 83–94. doi: 10.1046/j.1469-8137.2000.00614.x

Cock, J. M., and McCormick, S. (2001). A large family of genes that share homology with CLAVATA3. *Plant Physiol.* 126, 939–942. doi: 10.1104/pp.126.3.939

Cruz-Ramírez, A., Díaz-Triviño, S., Wachsman, G., Du, Y., Arteága-Vázquez, M., Zhang, H., et al. (2013). A SCARECROW-RETINOBLASTOMA Protein network controls protective quiescence in the arabidopsis root stem cell organizer. *PLoS Biol.* 11:e1001724. doi: 10.1371/journal.pbio.1001724

Czyzewicz, N., Shi, C.-L., Vu, L. D., Van De Cotte, B., Hodgman, C., Butenko, M. A., et al. (2015). Modulation of Arabidopsis and monocot root architecture by CLAVATA3/EMBRYO SURROUNDING REGION 26 peptide. *J. Exp. Bot.* 66, 5229–5243. doi: 10.1093/jxb/erv360

Dello Ioio, R., Linhares, F. S., Scacchi, E., Casamitjana-Martinez, E., Heidstra, R., Costantino, P., et al. (2007). Cytokinins determine Arabidopsis root-meristem size by controlling cell differentiation. *Current Biol.* 17, 678–682. doi: 10.1016/j.cub.2007.02.047

De Smet, I., Vassileva, V., De Rybel, B., Levesque, M., Grunewald, W., Van Damme, D. et al. (2008). Receptor-Like Kinase ACR4 restricts formative cell divisions in the Arabidopsis root. *Science* 322, 594–597. doi: 10.1126/science.1160158

Dolan, L., Janmaat, K., Willemsen, V., Linstead, P., Poethig, S., Roberts, K., et al. (1993). Cellular organisation of the *Arabidopsis thaliana* root. *Development* 119, 71–84.

Enstone, D. E., Peterson, C. A., and Ma, F. (2003). Root endodermis and exodermis: structure, function, and responses to the environment. *J. Plant Growth Regul.* 21, 335–351. doi: 10.1007/s00344-003-0002-2

FAO (2014). *Food and Agriculture Organization of the United Nations, FAOSTAT Database.* Available online at: http://faostat3.fao.org/home/E. Accessed 30 Oct 2016.

Fiers, M., Golemiec, E., Xu, J., Van Der Geest, L., Heidstra, R., Stiekema, W., et al. (2005). The 14 – Amino Acid CLV3 , CLE19 , and CLE40 peptides trigger consumption of the root meristem in Arabidopsis through a CLAVATA2 -dependent pathway. *Plant Cell* 17, 2542–2553. doi: 10.1105/tpc.105.034009.1

Fletcher, J. C., Brand, U., Running, M. P., Simon, R., and Meyerowitz, E. M. (1999). Signaling of cell fate decisions by CLAVATA3 in Arabidopsis shoot meristems. *Science* 283, 1911–1914. doi: 10.1126/science.283.5409.1911

Hackett, C. (1968). A study of the root system of barley- I. effects of nutrition on two varieties. *New Phytol.* 67, 287–299.

Hackett, C. (1969). A study of the root system of barley II. Relationships between root dimensions and nutrient uptake. *New Phytol.* 68, 1023–1030.

Hardtke, C. S., and Pacheco-Villalobos, D. (2015). "The Brachypodium distachyon Root System: A Tractable Model to Investigate Grass Roots," in *Genetics and Genomics of Brachypodium. Plant Genetics and Genomics: Crops and Models,* ed J. Vogel (Cham: Springer), 245–258.

Hejátko, J., Blilou, I., Brewer, P. B., Friml, J., Scheres, B., and Benkov,á, E. (2006). In situ hybridization technique for mRNA detection in whole mount Arabidopsis samples. *Nat. Protoc.* 1, 1939–1946. doi: 10.1038/nprot.2006.333

Henry, S., Divol, F., Bettembourg, M., Bureau, C., Guiderdoni, E., Périn, C., et al. (2016). Immunoprofiling of rice root cortex reveals two cortical subdomains. *Front. Plant Sci.* 6:1139. doi: 10.3389/fpls.2015.01139

Heyman, J., Kumpf, R. P., and De Veylder, L. (2014). A quiescent path to plant longevity. *Trends Cell Biol.* 24, 443–448. doi: 10.1016/j.tcb.2014.03.004

Hobe, M., Müller, R., Grünewald, M., Brand, U., and Simon, R. (2003). Loss of CLE40, a protein functionally equivalent to the stem cell restricting signal CLV3, enhances root waving in Arabidopsis. *Dev. Genes Evol.* 213, 371–381. doi: 10.1007/s00427-003-0329-5

Hochholdinger, F., Park, W. J., Sauer, M., and Woll, K. (2004a). From weeds to crops: genetic analysis of root development in cereals. *Trends Plant Sci.* 9, 42–48. doi: 10.1016/j.tplants.2003.11.003

Hochholdinger, F., Woll, K., Sauer, M., and Dembinsky, D. (2004b). Genetic dissection of root formation in maize (*Zea mays*) reveals root-type specific developmental programmes. *Ann. Bot.* 93, 359–368. doi: 10.1093/aob/mch056

Hong, J. H., Chu, H., Zhang, C., Ghosh, D., Gong, X., and Xu, J. (2015). A quantitative analysis of stem cell homeostasis in the Arabidopsis columella root cap. *Front. Plant Sci.* 6, 1–7. doi: 10.3389/fpls.2015.00206

Ivanov, V. B., and Dubrovsky, J. G. (2013). Longitudinal zonation pattern in plant roots: conflicts and solutions. *Trends Plant Sci.* 18, 237–243. doi: 10.1016/j.tplants.2012.10.002

Jackson, D. (1991). "*In-situ* hybridisation in plants," in *Molecular Plant Pathology: A Practical Approach,* eds S. J. Gurr, M. J. McPherson, and D. J. Bowles (Oxford: Oxford University Press), 163–174.

Jiang, K., and Feldman, L. J. (2005). Regulation of root apical meristem development. *Annu. Rev. Cell Dev. Biol.* 21, 485–509. doi: 10.1146/annurev.cellbio.21.122303.114753

Jiang, K., Meng, Y. L., and Feldman, L. J. (2003). Quiescent center formation in maize roots is associated with an auxin-regulated oxidizing environment. *Development* 130, 1429–1438. doi: 10.1242/dev.00359

Jiang, K., Zhu, T., Diao, Z., Huang, H., and Feldman, L. J. (2010). The maize root stem cell niche: a partnership between two sister cell populations. *Planta* 231, 411–424. doi: 10.1007/s00425-009-1059-3

Kerk, N., and Feldman, L. (1994). The quiescent center in roots of maize: initiation, maintenance and role in organization of the root apical meristem. *Protoplasma* 183, 100–106. doi: 10.1007/BF01276817

Kinoshita, A., Nakamura, Y., Sasaki, E., Kyozuka, J., Fukuda, H., and Sawa, S. (2007). Gain-of-function phenotypes of chemically synthetic CLAVATA3/ESR-Related (CLE) peptides in *Arabidopsis thaliana* and *Oryza sativa*. *Plant Cell Physiol.* 48, 1821–1825. doi: 10.1093/pcp/pcm154

Kiss, J. Z., Wright, J. B., and Caspar, T. (1996). Gravitropism in roots of intermediate-starch mutants of Arabidopsis. *Physiol. Plant* 97, 237–244. doi: 10.1034/j.1399-3054.1996.970205.x

Knipfer, T., and Fricke, W. (2011). Water uptake by seminal and adventitious roots in relation to whole-plant water flow in barley (*Hordeum vulgare* L.). *J. Exp. Bot.* 62, 717–733. doi: 10.1093/jxb/erq312

Kotogány, E., Dudits, D., Horváth, G. V., and Ayaydin, F. (2010). A rapid and robust assay for detection of S-phase cell cycle progression in plant cells and tissues by using ethynyl deoxyuridine. *Plant Methods* 6:5. doi: 10.1186/1746-4811-6-5

Lampropoulos, A., Sutikovic, Z., Wenzl, C., Maegele, I., Lohmann, J. U., and Forner, J. (2013). GreenGate - A novel, versatile, and efficient cloning system for plant transgenesis. *PLoS ONE* 8:83043. doi: 10.1371/journal.pone.0083043

Legland, D., Arganda-Carreras, I., and Andrey, P. (2016). MorphoLibJ: integrated library and plugins for mathematical morphology with ImageJ. *Bioinformatics* 32, 3532–3534. doi: 10.1093/bioinformatics/btw413

Lim, J., Helariutta, Y., Specht, C. D., Jung, J., Sims, L., Bruce, W. B., et al. (2000). Molecular analysis of the SCARECROW gene in maize reveals a common basis for radial patterning in diverse meristems. *Plant Cell* 12, 1307–1318. doi: 10.1105/tpc.12.8.1307

Lux, A., Morita, S., Abe, J., and Ito, K. (2005). An improved method for clearing and staining free-hand sections and whole-mount samples. *Ann. Bot.* 96, 989–996. doi: 10.1093/aob/mci266

Luxová, M. (1986). The Seminal Root Primordia in Barley and the Participation of their Non-Meristematic Cells in Root Construction. *Biol. Plant.* 28, 161–167. doi: 10.1007/BF02894591

Mayer, K. F. X., Waugh, R., Brown, J. W. S., Schulman, A., Langridge, P., Platzer, M., et al. (2012). A physical, genetic and functional sequence assembly of the barley genome. *Nature* 491, 711–716. doi: 10.1038/nature11543

Nawrath, C., Schreiber, L., Franke, R. B., Geldner, N., Reina-Pinto, J. J., and Kunst, L. (2013). Apoplastic diffusion barriers in Arabidopsis. *Arabidopsis Book* 11:e0167. doi: 10.1199/tab.0167

Ni, J., Shen, Y., Zhang, Y., and Wu, P. (2014). Definition and stabilisation of the quiescent centre in rice roots. *Plant Biol.* 16, 1014–1019. doi: 10.1111/plb.12138

Orman-Ligeza, B., Parizot, B., Gantet, P. P., Beeckman, T., Bennett, M. J., and Draye, X. (2013). Post-embryonic root organogenesis in cereals: branching out from model plants. *Trends Plant Sci.* 18, 459–467. doi: 10.1016/j.tplants.2013.04.010

Pallakies, H., and Simon, R. (2014). The CLE40 and CRN/CLV2 signaling pathways antagonistically control root meristem growth in Arabidopsis. *Mol. Plant* 7, 1619–1636. doi: 10.1093/mp/ssu094

Paquette, A. J., and Benfey, P. N. (2005). Maturation of the ground tissue of the root is regulated by Gibberellin and SCARECROW and requires SHORT-ROOT. *Plant Physiol.* 138, 636–640. doi: 10.1104/pp.104.058362

Pi, L., Aichinger, E., van der Graaff, E., Llavata-Peris, C. I., Weijers, D., Hennig, L., et al. (2015). Organizer-Derived WOX5 signal maintains root columella stem cells through chromatin-mediated repression of CDF4 EXPRESSION. *Develop. Cell* 33, 576–588. doi: 10.1016/j.devcel.2015.04.024

R Core Team (2015). *R: A Language and Environment for Statistical Computing*. Vienna: R Foundation for Statistical Computing.

Rebouillat, J., Dievart, A., Verdeil, J. L., Escoute, J., Giese, G., Breitler, J. C., et al. (2009). Molecular genetics of rice root development. *Rice* 2, 15–34. doi: 10.1007/s12284-008-9016-5

Ron, M., Dorrity, M. W., Lucas, M., De Toal, T., Hernandez, R. I., Little, S.A. et al. (2013). Identification of novel loci regulating interspecific variation in root morphology and cellular development in tomato. *Plant Physiol.* 162, 755–768. doi: 10.1104/pp.113.217802

Sarkar, A. K., Luijten, M., Miyashima, S., Lenhard, M., Hashimoto, T., Nakajima, K., et al. (2007). Conserved factors regulate signalling in *Arabidopsis thaliana* shoot and root stem cell organizers. *Nature* 446, 811–814. doi: 10.1038/nature05703

Schindelin, J., Arganda-Carreras, I., Frise, E., Kaynig, V., Longair, M., Pietzsch, T., et al. (2012). Fiji: an open-source platform for biological-image analysis. *Nat. Methods* 9, 676–682. doi: doi: 10.1038/nmeth.2019

Stahl, Y., Grabowski, S., Bleckmann, A., Kühnemuth, R., Weidtkamp-Peters, S., Pinto, K. G., et al. (2013). Moderation of Arabidopsis root stemness by CLAVATA1 and ARABIDOPSIS CRINKLY4 receptor kinase complexes. *Curr. Biol.* 23, 1–10. doi: 10.1016/j.cub.2013.01.045

Stahl, Y., Wink, R. H., Ingram, G. C., and Simon, R. (2009). A signaling module controlling the stem cell niche in Arabidopsis root meristems. *Curr. Biol.* 19, 909–914. doi: 10.1016/j.cub.2009.03.060

Suzaki, T., Toriba, T., Fujimoto, M., Tsutsumi, N., Kitano, H., and Hirano, H.-Y. (2006). Conservation and diversification of meristem maintenance mechanism in *Oryza sativa*: function of the FLORAL ORGAN NUMBER2 gene. *Plant Cell Physiol.* 47, 1591–1602. doi: 10.1093/pcp/pcl025

Suzaki, T., Yoshida, A., and Hirano, H.-Y. (2008). Functional diversification of CLAVATA3-related CLE proteins in meristem maintenance in rice. *Plant Cell* 20, 2049–2058. doi: 10.1105/tpc.107.057257

Truernit, E., Bauby, H., Dubreucq, B., Grandjean, O., Runions, J., Barthélémy, J., et al. (2008). High-resolution whole-mount imaging of three-dimensional tissue organization and gene expression enables the study of Phloem development and structure in Arabidopsis. *Plant Cell* 20, 1494–1503. doi: 10.1105/tpc.107.056069

van den Berg, C., Willemsen, V., Hendriks, G., Weisbeek, P., and Scheres, B. (1997). Short-range control of cell differentiation in the Arabidopsis root meristem. *Nature* 390, 287–289. doi: 10.1038/36856

Vanstraelen, M., Baloban, M., Da Ines, O., Cultrone, A., Lammens, T., Boudolf, V., et al. (2009). APC/C-CCS52A complexes control meristem maintenance in the Arabidopsis root. *Proc. Natl. Acad. Sci. U.S.A.* 106, 11806–11811. doi: 10.1073/pnas.0901193106

Wang, L., Chu, H., Li, Z., Wang, J., Li, J., Qiao, Y., et al. (2014). Origin and development of the root cap in rice. *Plant Physiol.* 166, 603–613. doi: 10.1104/pp.114.240929

Warner, C. A., Biedrzycki, M. L., Jacobs, S. S., Wisser, R. J., Caplan, J. L., and Sherrier, D. J. (2014). An optical clearing technique for plant tissues allowing deep imaging and compatible with fluorescence microscopy. *Plant Physiol.* 166, 1684–1687. doi: 10.1104/pp.114.244673

Conflict of Interest Statement: The authors declare that the research was conducted in the absence of any commercial or financial relationships that could be construed as a potential conflict of interest.

V. The Barley Root as a Model for Salinity and Drought Resistance

This chapter is a manuscript in preparation for submission.

Authors: Gwendolyn K. Kirschner[1], and Rüdiger Simon[1]

Affiliations:

[1]Institute for Developmental Genetics and Cluster of Excellence on Plant Sciences, Heinrich Heine University, Universitätsstr. 1, D-40225 Düsseldorf, Germany

Contributions:

The manuscript was written by Gwendolyn K. Kirschner with help from Rüdiger Simon.

1. Introduction

Plant growth and development is, among others, influenced by several different environmental factors. The roots, as below-ground organs, are especially exposed to abiotic factors originating from soil composition, and biotic factors in the root microbiota. Curiously, despite the obvious connection between plant biomass production and yield with root system architecture, hardly any research was conducted to understand the factors influencing barley root system development. Both for rice and barley, studies demonstrated that increased yield was directly correlated to the degree of root architectural plasticity (Sandhu et al., 2016; Chloupek et al., 2010; Streda et al., 2011). The correlation between root system architecture and yield might be due to a better drought tolerance and a better response to nutrient heterogeneity as summarized by Rogers and Benfey, 2015. On the other hand, there might be a genetic connection between shoot and root that is responsible for this correlation. Sandhu and colleagues found genomic loci in rice where grain yield and root architectural plasticity traits correlated (Sandhu et al., 2016). Thus, one hypothesis is that the high yield potential among rice genotypes with the highest degree of root architectural plasticity is linked to genetics rather than to functional tradeoffs. Accordingly, Naz and colleagues found that in barley, tiller number is positively correlated with root length, root dry weight and root volume and revealed chromosomal regions by quantitative trait locus (QTL) mapping where the introgression of wild barley alleles resulted in improved trait values in both root and shoot (Naz et al., 2014). Moreover, direct genetic interaction between the root and the shoot exist. Habte and colleagues found that osmotic stress in barley root alters the expression of circadian clock genes in the shoot, this photoperiodic regulation thereby also influences the flowering time and yield (Habte et al., 2014). But not only does root system size contribute to yield, the roots also help to stabilize the eco-system. Soil erosion by water is a serious environmental problem that results in on-site soil degradation and reducing the soil's productivity and water storage capacity. Roots prevent soil erosion by increasing the shear strength, physical retention of soil particles, addition of organic matter and alterations of the soil pore size. A high root length density would be favourable in this regard (Ola et al., 2015). In addition, it was suggested by Kell, 2011, that deeper roots would sequester more carbon from the atmosphere and would thus counter the increasing levels of CO_2 in the atmosphere (Kell, 2011).

In this review I want to give an overview about the state of research in barley roots in regard to the root system architecture and the root apical meristem. As barley ranks highly in regard to salt tolerance among the other cereal crop plants, achievements in barley root research might be transferred to other crop plants to improve their salt tolerance (Maas and Hoffman, 1977). Therefore, I will summarize the most important findings about the reaction of barley roots to salinity, and examples, where barley genes have already been successfully transferred to other plants.

2. Similarities to maize and rice root systems

The embryonic barley root system consists of two main root types, the primary and the seminal roots (Hackett, 1969; Luxová, 1986). In an early work, Luxová describes the root initiation: following germination of the barley seed, the coleorrhiza (root sheath) and the primary root primordium of the embryo elongate and, subsequently, the primordium breaks through the coleorrhiza and forms the primary root (Luxová, 1986) (Figure 1A). While the primary root primordium is initiated below the scutellar node close to the scutellum, further root primordia arise afterwards above the scutellar node in the mesocotyl, forming the seminal root system (Luxová, 1986). In contrast to that, Knipfer and colleagues do not describe the presence of a primary root in the cultivar (cv.) Golf, and also in the cv. Morex, no primary root could be distinguished on the basis of morphology (Knipfer and Fricke, 2011; Kirschner et al., 2017). The formation of a primary root might therefore only be observable at an embryonic scale and at very early growth stages or depending on the cultivar. The number of seminal roots of cultivars ranges from 5 – 7 , as described in Bengough et al., 2004; Grando & Ceccarelli, 1995; Hackett, 1968; Knipfer & Fricke, 2011; Luxová, 1986.

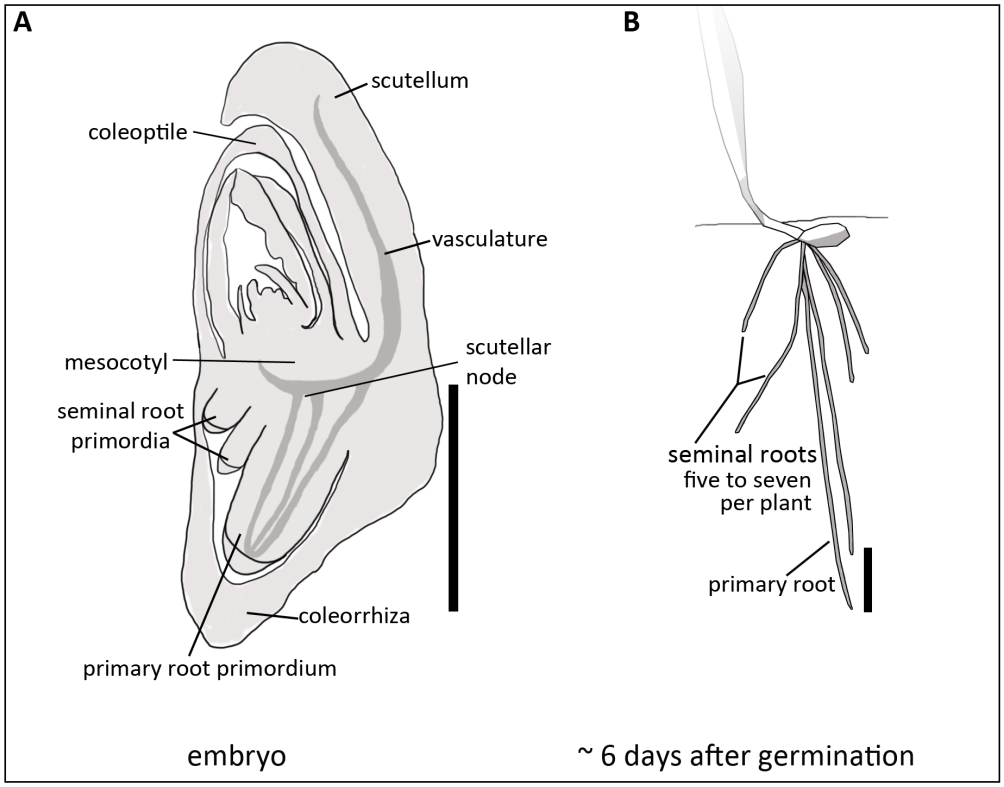

Figure 1: The root system of the barley embryo and the young barley plant.

A) The barley embryonic root system consists of the primary root primordium that is located close to the scutellum; primordia of seminal roots are initiated above the scutellar node; the root primordia are covered with the root sheat (coleorrhiza); scale bar 1 mm. **B)** The barley root system of a 6-day old seedling consists of 5-7 seminal roots and one primary root; scale bar 1 cm.

In contrast wild barley (*Hordeum spontaneum*) was described to exhibit 3 seminal roots on average (de Dorlodot et al., 2007; Grando and Ceccarelli, 1995; Bengough et al., 2004) (Figure 1B). In general, Grando and Ceccarelli found a correlation between seed weight and the number of seminal roots in cultivars and landraces (Grando and Ceccarelli, 1995). Two weeks after germination, lateral root development on the seminal roots can be observed (Hackett, 1969).

Besides the embryonic roots, monocots feature another root type: nodal roots, which include all postembryonic roots that arise during normal plant development, in particular the crown and the brace roots (Steffens and Rasmussen, 2016). Crown roots are formed at the lowermost belowground node ("crown"), while brace roots are formed at consecutive above-ground nodes of the shoots (Hochholdinger et al., 2004b). In barley, crown root formation can be observed depending on growth conditions and cultivar roughly 11 – 14 days after germination (Knipfer and Fricke, 2011; Hackett, 1969), or when 1 - 2 leaves have grown on the main stem (Wahbi, 1995).

Comparing the root systems of the major model plant species (*Arabidopsis thaliana*, rice, maize, *Brachypodium distachyon* and barley), it stands out that all plants exhibit a primary root, but only maize, rice and barley initiate seminal roots (Hochholdinger et al., 2004a; Coudert et al., 2010; Hardtke and Pacheco-Villalobos, 2015; Luxová, 1986; Schiefelbein and Benfey, 1991; Hackett, 1968; Wahbi, 1995; de Dorlodot et al., 2007; Knipfer and Fricke, 2011) (Figure 2). Crown root development is shared by all monocot model species, rice, maize, *Brachypodium* and barley, but only maize and *Brachypodium* are described to develop brace roots later in development (Figure 2) (Hochholdinger et al., 2004a; Coudert et al., 2010; Hardtke and Pacheco-Villalobos, 2015; Hackett, 1969; Knipfer and Fricke, 2011).

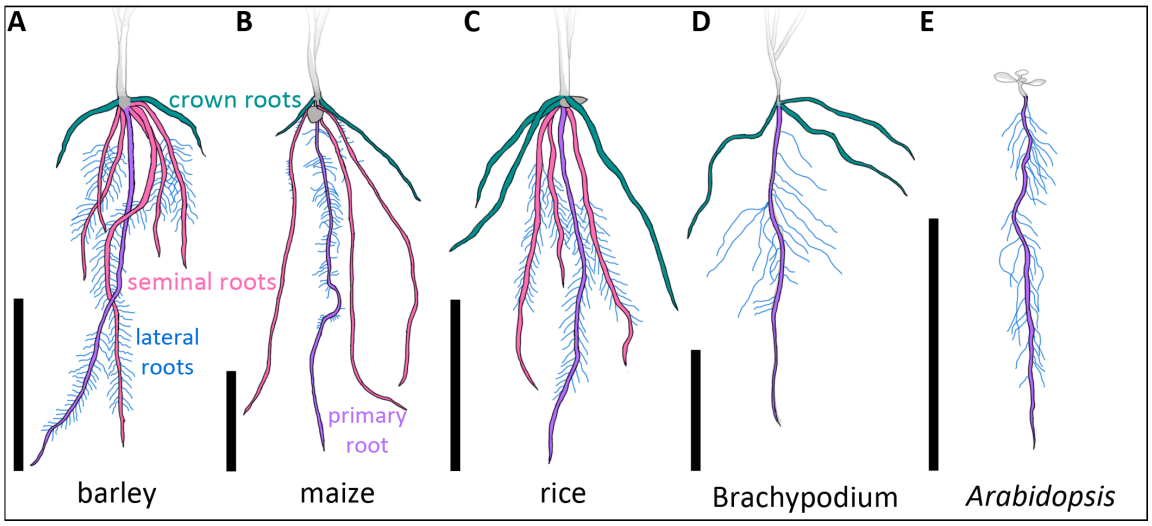

Figure 2: Schematic overview over the root systems of young barley, maize, rice, *Brachypodium* and *Arabidopsis* seedlings.

The young barley (**A)**, 14-day old seedling), maize (**B)**, 10-day-old seedling (Smith and De Smet, 2012)) and rice (**C)**, 14-day old seedling (Singh et al., 2016)) root system consists of the embryonic primary and the seminal roots, and shoot-borne crown roots; the *Brachypodium* (**D)**, 30-day old seedling (Pacheco-Villalobos and Hardtke, 2012)) and *Arabidopsis* (**E)**, 14-day old seedling (Smith and De Smet, 2012)) embryonic root system is formed by a primary root only; Brachypodium additionally develops crown roots; in the depicted developmental stages, the primary root and the seminal roots have initiated lateral roots; scale bars 5 cm.

These diverse root types have been shown to exhibit different functional specializations, as is reflected in their transcriptome, and results for instance in a different hydraulic conductivity (Knipfer and Fricke, 2011; Tai et al., 2016). The barley root system consists of the same root types as the two most important cereal crops, rice and maize. Therefore, barley represents an important plant for root research, as features of the barley root system can be translated to other cereal crop plants. Along with the fact that barley is the most salt-tolerant among the cereal crops, root research may especially contribute to this field (Maas and Hoffman, 1977). Examples of barley genes, which have already been used in cross-species approaches to improve salt and drought tolerance, are described below.

3. The transverse structure of the barley root

The root apex consists of different types of tissues that are radially arranged around the central cylinder. Four main tissue types can be distinguished in a transverse section of barley seminal roots, from the outside to the inside: one layer of epidermis, four to five cortical layers and one layer of endodermis which surrounds the central vascular tissue (Braszewska-Zalewska et al., 2013; Kirschner et al., 2017) (Figure 3). Under hydroponic growth conditions, no exodermis can be detected on the basis of suberine staining (Ranathunge et al., 2017). On the contrary, suberized casparian bands form in 2 mm distance from the root tip in the endodermis (Ranathunge et al., 2017). Crown roots differ in morphology and anatomy from seminal roots. They are 1.5- to 2-fold thicker than seminal roots and exhibit seven to eight cortical cell layers, 14 peripheral and 6 central metaxylem vessels, while seminal roots have one large

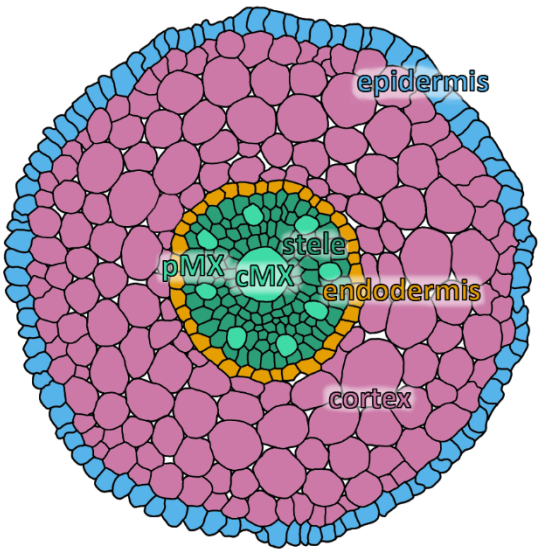

Figure 3: Schematic overview of the tissues in a barley seminal root (cross section).
In the barley seminal root, the vasculature contains eight peripheral metaxylem (pMX) vessels that are circular arranged around the central metaxylem (cMX); the vasculature is surrounded by the endodermis, four to five cortex cell layers and the epidermis.

central and eight smaller circularly arranged peripheral metaxylem vessels (Knipfer and Fricke, 2011). Furthermore, in seminal roots, the central metaxylem vessels become fully mature and the endodermis fully developed at 20 mm distance to the root tip, whereas in nodal roots maturation of the metaxylem occurs only at up to 60 mm from the tip (Knipfer and Fricke, 2011).

4. Unique features of the barley root apical meristem

Primary root growth is enabled by the root apical meristems that consist of small, rapidly dividing cells and harbour the stem cell niche. In general, root apical meristems can be divided on the basis of their cell arrangement into open and closed meristems. In closed meristems, the root cap can be clearly separated from the epidermis, the latter forming in the inner cell layer of the root cap. In open meristems, in contrast, cortex and root cap are of common origin and linkages between the epidermis and the root cap can be found (Clowes, 2000). Barley exhibits a closed meristem, which is typical for grasses (Clowes, 2000). The stem cell niche consists of stem cells surrounding a quiescent center (QC) that consists of cells with low cell-division activity (Clowes, 1984). The size of the QC was suggested to depend on the diameter of the root meristem, whereby roots with larger diameter have a larger QC (Clowes, 1984). The QC size of model plants ranges from 4 in *Arabidopsis* and rice, around 25 cells in *Brachypodium* to 800 – 1200 cells in maize (Dolan et al., 1993; Hardtke and Pacheco-Villalobos, 2015; Jiang et al., 2003; Ni et al., 2014). In an earlier study, we found that the barley QC consists of 20 – 30 cells (Figure 4) (Kirschner et al., 2017). In *Arabidopsis*, cell-ablation experiments revealed that the QC maintains the distal columella stem cells by short-range signals (van den Berg et al., 1997). It was furthermore hypothesized that the QC might act as source of cells that are protected from DNA damage by their low cell division rate and can replace adjacent stem cells (Cruz-Ramírez et al., 2013). This is supported by an earlier observation that distal QC cells from maize can regenerate the root cap, once it is mechanically damaged (Feldman, 1976). Detailled studies, however, are still lacking.

Just like the number of QC cells, the number of cortex cells also varies between different plant species, with one cortex cell layer in *Arabidopsis* (two, if the middle cortex is included), five in the seminal roots of rice, *Brachypodium* and barley and 8 – 15 in the seminal roots of maize (Hochholdinger et al., 2004b; Hardtke and Pacheco-Villalobos, 2015; Coudert et al., 2010; Kirschner et al., 2017; Paquette and Benfey, 2005; Dolan et al., 1993). As most plants have one single layer of endodermis and one single layer of epidermis, additionally to the number of stelar cells and the overall cell size, the number of cortex cell files determines the root diameter (Enstone et al., 2003). The hypothesis that the QC size is related to the root diameter, is therefore confirmed, with the exception of the rice QC (Clowes, 1984). A large QC might be needed as pool of DNA-damage free cells as replacement for more stem cells in roots with larger diameter, or the QC size is dictated by organizational reasons in regard to the cell arrangement.

The different number of cortex cell files among plant species implies a different cortex initiation mechanism. In *Arabidopsis*, cortex and endodermis share a common initial that is located lateral adjacent to the QC and creates a single endodermis and a single cortex cell file by periclinal division (Dolan et al., 1993). Later in development, a periclinal cell division of the cortex cells form the middle cortex (Paquette and Benfey, 2005). In *Brachypodium*, the cortex and the endodermis are produced by successive periclinal divisions of the endodermis-epidermis initial adjacent to the QC (Pacheco-Villalobos and Hardtke, 2012). In rice, the ground tissue stem cells laterally adjacent to the QC undergo an anticlinal cell division, and the daughter cell not abutting the QC divides periclinally several times to generate the single endodermis layer and the 5 cortex cell files (Ni et al., 2014). In barley, the cortex-endodermis initiation can be divided into the generation of the endodermis and the inner cortex by one common initial and the outer cortex by another initial, both initials located adjacent to the QC (Figure 4) (Kirschner et al., 2017). Studies with antibodies against cortical cell wall proteins in rice revealed two types of cortical tissue cells, the inner and outer cortex (Henry et al., 2016). Therefore, the formation of the inner and outer cortex in barley by different initials may also indicate a different cellular characteristic of inner and outer cortex here. So far, however, this has not been studied in detail. Moreover, clonal analysis to trace back the origin of cortex and endodermis in grasses are so far lacking. Cortex and endodermis formation was shown to depend among others on the transcription factor SHORT-ROOT (SHR). Expression of the monocot SHRs from rice and *Brachypodium* in *Arabidopsis* not only rescued the *Arabidopsis shr* mutant phenotype, but also produced supernumerary cortex cells files (Wu et al., 2014). Furthermore, the overexpression of the rice SHR and the *Arabidopsis* SHR in rice led to the formation of supernumerary cortex cells, indicating that the mechanism of cortex formation underlies the same genetic basics in monocts and dicots (Henry et al., 2017). Similar studies in barley have not been conducted so far.

Additionally to the formation of cortex and endodermis, the formation of the epidermis and lateral root cap is also different between the plant species, in particular between monocots and dicots. While in *Arabidopsis*, epidermis and lateral root cap share a common initial, in rice, maize and barley the root cap is clearly separated from the proximal meristem by a thick cell wall boundary called root cap junction (Dolan et al., 1993; Hochholdinger et al., 2004a; Kirschner et al., 2017; Wang et al., 2014). Both the presence of the root cap junction and the arrangement of cells indicate that, while in *Arabidopsis* the QC could replace the distal columella stem cells, the QC in monocots is completely separated from the root cap (Figure 4). A similar regulation of the columella stem cells by a negative feedback-loop between the QC and the differentiated columella cells like in *Arabidopsis* is therefore unlikely in monocots and could so far not be shown in barley (Stahl et al., 2009; Kirschner et al., 2017).

In summary, although the presence of the same tissue types and a similar structure among the root apical meristems of different plant species suggest a similar development, small but significant

variations exist, like the size of the QC, the generation of endodermis and cortex, and the presence of a root cap junction. These variations make a detailed research of root stem cell niches of different plant species necessary to find the universal underlying structures for root meristem development and maintenance.

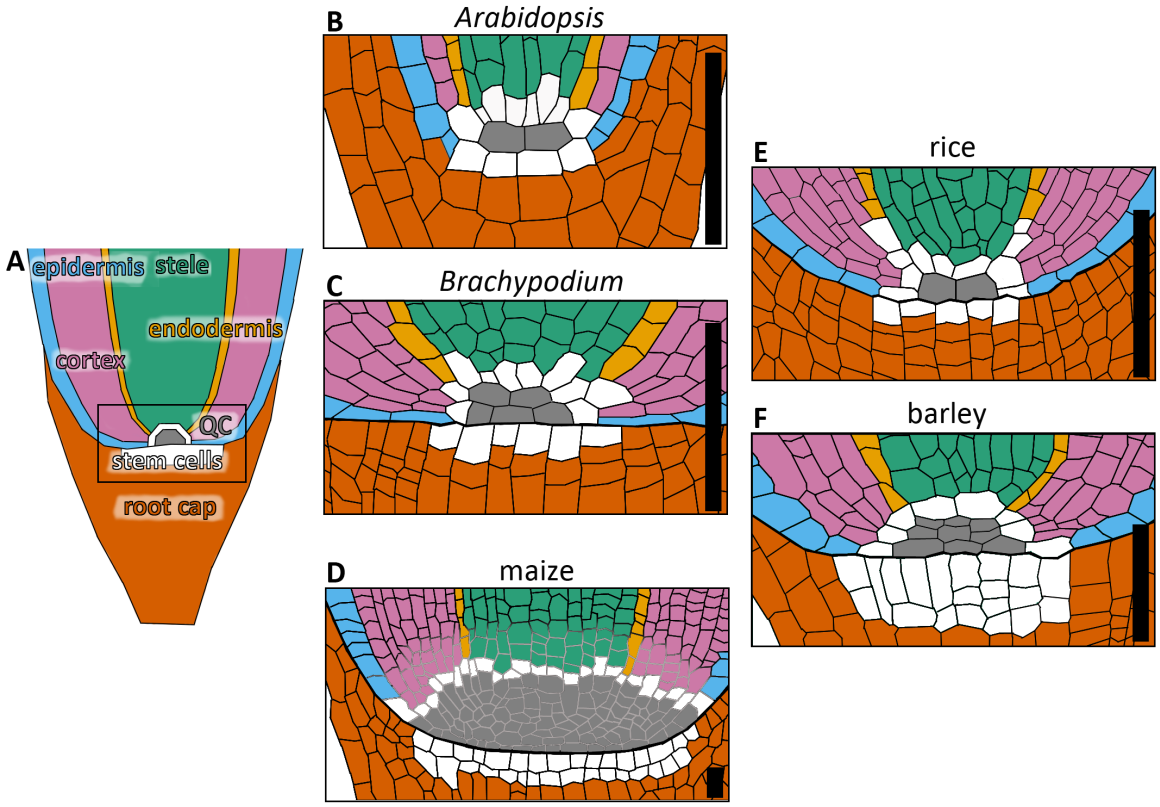

Figure 4: Schematic overview of the root meristem and the cell wall arrangement in the stem cell niches of *Arabidopsis*, *Brachypodium*, maize, rice and barley.
A) Schematic overview of root meristem structure; the QC is surrounded by stem cells that give rise to the different tissues. The stem cell niches of the main model plant species *Arabidopsis* (**B)**), *Brachypodium* (**C)**), maize (**D)**), rice (**E)**) and barley (**F)**) are similarly structured, but differ in some characteristics: the size of the QC ranges from 4 cells in *Arabidopsis* and rice to 800 – 1200 cells in maize; moreover, the formation of epidermis, cortex and endodermis varies; in *Arabidopsis*, the epidermis shares a common initial with the lateral root cap, and cortex and endodermis share another; as the monocot roots have a root cap junction that separates the proximal meristem including the QC from the root cap by a thick cell wall, the epidermis is here initiated separately from the root cap; in *Brachypodium*, epidermis, cortex and endodermis share the same initial; in rice, the cortex and endodermis are derived from the same initial independently of the epidermis; the latter applies to barley, but in regard to cortex and endodermis here, an initial gives rise to the inner cortex and the endodermis and another initial initiates the outer cortex; in maize, the cell division pattern of the epidermis, cortex and endodermis initiation has not yet been researched in detail (indicated by gray cell walls); scale bar 50 µm.

5. Lessons learned from barley in regard to salinity

Soil salinity has become an increasing problem in nowadays agriculture. High salt concentrations in the soil affect plants in many ways, the two major ones being: high salt concentrations decrease the ability of the roots to take up water from the soil. Second, high salinity can have toxic effects (reviewed in Munns et al., 2006). Maas and Hoffman compiled a list for crop plant salt tolerance, and ranked barley in first place as the most salt-tolerant crop species analyzed (including wheat and maize) in regard to the salt concentration tolerated until the yield decreases (Maas and Hoffman, 1977). Therefore, knowledge gained from barley root research in regard to salinity tolerance might be valuable to transfer to other monocot crops that are less salt-tolerant.

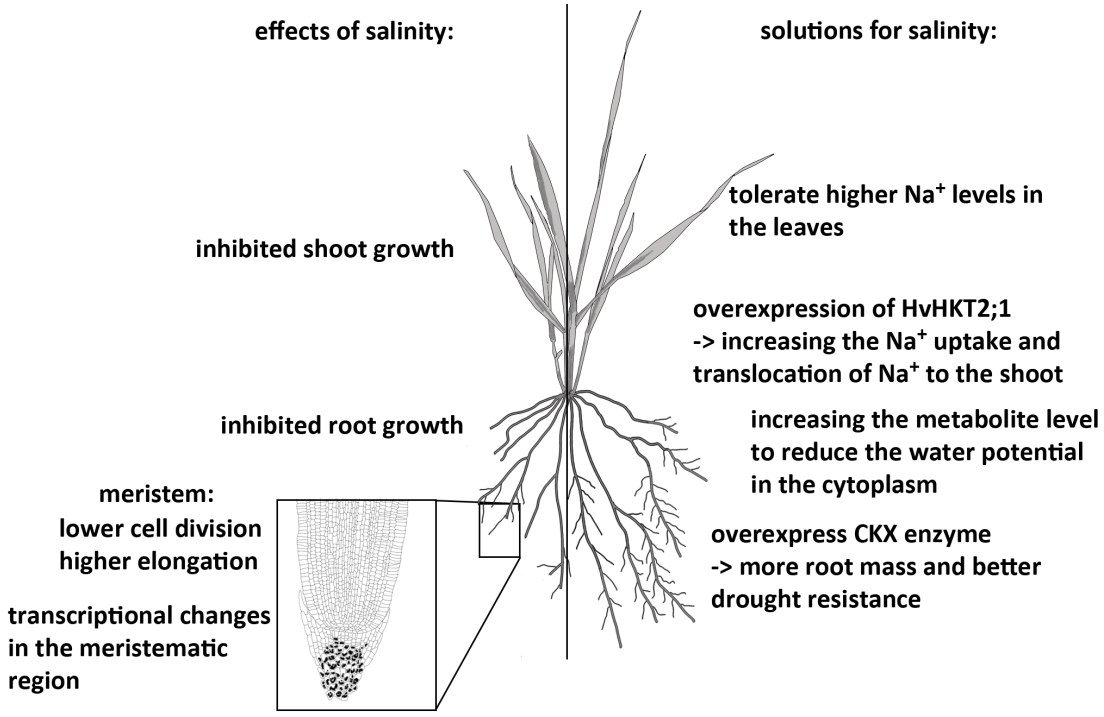

Figure 5: Influence of salt stress on barley plants and means to increase the salt tolerance.

5.1. Effects of salt stress on barley roots

Despite the high salt tolerance of barley, high salt concentrations still results in reduced root growth and less root biomass production (Horie et al., 2011; Bchini et al., 2010; Shelden et al., 2016). On a cellular level, salt stress causes inhibition of cell divisions in the procambium and in the root tip, and at the same time cause an increase in cell expansion in the elongation zone. However, this increase in cell size is not sufficient to compensate for the reduced number of cells, and hence overall root growth is inhibited (Figure 5) (Shelden et al., 2016). To reveal the genetic basics for these phenotypic changes, Hill and colleagues compared the transcriptome in distinct regions of the root, in particular the meristem, the elongation zone and the maturation zone in two barley cultivars with different levels of salt-tolerance, Clipper and Sahara. They found that the transcriptome in the meristematic region of

the more salt-susceptible cultivar exhibited more transcriptional changes in comparison to the more salt-tolerant cultivar (Figure 5) (Hill et al., 2016). Thus, the gene expression in the root meristem of the salt-tolerant cultivar seems to be less affected by salt stress, thereby being able to maintain the meristematic activity, and in this way the root growth, which helps to maintain a healthy plant under salt stress. Another way to cope with high salinity is to produce compatible solutes, small hydrophilic molecules which are not toxic at high concentrations but can contribute to reduce the water potential in the cytoplasm by outweighing the decreased water potential caused by the extracellular and vacuolar Na^+ accumulation. Widodo and colleagues compared the metabolome of two differently salt tolerant barley species upon drought stress and found that the more salt tolerant cultivar could cope better with high internal salt concentrations by either maintaining a higher K^+/Na^+ ratio in the cytoplasm through shifting Na^+ to the vacuole, or by increasing the metabolite levels to deal with the increased osmotic potential (Widodo et al., 2009). Furthermore, by comparing the proteome of two differently salt-tolerant barley cultivars upon salt stress, Witzel and colleagues found that one reason for higher salt tolerance might be the rapid up-regulation of proteins involved in proton and metal ion translocation in the salt-tolerant cultivar, so that a better Na^+ sequestration to the vacuole is enabled. Moreover, the induction of terpenoid biosynthetic proteins upon salt stress could result in an altered accumulation of structural sterols or sterol-derived hormones to cope with the salinity (Witzel et al., 2014).

5.2. Genetic engineering of barley towards an enhanced drought and salinity resistance

Changing the Na^+ translocation rate

The two main mechanisms of a plant's salt resistance are Na^+ exclusion, i.e. avoiding Na^+ uptake through the roots, or Na^+ inclusion, i.e. translocating Na^+ to the shoot where it is used as an osmoticum to decrease the water potential. Barley is considered a Na^+ includer (Glenn and Brown, 1999). Accordingly, Mian and colleagues were able the improve plant growth in the presence of high Na^+ concentrations by overexpression of HvHKT2;1, a high-affinity K^+ and Na^+ transporter for ion uptake, increasing the Na^+ uptake and at the same time the translocation of Na^+ to the shoot, and therefore reinforcing the includer behaviour of barley (Figure 5) (Mian et al., 2011).

Influencing cytokinin levels – a way to cope with drought and salinity

Drought and salt tolerance mechanisms in plants are highly intertwined, and maintaining a high root growth rate upon drought and high-salt conditions has been shown to be beneficial to both (Shelden et al., 2016). One approach to achieve this is to alter root cytokinin levels: Werner and colleagues demonstrated that reducing the cytokinin levels in *Arabidopsis* and tobacco can enhance root growth and the tolerance to drought without altering shoot growth (Werner et al., 2010). Means to change the cytokinin content in plants are the overexpression or silencing of key genes involved in cytokinin biosynthesis or degradation. The *ATP/ADP isopentenyltransferase* (*IPT*) genes encoding the rate-limiting enzymes in cytokinin biosynthesis, and the genes encoding CYTOKININ OXIDASE (CKX)

enzymes involved in cytokinin degradation are two examples for these key regulators. First studies on the silencing of *HvCKX1* in barley by RNA interference under the control of the Ubi1 intron promoter revealed that lower CKX enzyme activity leads to a higher number of seeds per plant, more grain filling and enhanced root growth (Zalewski et al., 2010). In contrast, silencing of *HvCKX2* in the same manner does not affect root weight and leads to reduced grain yield (Zalewski et al., 2012). An opposite approach was performed by Pospíšilová and colleagues who expressed the *Arabidopsis CKX1* (*AtCKX1*) under the weak root specific *β-glucosidase* promoter (*bGLU*) in barley and targeted the protein to different organelles, namely cytosol, apoplast and vacuoles (Pospíšilová et al., 2016). Despite the same decrease in cytokinin content in the roots of plants transformed with the different constructs, the plants exhibited a different root phenotype depending on the subcellular targeting. In general, the plants showed an increased tolerance to drought stress without negatively affecting yield, most likely due to a modification of root morphology and stronger lignification, which was supported by the finding that genes involved in lignin biosynthesis were up-regulated. Moreover, the overexpressing lines developed more lateral roots, together with an upregulation of auxin-response genes (Pospíšilová et al., 2016). Thus, the observed increase in the number of lateral roots could be explained by the effect of increased auxin response in pericycle cells for initiation of lateral root primordia. The altered root phenotype and the associated drought resistance in plants with reduced cytokinin levels might therefore be explained by an altered auxin signalling, as it was shown before that cytokinin and auxin signalling are highly interwoven (Ruzicka et al., 2009; Müller and Sheen, 2008). Overall, modifiying cytokinin levels in barley roots is one way to enhance the plant's tolerance to drought stress.

Applications in other plants - examples

Transgenic approaches in which genes from one plant species are transferred to another, are an useful approach to improve a plant's ability to cope with abiotic stresses. For example, the late embryogenesis abundant protein HVA1 from barley was successfully used in transgenic approaches in rice, wheat and maize to increase the tolerance to drought and salt stress when overexpressed (Xu et al., 1996; Nguyen et al., 2013; Chen et al., 2015; Sivamani et al., 2000). Babu and colleagues suggested that HVA1 conferred drought resistance in rice through cell membrane protection, i.e. protect the plasma membrane integrity and avoid electrolyte leakage from damaged tissues (Babu et al., 2004). Chen and colleagues found in a follow-up study that the increase in root growth in the HVA1 transgenic rice lines is caused by enhancement of lateral root initiation and elongation in an auxin-dependant manner (Chen et al., 2015). They furthermore suggest that the transgenic lines might have a greater water-holding capacity and higher relative water content in their leaves, and therefore are able to maintain photosynthesis and metabolic functions under stress conditions (Chen et al., 2015). In another approach, the calcium-activated protein calcineurin B-like protein CBL8, which perceives the second messenger $Ca2^{+}$, was cloned from a wild barley *Hordeum spontanum* line with

high salt tolerance. CBL8 overexpression in rice leads to increased salt tolerance by enhancing the plasma membrane protection and lower Na^+ uptake (Guo et al., 2016). Moreover, the CBL-interacting protein kinase CIPK2, a serine-threonine kinase which in complex with CBL is activated and regulates the expression and activity of downstream targets, was isolated from the halophytic grass *Hordeum brevisubulatum*. In *Arabidopsis*, overexpression of CIPK2 confers improved salt tolerance, probably by regulating the Na^+ transporter activity, but also of a K^+ transporter and thereby maintaining K^+/Na^+ homeostasis (Li et al., 2012).

In summary, the data compiled here demonstrate how some salt tolerance mechanisms of barley have already been successfully transferred to other plants to enhance their salt-tolerance.

6. Open questions in barley root science

Tamás and colleagues expressed the idea that growth inhibition in response to different abiotic stresses is a consequence of reduced cell division and elongation, as well as an alteration of cell differentiation (Tamás et al., 2010). Their experiments suggested that these changes might be associated with production of reactive oxygen species and an alteration in phytohormone levels, as the root growth inhibition and increased reactive oxygen species production were triggered by all abiotic stresses applied to the plants. As abiotic stresses are mostly sensed first by the plant's roots, the reaction of the roots should be investigated on a cellular level in regard to cell division, the creation of reactive oxygen species and phytohormone production and signalling. Except for the above-mentioned change in the cytokinin-levels that successfully altered the root structure towards drought resistance, the signalling of other phytohormones has not been studied sufficiently in barley so far. For example, a role for abscisic acid (ABA) in regulating water uptake by changing the aquaporin expression or changing the root hydraulic conductivity has previously been shown for maize (Parent et al., 2009). In barley, Sharipova and colleagues found that the barley mutant Az34, that exhibits lower ABA levels in all major tissues located along the radial path of water movement across roots, has decreased root hydraulic conductivity, most likely caused by a shorter root hair zone. In contrast exogenous application of ABA increases both root and root cell hydraulic conductivity caused by an increased abundance and activity of some aquaporines in root cortex cells (Sharipova et al., 2016). Also in regard to the important phytohormone auxin, there are only early studies on its effect on barley roots. Tagliani and colleagues found in connection to a study about an agravitropic mutant, that different auxins applied exogenously to barley seedlings inhibit root elongation (Tagliani et al., 1986). Besides phytohormone signalling, the gravitropism of roots is an interesting trait to focus on when it comes to drought or other abiotic factors, as for example a deeper rooting system allows a better uptake of deep-soil water (reviewed in Lynch and Wojciechowski, 2015). In rice, the *DEEPER ROOTING1* gene controls the root growth angle and introduction of the gene into a rice cultivar with a shallow root system increases its drought resistance (Uga et al., 2013). No similar gene has been identified in barley

yet, although in an early study Moore compared a graviresponse barley cultivar with a non-graviresponse mutant (Moore, 1985). Tagliani and colleagues further analysed the root growth of the non-graviresponse mutant and showed that the mutant exhibits more root elongation, probably to a disruption in auxin sensing (Tagliani et al., 1986). Further analyses of root mutants or quantitative trait loci-analysis of cultivars with varying root gravitropism are still lacking in barley but would provide a good tool for the crop science for the future.

7. References

Babu, R.C., Zhang, J., Blum, A., Ho, T.H.D., Wu, R., and Nguyen, H.T. (2004). HVA1, a LEA gene from barley confers dehydration tolerance in transgenic rice (Oryza sativa L.) via cell membrane protection. Plant Sci. **166**: 855–862.

Bchini, H., Naceur, M. Ben, Sayar, R., Khemira, H., and Kaab-Bettaeïb, L. Ben (2010). Genotypic differences in root and shoot growth of barley (Hordeum vulgare L.) grown under different salinity levels. Hereditas **147**: 114–122.

Bengough, A.G., Gordon, D.C., Al-Menaie, H., Ellis, R.P., Allan, D., Keith, R., Thomas, W.T.B., and Forster, B.P. (2004). Gel observation chamber for rapid screening of root traits in cereal seedlings. Plant Soil **262**: 63–70.

van den Berg, C., Willemsen, V., Hendriks, G., Weisbeek, P., and Scheres, B. (1997). Short-range control of cell differentiation in the Arabidopsis root meristem. Nature **390**: 287–289.

Braszewska-Zalewska, A.J., Wolny, E. a, Smialek, L., and Hasterok, R. (2013). Tissue-specific epigenetic modifications in root apical meristem cells of Hordeum vulgare. PLoS One **8**: e69204.

Chen, Y.S., Lo, S.F., Sun, P.K., Lu, C.A., Ho, T.H.D., and Yu, S.M. (2015). A late embryogenesis abundant protein HVA1 regulated by an inducible promoter enhances root growth and abiotic stress tolerance in rice without yield penalty. Plant Biotechnol. J. **13**: 105–116.

Chloupek, O., Dostl, V., Streda, T., Psota, V., and Dvorackova, O. (2010). Drought tolerance of barley varieties in relation to their root system size. Plant Breed. **129**: 630–636.

Clowes, F.A.L. (2000). Pattern in root meristem development in angiosperms. New Phytol. **146**: 83–94.

Clowes, F.A.L. (1984). Size And Activity Of Quiescent Centres Of Roots. New Phytol. **96**: 13–21.

Coudert, Y., Périn, C., Courtois, B., Khong, N.G., and Gantet, P. (2010). Genetic control of root development in rice, the model cereal. Trends Plant Sci. **15**: 219–26.

Cruz-Ramírez, A., Díaz-Triviño, S., Wachsman, G., Du, Y., Arteága-Vázquez, M., Zhang, H., Benjamins, R., Blilou, I., Neef, A.B., Chandler, V., and Scheres, B. (2013). A SCARECROW-RETINOBLASTOMA Protein Network Controls Protective Quiescence in the Arabidopsis Root Stem Cell Organizer. PLoS Biol. **11**.

Dolan, L., Janmaat, K., Willemsen, V., Linstead, P., Poethig, S., Roberts, K., and Scheres, B. (1993). Cellular organisation of the Arabidopsis thaliana root. Development **119**: 71–84.

de Dorlodot, S., Forster, B., Pagès, L., Price, A., Tuberosa, R., and Draye, X. (2007). Root system architecture: opportunities and constraints for genetic improvement of crops. Trends Plant Sci. **12**: 474–81.

Enstone, D.E., Peterson, C.A., and Ma, F. (2003). Root Endodermis and Exodermis: Structure, Function, and Responses to the Environment. J. Plant Growth Regul. **21**: 335–351.

Feldman, L.J. (1976). The de novo Origin of the Quiescent Center Regenerating Root Apices of Zea mays. Planta **128**: 207–212.

Glenn, E. and Brown, J.J. (1999). Salt Tolerance and Crop Potential of Halophytes. CRC. Crit. Rev. Plant Sci. **18**: 227–255.

Grando, S. and Ceccarelli, S. (1995). Seminal root morphology and coleoptile length in wild (Hordeum vulgare ssp. spontaneum) and cultivated (Hordeum vulgare ssp. vulgare) barley. Euphytica **86**: 73–80.

Guo, W., Chen, T., Hussain, N., Zhang, G., and Jiang, L. (2016). Characterization of Salinity Tolerance of Transgenic Rice Lines Harboring HsCBL8 of Wild Barley (Hordeum spontanum) Line from Qinghai-Tibet Plateau. Front. Plant Sci. **7**: 1–16.

Habte, E., Müller, L.M., Shtaya, M., Davis, S.J., and Von Korff, M. (2014). Osmotic stress at the barley root affects expression of circadian clock genes in the shoot. Plant, Cell Environ. **37**: 1321–1337.

Hackett, C. (1968). A study of the root system of barley I. effects of nutrition on two varieties. New Phytol. **67**: 287–299.

Hackett, C. (1969). A study of the root system of barley II. Relationships between root dimensions and nutrient uptake. New Phytol. **68**: 1023–1030.

Hardtke, C.S. and Pacheco-Villalobos, D. (2015). The Brachypodium distachyon Root System: A Tractable Model to Investigate Grass Roots. In Genetics and Genomics of Brachypodium, pp. 245–258.

Henry, S., Dievart, A., Fanchon, D., Pauluzzi, G., Meynard, D., Swarup, R., Wu, S., Lee, C.M., Gallagher, K., and Périn, C. (2017). SHR overexpression induces the formation of supernumerary cell layers with cortex cell identity in rice. Dev. Biol. **425**: 1–7.

Henry, S., Divol, F., Bettembourg, M., Bureau, C., Guiderdoni, E., Périn, C., and Diévart, A. (2016). Immunoprofiling of Rice Root Cortex Reveals Two Cortical Subdomains. Front. Plant Sci. **6**: 1139.

Hill, C.B., Cassin, A., Keeble-Gagnère, G., Doblin, M.S., Bacic, A., and Roessner, U. (2016). De novo transcriptome assembly and analysis of differentially expressed genes of two barley genotypes reveal root-zone-specific responses to salt exposure. Sci. Rep. **6**: 31558.

Hochholdinger, F., Park, W.J., Sauer, M., and Woll, K. (2004a). From weeds to crops: genetic analysis of root development in cereals. Trends Plant Sci. **9**: 42–48.

Hochholdinger, F., Woll, K., Sauer, M., and Dembinsky, D. (2004b). Genetic Dissection of Root Formation in Maize (Zea mays) Reveals Root-type Specific Developmental Programmes. Ann. Bot. **93**: 359–368.

Horie, T., Kaneko, T., Sugimoto, G., Sasano, S., Panda, S.K., Shibasaka, M., and Katsuhara, M. (2011). Mechanisms of Water Transport Mediated by PIP Aquaporins and Their Regulation Via Phosphorylation Events Under Salinity Stress in Barley Roots. Plant Cell Physiol. **52**: 663–675.

Jiang, K., Meng, Y.L., and Feldman, L.J. (2003). Quiescent center formation in maize roots is associated with an auxin-regulated oxidizing environment. Development **130**: 1429–1438.

Kell, D.B. (2011). Breeding crop plants with deep roots: their role in sustainable carbon, nutrient and water sequestration. Ann. Bot. **108**: 407–18.

Kirschner, G.K., Stahl, Y., Von Korff, M., and Simon, R. (2017). Unique and Conserved Features of the Barley Root Meristem. Front. Plant Sci. **8:** 1240.

Knipfer, T. and Fricke, W. (2011). Water uptake by seminal and adventitious roots in relation to whole-plant water flow in barley (Hordeum vulgare L.). J. Exp. Bot. **62**: 717–733.

Li, R., Zhang, J., Wu, G., Wang, H., Chen, Y., and Wei, J. (2012). HbCIPK2, a novel CBL-interacting protein kinase from halophyte Hordeum brevisubulatum, confers salt and osmotic stress tolerance. Plant, Cell Environ. **35**: 1582–1600.

Luxová, M. (1986). The Seminal Root Primordia in Barley and the Participation of their Non-Meristematic Cells in Root Construction. Biol. Plantarium **28**: 161–167.

Lynch, J.P. and Wojciechowski, T. (2015). Opportunities and challenges in the subsoil: Pathways to deeper rooted crops. J. Exp. Bot. **66**: 2199–2210.

Maas, E.V. and Hoffman, G.J. (1977). Crop salt tolerance - current assessment. J. Irrig. Drain. Div. **103**: 115–134.

Mian, A., Oomen, R.J.F.J., Isayenkov, S., Sentenac, H., Maathuis, F.J.M., and Véry, A.A. (2011). Over-expression of an Na^+- and K^+-permeable HKT transporter in barley improves salt tolerance. Plant J. **68**: 468–479.

Moore, R. (1985). A morphometric analysis of the redistribution of organelles in columella cells in primary roots of normal seedlings and agravitropic mutants of Hordeum vulgare. J. Exp. Bot. **36**: 1275–86.

Müller, B. and Sheen, J. (2008). Cytokinin and auxin interaction in root stem-cell specification during early embryogenesis. Nature **453**: 1094–7.

Munns, R., James, R.A., and Läuchli, A. (2006). Approaches to increasing the salt tolerance of wheat and other cereals. J. Exp. Bot. **57**: 1025–1043.

Naz, A.A., Arifuzzaman, M., Muzammil, S., Pillen, K., and Léon, J. (2014). Wild barley introgression lines revealed novel QTL alleles for root and related shoot traits in the cultivated barley (Hordeum vulgare L.). BMC Genet. **15**: 107.

Nguyen, T.X., Nguyen, T., Alameldin, H., Goheen, B., Loescher, W., and Sticklen, M. (2013). Transgene Pyramiding of the HVA1 and mtlD in T3 Maize (Zea mays L.) Plants Confers Drought and Salt Tolerance, along with an Increase in Crop Biomass. Int. J. Agron.: 1–10.

Ni, J., Shen, Y., Zhang, Y., and Wu, P. (2014). Definition and stabilisation of the quiescent centre in rice roots. Plant Biol. **16**: 1014–1019.

Ola, A., Dodd, I.C., and Quinton, J.N. (2015). Can we manipulate root system architecture to control soil erosion? SOIL Discuss. **2**: 603–612.

Pacheco-Villalobos, D. and Hardtke, C.S. (2012). Natural genetic variation of root system architecture from Arabidopsis to Brachypodium: towards adaptive value. Philos. Trans. R. Soc. B Biol. Sci. **367**: 1552–1558.

Paquette, A.J. and Benfey, P.N. (2005). Maturation of the Ground Tissue of the Root Is Regulated by Gibberellin and SCARECROW and Requires SHORT-ROOT. Plant Physiol. **138**: 636–640.

Parent, B., Hachez, C., Redondo, E., Simonneau, T., Chaumont, F., and Tardieu, F. (2009). Drought and Abscisic Acid Effects on Aquaporin Content Translate into Changes in Hydraulic Conductivity and Leaf Growth Rate: A Trans-Scale Approach. Plant Physiol. **149**: 2000–2012.

Pospíšilová, H., Jiskrová, E., Vojta, P., Mrízová, K., Kokáš, F., Čudejková, M.M., Bergougnoux, V., Plíhal, O., Klimešová, J., Novák, O., Dzurová, L., Frébort, I., and Galuszka, P. (2016).

Transgenic barley overexpressing a cytokinin dehydrogenase gene shows greater tolerance to drought stress. N. Biotechnol. **33**: 692–705.

Ranathunge, K., Kim, Y.X., Wassmann, F., Kreszies, T., Zeisler, V., and Schreiber, L. (2017). The composite water and solute transport of barley (Hordeum vulgare) roots: effect of suberized barriers. Ann. Bot. **119**: 629–643.

Rogers, E.D. and Benfey, P.N. (2015). Regulation of plant root system architecture: implications for crop advancement. Curr. Opin. Biotechnol. **32**: 93–98.

Ruzicka, K., Simásková, M., Duclercq, J., Petrásek, J., Zazímalová, E., Simon, S., Friml, J., Van Montagu, M.C.E., and Benková, E. (2009). Cytokinin regulates root meristem activity via modulation of the polar auxin transport. Proc. Natl. Acad. Sci. U. S. A. **106**: 4284–9.

Sandhu, N., Raman, K.A., Torres, R.O., Audebert, A., Dardou, A., Kumar, A., and Henry, A. (2016). Rice root architectural plasticity traits and genetic regions for adaptability to variable cultivation and stress conditions. Plant Physiol. **174**: pp.00705.2016.

Schiefelbein, J.W. and Benfey, P.N. (1991). The Development of Plant Roots: New Approaches to Underground Problems. Plant Cell **3**: 1147–1154.

Sharipova, G., Veselov, D., Kudoyarova, G., Fricke, W., Dodd, I.C., Katsuhara, M., Furuichi, T., Ivanov, I., and Veselov, S. (2016). Exogenous application of abscisic acid (ABA) increases root and cell hydraulic conductivity and abundance of some aquaporin isoforms in the ABA-deficient barley mutant Az34. Ann. Bot. **118**: 777–785.

Shelden, M.C., Dias, D.A., Jayasinghe, N.S., Bacic, A., and Roessner, U. (2016). Root spatial metabolite profiling of two genotypes of barley (Hordeum vulgare L.) reveals differences in response to short-term salt stress. J. Exp. Bot. **67**: 3731–45.

Singh, A., Kumar, P., Gautam, V., Rengasamy, B., Adhikari, B., Udayakumar, M., and Sarkar, A.K. (2016). Root transcriptome of two contrasting indica rice cultivars uncovers regulators of root development and physiological responses. Sci. Rep. **6**: 39266.

Sivamani, E., Bahieldin, A., Wraith, J.M., Al-Niemi, T., Dyer, W.E., Ho, T.H.D., and Qu, R. (2000). Improved biomass productivity and water use efficiency under water deficit conditions in transgenic wheat constitutively expressing the barley HVA1 gene. Plant Sci. **155**: 1–9.

Smith, S. and De Smet, I. (2012). Root system architecture: insights from Arabidopsis and cereal crops. Philos. Trans. R. Soc. B Biol. Sci. **367**: 1441–1452.

Stahl, Y., Wink, R.H., Ingram, G.C., and Simon, R. (2009). A Signaling Module Controlling the Stem Cell Niche in Arabidopsis Root Meristems. Curr. Biol. **19**: 909–914.

Steffens, B. and Rasmussen, A. (2016). The Physiology of Adventitious Roots. Plant Physiol. **170**: 603–617.

Streda, T., Dostal, V., Hajzler, M., and Chloupek, O. (2011). Yield and quality of spring barley in relation to root system size. 61. Tagung der Vereinigung der Pflanzenzüchter und Saatgutkaufleute Österreichs: 167–170.

Tagliani, L., Nissen, S., and Blake, T.K. (1986). Comparison of Growth, Exogenous Auxin Sensitivity, and Endogenous Indole-3-Acetic Acid Content in Roots of Hordeum vulgare L. and an Agravitropic Mutant. Biochem. Genet. **24**: 839–848.

Tai, H., Lu, X., Opitz, N., Marcon, C., Paschold, A., Lithio, A., Nettleton, D., and Hochholdinger, F. (2016). Transcriptomic and anatomical complexity of primary, seminal, and crown roots highlight root type-specific functional diversity in maize (Zea mays L.). J. Exp. Bot. **67**: 1123–1135.

Tamás, L., Mistrík, I., Huttová, J., Halušková, L., Valentovičová, K., and Zelinová, V. (2010). Role of reactive oxygen species-generating enzymes and hydrogen peroxide during cadmium, mercury and osmotic stresses in barley root tip. Planta **231**: 221–231.

Uga, Y., Sugimoto, K., Ogawa, S., Rane, J., Ishitani, M., Hara, N., Kitomi, Y., Inukai, Y., Ono, K., Kanno, N., Inoue, H., Takehisa, H., Motoyama, R., Nagamura, Y., Wu, J., Matsumoto, T., Takai, T., Okuno, K., and Yano, M. (2013). Control of root system architecture by DEEPER ROOTING 1 increases rice yield under drought conditions. Nat. Genet. **45**: 1097–102.

Wahbi, A. (1995). Growth and Development of Young Roots of Barley (Hordeum vulgare L.) Genotypes. Ann. Bot. **75**: 533–539.

Wang, L., Chu, H., Li, Z., Wang, J., Li, J., Qiao, Y., Fu, Y., Mou, T., Chen, C., and Xu, J. (2014). Origin and Development of the Root Cap in Rice. PLANT Physiol. **166**: 603–613.

Werner, T., Nehnevajova, E., Köllmer, I., Novák, O., Strnad, M., Krämer, U., and Schmülling, T. (2010). Root-Specific Reduction of Cytokinin Causes Enhanced Root Growth, Drought Tolerance, and Leaf Mineral Enrichment in Arabidopsis and Tobacco. Plant Cell **22**: 3905–3920.

Widodo, Patterson, J.H., Newbigin, E., Tester, M., Bacic, A., and Roessner, U. (2009). Metabolic responses to salt stress of barley (Hordeum vulgare L.) cultivars, Sahara and Clipper, which differ in salinity tolerance. J. Exp. Bot. **60**: 4089–4103.

Witzel, K., Matros, A., Strickert, M., Kaspar, S., Peukert, M., Mühling, K.H., Börner, A., and Mock, H.-P. (2014). Salinity Stress in Roots of Contrasting Barley Genotypes Reveals Time-Distinct and Genotype-Specific Patterns for Defined Proteins. Mol. Plant **7**: 336–355.

Wu, S., Lee, C.-M., Hayashi, T., Price, S., Divol, F., Henry, S., Pauluzzi, G., Perin, C., and Gallagher, K.L. (2014). A plausible mechanism, based upon SHORT-ROOT movement, for regulating the number of cortex cell layers in roots. Proc. Natl. Acad. Sci. **111**: 16184–16189.

Xu, D., Duan, X., Wang, B., Hong, B., Ho, T., and Wu, R. (1996). Expression of a Late Embryogenesis Abundant Protein Gene, HVA1, from Barley Confers Tolerance to Water Deficit and Salt Stress in Transgenic Rice. Plant Physiol. **110**: 249–257.

Zalewski, W., Galuszka, P., Gasparis, S., Orczyk, W., and Nadolska-Orczyk, A. (2010). Silencing of the HvCKX1 gene decreases the cytokinin oxidase/dehydrogenase level in barley and leads to higher plant productivity. J. Exp. Bot. **61**: 1839–51.

Zalewski, W., Orczyk, W., Gasparis, S., and Nadolska-Orczyk, A. (2012). HvCKX2 gene silencing by biolistic or Agrobacterium-mediated transformation in barley leads to different phenotypes. BMC Plant Biol. **12**: 206.

VI. Role of Auxin and Cytokinin in Barley Root Growth and Root Meristem Maintenance

This chapter is a manuscript in preparation for submission.

Authors:

Gwendolyn K. Kirschner[1], Yvonne Stahl[1], Jafargholi Imani[2], Maria von Korff Schmising[3] and Rüdiger Simon[1]

Affiliations:

[1]Institute for Developmental Genetics and Cluster of Excellence on Plant Sciences, Heinrich Heine University, Universitätsstr. 1, D-40225 Düsseldorf, Germany

[2]Research Centre for BioSystems, Land Use and Nutrition (IFZ), Justus Liebig University, Institute of Phytopathology and Applied Zoology, Heinrich-Buff-Ring 26-32, D-35392 Giessen, Germany

[3]Institute for Plant Genetics, Heinrich Heine University Düsseldorf, c/o Department of Plant Developmental Biology, Max Planck Institute for Plant Breeding Research, Carl-von-Linné-Weg 10, D-50829 Köln

Contributions:

The experiments were designed by Gwendolyn K. Kirschner, Yvonne Stahl, Maria von Korff Schmising and Rüdiger Simon. Molecular biology, plant work and microscopy were conducted by Gwendolyn Kirschner. Barley transformation was conducted in the group of Jafargholi Imani. The manuscript was written by Gwendolyn Kirschner with help from Yvonne Stahl and Rüdiger Simon.

1. Introduction

How phytohormones like auxin and cytokinin control root growth of plants is still an unresolved question. While the influence of the phytohormones on root growth is well analysed in the model dicot *Arabidopsis thaliana*, it is studied in monocot crop plants only to a little extent. In general, primary root growth in plants is enabled by root meristems at the tip of the roots, which harbour the stem cell niche and contribute to longitudinal root growth by their continuous cell division activity. The stem cell niche is located at the distal end of the root meristems above the root tip. In general, the root stem cell niche consists of the quiescent center (QC), cells with low mitotic activity, and the stem cells which surround the QC. The stem cells divide and their descendants differentiate to form all different root tissues, namely the proximal epidermis, cortex, endodermis and stele, and the distal root cap (columella and lateral root cap) (Clowes, 1978; Dolan et al., 1993; Ni et al., 2014). The cells that are displaced from the meristem in proximal direction first undergo several rounds of cell division, before they exit the meristematic transition zone to expand in size in the elongation zone and then differentiate in the differentiation zone. Following germination, the number of meristematic cells increases until a balance between cell division in the meristem and cell elongation and differentiation is reached and the meristem maintains a stable size (Ioio et al., 2008; Kirschner et al., 2017).

Genetic, molecular and environmental factors all contribute to control meristem size, stem cell niche formation and hence root growth. Two important regulators are the phytohormones auxin and cytokinin. Biosynthesis of auxin occurs in young aerial tissues and the phytohormone is then transported towards the roots via the mature phloem over long distances, whereas for short distances it is transported from cell to cell (reviewed in Saini et al., 2013). In the roots, an auxin maximum is formed in the columella initials (distal stem cells, DSCs), in the QC and in differentiated columella cells (Aida et al., 2004; Sabatini et al., 1999). This specific distribution is essential for root meristem patterning (Sabatini et al., 1999; Blilou et al., 2005). Accordingly, fine-tuned short-distance auxin transport is necessary. In *Arabidopsis,* the PINFORMED (PIN) proteins serve as auxin efflux carriers to establish a directional auxin flow to maintain the auxin maximum in the root tip (reviewed in Křeček et al., 2009). The different PINs are expressed in specific, partially overlapping domains within the root meristem and polarly localize to the cell membrane, thereby exporting the hormone only in one specific direction (Blilou et al., 2005; Grieneisen et al., 2007). Auxin response genes are transcriptionally activated by AUXIN RESPONSE FACTORS (ARFs), which bind to the auxin responsive elements (AuxRes) in the regulatory sequence of the target genes. At low auxin concentrations, the co-repressor TOPLESS represses auxin-regulated transcription by mediating the binding of AUXIN/ INDOLE-3-ACETIC ACID (Aux/IAA) proteins to ARFs. Perception of auxin by the TRANSPORT INHIBITOR RESPONSE 1/AUXIN SIGNALING F-BOX (TIR1/AFB) protein, subunit of the SCF E3-ligase protein complex, targets the Aux/IAA proteins for degradation via the ubiquitin-proteasome pathway, thereby leading to the activation of the ARFs and hence activation of

auxin responsive gene expression (reviewed in Saini et al., 2013). Among the genes downstream of auxin signalling in *Arabidopsis* are the *PLETHORA* (*PLT*) genes, which are members of the AINTEGUMENTA-like (AIL) subclass of the APETALA2/ethylene-responsive element binding protein (AP2/EREBP) family of transcription factors (Aida et al., 2004). *PLT1* and *PLT2* are redundantly required for the embryonic specification of the QC cells and for the maintenance of root stem cells (Aida et al., 2004). The *PLTs* are expressed in the stem cell niche forming a concentration gradient with a maximum in the QC and the DSCs, therefore mirroring auxin distribution (Aida et al., 2004; Galinha et al., 2007; Mähönen et al., 2014). Their expression is restricted by the action of PINs, while in turn, the *PLT* genes maintain *PIN* transcription (Blilou et al., 2005; Galinha et al., 2007).

Auxin signalling in the root is highly interwoven with cytokinin signalling. Cytokinins are perceived by histidine kinase receptors (AHKs) which carry an extracellular CHASE domain to sense the phytohormone. The cytokinin perception leads to autophosphorylation of the receptor kinase domain and subsequent transfer of the phosphoryl group onto a histidine phosphotransfer-protein (AHP). This enables AHP allocation to the nucleus and relay of the phosphoryl group to type-B response regulators (type-B ARRs) which in turn activate transcription of cytokinin responsive genes. Among their targets are type-A ARRs which negatively influence cytokinin signalling, thereby creating a negative feedback loop (reviewed in Bishopp et al., 2011). Auxin interferes at this point of the pathway by inducing A-type ARRs (Müller and Sheen, 2008). Likewise, cytokinin signalling interferes with auxin signalling: ARR1 targets the Aux/IAA gene *SHORT HYPOCOTYL2* (*SHY2*) that negatively regulates PIN expression, causing a reallocation of auxin (Ioio et al., 2008). Cytokinin furthermore downregulates the auxin influx carrier LIKE AUXIN RESISTANT 2 (Zhang et al., 2013). Moreover, also the expression of *PLT1* and *PLT2* is downregulated by cytokinin, connecting these two hormonal signalling pathways once more (Ioio et al., 2008).

The spatial domains of auxin and cytokinin signalling can be indirectly determined by following the expression of their downstream response genes, such as the ARRs for cytokinin or the ARFs for auxin. In addition, using known auxin- or cytokinin-responsive elements as promoters for reporter genes reveal the activity of phytohormone signalling. In case of auxin, commonly used constructs are the *DR5* and *DR5v2*, revealing the strongest auxin signalling in the QC, the columella, lateral root cap, pericycle and epidermal cells, as well as in proto- and metaxylem (Ulmasov et al., 1997; Liao et al., 2015). The cytokinin *Two Component signalling Sensor* (*TCS*) and *TCSnew* (*TCSn*) reporters display highest cytokinin signalling in the columella cells and the vasculature of *Arabidopsis* roots (Zürcher et al., 2013).

The effects of auxin and cytokinin signalling can easily be studied by manipulation of the hormone levels in the plant, for instance by externally adding excess of the hormones, or by inhibiting biosynthesis or signal perception. Application of synthetic auxin inhibits root elongation, increases lateral root production and induces adventitious roots in *Arabidopsis*. Equally, mutants that overproduce auxin have abundant lateral and adventitious roots, while mutants deficient in auxin

responses often tend to have long primary roots and few lateral roots (reviewed in Woodward and Bartel, 2005). In the root meristem, application of low auxin amounts enhance meristem length, while higher concentrations inhibit the meristem growth (Ruzicka et al., 2009). Furthermore, auxin application leads to differentiation of the DSCs (Ding and Friml, 2010). Reduction of cytokinin levels by overexpression of degradation enzymes lead to enhanced root growth and longer meristems (Werner et al., 2010), while application of cytokinin reduces the root and meristem length (Ruzicka et al., 2009; Dello Ioio et al., 2007).

While *Arabidopsis* is the best studied organism for auxin signalling, the influence of auxin on root growth of several crop plants has been studied to a minor extent. In maize, the application of auxins inhibits primary root growth (Martínez-de la Cruz et al., 2015). This inhibition is accompanied by a reduced root meristem and root cap size (Forestan et al., 2012). The application of the auxin indole-3-butyric acid (IBA) and the synthetic auxin 1-naphthalene acetic acid (NAA) increases the outgrowth of shoot-borne roots (crown roots) while treatment with the non-transportable auxin 2,4-dichlorophenoxyacetic acid (2,4D) inhibits it (Martínez-de la Cruz et al., 2015). In rice, application of NAA inhibits primary root growth in a dose-dependent manner, while the polar auxin transport inhibitor 1-N-naphthylphthalamic acid (NPA) blocks initiation and growth of nodal and adventitious roots, demonstrating that polar auxin transport is also critical for primary root elongation in rice (Da-Xi et al., 2003; Yang et al., 2017). Downstream targets of auxin and cytokinin signalling were identified in both, rice and maize. Zhang and colleagues identified nine maize *PLT* genes (Zhang et al., 2014). Out of those, the *AtBABYBOOM (AtBBM*/*PLT4*) homologues, *ZmPLT1* and *ZmBBM1*, as well as the *AtPLT3*/*AtPLT7* homologue *ZmSCF* are downregulated in the maize Aux/IAA mutant *ZmRUM1*, indicating that the maize *PLT* homologues are under transcriptional control of auxin (Zhang et al., 2014). Next to the *PLT* homologues, homologues of the PIN auxin transporters were identified and characterized in maize and rice. 12 members of the PIN family, as well as two PIN-like genes were identified in maize; seven of them being expressed in the root (ZmPIN1a, ZmPIN1b, ZmPIN1c, ZmPIN2, ZmPIN9, ZmPIN2, ZmPIN5a) (Forestan et al., 2012). Their expression can be influenced by external application of NAA or NPA (Forestan et al., 2012). The closest homologues of AtPIN1, ZmPIN1a and ZmPIN1b, are both expressed in roots and are localised in basal plasma membranes, therefore mirroring the expression and localisation of their *Arabidopsis* homologue (Carraro et al., 2006). In rice, 12 *PIN* genes were identified to likely encode auxin afflux carriers for polar auxin transport, most of them being expressed in the root (OsPIN1a, OsPIN1b, OsPIN1c, OsPIN1d, OsPIN2, OsPIN5a, OsPIN5b, OsPIN5b, OsPIN9) (Miyashita et al., 2010). Most of these *PIN* genes are induced by external application of auxin, while some are additionally induced by cytokinin application (Wang et al., 2009). *OsPIN1* is the closest homologue of *AtPIN1*, with which it shares the similar expression pattern, and is involved in the formation of nodal roots (Xu et al., 2005). OsPIN3t was shown to be important for the development of seminal and crown roots, and is involved in resistance towards drought stress (Zhang et al., 2012). For the *AtPLTs*, 10 homologues (called *OsPLt1-10*) were identified

in rice. Out of those, *OsPLT1 – OsPLT6* are expressed in the roots and their expression is induced by auxin and downregulated by cytokinin (Li and Xue, 2011).

Even though barley is the fourth most abundant crop plant in the world (FAO statistics 2014; http://faostat.fao.org) and highly salt tolerant in comparison to other cereal crops (Maas and Hoffman, 1977), therefore being a valuable model plant in regard to abiotic stresses, only a few studies exist about the function of auxin and cytokinins in barley roots. An early study shows that the application of auxin inhibits root elongation (Tagliani et al., 1986), but only one mutant has been described that is defective in auxin sensing. namely the *agravitropic* mutant that phenotypically normal except for its misguided roots (Tagliani et al., 1986). Much more is known about the cytokinin signalling and degradation pathways, as they were analysed in connection to drought resistance and yield in barley. Zalewski and colleagues identified barley homologues of CYTOKININ OXIDASE/DEHYDROGENASE (CKX) enzymes that are responsible for the cleavage of isoprenoid cytokinins in the cytokinin degradation pathway (Zalewski et al., 2014). Silencing of *HvCKX1* by RNA interference increases plant yield and results in a greater root mass (Zalewski et al., 2010). On the other hand, overexpression of *AtCKX1* under control of the weak maize beta-glucosidase promoter results in an increased number and length of lateral roots, but a reduction in primary and seminal root growth (Pospíšilová et al., 2016). These transgenic plants also exhibit a higher tolerance to drought stress (Pospíšilová et al., 2016), indicating a direct connection between cytokinin signalling and drought stress resistance, which so far has not been fully explored.

I have here analysed cytokinin distribution, downstream targets of auxin and cytokinin and crosstalk between these hormones in the barley root, with a focus on root meristem development. Application of the hormones to barley seedlings results in impaired root growth and meristem maintenance. I established transgenic reporter lines for hormone signalling and downstream targets and found that cytokinin signalling is strongest in the cells of the stele proximal to the QC and in the differentiated root cap cells. Furthermore I show that also the DSCs, the QC cells and surrounding initials are capable of cytokinin signalling. I show that a barley homologue of *AtPLT1*, *HvPLT1*, is expressed in a pattern similar to that of *AtPLT1* in *Arabidopsis*, namely in and around the QC. I then show that the PIN1 homologue HvPIN1a is expressed in the root meristem, that its expression is regulated by cytokinin and that HvPIN1a is subject to BFA-sensitive endocytosis and turnover. With this study, a foundation for future research on auxin and cytokinin signalling in barley is provided.

2. Material and Methods

2.1. Plant growth

To monitor root growth and expression of reporter genes in the root, seedlings were grown on square plates as described in Kirschner et al., 2017. For all experiments either the cultivar (cv.) Morex or Golden Promise were used as indicated in the figures.

2.2. Cloning

The *HvpPLT1:HvPLT1-mVENUS* construct was built by PCR amplification of a 1929 bp fragment upstream of the start codon of *HvPLT1* (MLOC_76811.2 on morex_contig_73008 (Mayer et al., 2012)) as the putative promoter region from Morex genomic DNA (gDNA) and cloned by restriction and ligation via a *Asc*I site into a modified pMDC99 vector (Curtis and Grossniklaus, 2003). The entire *HvPLT1* coding region lacking the stop codon (3433 bp) was amplified from Morex gDNA and inserted downstream of the promoter in the pMDC99 vector by Gateway cloning (Invitrogen). A C-terminal *mVENUS* (Koushik et al., 2006) was integrated downstream of the gateway site by restriction and ligation via *Pac*I and *Spe*I. The *HvpPIN1a:HvPIN1a-mV* construct was produced the same way, using 3453 bp upstream of the start codon of *HvPIN1a* (AK357068/MLOC_64867 on morex_contig_101983 (Mayer et al., 2012)) as putative promoter region and the whole *HvPIN1a* coding region including the stop codon. The *mVENUS* sequence was inserted by restriction and ligation via a *Sma*I restriction site into the sequence coding for the central hydrophilic region of the HvPIN1a protein, as described for a PIN1 reporter construct in *Arabidopsis* (Benková et al., 2003). The insertion of mVENUS is depicted in Supplementary figure 8B. For the *TCSn:VENUS-H2B* cytokinin reporter construct, the *TCSn* regulatory sequence (Zürcher et al., 2013) was obtained in the pDONR221 gateway vector from Invitrogen and subsequently inserted by Gateway cloning into the modified pMDC99 vector. The auxin reporter construct *DR5v2:VENUS-H2B* was built by amplifying the *DR5v2* promoter from the *pGIIK/DR5v2::NLS-tdTomato* plasmid (kind gift of Dolf Weijers (Liao et al., 2015)) and inserted by Gateway cloning into the modified pMDC99 vector. The pMDC99 modified for *TCSn:VENUS-H2B* and *DR5v2:VENUS-H2B* contained the gateway cassette, the coding sequence of *VENUS* (Nagai et al., 2002) and a T3A terminator, which were inserted by restriction and ligation with *Asc*I and *Sac*I from pAB114 (described in Bleckmann et al., 2010). Furthermore, it contains the coding sequence of *Arabidopsis HISTONE H2B* (AT5G22880) at the C terminus of the *VENUS* gene, inserted via restriction and ligation at a *Pac*I restriction site. The *DR5:ER-GFP* contains the auxin-response promoter *DR5* that consists of 9 inverted repeats of the 11 b-sequence 5′-CCTTTTGTCTC-3′, a 46-bp CaMV35S minimal promoter element, and a tobacco mosaic leader sequence as translational enhancer fused to endoplasmatic reticulum -targeted GFP (Benková et al., 2003; Friml et al., 2002). The plasmid was a kind gift from the Benková lab.

2.3. Barley transformation

Barley transformation was performed at the Justus-Liebig University in Gießen, Germany, in the research group Plant biotechnology as described by Imani and colleagues with the barley cv. Golden Promise and tested for hygromycin resistance by growth on medium containing hygromycin and PCR on the hygromycin gene (Imani et al., 2011). For root expression analysis, the seeds of the plants recovered from the transformed scutella were used (T1) and again tested for the presence of the reporter construct by PCR with primers binding in the gene of interest and the downstream reporter gene.

2.4. Preparation of the reporter line samples

Clearing of the transgenic reporter lines was performed as described by Warner and colleagues for pea root nodules with an altered fixation step (Warner et al., 2014). Root samples were fixed with 4 % para-formaldehyde in phosphate buffered saline (PBS) for 1 h with applied vaccuum. Samples were incubated in the clearing solution for 1 week in darkness at 4 °C. The roots of plant lines with weak expression, or to be examined uncleared, were embedded in liquid 5 % (w/v) agarose in dH_2O for stabilization and sectioned longitudinally in the center by hand with a razor blade.

2.5. Cell wall and starch staining

Modified pseudo-Schiff propidium iodide (mPS-PI) staining and microscopy of the stained samples was performed as described previously (Kirschner et al., 2017).

2.6. Treatments

The cytokinins 6-benzylaminopurine (6-BA) (Duchefa) and *trans*-zeatin (t-Z) (Sigma-Aldrich) were used, as well as the auxins NAA (Duchefa) and 2,4D (Duchefa). For phytohormone treatments of wild type plants, the hormones were added to the growth medium at the concentrations indicated in the results section. The mock control was treated with water. For phytohormone treatment of the *TCSn:VENUS-H2B* and *HvpPIN1a:HvPIN1a-mVENUS* and *DR5v2:VENUS-H2B* reporter lines, the phytohormones were added to PBS and the plates with 7 day-old seedlings were flooded with the hormone solution or pure PBS as mock control and incubated for 2 -3 h to allow phytohormone uptake into the medium. Then, the liquid medium was removed, the plates were placed back into the phytochamber in a 45 ° angle and examined 24 h later. The brefeldin-A (BFA) treatment of the *HvpPINa1:HvPINa1-mVENUS* reporter line was performed according to Geldner and colleagues (Geldner et al., 2001). In particular, the roots were cut around 1 cm above the root tip and the root tip was placed in pure PBS as mock control or PBS containing 50 µM BFA. Pictures of the outer cortex cell layers were taken at the time of the treatment (0 h) and 2 h later.

2.7. RNA *in situ* hybridisations

Probes for the *HvPLT1* mRNA were prepared from gDNA of the cv. Morex from the *HvPLT1* start to stop codon (3433 bp). The DNA was cloned into the pGGC000 entry vector of the GreenGate cloning system (Lampropoulos et al., 2013) and then amplified including the T7 and SP6 promoter sites by PCR. RNA probes were produced as described by Hejátko and colleagues (Hejátko et al., 2006). The RNA probes were hydrolysed by adding 50 µl carbonate buffer (0.08 M $NaHCO_3$, 0.12 M Na_2CO_3) to 50 µl RNA probe and incubation at 60 °C for 58 min. On ice, 10 µl 10 % acetic acid, 12 µl sodium acetate and 312 µl EtOH were added, the RNA was precipitated and dissolved in RNase-free dH_2O. RNA *in situ* hybridisations were performed on roots of plants 8 days after germination (DAG) as described previously (Kirschner et al., 2017). Polyvinyl alcohol was added to a final concentration of 10 % to the NBT/BCIP staining buffer. Permanent specimens were created by washing the slides in 50 % EtOH, 70 % EtOH, 95 % EtOH and 100 % EtOH for 2 min each and for 10 s in xylol, and after drying, a few drops of Entellan (Merck) and a cover slip were added.

2.8. Microscopy

The transgenic reporter lines with mVENUS or VENUS fluorophores were examined with a 40x water objective with a numeric aperture (NA) of 1.20 using the Zeiss confocal laser scanning microscope (LSM) 780. Yellow fluorescence was excited using a 514 nm Argon laser and the emission was detected between 519 and 620 nm. The pinhole was set to 2,24 airy units. Transmitted light pictures were recorded with a transmitted light detector (T-PMT). Pictures were recorded with the tile scan function with 10 % overlap, a threshold of 0.70 and automatically stitched using the microscope software. RNA *in situ* hybridizations were examined using a plan-neofluar 20x objective with a NA of 0.50 or a plan-neofluar 40x objective with a NA of 0.75 using the Zeiss Axioskop light microscope.

2.9. Data Analysis

Picture analyses were carried out using Fiji (Schindelin et al., 2012). For root length measurements, the mean root length of all roots from a single plant were measured. For meristem length measurements, the border between meristem and elongation zone was defined by the first cell in the outermost cortex cell layer that doubled in cell length compared to its distal neighbour and analysis was carried out qualitatively from direct observation (as described in Dello Ioio et al. 2007). For analysing the DSC layers the starch-free cells of three colums in the center of the root cap below the QC were counted and the mean for one column was calculated. For information about creation of the phylogenetic trees see Supplementary figure 6 and Supplementary figure 8A. The transmembrane domains of the PIN proteins were predicted using the TMHMM method on the website provided by Krogh and colleagues (Krogh et al., 2001). Plots and statistics were created in R (R Core Team, 2015). Significance was determined by a two-tailed Student's T-Test with the given p value. For image processing, Adobe Photoshop was used. Contrast and brightness were adjusted in the mPS-PI sample

pictures manually to increase the cell wall and starch visibility. When the fluorescence brightness was compared, identical settings were used for all samples.

3. Results

3.1. Auxin application affects root length negatively and root meristem size after long exposure

Previously, it was shown that the external application of phytohormones such as auxin and cytokinin affects the root architecture of plants in regard to root length, meristem size and structure (Martínez-de la Cruz et al., 2015; Dello Ioio et al., 2007; Ruzicka et al., 2009; Carraro et al., 2006). Tagliani and colleagues performed basic experiments on the influence of different auxins at various concentrations on root length in barley (Tagliani et al., 1986). Here, root growth was inhibited by all auxins tested and at all concentrations, even though to different degrees. To gain a better understanding of the effects of auxin and cytokinin on barley root growth, similar root length measurements were performed in the present study and the analysis was extended to include root meristem length, as the root meristem is the source of new cells for longitudinal root growth. For the auxin treatment, the synthetic auxins NAA and 2,4D were used, the first being the closest in structure and effect to the natural auxin, while the latter cannot be transported out of cells by auxin efflux carriers (Delbarre et al., 1996). Low (10 nM) and high concentrations (1 µM and 10 µM) were used for comparison, as auxins are known to have opposite effects on meristem size at different concentrations (Ruzicka et al., 2009).

Growing barley plants on medium containing either no phytohormone or the different auxins for 6 or 10 days revealed that root length is not affected by low concentrations (10 nM) of NAA or 2,4D but is significantly decreased at higher concentrations (1µM 2,4D, 1µM and 10µM NAA) (Figure 1A, Supplementary figure 1A). Effects on the meristem size, however, were less pronounced and only became significant when plants were treated for 10 days with high auxin concentrations (1 µM or 10 µM) (Figure 1B, C), although a weak, yet statistically not significant effect was already observable at 6 days (Supplementary figure 1C). Only in case of treatment with 1 µM 2,4D, this reduction in meristem size after 10 days correlated with a significant reduction in meristem cell number (Figure 1 D). Additionally, treatments with high concentrations (1 µM and 10 µM) increased meristem width (Supplementary figure 3A). In *Arabidopsis*, Ding and Friml showed that auxin is involved in the DCS maintenance (Ding and Friml, 2010), since auxin application results in differentiation of these stem cells indicated by the accumulation of starch granules. In barley, no significant difference in the number of DSC layers was detected after auxin application (Figure 1B, Supplementary figure 1B).

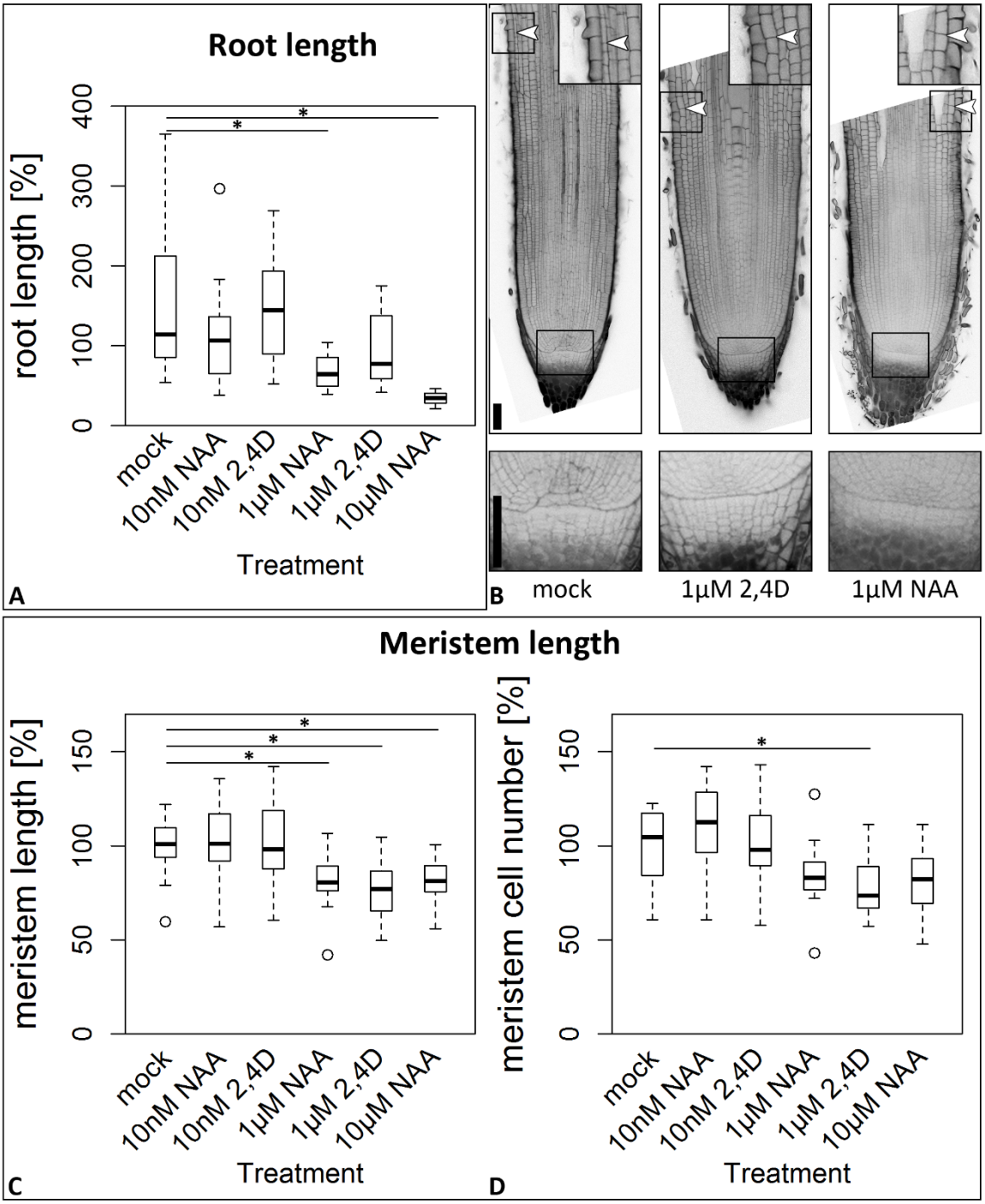

Figure 1: Root length and meristem size given as percent of the respective mock-treated plants 6 DAG and DSC phenotype of the cv. Morex upon auxin treatment for 10 days.

A) Root length after 10 day-treatment with auxin; experiment was performed twice; for a better comparison between the experiments, all values were normalized to the respective mock-treated plants 6 DAG (Supplementary figure 1A); n = 4-18 plants per data point. **B)** Upper panels show representative pictures of the meristem phenotype of roots at 10 DAG upon hormone treatment according to the captions; arrow heads mark the transition zones, i.e. the proximal end of the meristem; insets show magnifications of the transition zones; lower panels show magnifications of the stem cell niche and root cap as indicated by the black frames in the

upper panels; scale bars 100 µm. **C)**, **D)** Meristem size upon hormone treatment, measured by meristem length (C)) or meristem cell number (D)); experiment was performed twice; all values are normalized to the mock-treated control 6 DAG (Supplementary figure 1C, D); n = 7-17 roots per data point; significance was determined using the two-tailed Student's t test, * = $p<0.05$, **= $p<0.001$.

3.2. The cytokinin 6-benzylaminopurine (6-BA) inhibits root growth and both cytokinins, 6-BA and *trans*-zeatin (t-Z), influence root meristem maintenance negatively

To test the effect of cytokinin, both t-Z, a naturally occurring isoprenoid-type cytokinin (Podlešáková et al., 2012), and the synthetic cytokinin 6-BA were used, both of which were shown to affect root and meristem length upon application in *Arabidopsis* (Ruzicka et al., 2009; Dello Ioio et al., 2007). 6-BA had a negative effect on root length in both used concentrations (1 µM and 10 µM) in barley, while t-Z did not affect root growth significantly (Figure 2A, Supplementary figure 2A). Interestingly, the effect on the root meristems was much stronger for both, 6-BA and t-Z, and resulted in a reduction in meristem size (Figure 2C, Supplementary figure 2C). Both hormones seem to affect meristem size by changes in cell division and/or differentiation rate, since a reduced cell number was responsible for the difference in overall meristem size, rather than the mean length of the meristematic cells (Figure 2D, Supplementary figure 2D). Measuring the width of the root meristems revealed that cytokinin influences the width negatively (Supplementary figure 3B). Like auxin treatment, cytokinin treatment did not affect the differentiation of the DSCs (Supplementary figure 2B).

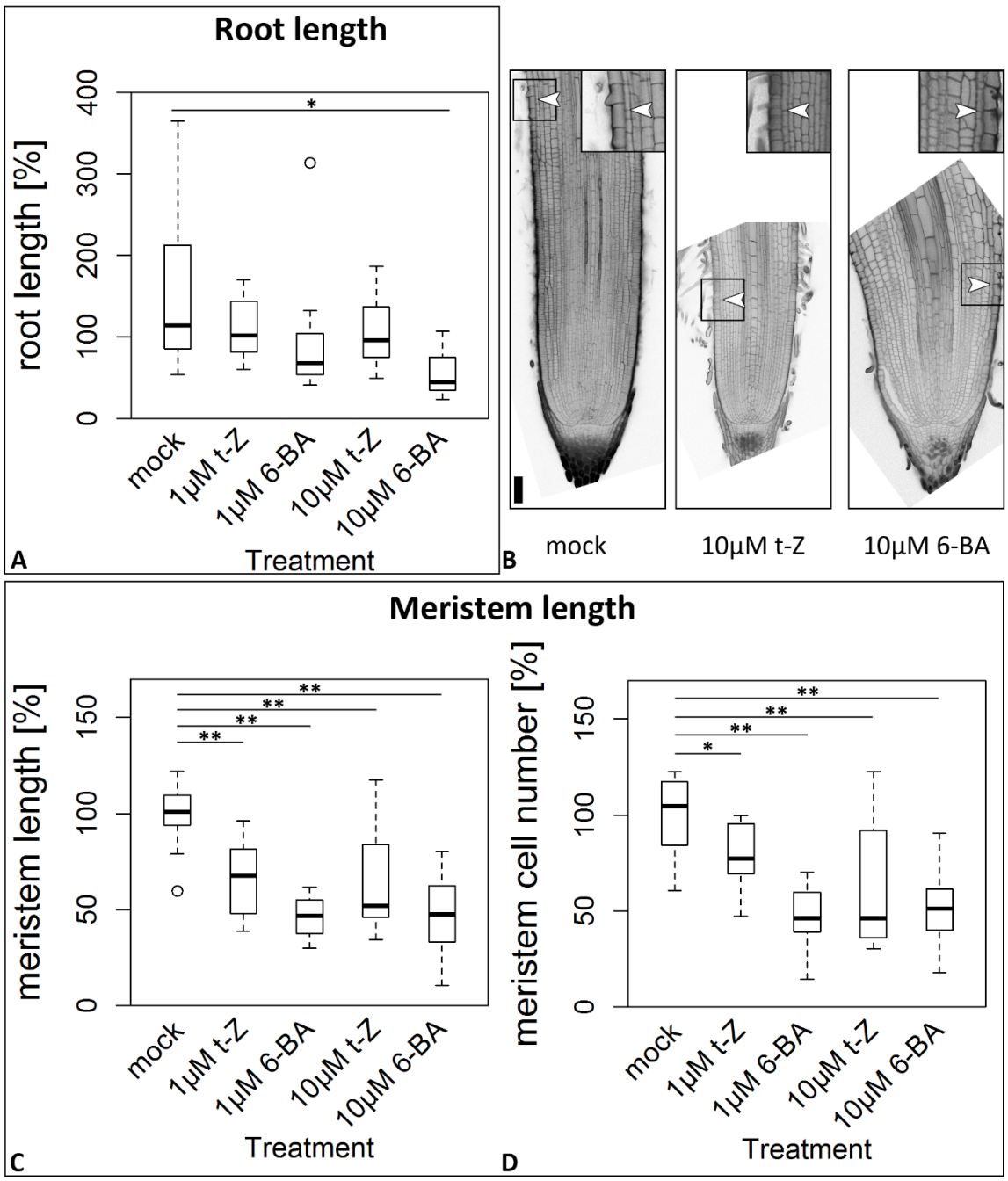

Figure 2: Root length and meristem size given as percent of the respective mock-treated plants 6 DAG of the barley cv. Morex upon cytokinin treatment for 10 days.

A) Root length after 10 day-treatment with cytokinin; experiment was performed twice; for a better comparison between the experiments, all values were normalized to the respective mock-treated plants 6 DAG (Supplementary figure 2A); n = 7-18 plants per data point. **B)** Representative pictures of the meristem phenotype of roots 10 DAG upon cytokinin treatment according to the captions; arrow heads mark the transition zones; insets show magnifications of the transition zones; scale bars 100 µm. **C)**, **D)** Meristem size upon 10-day cytokinin treatment, measured by meristem length (C)) or meristem cell number (D)); experiment was performed twice; all values are normalized to the mock-treated control 6 DAG (Supplementary figure 2C, D); n = 11-16

roots per data point; significance was determined using the two-tailed Student's t test, * = $p<0.05$, **= $p<0.001$.

3.3. Expression of auxin and cytokinin reporters

As both auxin and cytokinin had an effect on root length and meristem size, revealing the distribution of the phytohormones in the root would indicate their sites of action. Therefore, synthetic reporters were created that use repeating elements targeted by auxin or cytokinin response factors, respectively, to drive the expression of the *VENUS* reporter gene.

For cytokinin, the *TCSn* promoter was used to drive the expression of *VENUS*. Here, concatemeric binding motifs for type-B ARRs are combined with a minimal promoter and display the activity of cytokinin signalling (Zürcher et al., 2013). It was shown that applications of cytokinin enhanced the activity of the promoter in *Arabidopsis* and maize protoplasts (Zurcher et al., 2013). In mature barley root apical meristems, expression of the cytokinin reporter *TCSn:VENUS-H2B* could be observed in the differentiated root cap and the stele (Figure 3A') with the exception of metaxylem (Figure 3A', white arrow head), but not in the QC or the surrounding initials (Figure 3A', gray arrow head). 24 h treatment with 6-BA, but not t-Z, increased the expression in the stele, measured by the mean gray value (Figure 3B, C). Moreover, 6-BA treatment also induced *TCSn:VENUS-H2B* expression in the stele up to the transition zone (light gray arrow head in Figure 3F'). As cytokinin and auxin signalling were shown to be highly interconnected (Müller and Sheen, 2008; Ioio et al., 2008; Zhang et al., 2013), also the influence of externally applied auxin on the *TCSn:VENUS-H2B* expression was tested. However, auxin treatments did not change the expression in the stelar region nor did it induce expression in other spatial domains than the mock treatment (Supplementary figure 4D, E). Additional to the increased expression in the stele, treatment with both cytokinins caused expression in the DSCs, in the cortex and endodermis initials, the epidermis initials and in the layer of the QC adjacent to the root cap (Figure 3D). In control plants, expression in the DSCs, the QC or the surrounding initials could never be observed (Figure 3D). The same induction of expression in the QC surrounding region was observed in younger barley plants (3 DAG), an age, when the root meristem is not yet fully mature (Kirschner et al., 2017) (Supplementary figure 4 A, B). Quantifications of the mean gray value in this region showed that the induction by cytokinin here was even stronger than in older plants (Supplementary figure 4C). In summary, the *TCSn* expression pattern in barley resembles the expression in *Arabidopsis* (Zurcher et al., 2013) and increasing the cytokinin concentration by external application induces the *TCSn* expression.

As auxin reporters, two widely used regulatory sequences are the *DR5* and the *DR5v2*, the former consisting of 9 inverted repeats of the auxin responsive element TGTCTC (Ulmasov et al., 1997) and the latter of 9 repeats of the higher affinity auxin binding-site TGTCGG (Liao et al., 2015). Here, the presence of auxin in a cell is indirectly determined through the activation of ARFs that bind to the synthetic promoters in an auxin-dependent manner, activating expression of the reporter genes. In

Arabidopsis, the responsiveness of these reporters to auxin was confirmed by auxin application to the roots, leading to an enhanced expression of the reporter gene and a broadening of the expression domain (Liao et al., 2015). The same reporters were successfully used in maize and rice to display the spatial domain of auxin signalling (Gallavotti et al., 2008; Yang et al., 2017), therefore, the *DR5* and *DR5v2* regulatory sequences might also be feasible for representing auxin signalling in barley.

However, no expression of the *DR5:GFP* reporter could be detected in transgenic lines, and the expression of the *DR5v2:VENUS-H2B* reporter lines was very weak and inconsistent between different roots and plant lines (Supplementary figure 5A'). Furthermore, no increase of the *DR5v2:VENUS-H2B* expression was detected even upon high auxin concentrations (10 µM 2,4D) (Supplementary figure 5B'). Thus, the *DR5* and *DR5v2* reporters do not seem to be suitable for reflecting the auxin signalling in barley.

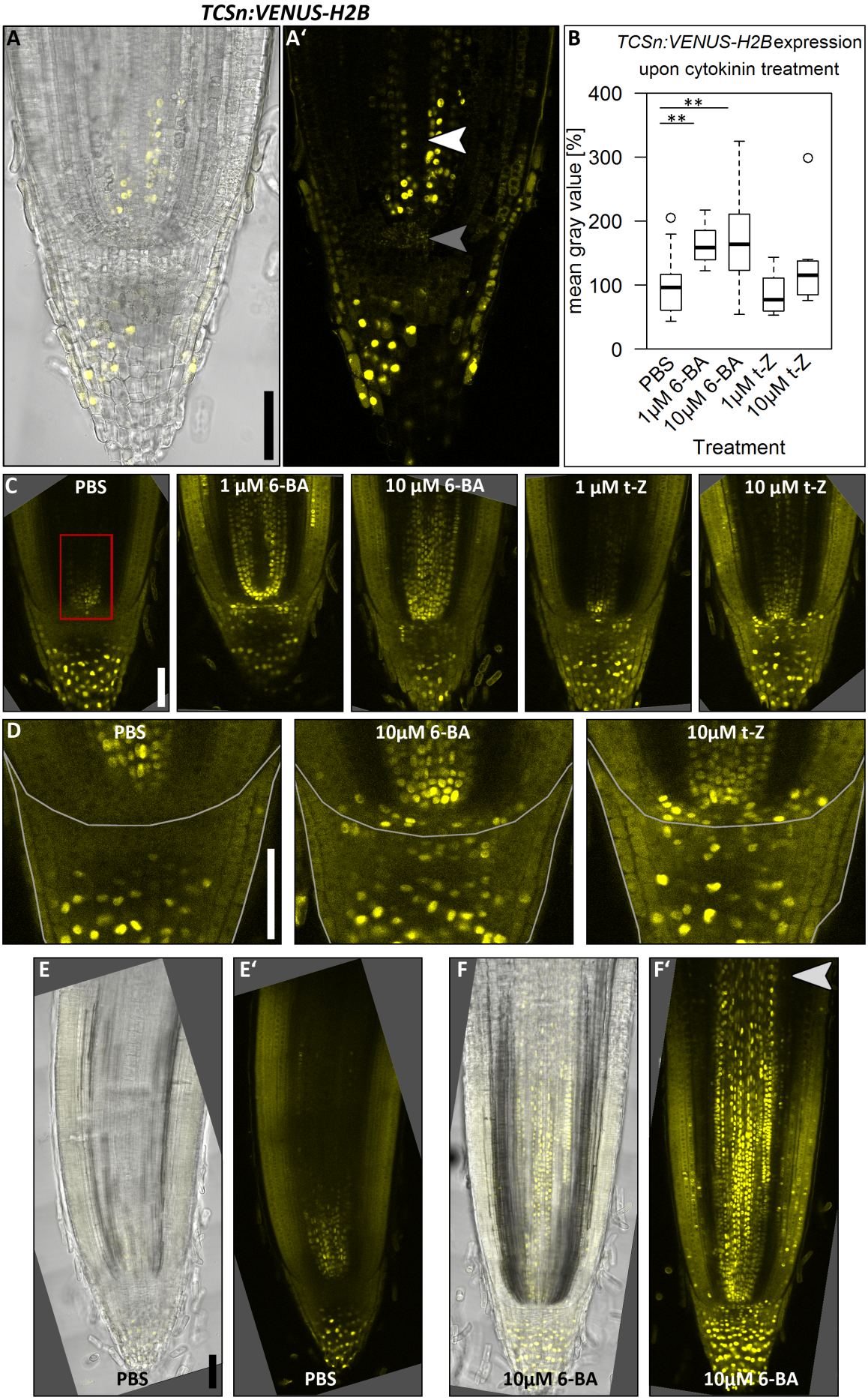
TCSn:VENUS-H2B
A
A'
B
TCSn:VENUS-H2B expression
upon cytokinin treatment
mean gray value [%]
400
300
200
100
0
**
**
PBS
1µM 6-BA
10µM 6-BA
1µM t-Z
10µM t-Z
Treatment
C
PBS
1 µM 6-BA
10 µM 6-BA
1 µM t-Z
10 µM t-Z
D
PBS
10µM 6-BA
10µM t-Z
E
E'
F
F'
PBS
PBS
10µM 6-BA
10µM 6-BA

Figure 3: Expression of the cytokinin reporter *TCSn:VENUS-H2B* in the root meristem of the barley cv. Golden Promise 8 DAG.

A), A') *TCSn:VENUS-H2B* expression in untreated roots; transmitted light and VENUS emission (A)) and VENUS emission only (A')); white arrow head in A') points to the metaxylem; gray arrow head in A') indicates QC; seven independent transgenic lines were examined and exhibit a similar expression pattern; hand-sections. **B)** Quantification of the *TCSn:VENUS-H2B* expression by the mean gray value of the region marked with the red box in C); mean gray value is normalized to the PBS control; significance was determined using the two-tailed Student's t test, ** = $p<0.001$. **C)** Representative pictures of the *TCSn:VENUS-H2B* expression in root meristems upon 24 h of cytokinin treatment according to the captions; PBS only was used as control; three independent transgenic lines were examined; experiment was performed three times; n = 8-31 per treatment. **D)** Magnification of the stem cell niche and root cap of roots upon treatments indicated by the captions; treatment with both cytokinins leads to expression in the cortex/ endodermis initials, the DSCs, the QC layer adjacent to the root cap and the epidermis initials (PBS: 0/21 roots, 1 µM 6-BA: 1/9 roots, 10 µM 6-BA 8/18 roots, 1 µM t-Z 2/9 roots, 10 µM t-Z 5/8 roots); root cap border is marked with a white frame. **E), F)** Representative pictures of *TCSn:VENUS-H2B* expression in the whole root meristem treated with PBS (E)) or 10 µM 6-BA (F)); transmitted light and VENUS emission (E), F)) and VENUS emission only (E'), F')); light gray arrow head in F') indicates transition zone; for a better comparison between samples, roots were cleared for one week before microscopy (C), D), E)); scale bars 100 µm.

3.4. Expression pattern of *HvPLT1*

From the phenotypic effects of auxin and cytokinin treatment on meristem size, as well as the expression pattern of the *TCSn* reporter, it can be concluded that both phytohormones are active in the root meristem. Therefore, possible target genes of auxin and cytokinin signalling were identified. Based on the research conducted in other model plants such as *Arabidopsis*, rice and maize, a possible role of the PLT transcription factors was analysed, which are expressed in the root meristem. In *Arabidopsis*, the *PLT* genes are downregulated by cytokinin, and require auxin signalling for expression (Aida et al., 2004; Blilou et al., 2005; Ioio et al., 2008). The rice *OsPLTs* are likewise expressed in roots and transcription is induced by auxin and downregulated by cytokinin (Li and Xue, 2011). To identify possible *PLT* homologues of barley and to examine the phylogenetic relationship between the *Arabidopsis*, rice, maize and barley PLTs, the barley proteome was searched (Mayer et al., 2012) and an unrooted tree was created from whole protein sequences (Supplementary figure 6). Because OsPLT1 grouped phylogenetically together with AtPLT1-3 and AtBBM (AtPLT4) in the study by Li and Xue and therefore might have a similar function in the stem cell niche maintenance (Li and Xue, 2011), it was focused on MLOC_76811 as the closest homologue of OsPLT1 (Supplementary figure 6) and named HvPLT1 accordingly. In the annotation database for the barley genome, the gene is annotated as "AP2-like ethylene-responsive transcription factor" (http://pgsb.helmholtz-muenchen.de/plant/barley/). As the annotation suggests, *HvPLT1* consists of

two repeats of the conserved AP2 DNA binding domain and a conserved linker region (Figure 4A) like its two homologues *AtPLT1* and *AtPLT2* in *Arabidopsis*. To reveal the expression pattern of *HvPLT1*, transgenic reporter lines were created that expressed *HvPLT1* fused to *mVENUS* under the control of the putative endogenous *HvPLT1* regulatory sequence. The reporter lines showed a gradual expression pattern of HvPLT1 with the maximum in the QC and the surrounding cells, gradually decreasing towards the root cap, the proximal meristems and the outer root layers (Figure 4B, B'). Non-transgenic control plants did not show any expression (Supplementary figure 7A, A'). RNA *in situ* hybridisations with a probe for *HvPLT1* confirmed this expression pattern (Figure 4C).

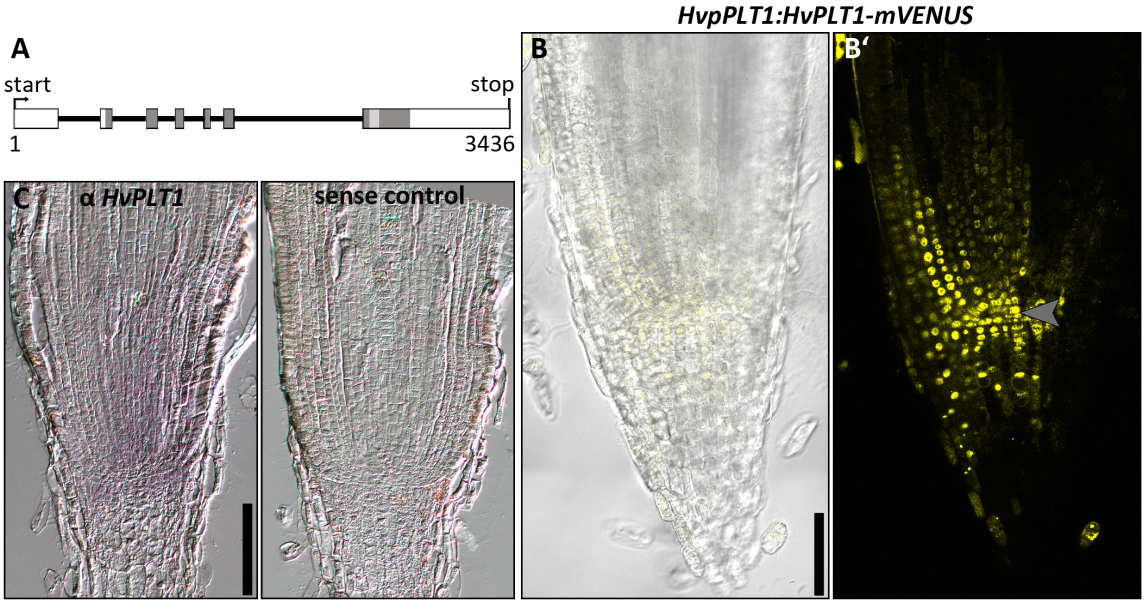

Figure 4: *HvPLT1* gene structure, promoter activity and protein localization in the root meristem of the barley cv. Golden Promise 8 DAG.

A) Genomic structure of the *HvPLT1* coding sequence; boxes represent exons, black horizontal lines represents introns; dark gray boxes indicate coding sequence for AP2 domains, light gray boxes indicate coding sequence for the linkers between AP2 domains. **B)** Representative picture of the *HvpPLT1:HvPLT1-mVENUS* emission in the root meristem; transmitted light and mVENUS emission (B)), mVENUS emission only (B')); gray arrow head in B') points to the QC; hand sections; seven independent transgenic lines were examined and exhibit a similar expression pattern. **C)** Representative picture of RNA in situ hybridizations with a probe for *HvPLT1* (purple staining) or the respective sense probe; scale bars 100 µm.

3.5. Identification of a PIN1 homologue in barley

In *Arabidopsis*, the expression of the AtPLTs is dependent on auxin signalling (Mähönen et al., 2014; Galinha et al., 2007). The *HvPLT1* expression pattern suggests the presence of an auxin maximum in the QC and the root stem cell niche also in barley. To create such an auxin maximum, auxin transport

is necessary in a directed, polar manner. Auxin biosynthesis occurs in young aerial tissues and auxin is transported towards the root via the phloem (Saini et al., 2013), and for many plants such as *Arabidopsis*, rice and maize it has been shown that the subsequent cell-to-cell transport is facilitated by PIN proteins (Wang et al., 2009; Carraro et al., 2006; Blilou et al., 2005). Computational analysis of the structure of PIN proteins predicts that they consist of hydrophobic regions that span the cell membranes and of hydrophilic regions that are exposed on the intracellular side of the plasma membranes (Křeček et al., 2009). Křeček and colleagues sorted the eight *Arabidopsis* PINs into two subfamilies, namely the “long” and the “short” PINs according to the length of their hydrophilic region (Křeček et al., 2009). The “long” PIN subfamily is characterised by its central hydrophilic loop, separating two hydrophilic domains, each consisting of five trans-membrane regions. They are primarily localised to the plasma membrane in the cell (Benková et al., 2003; Blilou et al., 2005; Friml et al., 2003). The "short" PINs, however, possess a short central hydrophilic region and localise to internal cell membranes (Ganguly et al., 2010). To identify PINs in barley, the barley protein database was searched for homologues of AtPINs and 13 possible HvPIN protein sequences were found that were used to build a phylogenetic tree and analyze their topology (Mayer et al., 2012) (Supplementary figure 8A, B). In the phylogenetic tree, MLOC_64867.2 (HvPIN1a), MLOC_12686.1 (HvPIN1b) and MLOC_293.2 (HvPIN1c) grouped with AtPIN1 and the PIN1 homologues from rice and maize, AK366549 (HvPIN2) grouped together with OsPIN2 and AtPIN2 (Supplementary figure 8A), therefore these barley homologues can be regarded as PIN1 and PIN2 homologues, respectively. A transmembrane helices prediction analysis moreover revealed that these barley PIN1 and PIN2 homologues carry 4 - 5 transmembrane domains that group around a central hydrophilic region (Supplementary figure 8B). Therefore, these HvPINs can be classified as being part of the "long" PIN subfamily. On the other hand, PINs that cluster with the "short" PINs from *Arabidopsis* could be identified: MLOC_60446.1 (HvPIN5a) and MLOC_71135.1 (HvPIN5b) grouped together with PIN5, MLOC_61956.2 (HvPIN8) grouped together with PIN8, and MLOC_38112.1 (HvPIN9a) and MLOC_53867.1 (HvPIN9b) belong to the clade of PIN9 which has no homologue in *Arabidopsis* but only exists in maize and rice (Supplementary figure 8A). Indeed, these proteins exhibited only a short central hydrophilic region (Supplementary figure 8B). MLOC_6128.3 (HvPIN3a), MLOC_38023.1 (HvPIN3b), MLOC_38022.1 (HvPIN10a) and MLOC_60432.1 (HvPIN10b), on the other hand, grouped together with the clade of ZmPIN10 and OsPIN3. Like in maize and rice, also the barley genome did not harbour *PIN4* and *PIN7* homologues (Wang et al., 2009; Forestan et al., 2012). In regard to their structure, the HvPIN3s and HvPIN10s did not show the typical structure of neither "short" nor "long" PINs. They either have no large hydrophilic region (HvPIN10a, HvPIN10b and HvPIN3b) or the hydrophilic region is not central (HvPIN3a) (Supplementary figure 8B). For the subsequent work on PIN protein localization in barley, it was focussed on PIN1, as this is the best studied PIN protein in other model plants. Both in maize and rice, the two maize PIN1-like proteins and OsPIN1 show a similar transmembrane helices prediction profile, with two hydrophobic domains

at the N and C termini and a central hydrophilic region (Xu et al., 2005; Wang et al., 2009; Carraro et al., 2006). From the HvPINs that grouped together with the other PIN1s, HvPIN1a is the one with the transmembrane helices prediction profile most similar to AtPIN1 (Supplementary figure 8B).

3.6. Expression pattern and polar localization of HvPIN1a

In the *Arabidopsis* root, *PIN1* is expressed in the root meristem, in particular in the vasculature and endodermis, and weaker in the epidermis and cortex (Blilou et al., 2005). *PIN1* homlogues of maize and rice are also expressed in the root meristem, but also in the root cap (Forestan et al., 2012; Wang et al., 2009). In barley, the expression of *HvPIN1a* was examined by means of transgenic reporter lines with the genomic *HvPIN1a* sequence, under control of the putative endogenous *HvPIN1a* regulatory sequences, consisting of 3453 bp upstream of the start codon. The sequence of the fluorophore *mVENUS* was inserted into the part of the *HvPIN1a* gene sequence that encodes for the intracellular hydrophilic region of the protein, as it was described for the *AtPIN1-GFP* construct (Benková et al., 2003) (Supplementary figure 8B). Strong expression was detected in the whole root meristem, except for the cell area of the presumed QC, where expression was weaker compared to surrounding tissues (Figure 5 A', D'). High expression was observed in the stele, the endodermis, the cortex and the DSCs, and the differentiated root cap (Figure 5D'). The PIN1s from *Arabidopsis*, maize and rice were shown to be mostly polarly localised to the plasma membranes at defined sides of the cells. In *Arabidopsis* roots, AtPIN1 is localized to the basal plasma membranes (Blilou et al., 2005), and a basal localisation was also observed for ZmPIN1 in the epidermis, the meristematic regions and the central cylinder in maize, whereas ZmPIN1 appeared to be cytosolic in the root cap (Forestan et al., 2012; Carraro et al., 2006). In barley, a basal plasma membrane localisation was detected in the stele, endodermis and the inner cortex cell layers (gray arrow heads in Figure 5B, D'), but apical localisation was observed in the outermost cortex cell layer and the lateral root cap (white arrow head in Figure 5B, D'). In the central region of the root cap, polar localisation was not detectable, but HvPIN1a was evenly distributed in the plasma membrane (Figure 5D').

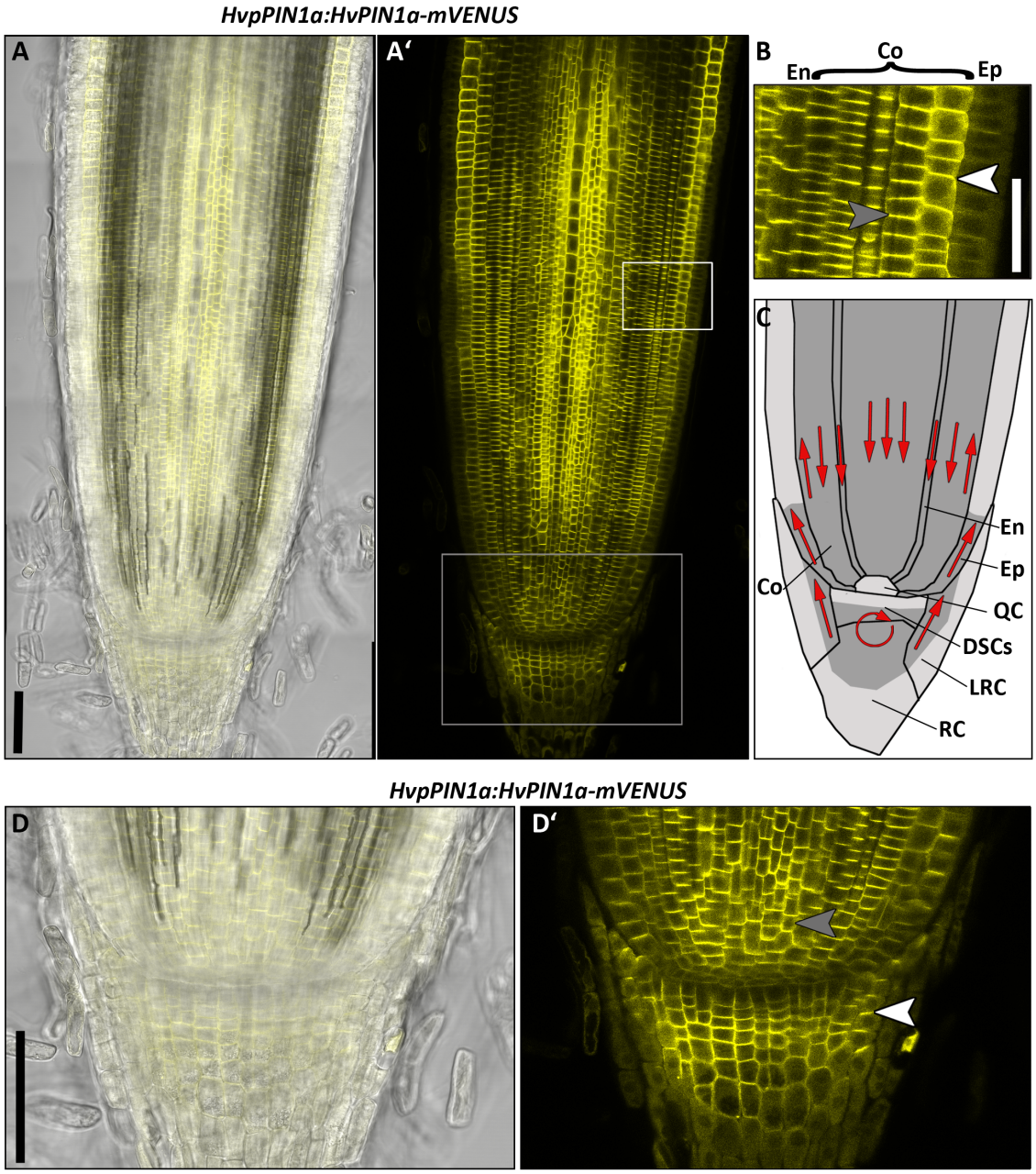

Figure 5: HvPIN1a expression in the root meristem of the barley cv. Golden Promise 8 DAG.

A) Representative picture of *HvpPIN1a:HvPIN1a-mVENUS* expression; six independent transgenic lines were examined; white box in A') marks magnification in B); gray box in A') marks magnification in D). **B)** Magnification of the epidermal, cortical and endodermal cell layers depicted with white frame in A'). **C)** Schematic illustration of *HvPIN1a* expression in the root meristem, high = dark gray, low = gray; red arrows indicate possible auxin flow created by localisation of PIN1a auxin transporters; En = endodermis, Co = cortex, Ep = epidermis, LRC = lateral root cap, RC = root cap. **D)** Magnification of the stem cell niche depicted with gray frame in A'); transmitted light and mVENUS emission (A), D)), mVENUS emission only (A'), D')); white arrow heads mark apically localised PIN1a, gray arrow heads mark basally localised PIN1a; brightness adjusted in B and D'); scale bars 100 µm in A), D); 50 µm in B).

3.7. HvPIN1a-mVENUS is found in vesicles upon Brefeldin-A (BFA) treatment

PINs are continuously recycled from the cell membrane to endosomes. Involved in the trafficking of basally localised PINs in *Arabidopsis*is are the GDP/GTP exchange factor for small G proteins of the ADP-ribosylation factor class (ARF-GEFs), which contain Sec7 domains (Kleine-Vehn et al., 2009; Steinmann et al., 1999; Geldner et al., 2003). The inhibitor of protein secretion BFA stabilizes an intermediate of the reaction of the ARF-GEF Sec7 domain with GDP, thereby blocking the cycle of activation of the ARF-GEFs and the thereto related recycling pathways (Peyroche et al., 1999). Therefore, BFA can be used to reveal the involvement of BFA-sensitive ARF-GEFs in the PIN recycling pathways. Treatment with BFA induces intracellular accumulation of AtPIN1 by blocking the exocytosis of PIN1, which normally cycles rapidly between plasma membrane and endosomal compartments (Geldner et al., 2001, 2003). To test if the PIN1 recycling mechanism is conserved in barley, *HvpPIN1aHvPIN1a-mVENUS* expressing roots were treated with 50 µM BFA and the HvPIN1a-mVENUS localisation was monitored in the outer cortex cell file after 2 h. While HvPIN1a-mVENUS was exclusively localised at the apical cell membranes before the BFA treatment and upon mock controls, the formation of vesicles within the cells could be observed after 2 h of BFA treatment (gray arrow heads in Figure 6A). This indicates the existence of a conserved mechanism of PIN1 recycling between endosomal compartments and the plasma membrane in barley.

3.8. *HvPIN1a* expression is regulated by cytokinin

As the recycling of the HvPIN1a protein is similarly affected by BFA like in *Arabidopsis*, it was examined if gene expression of *HvPIN1a* is regulated by the same factors as in *Arabidopsis*. Dello Ioio and colleagues showed that *AtPIN1* expression is downregulated by cytokinin (Ioio et al., 2008). In barley, treatment with the cytokinin 6-BA for 24 h reduced *HvPIN1a-mVENUS* expression as well (Figure 6B, C).

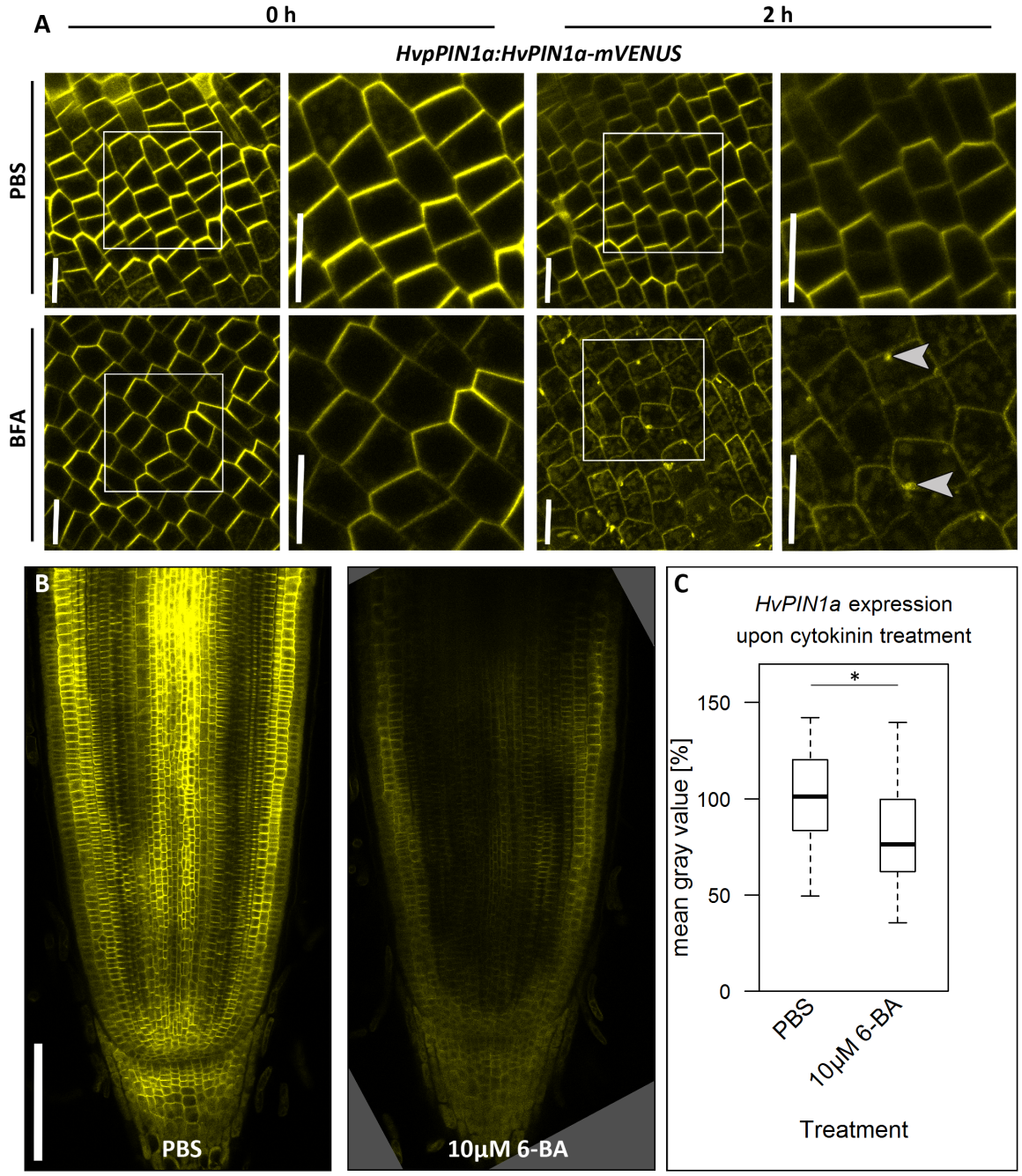

Figure 6: HvPIN1a localisation is influenced by BFA and its expression is influenced by cytokinin.

A) Representative pictures of the *HvpPIN1a:HvPIN1a-mVENUS* expression in the outer cortex cell layer immediately (0 h) or 2 h after mock (PBS) or 50 µM BFA treatment; the respective right pictures display magnifications of the areas framed in white in the left pictures; gray arrow heads point to vesicles; scale bar 20 µm; three independent transgenic lines were examined; experiments were performed twice; n = 4 - 6. **B)** Representative pictures of *HvpPIN1a:HvPIN1a-mVENUS* expression upon mock (PBS) or cytokinin treatment as indicated; scale bar 200 µm. **C)** Quantification of the *HvpPIN1a:HvPIN1a-mVENUS* expression in B), measured by the mean gray value of the whole meristem and the root cap; values are normalized to the PBS-control; five different independent transgenic lines were used; experiment was performed twice; n = 24 per

treatment; significance was determined using the two-tailed Student's t test, * = $p<0.05$.

4. Discussion

4.1. Meristem length measurements and expression of the cytokinin reporter *TCSn:VENUS-H2B* reveal a role for cytokinin in meristem maintenance

In this study, the role of the phytohormones auxin and cytokinin on barley root growth and the root apical meristem maintenance was analysed. Growing barley seedlings on medium with the cytokinin 6-BA caused a reduction in root growth (Figure 2A, Supplementary figure 2A). The same was shown for *Arabidopsis*, where application of 6-BA already at low concentrations between 10 nM and 100 nM reduces root growth (Ruzicka et al., 2009). Application of the cytokinin t-Z, however, did not cause any significant reduction in barley root growth at the concentrations tested (Figure 2A, Supplementary figure 2A). It was shown for *Arabidopsis* CKXs, enzymes that participate in the cytokinin degradation pathway, that they preferentially cleave isoprenoid cytokinins, which include t-Z but not 6-BA (Galuszka et al., 2007), and for CKX1 from maize that it predominately cleaves free cytokinin bases, including t-Z (Mrízová et al., 2013). In barley, thirteen putative members of the HvCKX family were identified (Zalewski et al., 2014). Their presence could lead to an enhanced degradation of the externally added t-Z, thereby leading to a reduced influence on root growth in comparison to 6-BA. In *Arabidopsis*, application of both, t-Z and 6-BA, in only low concentrations of about 50 nM leads to a reduction in meristem size (Ruzicka et al., 2009; Dello Ioio et al., 2007). In barley, both t-Z and 6-BA treatments reduced the meristem size, however, the effect was again more pronounced in roots treated with 6-BA (Figure 2B, C, D, Supplementary figure 2C, D). In this case again, the observed difference of effect of the two synthetic cytokinins could be caused by the degradation of t-Z by the endogenous HvCXKs. Nevertheless, in barley, cytokinin application led to a reduced meristem size, caused by a reduced number of meristematic cells (Figure 2B, C, D, Supplementary figure 2C, D). In *Arabidopsis* it was shown that cytokinin mediates the cell differentiation at the transition zone and cytokinin application reduces the mitotic activity in the root meristem (Dello Ioio et al., 2007; Ruzicka et al., 2009). As displayed by the barley cytokinin reporter line *TCSn:VENUS-H2B*, application of 6-BA, but again not of t-Z, induces the reporter gene expression in the stele up to the transition zone of the meristem, indicating that also in barley cytokinin, more precise 6-BA, is involved in the transition between the meristematic and the elongation-differentiation zone (Figure 3F'). If cytokinin is also involved in the mitotic activity in barley, however, has not yet been analysed. The reduction in root growth upon cytokinin application could be explained by a premature differentiation of the meristematic cells and thereby a lower production of new cells.

Besides its influence on root length and meristem size, cytokinins also influence the root diameter. The impact of cytokinin on root diameter was previously shown in *Arabidopsis* plants harbouring a *35S:AtCKX7* construct and a 30 % reduction in overall cytokinin content. These plants developed fewer vascular cell files in the central cylinder (Köllmer et al., 2014). Increasing cytokinin concentrations by external application could, on the other hand, result in the formation of additional

vascular cell files, and hence a greater root diameter. However, cytokinin application in barley had in the opposite effect, as it significantly reduced the diameter of the barley roots in the meristematic region (Supplementary figure 3B). This outcome is partially surprising, however, earlier studies in *Arabidopsis* have already shown that overexpression of different CKX isoforms resulted in opposite effects on root growth (Werner et al., 2003; Köllmer et al., 2014). Therefore, it is possible that it is not overall cytokinin concentrations, but rather local cytokinin distribution that influences root size.

4.2. Cytokinin signalling is active in the root cap and the stele and activated by cytokinin application in the root stem cell niche

In *Arabidopsis*, reporter genes under control of the *TCSn* regulatory sequence are expressed in the differentiated columella cells and in the vasculature of roots (Zürcher et al., 2013). In maize, Saleem and colleagues found a predominant localization of the cytokinin cis-zeatin, one cis- zeatin precursor, and its conjugate cis-zeatin O-glucoside in the cortex, indicating that cytokinin biosynthesis is primarily occuring in the cortex (Saleem et al., 2010). The *TCSn:VENUS-H2B* barley reporter line revealed that cytokinin signalling occurs in the differentiated root cap cells and the stele, but, however, did not express in the cortex (Figure 3A), implying that the localisation of the barley cytokinin signalling rather resembles the cytokinin signalling in *Arabidopsis* than the cytokinin distribution in maize (Saleem et al., 2010; Zürcher et al., 2013). The *TCSn* sensor was initially designed for *Arabidopsis*, and additionally tested for cytokinin response in maize protoplasts, but so far, the functionality in monocot roots has not been proven. Therefore, the *TCSn:VENUS-H2B* barley reporter lines were tested for their cytokinin response in the roots. Noteworthy, although externally applied cytokinin is most likely taken up through all root tissues, enhanced expression of the reporter appeared to be restricted to specific cell types. The *TCSn* reporter consists of concatemeric repeats of the DNA-binding motif of the *Arabidopsis* type-B ARR (Zürcher et al., 2013). Therefore, some cells may lack expression of genes that are necessary for the multistep phosphorelay signalling cascade for cytokinin, for instance cytokinin receptors, so that the type-B ARRs are not phosphorylated despite a high cytokinin concentration in the cell. Furthermore, the *TCSn* was designed by analysing the DNA-binding motifs of the *Arabidopsis* type-B ARRS, which might differ from those of barley. 6-BA treatment enhanced expression of *TCSn:VENUS-H2B* in the stelar cells (Figure 3 B, C) and treatment with both used cytokinins resulted in additional expression of the reporter in the QC cells adjacent to the root cap, the DSCs, the cortex/endodermis initial, the epidermis initial, and older cortex, endodermis and epidermis cells (Figure 3 D). Moreover, this induction of reporter gene expression in the stem cell niche was even more pronounced when 3-day old seedlings were treated with cytokinin in comparison to older seedlings (Supplementary figure 4A, B, C). At this age, the meristem has not yet reached its final size (Kirschner et al., 2017). The enhanced expression of *TCSn:VENUS-H2B* in the root initials especially in young roots implies that these cells are targets of cytokinin activity and that cytokinin is involved in determining the cell fate. In summary, these data suggest that the *TCSn*

reporter is applicable for reflecting cytokinin signalling in barley roots, as the *TCSn* expression pattern resembles the expression in *Arabidopsis* (Zürcher et al., 2013) and increasing cytokinin concentration by external application induces the *TCSn* expression. The *TCSn* expression indicates an involvement of the cytokinin 6-BA in root meristem maintenance, while both 6-BA and t-Z play a role in specification of the root tissue.

4.3. Auxin reduces barley root growth, but root meristem maintenance is only influenced to a minor extent

Cytokinin signalling in the root is highly interwoven with auxin signalling (Müller and Sheen, 2008; Ioio et al., 2008; Zhang et al., 2013). Like cytokinin, auxin application influences the root growth and root meristem size in many plants, such as *Arabidopsis* and maize (Evans et al., 1994; Martínez-de la Cruz et al., 2015; Ruzicka et al., 2009). At low concentrations of 0.001-10 nM auxin was shown to have a positive effect on root growth of *Arabidopsis* by stimulating cell elongation (Müssig et al., 2003; Evans et al., 1994), while the root growth is affected negatively at higher concentrations in many plant species, such as *Arabidopsis*, maize and rice (Evans et al., 1994; Martínez-de la Cruz et al., 2015; Yang et al., 2017). In the present study, the influence of the synthetic auxin NAA and the non-transportable synthetic auxin 2,4D on barley root growth was analysed. NAA can enter the cells by passive diffusion and is transported by the auxin efflux carriers. Accordingly, NAA treatment will elevate the auxin concentration within the wild type distribution pattern in the root. 2,4D, on the other hand, is taken up with influx carriers, but not secreted by efflux carriers, so that it cannot be transported within the plant (Delbarre et al., 1996). This results in elevated auxin concentrations in all cells of the root. Therefore, a stronger effect of 2,4D on root growth would be expected in comparison to NAA. Accordingly, many studies showed that low concentrations of 2,4D were sufficient to decrease the root growth to the same extend as high concentrations of NAA (Tagliani et al., 1986; Martínez-de la Cruz et al., 2015; Müssig et al., 2003). In barley, however, 2,4D and NAA had an equally strong negative effect on root growth when applied at a concentration of 1 µM (Figure 1A). This might be caused by the applied plant growth methods. Tagliani and colleagues measured the root length of barley by placing the seedlings between wet filter paper, soaked with the phytohormone or the control solution (Tagliani et al., 1986), while Martínez-de la Cruz and colleagues used liquid medium for maize root growth, ensuring that the roots were completely immersed in the solution (Martínez-de la Cruz et al., 2015). In the present study, the plants were grown on the surface of solid growth medium containing the phytohormones (see Material and Methods), so that the roots only took up the hormones at the contact points with the medium. Thus, NAA can be taken up and redistributed into different cells via active transport, while 2,4D concentrations are elevated at the sites of root to medium contact, possibly explaining the unexpected low effect of 2,4D. In contrast to studies in *Arabidopsis*, where low concentrations of auxins were shown to increase the root growth rate (Evans et al., 1994; Müssig et al., 2003), no enhancement of root growth rates upon applications of low

concentrations of NAA and 2,4D (10 nM) was observed in barley (Figure 1B). Root longitudinal growth can primarily be attributed to cell divisions in the meristematic zone and cell elongation in the elongation zone. Both of these processes are, among other factors, regulated by auxin signalling pathways. A reduction in meristem size upon treatment with high auxin concentrations (1 µM or 10 µM) was observed, both in regard to cell number and meristem length (Supplementary figure 1C, D). This effect, however, was only significant compared to the control after 10 days of auxin treatment, while overall root growth was already inhibited after 6 days (Figure 1C, D). Ruzicka and colleagues observed a similar effect for root length and meristem size in *Arabidopsis*, where root length was stronger affected by auxin application than the meristem length (Ruzicka et al., 2009). Thus, it is most likely that auxin affects root growth not by affecting the meristematic activity, or at least only to a minor proportion, but mainly through reduction of the cell elongation in the differentiated part of the root. This effect of externally applied auxin at micromolar concentrations was shown before in *Arabidopsis* (Perrot-Rechenmann, 2010). However, a closer examination of average cell length of differentiated barley root cells and meristematic cell division rates upon auxin treatment is necessary to reveal the underlying mechanism of how auxin affects root growth in barley.

Besides the effect of auxin application on longitudinal root growth and meristem size in *Arabidopsis*, the phytohormone also influences the DSC that give rise to the columella cells. Auxin application leads to differentiation of these stem cells, marked by accumulation of starch granules (Ding and Friml, 2010). In barley, however, no starch granule accumulations could be observed in any additional DSC file in barley (Figure 1B, Supplementary figure 1B). Previously, similar observations for the application of a CLE peptide were published. CLE peptides were shown to cause both a differentiation of the proximal root meristem and the DSCs in *Arabidopsis*, whereas application of CLE peptides did only affect the proximal root meristem but not the DSC differentiation in barley (Kirschner et al., 2017; Stahl et al., 2009). This indicates that DSC maintenance, in contrast to root meristem maintenance, is regulated differently in barley than in *Arabidopsis*. In *Arabidopsis*, the DSCs are maintained by signalling from the QC, shown among other experiments by laser ablation (van den Berg et al., 1997). In monocots, however, similar studies are lacking. Nevertheless, also in monocots there is evidence for signalling between the cells of the QC and the root cap. When the root cap is excised in maize, the remaining root changes its developmental programme to regenerate a new cap (Feldman, 1976). Furthermore, Campos and colleagues could show that the expression of some root cap specific genes is dependent on the presence of the QC in maize (Ponce et al., 2000). This suggests that in monocots there is indeed communication between the QC and the root cap, although the underlying genetic and molecular mechanisms appear to be different from the dicot *Arabidopsis*.

4.4. The expression patterns of *HvPLT1* and *HvPIN1a* indicate an auxin distribution in the root tip similar to *Arabidopsis*, rice and maize

These findings raise the question, where auxin signalling is active in the barley root meristem. The synthetic reporters *DR5* and *DR5v2*, consisting of auxin responsive elements as regulatory sequence, revealed that in *Arabidopsis* an auxin maximum is formed in the QC, the root cap, the lateral root cap and the epidermal cells (Liao et al., 2015). The same auxin distributions were observed in rice with the *DR5* reporter, although here, the reporter is also expressed additionally in the epidermis in the meristematic and elongation zone (Yang et al., 2017). In maize, activity of the *DR5* reporter was reported in the tip of the root cap and the vasculature (Forestan et al., 2012). External application of auxin extends the expression of the reporter, whereas the expression pattern is disrupted by the application of the auxin transport inhibitor NPA, suggesting that the expression patterns of the reporters reflect the actual auxin distribution (Yang et al., 2017; Forestan et al., 2012). However, no expression of the *DR5:GFP* nor a consistent expression pattern of the *DR5v2:VENUS-H2B* was detected in transgenic barley lines (Supplementary figure 5A'). In *Arabidopsis*, the two auxin reporters *DR5* and *DR5v2* exhibit a difference in expression patterns, indicating that the ARFs have a different binding affinity towards the auxin responsive elements TGTCTC (*DR5*) and TGTCGG (*DR5v2*) (Liao et al., 2015). Moreover, it was shown that spacing in between the auxin responsive elements, flanking sequences and the number of repeats are important for the reactivity of the reporter to auxin (Ulmasov et al., 1997). The present results suggest that in barley different auxin responsive elements and/or a different composition of the reporters are necessary for an induction by auxin.

As the *DR5* and *DR5v2* reporter did not deliver a satisfactory reflection of the auxin distribution in barley roots, the expression of auxin downstream targets was analysed. In other plants like rice, maize and *Arabidopsis*, downstream targets of auxin and cytokinin signalling are the *PLTs* (Li and Xue, 2011; Zhang et al., 2014). In *Arabidopsis*, the *PLT* promoters produce an expression gradient in roots with an expression maximum in the stem cell niche, which is broad for *AtPLT1* and *AtPLT2* and more restricted for *AtPLT3* and *AtPLT4*/*BBM* (Galinha et al., 2007). In rice, the root-specific *PLTs* also show an expression maximum around the QC (Li and Xue, 2011). In barley, a similar expression pattern of *HvPLT1* was detected, both on RNA and protein level (Figure 4). This suggests that the expression of *PLTs* is conserved between the plant species, indicating that the well described auxin- and PLT-mediated cell specification mechanism in the root meristem is conserved between *Arabidopsis* and barley (Aida et al., 2004; Galinha et al., 2007; Mähönen et al., 2014).

Auxin distribution in the root is mediated primarily by PIN auxin efflux carriers (Wang et al., 2009; Carraro et al., 2006; Blilou et al., 2005). In barley, 13 proteins were identified that, based on protein sequence homology, probably belong to the PIN family (Supplementary figure 8A). Four PINs can be classified into the subfamily of "long" PINs in regard to their transmembrane topology (HvPIN1a, HvPIN1b, HvPIN1c and HvPIN2, Supplementary figure 8B). The subcellular localisation of HvPIN1a

revealed that it is localised at the plasma membrane in barley root meristems, and polarly localised in certain tissues, just as it was observed for other "long" PINs in *Arabidopsis* and maize (Figure 5B, D') (Gallavotti et al., 2008; Blilou et al., 2005). The PINs of the "short" subfamily in *Arabidopsis* contain only a short central hydrophilic loop and are probably involved in intracellular auxin homeostasis and localise to the ER (Křeček et al., 2009; Mravec et al., 2009). In barley, five PINs were identified that potentially belong to this subfamily: HvPIN8, HvPIN9a, HvPIN9b, HvPIN5a and HvPIN5b, however, their cellular localisation remains to be analysed (Supplementary figure 8A,B). As in rice and in maize, distinct homologues of AtPIN3, AtPIN4 and AtPIN7 could not be identified (Wang et al., 2009; Forestan et al., 2012). For maize it was hypothesized that in the root apex, the three ZmPIN1s could take over the role for PIN3, PIN4 and PIN7 efflux carriers (Forestan et al., 2012). The same distribution of functions could hold true for barley. HvPIN3a, HvPIN3b, HvPIN10a and HvPIN10b are PIN homologues that cannot be assigned as "long" or "short" PIN because their transmembrane topology does not follow either structure (Supplementary figure 8B). This divergence in transmembrane topology has not been reported for PINs in *Arabidopsis*, rice and maize and therefore, the localisation and function of these PINs should be subjected to a closer examination.

PIN1 homologues were found in many plant species. In *Arabidopsis*, AtPIN1 is expressed in the vasculature and weaker in epidermis and cortex (Blilou et al., 2005). In maize, the three PIN1 homologues ZmPIN1s are expressed in the root, with ZmPIN1a expression in the DSCs and the meristematic region, ZmPIN1b expression in the epidermis, root cap and vasculature and ZmPIN1c expression in the epidermis and vasculature of the central cylinder (Forestan et al., 2012). The rice *OsPIN1s* are also expressed in the root, *OsPIN1a* is expressed in the stem cell niche and the root cap, *OsPIN1b* and *c* are additionally expressed in the stele (Wang et al., 2009). In barley, strong HvPIN1a expression was detected in the stele, the endodermis, the cortex, the DSCs and the differentiated root cap, and weak expression in the QC, the first layer of DSCs and the proximal epidermis (Figure 5A'). Thus, the expression of PIN1 in the root is conserved between species, while expression in individual tissues differs (Wang et al., 2009; Blilou et al., 2005; Forestan et al., 2012). On a cellular level, PIN1s localise to the cell membrane, as they act as carriers that provide auxin efflux from the cells. AtPIN1 in *Arabidopsis* localizes to the basal membrane of the vascular cells, while other AtPINs show a localisation to either the basal or apical side of the cells depending on the tissue. AtPIN2, for example, localises apically in the epidermis and basally in the cortex (Blilou et al., 2005). Forestan and colleagues found that ZmPIN1 is polarly localized in the epidermis, in the meristematic regions and the central cylinder at basal membrane (Forestan et al., 2012). Nevertheless, there are exceptions: in the root cap cells, ZmPIN1 is localised in the cytosol (Forestan et al., 2012). The expression pattern as well as the polar localization of the PINs create an auxin flux that is directed to the tip via the vasculature of the roots (Forestan et al., 2012; Carraro et al., 2006; Blilou et al., 2005). In barley, HvPIN1a is basally localized only in the stele, the endodermis and the inner cortex layers, while it is apically localised in the outer cortex layers and the lateral root cap. In the root cap and the QC, no

polar localisation can be observed (Figure 5B, D'). In contrast to the dicot PIN1 (*Arabidopsis*), PIN1s in monocots might therefore have a broader role for the auxin distribution as their expression is not only restricted to the vasculature and their localisation differs according to the tissue type (Figure 5A, B, D) (Blilou et al., 2005; Carraro et al., 2006). Nevertheless, the expression pattern and polar localization of HvPIN1a indicates that also in barley, an auxin flow is created that is directed towards the QC, the stem cell niche and the root cap and also a flow from the stem cell niche to the proximal meristem via the outer cortex cell layers (Figure 5C), as it was proposed for the *Arabidopsis* PINs (Blilou et al., 2005).

4.5. HvPIN1a polar localization is controlled via a BFA sensitive recycling mechanism

Genetic analysis and BFA-treatment experiments revealed that in *Arabidopsis*, the basal localisation of PINs is dependent on the ARF-GEF GNOM (Geldner et al., 2003). The kinase PID regulates the PIN localization by phosphorylating the PINs at the plasma membrane, making them less affine to the GNOM-dependent basal recycling pathway. The phosphorylated PIN proteins are then recruited to the apical GNOM-independent trafficking pathways (Kleine-Vehn et al., 2009; Steinmann et al., 1999; Geldner et al., 2003). For the apically localised AtPIN2 in the *Arabidopsis* epidermis, however, it was shown that its vacuolar trafficking is independent of GNOM and involves an additional, BFA-sensitive ARF-GEF (Kleine-Vehn et al., 2008). In the outer cortex cell layer, where HvPIN1a is localised apically, BFA caused the accumulation of HvPIN1a in vesicles (Figure 6A), indicating that in barley, too, BFA-sensitive components are involved in PIN1 trafficking.

4.6. HvPIN1a expression is downregulated by cytokinin

Besides intracellular localisation of the PIN1 protein, also the expression of *PIN1* is subject to regulation by other factors. Dello Ioio and colleagues showed that in *Arabidopsis*, *AtPIN1* expression is downregulated by cytokinin (Ioio et al., 2008). In rice, the PIN1 homologues *OsPIN1a*, *OsPIN1b* and *OsPIN1c*, however, are not transcriptionally regulated by cytokinin (Wang et al., 2009). In barley, *HvPIN1a* expression is downregulated by cytokinin treatment (Figure 6B, C). Thus, *HvPIN1a* expression is similarly regulated in barley as it is in *Arabidopsis*, but different from rice (Ioio et al., 2008; Wang et al., 2009). Auxin treatment of the barley *TCSn:VENUS-H2B* reporter line furthermore revealed that at least in the stele, cytokinin signalling is not affected by auxin application (Figure 4D, E), suggesting that there is no direct regulation of the cytokinin signalling by auxin.

In summary, barley exhibits many apparently conserved mechanisms with *Arabidopsis*, maize and rice in regard to cytokinin and auxin signalling. External application of both phytohormones causes a reduction in root growth which is probably due to reduced cell elongation in case of auxin and due to a

premature meristem differentiation in case of cytokinin, as it was also observed in other plants. Cytokinin signalling reflected by the *TCSn* reporter occurs in the stele and the differentiated root cap cells, but reporter gene expression can be induced by cytokinin application in the root stem cell niche. Furthermore, the barley genome contains homologues of the *PIN* and *PLT* genes that are connected to auxin and cytokinin signalling in other plants. *HvPLT1* is expressed in a gradient with the maximum in the QC, while *HvPIN1a* is expressed in the whole root meristem, but weaker in the epidermis and the QC. *HvPIN1a* expression is downregulated by cytokinin application, as it was shown for *Arabidopsis*, and its intracellular localisation is regulated in a BFA-sensitive manner.

5. Supplementary figures

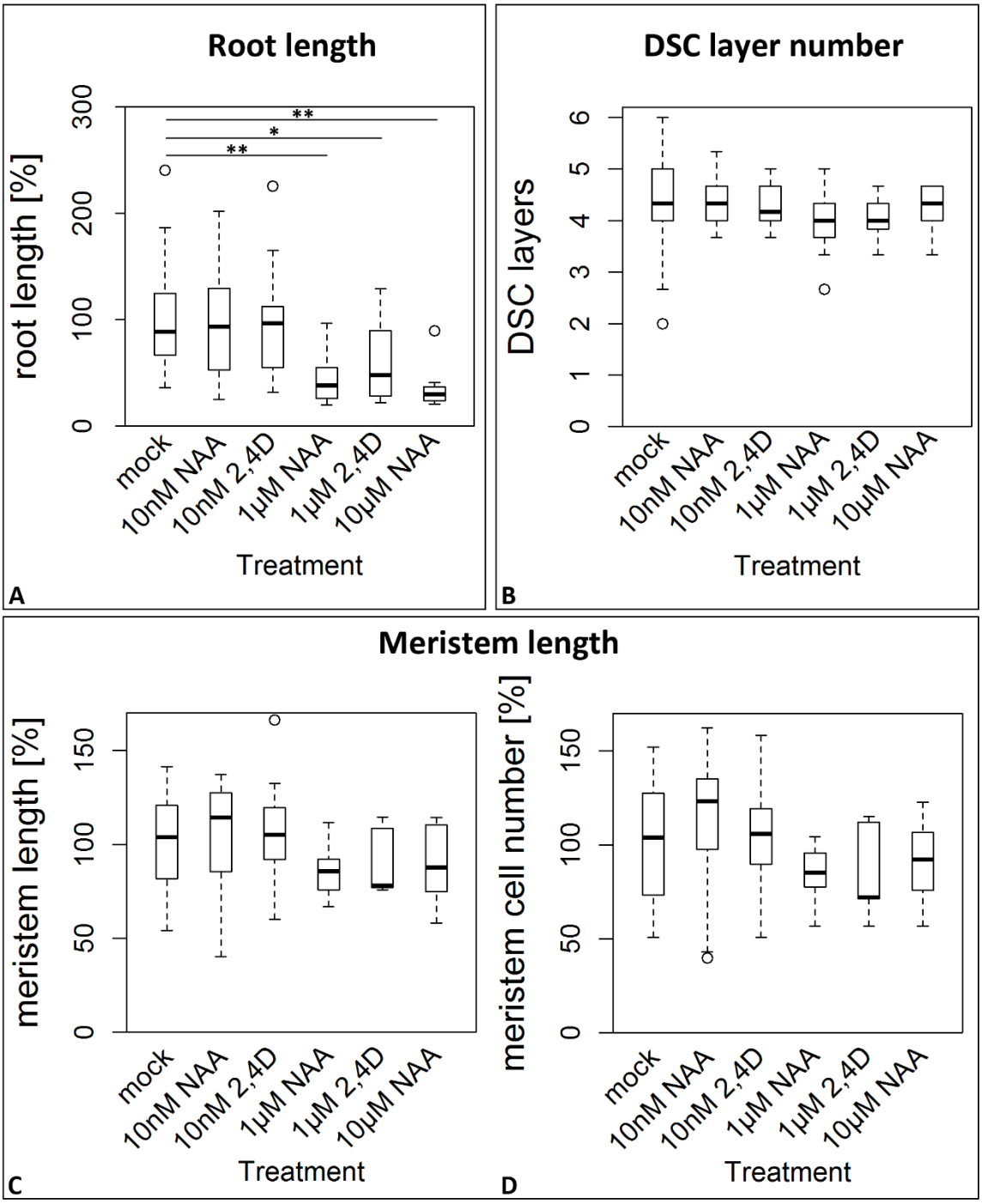

Supplementary figure 1: Root length and meristem size given as percent of the respective mock-treated plants and DSC layer number of the cv. Morex upon 6-day treatment with auxin.

A) Root length after 6-day treatment with auxin; experiment was performed twice; for a better comparison between the experiments, all values were normalized to the respective mock-treated plants; n = 12-31 plants per data point. **B)** Number of DSC layers upon 6-day treatment with auxin; experiment was performed twice; n = 6-21 per data point. **C), D)** Meristem size upon 6-day auxin treatment, measured by meristem length (C)) or meristem cell number (D)); experiment was performed twice; all values are normalized to the mock-treated

control; n = 6-27 roots per data point; significance was determined using the two-tailed Student's t test, * = $p<0.05$, **= $p<0.001$.

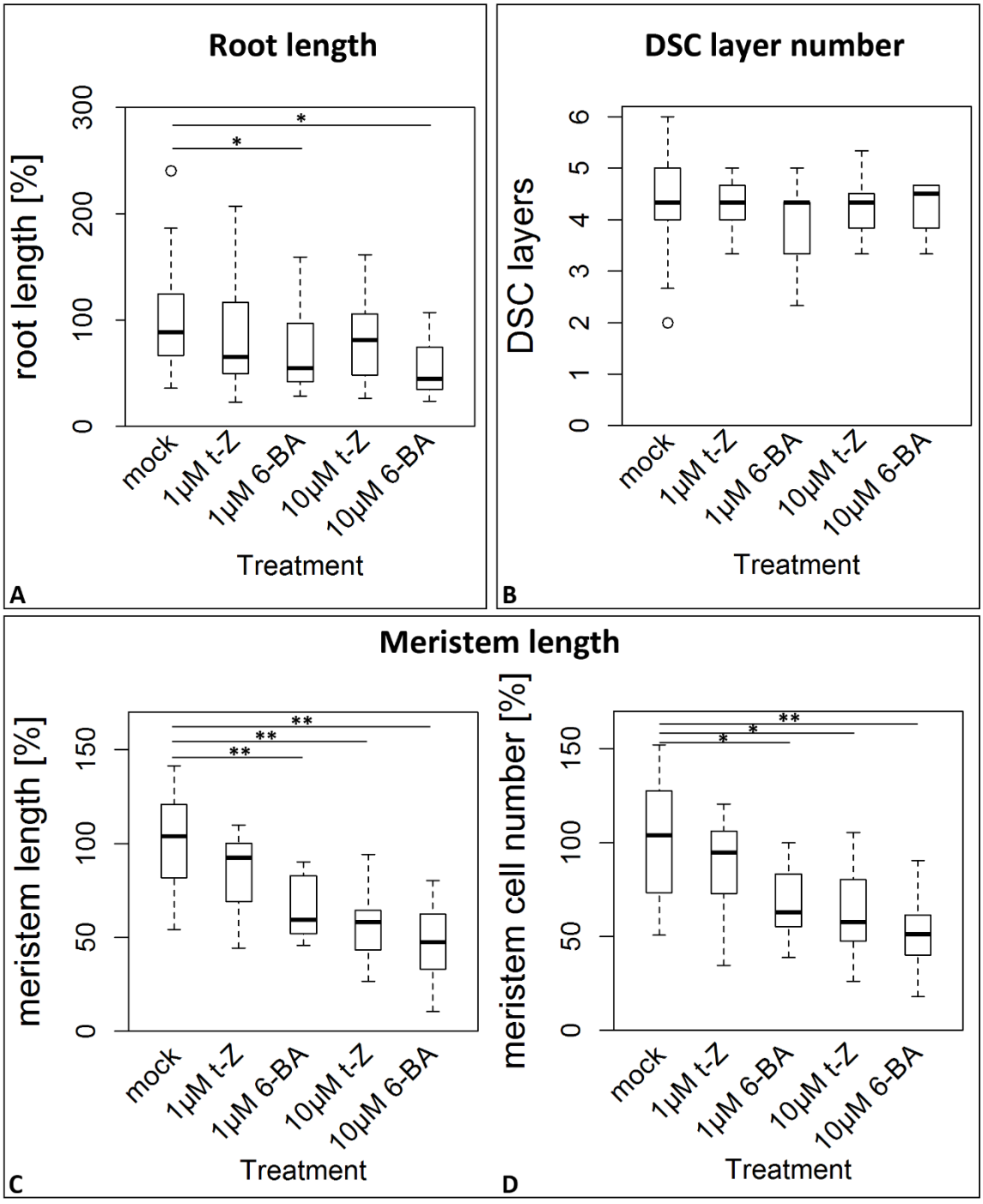

Supplementary figure 2: Root length and meristem size given as percent of the respective mock-treated plants and DSC layer number of the cv. Morex upon 6-day treatment with cytokinin.
A) Root length after 6-day treatment with cytokinin; experiment was performed twice; for a better comparison between the experiments, all values were normalized to the respective mock-treated plants; n = 15-31 plants per data point. **B)** Number of DSC layers upon 6-day treatment with cytokinin; experiment was performed twice;

n = 4-21 per data point. **C), D)** Meristem size upon 6-day cytokinin treatment, measured by meristem length (C)) or meristem cell number (D)); experiment was performed twice; all values are normalized to the mock-treated control; n = 13-27 roots per data point; significance was determined using the two-tailed Student's t test, * = $p<0.05$, **= $p<0.001$.

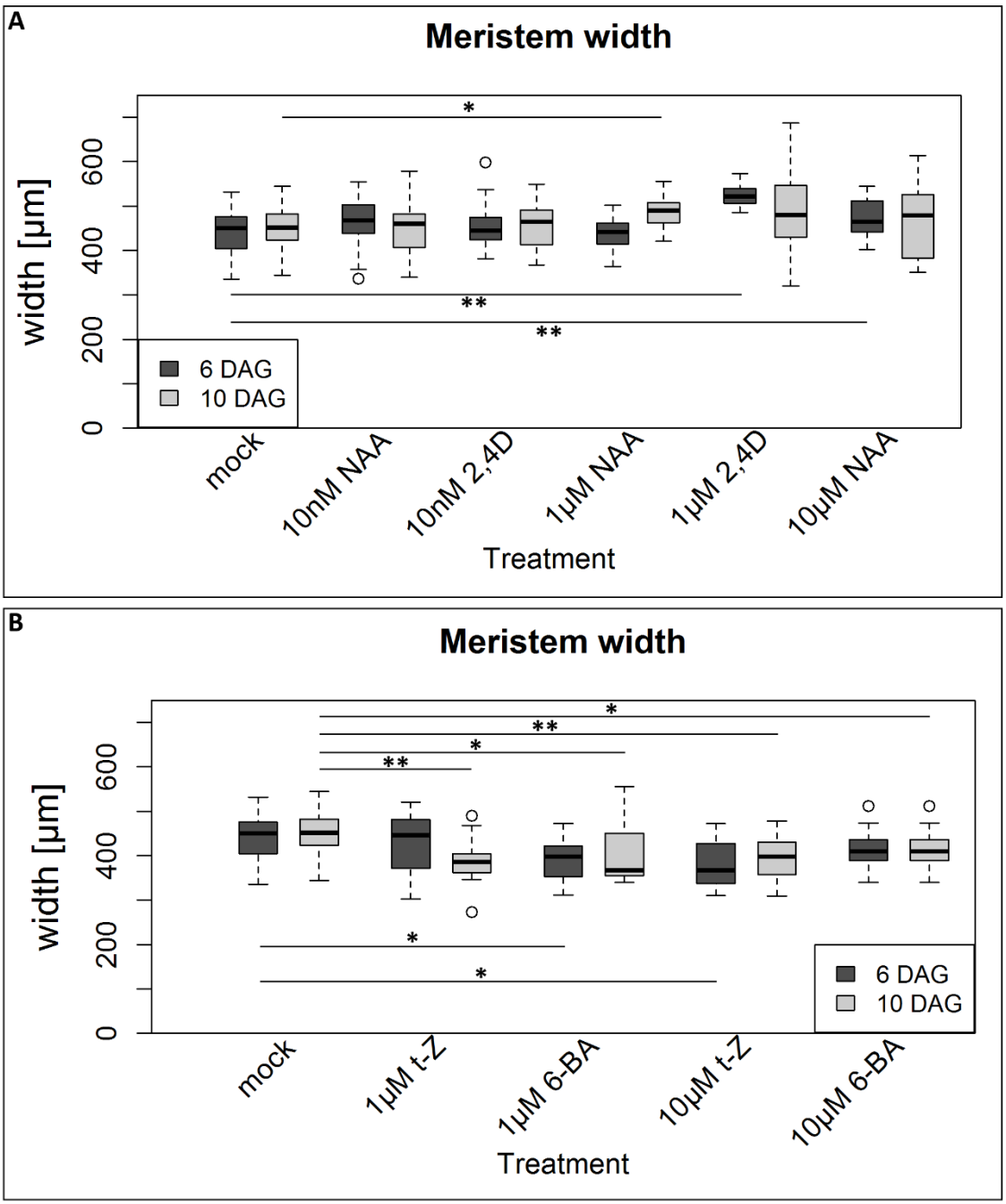

Supplementary figure 3: Root meristem width upon auxin and cytokinin treatment.

Meristem width measured at the transition zone from root meristems exemplarily shown in Figure 1B and Figure 2B. **A)** Roots were treated with auxin for 6 or 10 days according to the colour of the boxplots;

experiment was performed twice; n = 7-27 (6 DAG), n = 12-25 (10 DAG) roots per data point. **B)** Roots were treated with cytokinin for 6 or 10 days according to the colour of the boxplots; experiments were performed twice; n = 13-27 (6 DAG), n = 15-25 (10 DAG) roots per data point; significance was determined using the two-tailed Student's t test, * = p<0.05, **= p<0.001.

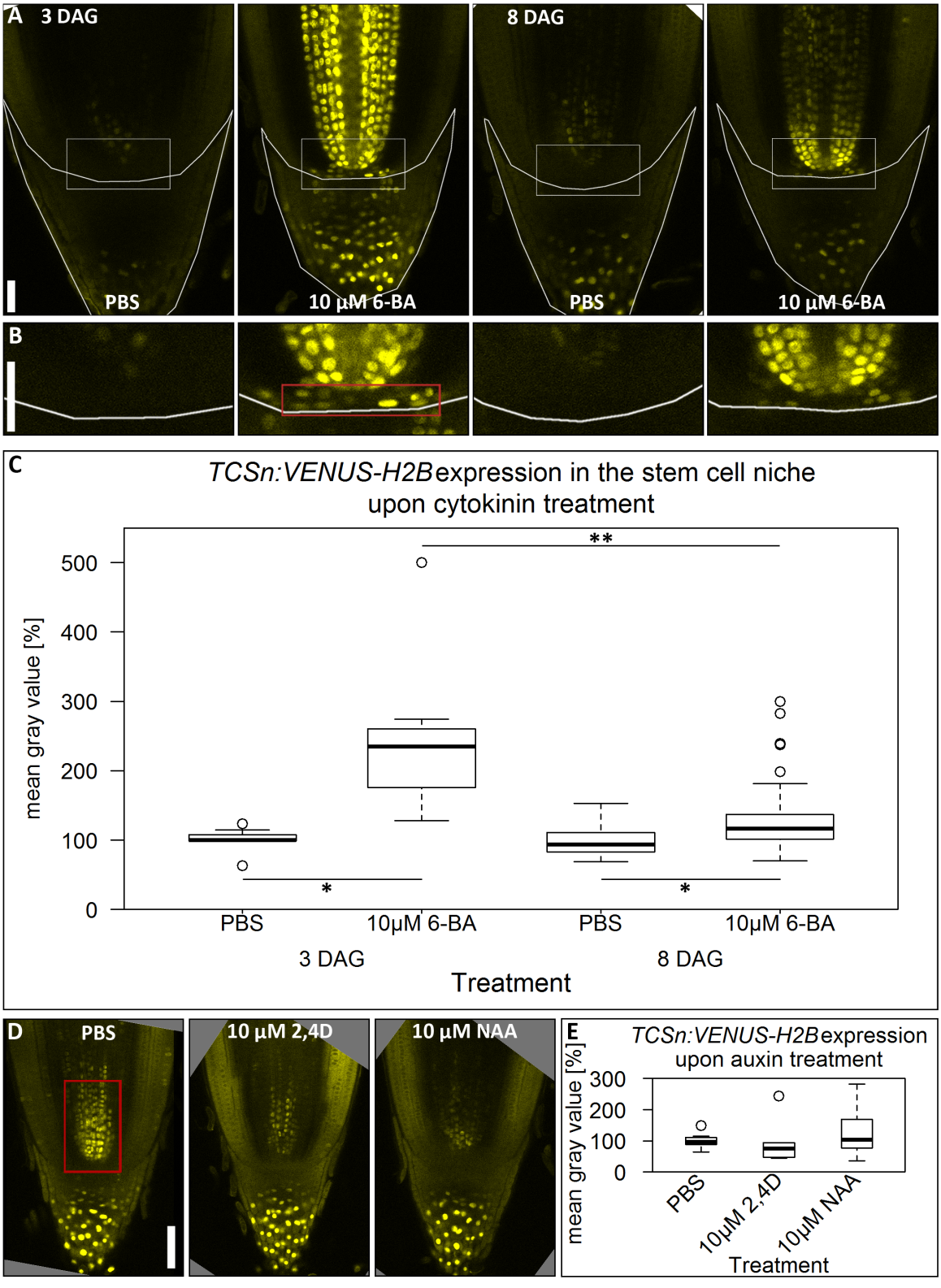

Supplementary figure 4: Expression of *TCSn:VENUS-H2B* in 3-day old seedlings in comparison to roots 8 DAG and auxin treatments in the cv. Golden Promise.

A) Expression of *TCSn:VENUS-H2B* in roots 3 or 8 DAG upon mock (PBS only) or 10 µM 6-BA treatment according to the captions; white outlines mark the root cap. **B)** Magnification of the region marked with the white rectangle in A); scale bars 50 µm. **C)** Quantification of the VENUS expression by mean gray value of the region marked with the red rectangle in B); experiment was performed twice; three independent transgenic lines were examined; n = 7-41 significance was determined using the two-tailed Student's t test, * = $p<0.05$, **= $p<0.001$. **D)** Representative pictures of the *TCSn:VENUS-H2B* expression in root meristems upon 24 h of auxin treatment according to the captions. **E)** Quantification of the *TCSn:VENUS-H2B* expression in the stele by the mean gray value of the region marked with the red box in E); mean gray value is normalized to the PBS control; experiment was performed once; n = 5-15; significance was determined using the two-tailed Student's t test, **= $p<0.001$; scale bar 100 µm; for a better comparison between samples, roots were cleared as described in Material and Methods (A), B), D)).

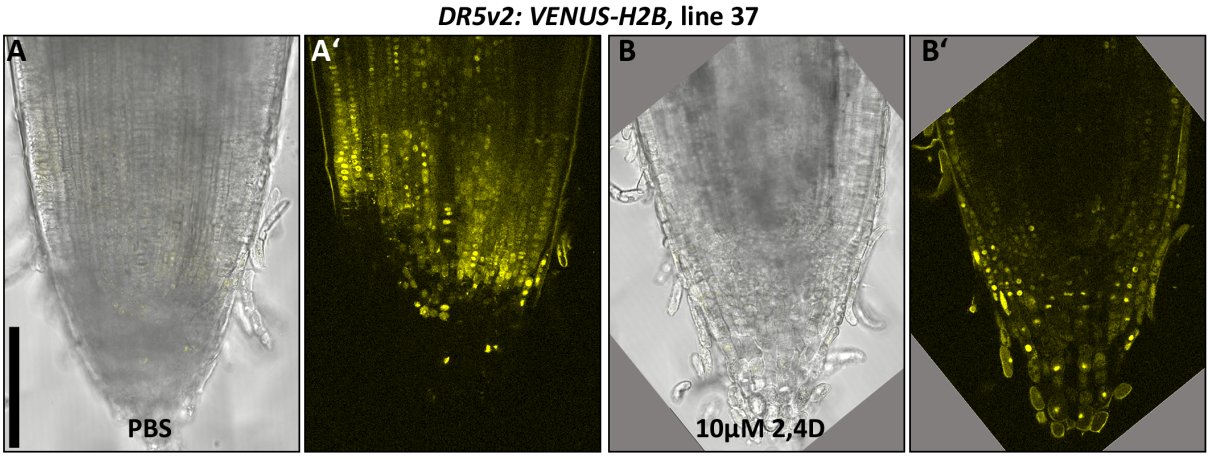

Supplementary figure 5: Expression of the auxin reporter *DR5v2:VENUS-H2B* in the root meristem of the barley cv. Golden Promise 8 DAG.

A) Exemplary picture of *DR5v2:VENUS-H2B* expression in the transgenic line 37; transmitted light and VENUS emission (A)), VENUS emission only (A')); VENUS expression is very weak and inconsistent between roots and independent transgenic lines. **B)** *DR5v2:VENUS-H2B* expression upon treatment with 10 µM 2, 4D for 24 h; transmitted light and VENUS emission (B)), VENUS emission only (B')); *DR5v2:VENUS-H2B* expression intensity is unchanged upon treatment with the non-transportable auxin 2,4D in comparison to PBS treatment (A)), indicating that the *DR5v2:VENUS-H2B* construct does not reflect auxin signalling; hand-sections; scale bars 200 µm.

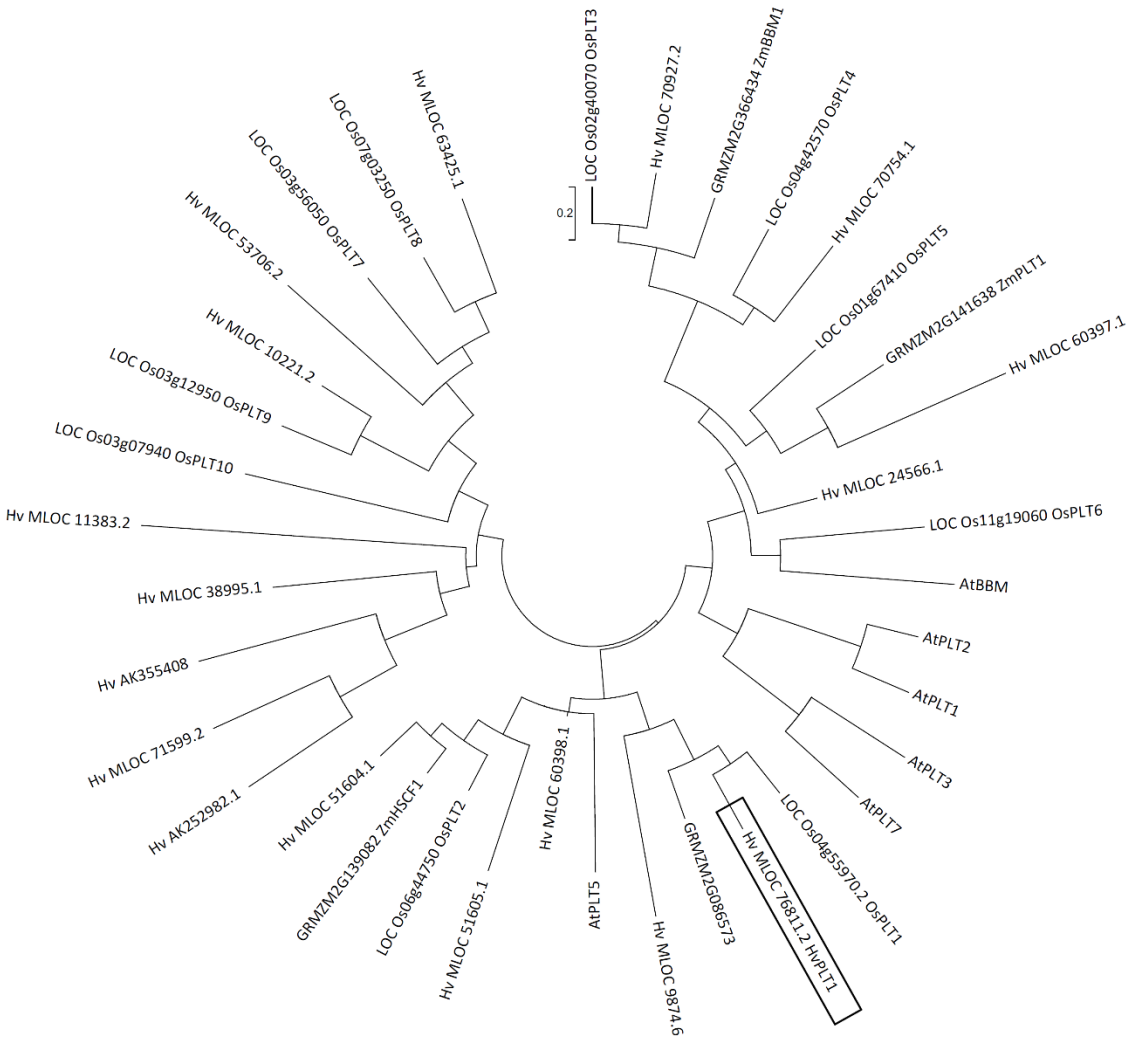

Supplementary figure 6: Phylogenetic tree of PLT homologue proteins in rice, maize, *Arabidopsis* and barley.

Rice PLT sequences were named according to Li and Xue (Li and Xue, 2011), *Arabidopsis* PLT sequences were taken from arabidopsis.org; maize PLT sequences were identified in a BLAST search with AtPLT1 as template (e-value below 5e-75) on the Phytozomev.12.0 website and named according to Zhang et al., 2014; barley genes were identified by BLAST-p search on http://webblast.ipk-gatersleben.de/barley/ with AtPLT1 as template (e-value below 4e-47 for high-confidence genes and 2e-11 for low-confidence genes; "Hv" was added to mark all barley genes; the chosen candidate as PLT1 homologue HvPLT1 is marked with a black frame. Alignments were performed using MEGA7. 0 (Molecular Evolutionary Genetics Analysis version 7.0 for bigger datasets (Kumar, Stecher and Tamura 2015)) and a MUSCLE alignment; the phylogenetic tree was obtained using MEGA7.0 by the Maximum Likelihood method; the tree with the highest log likelihood (-25123.8247) is shown; initial tree(s) for the heuristic search were obtained automatically by applying Neighbor-Join and BioNJ algorithms to a matrix of pairwise distances estimated using a JTT model, and then selecting the topology with superior log likelihood value; the tree is drawn to scale, with branch lengths measured in the number of substitutions per site; all

positions containing gaps and missing data were eliminated.

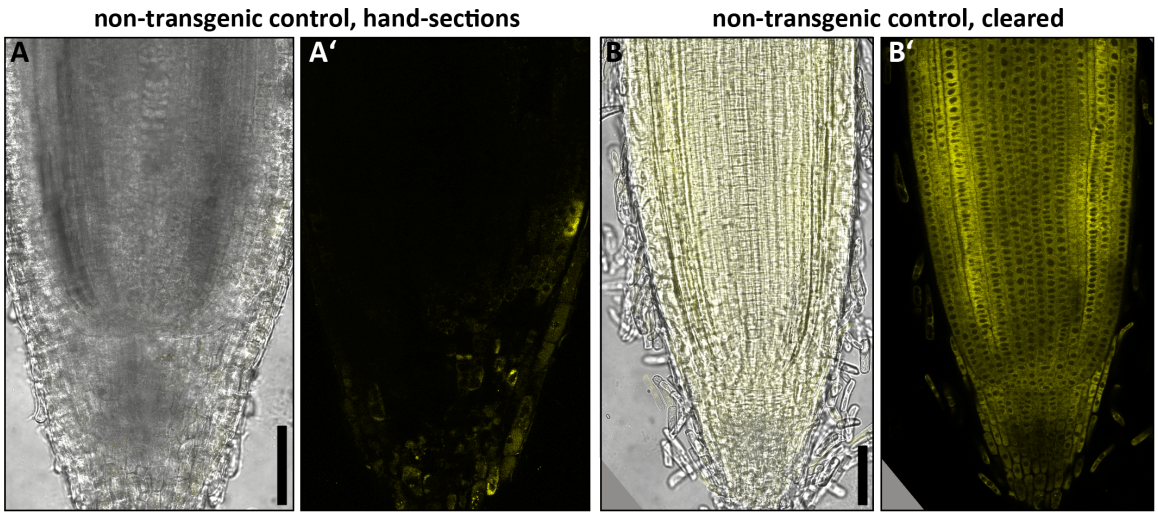

Supplementary figure 7: Barley cv. Golden Promise as non-transgenic control.

A) Representative picture of the root meristem of a non-transgenic Golden Promise seedling 8 DAG; transmitted light and mVENUS emission (A)), mVENUS emission only (A’)), same settings as in Figure 4B, B’; hand-sections as described in Material and Methods; only background signal with mVENUS excitation. **B)** Representative picture of the root meristem of a non-transgenic Golden Promise seedling 8 DAG; transmitted light and mVENUS emission (B)), mVENUS emission only (B’)), same settings as in Figure 5A’; cleared as described in Material and Methods; only background signal with mVENUS excitation; scale bars 100 µm.

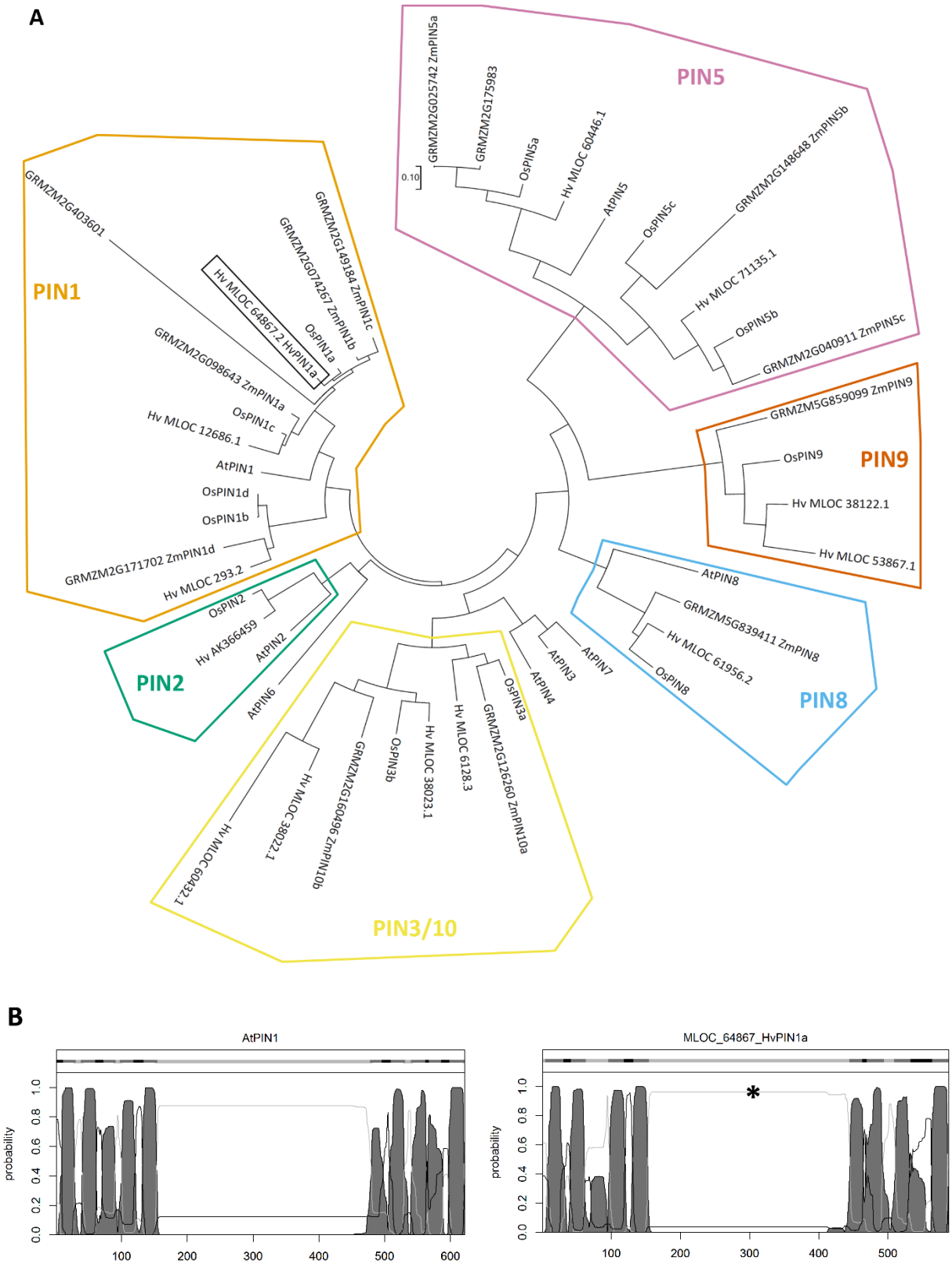
A
PIN5
GRMZM2G025742 ZmPIN5a
GRMZM2G175983
OsPIN5a
Hv MLOC 60446.1
AtPIN5
OsPIN5c
GRMZM2G148648 ZmPIN5b
Hv MLOC 71135.1
OsPIN5b
GRMZM2G040911 ZmPIN5c
0.10
PIN1
GRMZM2G403601
GRMZM2G149184 ZmPIN1c
GRMZM2G074267 ZmPIN1b
Hv MLOC 64867.2 HvPIN1a
OsPIN1a
GRMZM2G098643 ZmPIN1a
OsPIN1c
Hv MLOC 12686.1
AtPIN1
OsPIN1d
OsPIN1b
GRMZM2G171702 ZmPIN1d
Hv MLOC 293.2
PIN9
GRMZM5G859099 ZmPIN9
OsPIN9
Hv MLOC 38122.1
Hv MLOC 53867.1
PIN2
OsPIN2
Hv AK366459
AtPIN2
AtPIN6
PIN8
AtPIN8
GRMZM5G839411 ZmPIN8
Hv MLOC 61956.2
OsPIN8
AtPIN3
AtPIN7
AtPIN4
PIN3/10
OsPIN3a
GRMZM2G126260 ZmPIN10a
Hv MLOC 6128.3
Hv MLOC 38023.1
OsPIN3b
GRMZM2G160496 ZmPIN10b
Hv MLOC 38022.1
Hv MLOC 60432.1
B
AtPIN1
MLOC_64867_HvPIN1a
probability
0.0
0.2
0.4
0.6
0.8
1.0
100
200
300
400
500
600
*

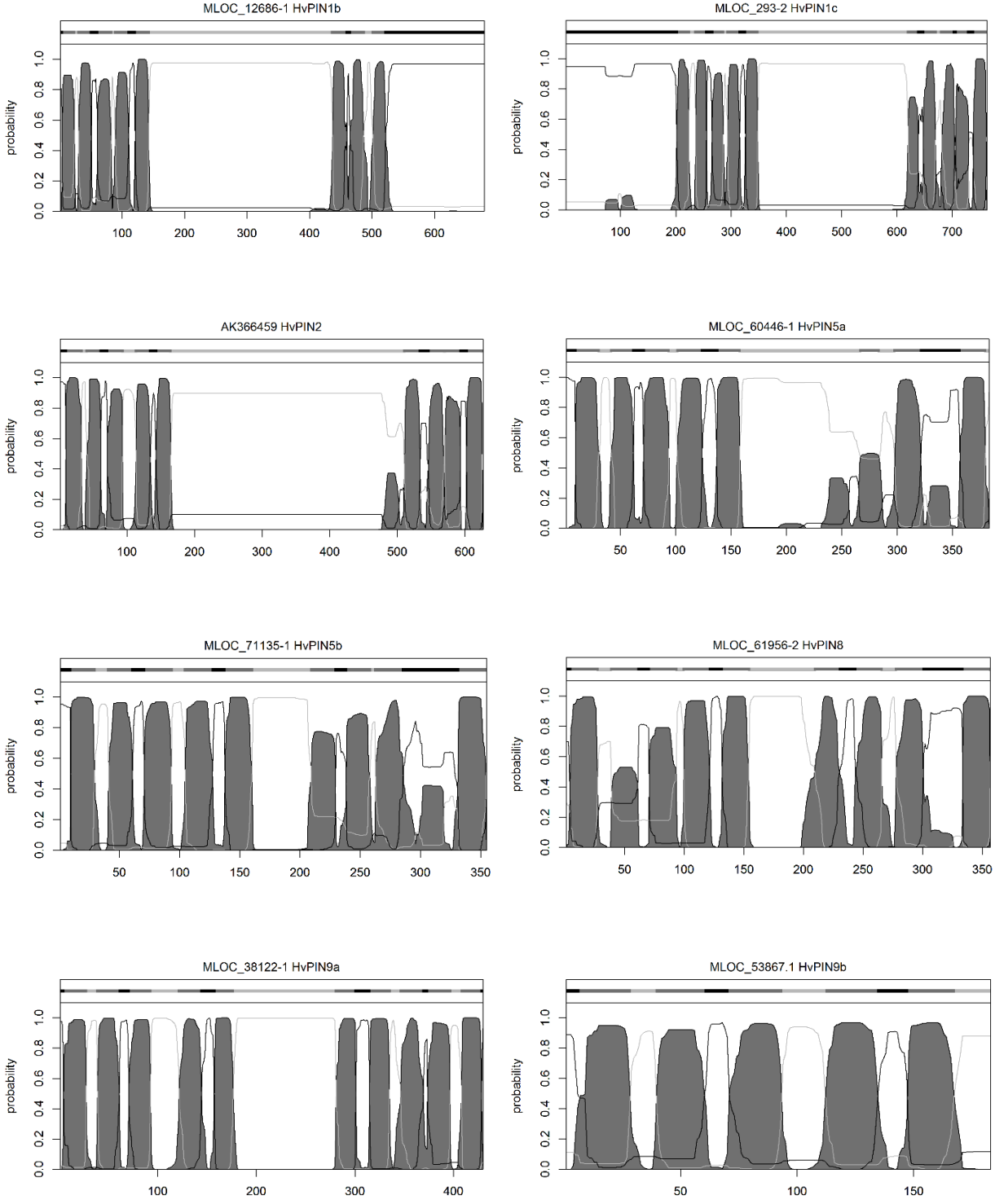
MLOC_12686-1 HvPIN1b
MLOC_293-2 HvPIN1c
AK366459 HvPIN2
MLOC_60446-1 HvPIN5a
MLOC_71135-1 HvPIN5b
MLOC_61956-2 HvPIN8
MLOC_38122-1 HvPIN9a
MLOC_53867.1 HvPIN9b
probability

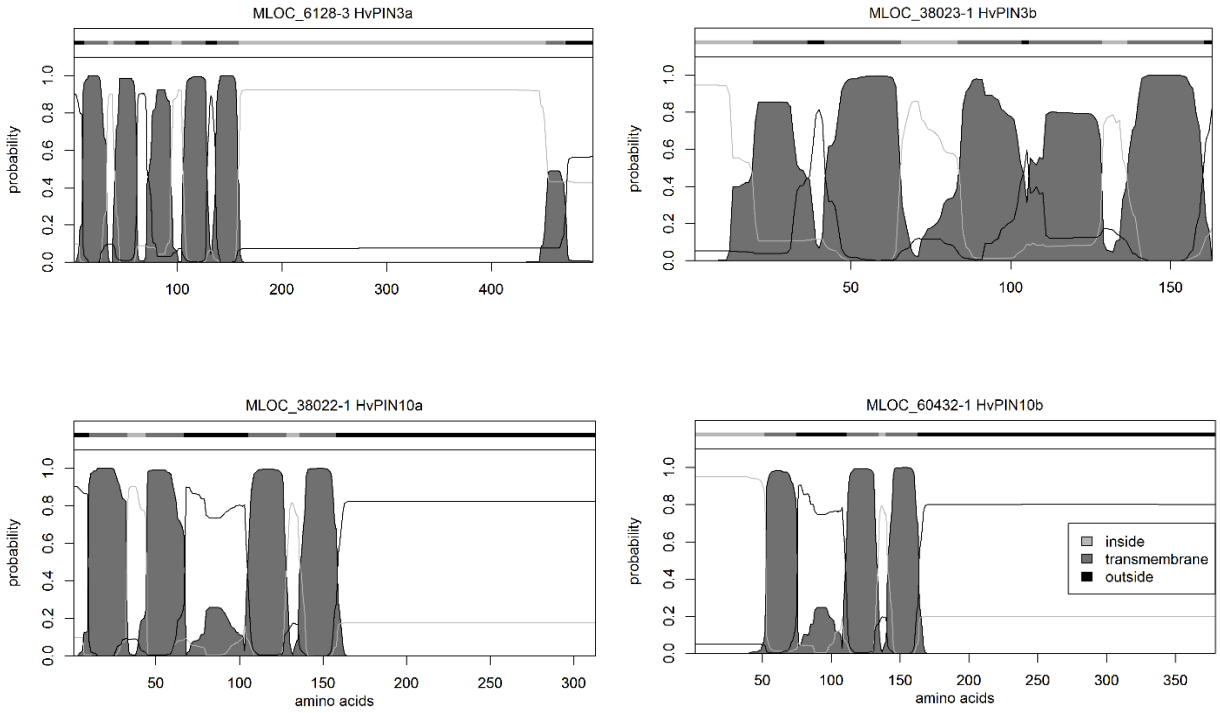

Supplementary figure 8: Phylogeny and topology of barley PINs.

A) Phylogenetic tree of maize, *Arabidopsis*, rice and barley PINs; barley PINs were taken from http://webblast.ipk-gatersleben.de/barley/ with BLAST-p with HvPIN1a (MLOC_64867) as template (e-value below 1e-41 for high and low-confidence genes); rice sequences are taken from Miyashita et al., 2010; *Arabidopsis* PINs were searched at arabidopsis.org; maize PINs were taken from Phytozome v12 (e-value below 4.3e-29) and named according to Forestan et al., 2012. Alignments were performed using MEGA7. 0 (Molecular Evolutionary Genetics Analysis version 7.0 for bigger datasets, Kumar, Stecher and Tamura 2015) and a MUSCLE alignment; the phylogenetic tree was obtained using MEGA7.0 by the Maximum Likelihood method; the tree with the highest log likelihood (-25123.8247) is shown; initial tree(s) for the heuristic search were obtained automatically by applying Neighbor-Join and BioNJ algorithms to a matrix of pairwise distances estimated using a JTT model, and then selecting the topology with superior log likelihood value; the tree is drawn to scale, with branch lengths measured in the number of substitutions per site; proteins of the same subfamily are framed with the same colour; black frame marks HvPIN1a. **B)** Topology of the transmembrane barley PIN proteins in comparison to AtPIN1; domains predicted to the inside of the cell are shown in light-gray, transmembrane domains are shown in dark-gray and domains outside the cell are depicted in black according to the legend; in the protein topology of MLOC_64867 - HvPIN1a the asterisk marks the site where mVENUS is inserted for the reporter line shown in Figure 5; newly identified HvPINs are named according to their topology and the cluster of the *Arabidopsis*, maize and rice PIN family to which they belong.

6. References

Aida, M., Beis, D., Heidstra, R., Willemsen, V., Blilou, I., Galinha, C., Nussaume, L., Noh, Y., Amasino, R., and Scheres, B. (2004). The PLETHORA Genes Mediate Patterning of the Arabidopsis Root Stem Cell Niche. Cell **119**: 109–120.

Benková, E., Michniewicz, M., Sauer, M., Teichmann, T., Seifertová, D., Jürgens, G., and Friml, J. (2003). Local, Efflux-Dependent Auxin Gradients as a Common Module for Plant Organ Formation. Cell **115**: 591–602.

van den Berg, C., Willemsen, V., Hendriks, G., Weisbeek, P., and Scheres, B. (1997). Short-range control of cell differentiation in the Arabidopsis root meristem. Nature **390**: 287–289.

Bishopp, A., Benková, E., and Helariutta, Y. (2011). Sending mixed messages: auxin-cytokinin crosstalk in roots. Curr. Opin. Plant Biol. **14**: 10–6.

Bleckmann, A., Weidtkamp-Peters, S., Seidel, C.A.M., and Simon, R. (2010). Stem Cell Signaling in Arabidopsis Requires CRN to Localize CLV2 to the Plasma Membrane. Plant Physiol. **152**: 166–76.

Blilou, I., Xu, J., Wildwater, M., Willemsen, V., Paponov, I., Friml, J., Heidstra, R., Aida, M., Palme, K., and Scheres, B. (2005). The PIN auxin efflux facilitator network controls growth and patterning in Arabidopsis roots. Nature **433**: 39–44.

Carraro, N., Forestan, C., Canova, S., Traas, J., and Varotto, S. (2006). ZmPIN1a and ZmPIN1b Encode Two Novel Putative Candidates for Polar Auxin Transport and Plant Architecture Determination of Maize. Plant Physiol. **142**: 254–64.

Clowes, F.A.L. (1978). Origin of the Quiescent Centre in Zea Mays. New Phytol. **80**: 409–419.

Curtis, M.D. and Grossniklaus, U. (2003). A Gateway Cloning Vector Set for High-Throughput Functional Analysis of Genes in Planta. Plant Physiol. **133**: 462–469.

Da-Xi, Z., Ke, Y., Zhi-Hong, X., and Hong-Wei, X. (2003). Effect of Polar Auxin Transport on Rice Root Development. Acta Bot. Sin. **45**: 1421–1427.

Delbarre, A., Muller, P., Imhoff, V., and Guern, J. (1996). Comparison of mechanisms controlling uptake and accumulation of 2,4-dichlorophenoxy acetic acid, naphthalene-1-acetic acid, and indole-3-acetic acid in suspension-cultured tobacco cells. Planta **198**: 532–541.

Ding, Z. and Friml, J. (2010). Auxin regulates distal stem cell differentiation in Arabidopsis roots. Proc. Natl. Acad. Sci. U. S. A. **107**: 12046–12051.

Dolan, L., Janmaat, K., Willemsen, V., Linstead, P., Poethig, S., Roberts, K., and Scheres, B. (1993). Cellular organisation of the Arabidopsis thaliana root. Development **119**: 71–84.

Evans, M.L., Ishikawa, H., and Estelle, M.A. (1994). Responses of Arabidopsis roots to auxin studied with high temporal resolution: Comparison of wild type and auxin-response mutants. Planta **194**: 215–222.

Feldman, L.J. (1976). The de novo Origin of the Quiescent Center Regenerating Root Apices of Zea

mays. Planta **128**: 207–212.

Forestan, C., Farinati, S., and Varotto, S. (2012). The Maize PIN Gene Family of Auxin Transporters. Front. Plant Sci. **3**: 1–23.

Friml, J., Benkova, E., Blilou, I., Wisniewska, J., Hamann, T., Ljung, K., Woody, S., Sandberg, G., Scheres, B., Jürgens, G., and Palme, K. (2002). AtPIN4 Mediates Sink-Driven Auxin Gradients and Root Patterning in Arabidopsis. Cell **108**: 661–673.

Friml, J., Vieten, A., Sauer, M., Weijers, D., Schwarz, H., Hamann, T., Offringa, R., and Jürgens, G. (2003). Efflux-dependent auxin gradients establish the apical-basal axis of Arabidopsis. Nature **426**: 147–53.

Galinha, C., Hofhuis, H., Luijten, M., Willemsen, V., Blilou, I., Heidstra, R., and Scheres, B. (2007). PLETHORA proteins as dose-dependent master regulators of Arabidopsis root development. Nature **449**: 1053–7.

Gallavotti, A., Yang, Y., Schmidt, R.J., and Jackson, D. (2008). The Relationship between Auxin Transport and Maize Branching. Plant Physiol. **147**: 1913–1923.

Galuszka, P., Popelková, H., Werner, T., Frébortová, J., Pospíšilová, H., Mik, V., Köllmer, I., Schmülling, T., and Frébort, I. (2007). Biochemical Characterization of Cytokinin Oxidases/Dehydrogenases from Arabidopsis thaliana Expressed in Nicotiana tabacum L. J. Plant Growth Regul. **26**: 255–267.

Ganguly, A., Lee, S.H., Cho, M., Lee, O.R., Yoo, H., and Cho, H.-T. (2010). Differential Auxin-Transporting Activities of PIN-FORMED Proteins in Arabidopsis Root Hair Cells. Plant Physiol. **153**: 1046–1061.

Geldner, N., Anders, N., Wolters, H., Keicher, J., Kornberger, W., Muller, P., Delbarre, A., Ueda, T., Nakano, A., and Jürgens, G. (2003). The Arabidopsis GNOM ARF-GEF Mediates Endosomal Recycling, Auxin Transport, and Auxin-Dependent Plant Growth. Cell **112**: 219–230.

Geldner, N., Friml, J., Stierhof, Y.D., Jürgens, G., and Palme, K. (2001). Auxin transport inhibitors block PIN1 cycling and vesicle trafficking. Nature **413**: 425–428.

Grieneisen, V.A., Xu, J., Marée, A.F.M., Hogeweg, P., and Scheres, B. (2007). Auxin transport is sufficient to generate a maximum and gradient guiding root growth. Nature **449**: 1008–13.

Hejátko, J., Blilou, I., Brewer, P.B., Friml, J., Scheres, B., and Benková, E. (2006). In situ hybridization technique for mRNA detection in whole mount Arabidopsis samples. Nat. Protoc. **1**: 1939–1946.

Imani, J., Li, L., Schäfer, P., and Kogel, K.-H. (2011). STARTS - A stable root transformation system for rapid functional analyses of proteins of the monocot model plant barley. Plant J. **67**: 726–735.

Dello Ioio, R., Linhares, F.S., Scacchi, E., Casamitjana-Martinez, E., Heidstra, R., Costantino, P., and Sabatini, S. (2007). Cytokinins determine Arabidopsis root-meristem size by controlling

cell differentiation. Curr. Biol. **17**: 678–682.

Ioio, R.D., Nakamura, K., Moubayidin, L., Perilli, S., Taniguchi, M., Morita, M.T., Aoyama, T., Costantino, P., and Sabatini, S. (2008). A Genetic Framework for the Control of Cell Division and Differentiation in the Root Meristem. Science **322**: 1380–1384.

Kirschner, G.K., Stahl, Y., Von Korff, M., and Simon, R. (2017). Unique and Conserved Features of the Barley Root Meristem. Front. Plant Sci. **8:** 1240.

Kleine-Vehn, J., Huang, F., Naramoto, S., Zhang, J., Michniewicz, M., Offringa, R., and Friml, J. (2009). PIN Auxin Efflux Carrier Polarity Is Regulated by PINOID Kinase-Mediated Recruitment into GNOM-Independent Trafficking in Arabidopsis. Plant Cell **21**: 3839–3849.

Kleine-Vehn, J., Leitner, J., Zwiewka, M., Sauer, M., Abas, L., Luschnig, C., and Friml, J. (2008). Differential degradation of PIN2 auxin efflux carrier by retromer-dependent vacuolar targeting. Proc. Natl. Acad. Sci. U. S. A. **105**: 17812–17817.

Köllmer, I., Novák, O., Strnad, M., Schmülling, T., and Werner, T. (2014). Overexpression of the cytosolic cytokinin oxidase/dehydrogenase (CKX7) from Arabidopsis causes specific changes in root growth and xylem differentiation. Plant J. **78**: 359–371.

Koushik, S. V, Chen, H., Thaler, C., Puhl, H.L., and Vogel, S.S. (2006). Cerulean, Venus, and VenusY67C FRET Reference Standards. Biophys. J. **91**: L99–L101.

Křeček, P., Skůpa, P., Libus, J., Naramoto, S., Tejos, R., Friml, J., and Zažímalová, E. (2009). The PIN-FORMED (PIN) protein family of auxin transporters. Genome Biol. **10**: 1–11.

Krogh, A., Larsson, B., von Heijne, G., and Sonnhammer, E.L.. (2001). Predicting transmembrane protein topology with a hidden markov model: application to complete genomes. J. Mol. Biol. **305**: 567–580.

Lampropoulos, A., Sutikovic, Z., Wenzl, C., Maegele, I., Lohmann, J.U., and Forner, J. (2013). GreenGate - A Novel, Versatile, and Efficient Cloning System for Plant Transgenesis. PLoS One **8**: e83043.

Li, P. and Xue, H. (2011). Structural characterization and expression pattern analysis of the rice PLT gene family. ActaBiochim Biophys Sin **43**: 688–697.

Liao, C., Smet, W., Brunoud, G., Yoshida, S., Vernoux, T., and Weijers, D. (2015). Reporters for sensitive and quantitative measurement of auxin response. Nat. Methods **12**: 207–210.

Maas, E.V. and Hoffman, G.J. (1977). Crop salt tolerance - current assessment. J. Irrig. Drain. Div. Am. Soc. Civ. Eng. **103**: 115–134.

Mähönen, A.P., Tusscher, K. ten, Siligato, R., Smetana, O., Díaz-Triviño, S., Salojärvi, J., Wachsman, G., Prasad, K., Heidstra, R., and Scheres, B. (2014). PLETHORA gradient formation mechanism separates auxin responses. Nature **515**: 125–129.

Martínez-de la Cruz, E., García-Ramírez, E., Vázquez-Ramos, J.M., Reyes de la Cruz, H., and López-Bucio, J. (2015). Auxins differentially regulate root system architecture and cell cycle

protein levels in maize seedlings. J. Plant Physiol. **176**: 147–156.

Mayer, K.F.X. et al., The International Barley Genome Sequencing Consortium (2012). A physical, genetic and functional sequence assembly of the barley genome. Nature **491**: 711–716.

Miyashita, Y., Takasugi, T., and Ito, Y. (2010). Identification and expression analysis of PIN genes in rice. Plant Sci. **178**: 424–428.

Mravec, J. et al. (2009). Subcellular homeostasis of phytohormone auxin is mediated by the ER-localized PIN5 transporter. Nature **459**: 1136–1140.

Mrízová, K., Jiskrová, E., Vyroubalová, S., Novák, O., Ohnoutková, L., Pospíšilová, H., Frébort, I., Harwood, W. a, and Galuszka, P. (2013). Overexpression of Cytokinin Dehydrogenase Genes in Barley (Hordeum vulgare cv. Golden Promise) Fundamentally Affects Morphology and Fertility. PLoS One **8**: e79029.

Müller, B. and Sheen, J. (2008). Cytokinin and auxin interaction in root stem-cell specification during early embryogenesis. Nature **453**: 1094–7.

Müssig, C., Shin, G.-H., and Altmann, T. (2003). Brassinosteroids promote root growth in Arabidopsis. Plant Physiol. **133**: 1261–1271.

Nagai, T., Ibata, K., Park, E.S., Kubota, M., Mikoshiba, K., and Miyawaki, A. (2002). A variant of yellow fluorescent protein with fast and efficient maturation for cell-biological applications. Nat. Biotechnol. **20**: 87–90.

Ni, J., Shen, Y., Zhang, Y., and Wu, P. (2014). Definition and stabilisation of the quiescent centre in rice roots. Plant Biol. **16**: 1014–1019.

Perrot-Rechenmann, C. (2010). Cellular responses to auxin: division versus expansion. Cold Spring Harb. Perspect. Biol. **2**: 1–15.

Peyroche, A., Antonny, B., Robineau, S., Acker, J., Cherfils, J., and Jackson, C.L. (1999). Brefeldin A Acts to Stabilize an Abortive ARF–GDP–Sec7 Domain Protein Complex. Mol. Cell **3**: 275–285.

Podlešáková, K., Zalabák, D., Čudejková, M., Plíhal, O., Szücová, L., Doležal, K., Spíchal, L., Strnad, M., and Galuszka, P. (2012). Novel Cytokinin Derivatives Do Not Show Negative Effects on Root Growth and Proliferation in Submicromolar Range. PLoS One **7**: e39293.

Ponce, G., Luján, R., Campos, M.E., Reyes, a, Nieto-Sotelo, J., Feldman, L.J., and Cassab, G.I. (2000). Three maize root-specific genes are not correctly expressed in regenerated caps in the absence of the quiescent center. Planta **211**: 23–33.

Pospíšilová, H. et al. (2016). Transgenic barley overexpressing a cytokinin dehydrogenase gene shows greater tolerance to drought stress. N. Biotechnol. **33**: 692–705.

R Core Team (2015). R: A language and environment for statistical computing. R Foundation for Statistical Computing.

Ruzicka, K., Simásková, M., Duclercq, J., Petrásek, J., Zazímalová, E., Simon, S., Friml, J., Van Montagu, M.C.E., and Benková, E. (2009). Cytokinin regulates root meristem activity via

modulation of the polar auxin transport. Proc. Natl. Acad. Sci. U. S. A. **106**: 4284–9.

Sabatini, S., Beis, D., Wolkenfelt, H., Murfett, J., Guilfoyle, T., Malamy, J., Benfey, P., Leyser, O., Bechtold, N., Weisbeek, P., and Scheres, B. (1999). An Auxin-Dependent Distal Organizer of Pattern and Polarity in the Arabidopsis Root. Cell **99**: 463–72.

Saini, S., Sharma, I., Kaur, N., and Pati, P.K. (2013). Auxin: A master regulator in plant root development. Plant Cell Rep. **32**: 741–757.

Saleem, M., Lamkemeyer, T., Schützenmeister, A., Madlung, J., Sakai, H., Piepho, H.-P., Nordheim, A., and Hochholdinger, F. (2010). Specification of Cortical Parenchyma and Stele of Maize Primary Roots by Asymmetric Levels of Auxin, Cytokinin, and Cytokinin-Regulated Proteins. Plant Physiol. **152**: 4–18.

Schindelin, J. et al. (2012). Fiji: an open-source platform for biological-image analysis. Nat. Methods **9**: 676–682.

Stahl, Y., Wink, R.H., Ingram, G.C., and Simon, R. (2009). A Signaling Module Controlling the Stem Cell Niche in Arabidopsis Root Meristems. Curr. Biol. **19**: 909–914.

Steinmann, T., Geldner, N., Grebe, M., Mangold, S., Jackson, C.L., Paris, S., Gälweiler, L., Palme, K., and Jürgens, G. (1999). Coordinated Polar Localization of Auxin Efflux Carrier PIN1 by GNOM ARF GEF. Science. **286**: 316–18.

Tagliani, L., Nissen, S., and Blake, T.K. (1986). Comparison of Growth, Exogenous Auxin Sensitivity, and Endogenous Indole-3-Acetic Acid Content in Roots of Hordeum vulgare L. and an Agravitropic Mutant. Biochem. Genet. **24**: 839–848.

Ulmasov, T., Murfett, J., Hagen, G., and Guilfoyle, T.J. (1997). Aux/IAA Proteins Repress Expression of Reporter Genes Containing Natural and Highly Active Synthetic Auxin Response Elements. Plant Cell **9**: 1963–1971.

Wang, J.R., Hu, H., Wang, G.H., Li, J., Chen, J.Y., and Wu, P. (2009b). Expression of PIN genes in rice (Oryza sativa L.): Tissue specificity and regulation by hormones. Mol. Plant **2**: 823–831.

Warner, C.A., Biedrzycki, M.L., Jacobs, S.S., Wisser, R.J., Caplan, J.L., and Sherrier, D.J. (2014). An Optical Clearing Technique for Plant Tissues Allowing Deep Imaging and Compatible with Fluorescence Microscopy. Plant Physiol. **166**: 1684–1687.

Werner, T., Motyka, V., Laucou, V., Smets, R., Onckelen, H. Van, and Schmuelling, T. (2003). Cytokinin-Deficient Transgenic Arabidopsis Plants Show Functions of Cytokinins in the Regulation of Shoot and Root Meristem Activity. Plant Cell **15**: 2532–2550.

Werner, T., Nehnevajova, E., Köllmer, I., Novák, O., Strnad, M., Krämer, U., and Schmülling, T. (2010). Root-Specific Reduction of Cytokinin Causes Enhanced Root Growth, Drought Tolerance, and Leaf Mineral Enrichment in Arabidopsis and Tobacco. Plant Cell **22**: 3905–3920.

Woodward, A.W. and Bartel, B. (2005). Auxin: Regulation, action, and interaction. Ann. Bot. **95**: 707–735.

Xu, M., Zhu, L., Shou, H., and Wu, P. (2005). A PIN1 Family Gene, OsPIN1, involved in Auxin-

dependent Adventitious Root Emergence and Tillering in Rice. Plant Cell Physiol. **46**: 1674–1681.

Yang, J., Yuan, Z., Meng, Q., Huang, G., Périn, C., Bureau, C., Meunier, A.-C., Ingouff, M., Bennett, M.J., Liang, W., and Zhang, D. (2017). Dynamic Regulation of Auxin Response during Rice Development Revealed by Newly Established Hormone Biosensor Markers. Front. Plant Sci. **8**: 256.

Zalewski, W., Galuszka, P., Gasparis, S., Orczyk, W., and Nadolska-Orczyk, A. (2010). Silencing of the HvCKX1 gene decreases the cytokinin oxidase/dehydrogenase level in barley and leads to higher plant productivity. J. Exp. Bot. **61**: 1839–51.

Zalewski, W., Gasparis, S., Boczkowska, M., Rajchel, I.K., Kała, M., Orczyk, W., and Nadolska-Orczyk, A. (2014). Expression patterns of HvCKX Genes indicate their role in growth and reproductive development of barley. PLoS One **9**: 1–20.

Zhang, Q., Li, J., Zhang, W., Yan, S., Wang, R., Zhao, J., Li, Y., Qi, Z., Sun, Z., and Zhu, Z. (2012). The putative auxin efflux carrier OsPIN3t is involved in the drought stress response and drought tolerance. Plant J. **72**: 805–816.

Zhang, W., Swarup, R., Bennett, M., Schaller, G.E., and Kieber, J.J. (2013). Cytokinin induces cell division in the quiescent center of the Arabidopsis root apical meristem. Curr. Biol. **23**: 1979–89.

Zhang, Y., Paschold, A., Marcon, C., Liu, S., Tai, H., Nestler, J., -Ting Yeh, C., Opitz, N., Lanz, C., Schnable, P.S., and Hochholdinger, F. (2014). The Aux/IAA gene rum1 involved in seminal and lateral root formation controls vascular patterning in maize (Zea mays L.) primary roots. J. Exp. Bot. **65**: 4919–4930.

Zürcher, E., Tavor-Deslex, D., Lituiev, D., Enkerli, K., Tarr, P.T., and Müller, B. (2013). A Robust and Sensitive Synthetic Sensor to Monitor the Transcriptional Output of the Cytokinin Signaling Network in Planta. Plant Physiol. **161**: 1066–1075.

VII. Conserved Pathways in the Barley Root and Shoot Apical Meristem

This chapter is a manuscript in preparation for submission.

Authors:

Gwendolyn K. Kirschner[1], Yvonne Stahl[1], Jafargholi Imani[2], Maria von Korff Schmising[3] and Rüdiger Simon[1]

Affiliations:

[1]Institute for Developmental Genetics and Cluster of Excellence on Plant Sciences, Heinrich Heine University, Universitätsstr. 1, D-40225 Düsseldorf, Germany

[2]Research Centre for BioSystems, Land Use and Nutrition (IFZ), Justus Liebig University, Institute of Phytopathology and Applied Zoology, Heinrich-Buff-Ring 26-32, D-35392 Giessen, Germany

[3]Institute for Plant Genetics, Heinrich Heine University Düsseldorf, c/o Department of Plant Developmental Biology, Max Planck Institute for Plant Breeding Research, Carl-von-Linné-Weg 10, D-50829 Köln

Contributions:

The experiments were designed by Gwendolyn K. Kirschner, Yvonne Stahl, Maria von Korff Schmising and Rüdiger Simon. Molecular biology, plant work and microscopy were conducted by Gwendolyn Kirschner. Barley transformation was conducted in the group of Jafargholi Imani. The manuscript was written by Gwendolyn Kirschner with help from Yvonne Stahl and Rüdiger Simon.

1. Introduction

Post-embryonic development of plant organs depends on the activity of meristems which harbour the plant stem cell niches. In the meristem, cells are undifferentiated and have a high division potential. All above-ground organs are produced by the shoot apical meristem (SAM), whereas longitudinal root growth is enabled by the root apical meristem (RAM) (reviewed in Stahl and Simon, 2005). Cells in the SAM center have a low mitotic activity, while cells in the surrounding peripheral zone divide more often (Laufs et al., 1998). The stem cell population is located in the outermost cell layers in the central region. Stem cell progenitors are displaced from the stem cell niche into the peripheral zone where they proliferate before differentiating in the organ primordia at the flanks of the meristem (reviewed in Stahl and Simon, 2005). Right below the stem cell niche resides the organizing center (OC) which is essential to maintain a stable pool of stem cells (Mayer et al., 1998). Here, the homeodomain transcription factor WUSCHEL (WUS) is expressed and acts non-cell autonomously to maintain the overlying stem cells (Mayer et al., 1998; Laux et al., 1996). The stem cells in turn produce the small secreted peptide CLAVATA3 (CLV3) which acts through the receptor kinase CLAVATA1 (CLV1) and the receptor/kinase pair CLAVATA2 (CLV2)/CORYNE (CRN) to negatively regulate *WUS* expression in the OC, thereby establishing a negative feedback loop (Yadav et al., 2011; Brand et al., 2000; Ogawa et al., 2008; Jeong et al., 1999; Bleckmann et al., 2010; Müller et al., 2008; Schoof et al., 2000).

It is assumed that the RAM has evolutionarily evolved from the SAM, since many of the key regulators act in both tissues and the earliest discovered roots are morphologically similar to shoots (Jiang and Feldman, 2005). Thus, the role of the OC in the SAM is resembled by the cells of the quiescent center (QC) in the RAM, that maintain the surrounding cells in stem cell state (Clowes, 1978). In *Arabidopsis thaliana.* the four QC cells are almost mitotically inactive but send short-range signals to the surrounding cell layer to prevent these cells from differentiating (Dolan et al., 1993; van den Berg et al., 1997). One of these signals is the WUS homologue WUSCHEL-RLEATED HOMEOBOX5 (WOX5) that maintains the distal columella stem cells (DSCs) in a pathway involving the receptor-like kinase ARABIDOPSIS CRINKLY4 (ACR4), CLV1 and the CLE-peptide CLV3/ ENDOSPERM SURROUNDING REGION40 (CLE40) which is closely related to CLV3 (Sarkar et al., 2007; Stahl et al., 2009, 2013). The proximal root meristem in *Arabidopsis* is maintained by the CLE40 peptide via a CLV2- and CRN-dependent pathway (Fiers et al., 2005). The GRAS family members SCARECROW (SCR) and SHORTROOT (SHR) are necessary for specification of endodermis and QC (Di Laurenzio et al., 1996; Sabatini et al., 2003; Cui et al., 2007).

While most of this knowledge was gained from the dicot model system *Arabidopsis*, there is accumulating evidence that the pathways described above are at least partially conserved in other plants, from monocots to dicots. CLV1 homologues, the leucine-rich repeat receptor kinases THICK TASSEL DWARF1 (TD1) and FLORAL ORGAN NUMBER1 (FON1) were identified in maize and

rice, respectively (Bommert et al., 2005; Suzaki et al., 2004). FLORAL ORGAN NUMBER2 (FON2, also identified and named independently FON4) represents a rice CLV3 homologue (Chu et al., 2006; Suzaki et al., 2008, 2006). Furthermore, FASCIATED EAR2 (FEA2) was identified as CLV2 homologue in maize and mutations in the *FEA2* gene lead to a resistance to the *Arabidopsis* CLV3 peptide, suggesting an involvement in the CLE signalling pathway (Taguchi-Shiobara et al., 2001; Je et al., 2016).

Mutations in the genes coding for these homologues lead to enlarged inflorescence meristems, indicating that they participate in stem cell maintenance like their homologues in *Arabidopsis* (Bommert et al., 2005; Suzaki et al., 2004; Nagasawa et al., 1996; Taguchi-Shiobara et al., 2001). In contrast, no functional WUS homologues have been identified in monocots so far. *OsWUS* and *ZmWUS1* and *ZmWUS2* represent *WUS* homologues in rice and maize respectively, but none of these genes show an OC-specific expression in the SAMs (Nardmann and Werr, 2006). For the WUS-related WOX5, however, homologues were found in maize and rice (named QUIESCENT-CENTER-SPECIFIC HOMEOBOX (QHB) in rice and ZmWOX5B in maize) that are expressed specifically in the QC in the RAM (Nardmann et al., 2007; Kamiya et al., 2003b; Chu et al., 2013). The rice homologue of CLE40, FON2-LIKE CLE PROTEIN1 (FCP1), is involved in the maintenance of the SAM during the vegetative phase of development (Suzaki et al., 2008). Furthermore, FCP1, as well as the recently described barley CLE40 homologue HvCLE402, participate in the maintenance of the proximal RAM (Suzaki et al., 2008; Kinoshita et al., 2007; Kirschner et al., 2017). CR4 represents a homologue of the *Arabidopsis* ACR4 in maize, where it controls cell differentiation particularly in the shoot epidermis and in the aleurone of the endosperm (Becraft et al., 2001). A conserved expression pattern in the root was also examined for the maize and rice homologues of SCR, *ZmSCR*, *OsSCR* and *OsSHR*, in particular in the endodermis in case of *ZmSCR* and *OsSCR*, and in the stele in case of *OsSHR* (Lim et al., 2000; Cui et al., 2007; Kamiya et al., 2003a). Thus, similar pathways involving GRAS family members, CLE peptides, CLV genes and WUS-related proteins exist in both dicots and monocots and control stem cell specification and maintenance in the shoot as well as in the root.

Roots of monocots like rice, maize and barley consist of the same tissues as *Arabidopsis* and the stem cell niche in the RAM is structured in a similar way, however, monocots form a larger number of cortical and stelar cell files (Rebouillat et al., 2009; Hochholdinger et al., 2004b; Kirschner et al., 2017). Inevitably, the formation of cortex and endodermis occurs by a different mechanism than in *Arabidopsis* in rice and barley (Ni et al., 2014; Kirschner et al., 2017). Furthermore, the QC size is different between the species, with 4 QC cells in *Arabidopsis* and rice, around 30 in barley and 800 - 1200 in maize (Jiang et al., 2003; Kirschner et al., 2017; Ni et al., 2014; Dolan et al., 1993). In this given manuscript, more homologues of key regulators in RAM and SAM maintenance were identified in barley. Moreover, it was analysed how the HvCLE402 peptide affects these patterns. To this end, the barley homologues of CR4, CLV1, WOX5, CLE40, SHR and SCR were cloned and their expression patterns were mapped *in planta*. It was found that, like its *Arabidopsis* homologue,

HvCLE402 is expressed in the stele and the differentiated root cap. However, unlike the CLE40 homologues in *Arabidopsis* and rice, HvCLE402 does not affect expression of the barley WOX5 homologue *HvWOX5*. Furthermore, HvWOX5 is not expressed in the cells of the QC, but in the metaxylem, indicating that homologues of the RAM regulators in barley are indeed expressed in the root, but their specific function might differ from their homologues in *Arabidopsis* and other monocots such as rice. *HvSCR* and *HvSHR* are expressed in the stele, or endodermis, respectively, like homologues in *Arabidopsis* and rice, but *HvSCR* expression levels are much lower in the QC. Notably, it appeared that HvCLV1 and HvCR4 are expressed exclusively in the SAM, but are absent from the RAM, again pointing towards a different mechanism for RAM establishment and maintenance in barley.

2. Material and Methods

2.1. Plant growth

For monitoring root growth and expression of reporter genes in the root, seedlings were grown on square plates as it was described previously (Kirschner et al., 2017) for 8 days after germination (DAG). For all experiments either the cultivars (cv.) Golden Promise or Morex were used as indicated. SAMs were monitored in plants grown 8 DAG on agar plates (Waddington stage I, "transition apex") or plants grown on soil under greenhouse conditions for around 3 weeks (Waddington stage II "double-ridge") (Waddington et al., 1983).

2.2. Cloning

The *HvpWOX5:HvWOX5-mVENUS* construct was constructed by PCR amplification of a 5228 bp fragment upstream of the start codon of *HvWOX5* (MLOC_74758.1 on morex_contig_66485, Mayer et al., 2012) as putative regulatory sequence from Morex genomic DNA (gDNA) and cloned by restriction and ligation via a *Asc*I site into a modified pMDC99 (Curtis and Grossniklaus, 2003). The whole *HvWOX5* coding region without stop codon (755 bp) was amplified from Morex gDNA and inserted downstream of the promoter by Gateway cloning (Invitrogen). A C-terminal *mVENUS* (Koushik et al., 2006) was integrated downstream of the gateway site by restriction and ligation via *Pac*I and *Spe*I. The *HvpSCR:HvSCR-mVENUS* construct was cloned in the same way, the *HvSCR* regulatory sequence included 2539 bp upstream of the start codon of *HvSCR* (AK359827 on morex_contig_49323) and the whole *HvSCR* coding region without stop codon (2359 bp) was amplified from Morex gDNA. The *HvpCR4:HvCR4-mVENUS* construct included the regulatory sequence of 1266 bp upstream of the start codon and 2691 bp as coding region, the *HvpCLV1:HvCLV1-mVENUS* construct comprised a regulatory sequence of 2826 bp upstream of the start codon and 3573 bp as coding sequence amplified from Morex gDNA and cloned similarly as the above described reporter constructs. The *HvpCLE402:VENUS-H2B* construct was cloned by amplifying the regulatory sequence including 2034 bp upstream of the start codon and inserted by Gateway cloning (Invitrogen) into the modified pMDC99 (Curtis and Grossniklaus, 2003). This modified pMDC99 contained the gateway cassette, the coding sequence of *VENUS* (Nagai et al., 2002) and a T3A terminator, which were inserted by restriction via *Asc*I and *Sac*I from pAB114 (described in Bleckmann et al., 2010). Furthermore, it contains the coding sequence of *Arabidopsis HISTONE H2B* (AT5G22880) at the C terminus of VENUS, inserted via restriction and ligation at a *Pac*I restriction site.

2.3. Barley transformation

Barley transformation was performed at the Justus-Liebig University in Gießen, Germany, in the research group Plant biotechnology as described by Imani and colleagues in the barley cultivar Golden Promise and tested for hygromycin resistance by growth on medium containing hygromycin and PCR

on the hygromycin gene (Imani et al., 2011). For root expression analysis, the seeds of the plants recovered from the transformed scutella were used (T1) and again tested for the presence of the reporter construct by PCR with primers binding in the gene of interest and the downstream reporter gene.

2.4. Preparation of the reporter line samples

Clearing of the transgenic reporter lines was performed as described by Warner and colleagues for pea root nodules with a different fixation, in particular with 4 % para-formaldehyde in phosphate buffered saline (PBS) for 1 h in vaccuum (Warner et al., 2014). Samples were incubated in the clearing solution for 1 week in darkness at 4 °C. In case of lines with weak expression and to examine expression in uncleared roots, the roots were embedded in liquid 5 % agarose in dH_2O for stabilization and sectioned longitudinally in the middle by hand with a sharp razor blade.

2.5. Stainings

Berberine hemisulfate staining, and microscopy of the stained samples were performed as described previously (Kirschner et al., 2017). SAM preparation and propidium iodide (PI) staining of cell walls of the SAMs was carried out by removing all leaves from the SAMs and incubate the SAMs in 5 mM PI for 5 min, and washed with dH_2O afterwards.

2.6. Treatments

Peptide treatments were carried out as described previously (Kirschner et al., 2017).

2.7. RNA *in situ* hybridisations

Probes for the *HvWOX5* mRNA were prepared from complementary DNA (cDNA) of the cv. Morex from start to stop codon of the *HvWOX5* gene (630 bp). For *HvSCR* probes, cDNA of cv. Morex was amplified from start to stop codon of *HvSCR* (1755 bp) or a fragment containing the VHIID motif (Lim et al., 2000) (373 bp) from Morex gDNA. For *HvSHR* probes, parts of exon 1 were amplified from Morex gDNA including 421 bp downstream of the start codon. The DNA was cloned into the pGGC000 entry vector of the GreenGate cloning system (Lampropoulos et al., 2013) and amplified including the T7 and sp6 promoter sites by PCR. RNA probes were produced as described previously (Hejátko et al., 2006). The RNA probes for *HvWOX5* were hydrolysed by adding 50 µl carbonate buffer (0.08 M $NaHCO_3$, 0.12 M Na_2CO_3) to 50 µl RNA probe and incubation at 60 °C for 46 min. On ice, 10 µl 10 % acetic acid, 12 µl sodium acetate and 312 µl EtOH were added, the RNA was precipitated and dissolved in RNase-free dH_2O. RNA *in situ* hybridisations were performed on roots of plants 8 DAG as described before (Kirschner et al., 2017). For hybridisations of *HvWOX5* and *HvSHR*, 10 % polyvinyl alcohol were added to the nitro-blue tetrazolium chloride (NBT)/ 5-bromo-4-chloro-3'-indolyphosphate p-toluidine salt (BCIP) staining buffer. In cases of strong staining, permanent specimens were created by washing the slides in 50 % ethanol (EtOH), 70 % EtOH, 95 %

EtOH and 100 % EtOH for 2 min each and for 10 s in xylol, and after drying, addition of a few drops of Entellan (Merck) and a cover slip. For examining the *HvWOX5* expression upon mock-and peptide-treated plants, root sections of roots 5 DAG with the control treatment and peptide treatment were placed next to each other on the same slide to guarantee an equal RNA probe hybridisation, antibody incubation and staining.

2.8. Microscopy

The transgenic reporter lines with mVENUS and VENUS were examined with a 40x water objective with a numeric aperture (NA) of 1.20 using the confocal microscope Zeiss LSM 780. Yellow fluorescence was excited with a 514 nm Argon laser with emission detection at 519 to 620 nm. The pinhole was set to 2,24 Airy units. Transmitted light pictures were recorded with a transmitted light detector (T-PMT). Pictures were recorded with the tile scan function with 10 % overlap, a threshold of 0.70 and automatically stitched by the LSM Zen software. RNA *in situ* hybridizations were examined with a plan-neofluar 20x objective with a NA of 0.50 or a plan-neofluar 40x objective with a NA of 0.75 using the Zeiss Axioskop light microscope.

2.9. Analysis

Picture analyses were carried out in Fiji (Schindelin et al., 2012). For information about creation of the phylogenetic tree see captions in the respective supplementary figure. For image compilation, Adobe Photoshop was used. If contrast and brightness were adjusted manually, the same changes were applied equally on the whole picture and on the pictures of all compared samples.

3. Results

3.1. Expression pattern of *HvSCR* and *HvSHR*

In *Arabidopsis* roots, endodermis and cortex are single-layered and the QC is formed by 4 cells (Dolan et al., 1993). Most monocot roots, however, consist of more cortex cell files and a larger QC area (Hardtke and Pacheco-Villalobos, 2015; Rebouillat et al., 2009; Hochholdinger et al., 2004a; Kirschner et al., 2017; Jiang et al., 2003; Ni et al., 2014). While in *Arabidopsis* and rice, one (in *Arabidopsis*) or several (in rice) periclinal divisions of the cortex-endodermis initial (CEI) create the single endodermis and the cortex cell layers (Dolan et al., 1993; Ni et al., 2014), in barley, the inner cortex cell layers and the endodermis are derived from a shared initial (inner cortex endodermis initial, ICEI) and the outer cortex cell layers are derived from another initial (outer cortex initial, OCI) (Figure 1A) (Kirschner et al., 2017). In *Arabidopsis*, the transcription factors SHR and SCR are important for QC specification and cortex/endodermis formation (Sabatini et al., 2003; Di Laurenzio et al., 1996). To figure out if a similar regulatory mechanism might be conserved in barley, the barley genome was searched for SCR and SHR homologues and MLOC_64716 (AK359827) was identified as a SCR homologue in barley (called HvSCR hereafter) and MLOC_62665.1 as the closest SHR homologue (called HvSHR hereafter) based on their amino acid sequences (Supplementary figure 1). As its homologue AtSCR, HvSCR localized to the nucleus when tagged to mVENUS in barley reporter lines (Figure 1I). The expression pattern, however, could not be analysed with the reporter line, as only one transgenic reporter line with mVENUS expression could be recovered from T0 and this line showed a ubiquitous expression (Figure 1H'). Therefore, the chosen promoter of 2539 bp might miss regulatory elements or the construct integrated in a position in the genome where it is controlled by different regulatory elements. Expression pattern analysis by RNA *in situ* hybridisation revealed that *HvSCR* is expressed in the endodermis and in the ICEI in the root meristem (10/10 roots), but only weakly (3/10 roots) or not expressed in the QC region (7/10 roots) (Figure 1 B, B', D). *HvSHR* mRNA was detected in the stelar cells of the root meristem, but as for *HvSCR*, *HvSHR* mRNA could not be detected in the QC region (Figure 1F, F'). This expression pattern is conserved between monocots and dicots, suggesting that despite of the different root anatomy, cortex and endodermis specification might be regulated by a conserved mechanism involving *SHR* and *SCR*. In *Arabidopsis*, rice and maize, however, *SCR* is additionally expressed in the QC (Di Laurenzio et al., 1996; Sabatini et al., 2003; Ni et al., 2014; Lim et al., 2000). As only weak, if any, *HvSCR* expression was observed in the barley QC in the analysed stages, QC specification might depend on another factor than *HvSCR* in barley.

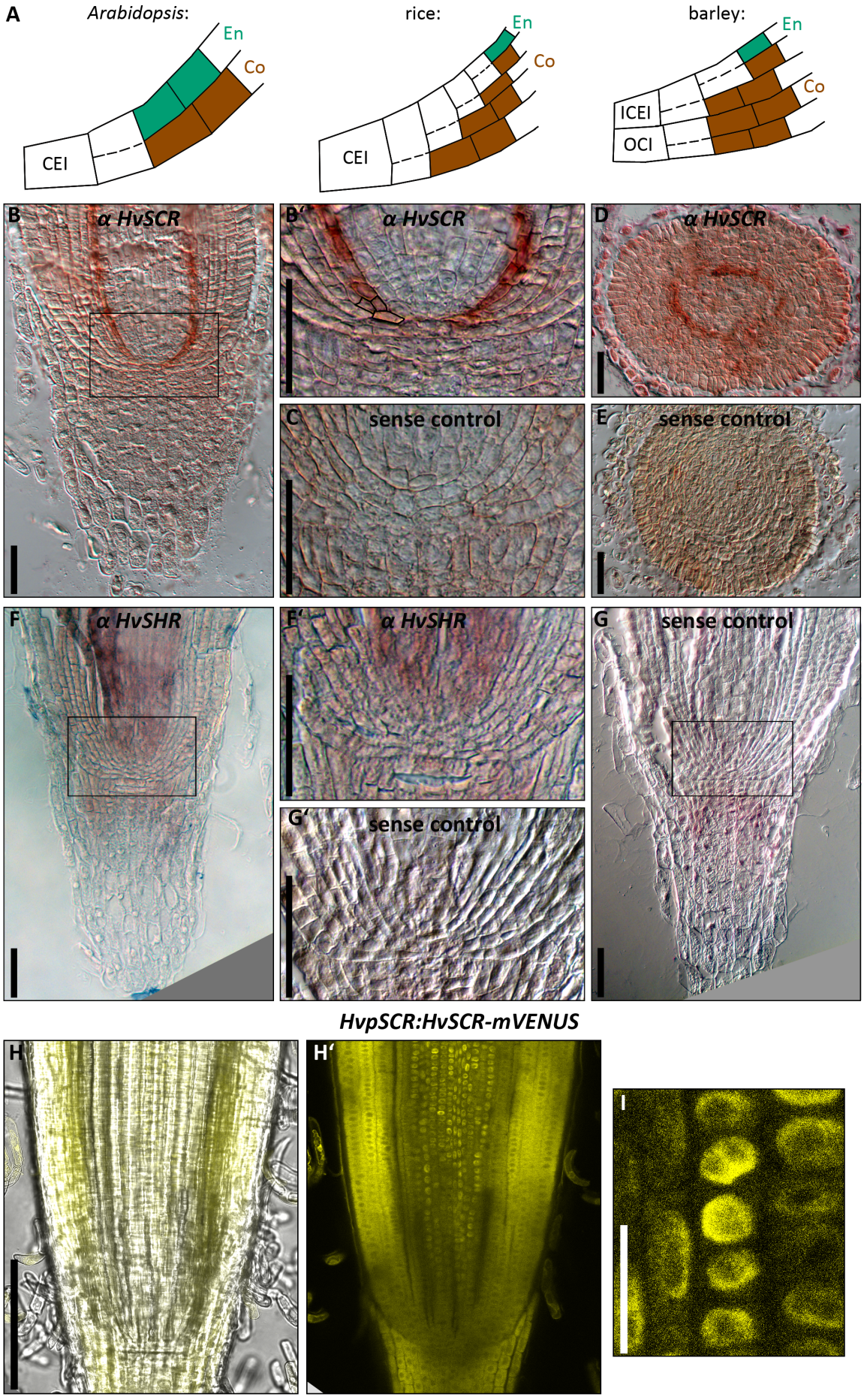
A
Arabidopsis:
En
Co
CEI
rice:
En
Co
CEI
barley:
En
Co
ICEI
OCI
B
α HvSCR
B'
α HvSCR
D
α HvSCR
C
sense control
E
sense control
F
α HvSHR
F'
α HvSHR
G
sense control
G'
sense control
HvpSCR:HvSCR-mVENUS
H
H'
I

Figure 1: Cortex and endodermis formation in *Arabidopsis*, rice and barley.

A) Schematic representation of ground tissue formation in *Arabidopsis*, rice and maize (according to Kirschner et al., 2017; Dolan et al., 1993; Ni et al., 2014; Coudert et al., 2010; Rebouillat et al., 2009); dashed lines represent cell divisions; En = endodermis, Co = cortex. B) – G) Localisation of the *HvSCR* and *HvSHR* mRNA in the roots of 8 DAG-old barley plants by RNA *in situ* hybridization in the cv. Morex (B), C), F), G)) or Golden Promise (D), E)). **B)** Probe for *HvSCR*. **B')** Magnification of the region framed in B); black lines indicate the position of the ICEI and the ICEI daughters. **C)** Sense control for *HvSCR* **D)** Cross section in the meristematic region and hybridization with probe for *HvSCR*. **E)** Sense control for *HvSCR*. **F)** Probe for *HvSHR*. **F')** Magnification of the region framed in F). **G)** Sense control for *HvSHR*. **G')** Magnification of the region framed in G); **H), H')** Expression of *HvpSCR:HvSCR-mVENUS* in roots of the barley cv. Golden Promise 8 DAG; roots were cleared for one week as described in Material and Methods; only one transgenic reporter line with the *HvpSCR:HvSCR-mVENUS* construct could be recovered after transformation. **I)** Magnification of nuclei with mVENUS expression; brightness adjusted. H), I) mVENUS emission and transmitted light, H') mVENUS emission only; scale bars 50 µm (A) – G)), 200 µm (H)), 20 µm (I)).

3.2. Identification of a WOX5 homologue in barley

Another gene, which is expressed in the QC in rice and *Arabidopsis*, is WOX5 (Ni et al., 2014; Sarkar et al., 2007). In *Arabidopsis*, *WOX5* signalling from the QC maintains the DSCs (Sarkar et al., 2007). Based on the closest phylogenetic relationship of the whole protein sequence to ZmWOX5A and ZmWOX5B, rice QHB, the wheat WOX5 homologues and the *Arabidopsis* WOX5, MLOC_74758 was identified as a barley WOX5 homologue (called HvWOX5 hereafter) (Supplementary figure 2). The same phylogenetic analysis including the homeobox domain of the proteins only (as described by Nardmann et al., 2007) revealed similar results. Expression analysis revealed that both the *HvWOX5* mRNA and protein are present in the metaxylem in the root meristem (Figure 2). No expression, however, was detected in the QC (Figure 2). Non-transgenic control lines did not show any expression (Supplementary figure 5B'). The expression pattern of *HvWOX5* therefore seems to be more closely related to the rice *WOX5* homologue *QHB*, which is expressed in both the QC and the metaxylem of roots (Chu et al., 2013; Ni et al., 2014). Interestingly, though, *QHB* expression is regulated by the rice CLE peptide OsFCP2, just like *AtWOX5* expression by the *Arabidopsis* CLE peptide AtCLE40, which could be equally possible for *HvWOX5*/HvCLE402 (Chu et al., 2013; Stahl et al., 2009; Kirschner et al., 2017).

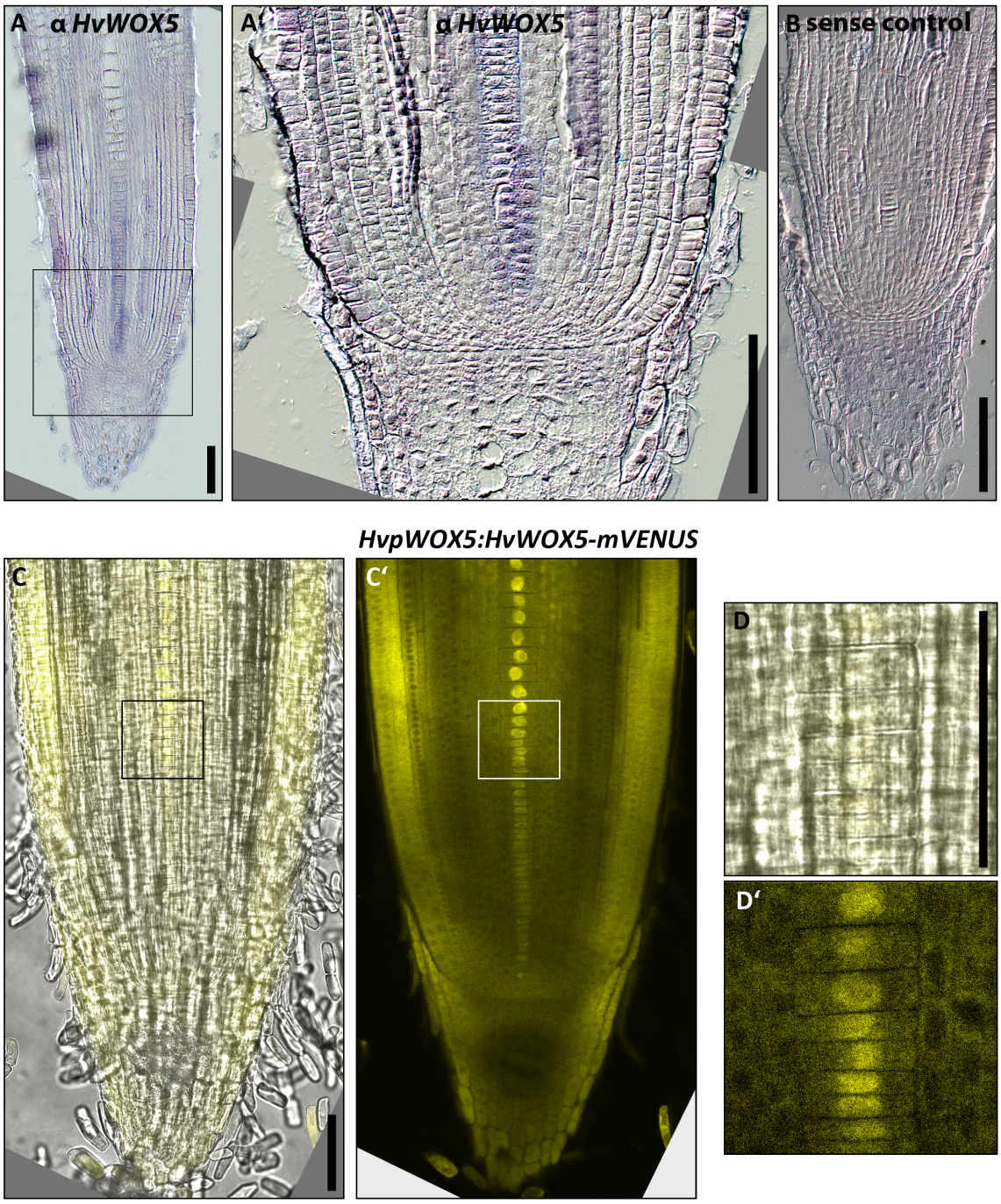

Figure 2: *HvWOX5* expression in the root of the barley cv. Golden Promise.

Localisation of *HvWOX5* mRNA and protein in the roots of 8 DAG-old barley plants by RNA *in situ* hybridization and transgenic reporter lines. **A)** RNA *in situ* hybridisation with a probe for *HvWOX5*. **A')** magnification of the region outlined in A). **B)** sense control for *HvWOX5*. **C)**, **C')** Transgenic lines expressing *HvpWOX5:HvWOX5-mVENUS*; roots were cleared as described in Material and Methods. **D)**, **D')** magnification of region indicated with the white frame in C') with adjusted brightness. C), D) transmitted light (TM) and mVENUS emission, C'), D') mVENUS emission only. Three independent transgenic lines were examined, which showed the same expression pattern; scale bars 100µm.

3.3. *HvCLE402* is expressed in differentiated root cap cells and the stele

In order to investigate whether *HvWOX5* expression is possibly affected by HvCLE402, the expression pattern of *HvCLE402* was examined. The transcriptional barley reporter line *HvCLE402p:VENUS-H2B* line revealed that the putative *HvCLE402* promoter consisting of 2034 bp upstream of the *HvCLE402* start codon is active in the differentiated root cap cells and in the stele (Figure 3), thereby reflecting the expression pattern of AtCLE40 (Stahl et al., 2009). However, when the plants were grown on medium containing 1 µM HvCLE402 peptide (HvCLE402p), no change in the *HvWOX5* expression pattern could be detected, nor any change in the metaxylem structure in regard to the cell arrangement in differentiated metaxylem (Supplementary figure 3). This indicates that *HvWOX5* expression is independent of HvCLE402 signalling, therefore suggesting that, while *HvWOX5* and *HvCLE402* are expressed in a similar pattern to their *Arabidopsis* and rice homologues, they seem to function differently.

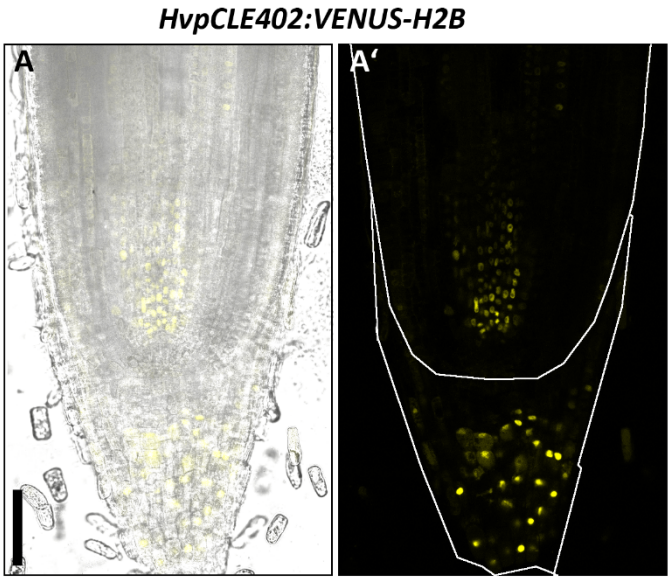

Figure 3: *HvCLE402* expression in the root of the barley cv. Golden Promise.

Activity of the *HvCLE402* promoter in the barley root 8 DAG in the stele and the differentiated root cap, displayed by expression of the *HvpCLE402:VENUS-H2B* construct; roots were cleared for one week as described in Material and Methods; two independent transgenic lines were examined and showed a similar expression pattern in the root. **A)** VENUS emission and transmitted light **A')** VENUS emission; white frame indicates the root outlines of the root and the root cap junction; scale bar 100µm.

3.4. Expression of HvCLV1, HvCR4 and *HvCLE402* in the SAM

Subsequently, the expression patterns of the potential HvCLE402 receptors HvCR4 and HvCLV1 were analysed. MLOC_66232.2 was identified as possible CLV1 homologue in barley, as it clusters

closely together with the maize and rice CLV1 homologues TD1 and FON1 and the *Arabidopsis* CLV1 based on their protein sequence (Supplementary figure 4). The CR4 homologue from barley HvCR4 was previously described by Olsen and colleagues (Olsen et al., 2008) and consists of a single exon like the *Arabidopsis* ACR4 (The Arabidopsis Information Resource, TAIR). To monitor the expression and subcellular localisation of HvCLV1 and HvCR4, translational barley reporter lines were created. Interestingly though, no expression in the RAM was detected. As CLE40, ACR4 and CLV1 are also known to be involved in SAM maintenance in *Arabidopsis*, maize and rice (Bommert et al., 2005; Suzaki et al., 2004; Clark et al., 1997; Hobe et al., 2003; Gifford et al., 2005; Stahl et al., 2013; Gifford et al., 2003; Nimchuk et al., 2011), the expression of the barley homologues was also investigated in the SAM. The SAM of barley is structured similarly to SAMs of other monocots. While in dicots, the tunica region consists of the clonal layers L1 and L2, the tunica only comprises one layer in monocots (L1, Figure 4 A, E) and the L2 belongs to the corpus (reviewed in Carles and Fletcher, 2003). The *HvpCLE402:VENUS-H2B* reporter line revealed that the *HvCLE402* promoter is active in the whole SAM in both examined SAM stages (Figure 4B', F'). *HvpCR4:HvCR4-mVENUS* was expressed in the whole SAM as well (Figure 4 C', G'), with an apparent maximum in the L1 layer (epidermis) (inset in Figure 4 G'). This difference, however, might be due to the imaging method, as the fluorescence intensity decreases within the tissue. Overall, the expression was quite weak, but still distinguishable from the background of non-transgenic plants (Supplementary figure 5). Interestingly in *Arabidopsis*, AtACR4 is also expressed mainly in the L1 in the SAM and is thought to signal to the meristem center from the epidermis (Gifford et al., 2003). It was shown for the *Arabidopsis* ACR4 and maize CR4, that they localize to plasmodesmata in the *Arabidopsis* cotyledon epidermis or the maize aleurone layer, respectively (Tian et al., 2007; Stahl et al., 2013). In the barley SAM, however, no specific localization to plasmodesmata was detected (Figure 4 G'), maybe due to the low expression level. *HvpCLV1:HvCLV1-mVENUS* expression was detected in the whole SAM in Waddington stage I and II (Figure 4 D, H). HvCLV1-mVENUS was apparently mostly localized at the plasma membrane, but also in vesicles within the cells, indicating internalized HvCLV1-mVENUS, similar to AtCLV1 localization (Nimchuk et al., 2011). It is to note, however, that the expression intensity between the different layers within the established pattern slightly varied between plants of the same transgenic line. Sometimes, the expression was higher in the L1 and corpus and lower expression in the L2 (8/14 SAMs in Waddington stages I or II, Figure 4 D', H'). In the other cases, the expression was higher in the L1 and L2 and lower in the corpus (6/14 SAMs in Waddington stages I or II). In summary, while *HvCLE402* is expressed in both RAMs and SAMs of barley, the ACR4 and CLV1 homologues HvCR4 and HvCLV1 homologues are not expressed in the RAMs, but only in the SAMs. Accordingly, it appears that similar, conserved pathways control stem cell maintenance in the SAM of *Arabidopsis* and barley, but RAM maintenance must be controlled by a different regulatory system, involving some of the same key players, but not all of them.

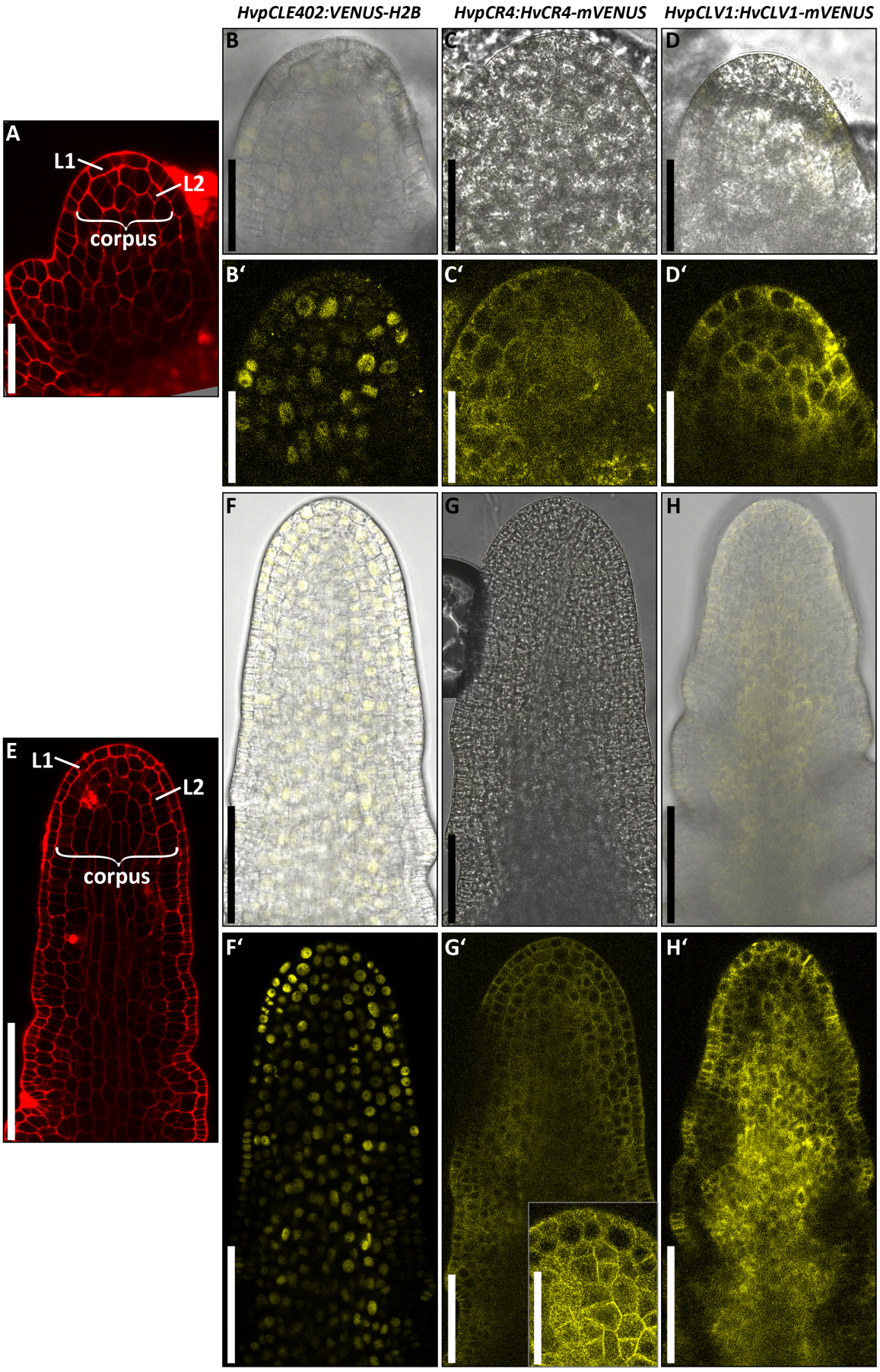
HvpCLE402:VENUS-H2B
HvpCR4:HvCR4-mVENUS
HvpCLV1:HvCLV1-mVENUS
A
L1
L2
corpus
B
C
D
B‘
C‘
D‘
E
L1
L2
corpus
F
G
H
F‘
G‘
H‘

Figure 4: SAM structure and expression of *HvCLE402*, HvCLV1 and HvCR4 in the SAM of the barley cv. Golden Promise.

A), **E)** Cell layers in barley SAMs can be distinguished in the outer layer (L1) and the corpus, that includes the second-inner layer (L2) in monocots; cell walls in SAMs counterstained with PI. **B)**, **B')**, **F)**, **F')** Promoter activity of the *HvpCLE402* promoter in the SAM displayed by *HvpCLE402:VENUS-H2B* expression; 5 independent transgenic lines show a similar expression pattern. **C)**, **C')**, **G)**, **G')** Expression of HvCR4 in the SAM visualized with the *HvpCR4:HvCR4-mVENUS* construct; inset in G') shows focus on the epidermis of the tip of the SAM, scale bar 50 µm in the inset, same settings like in G'); 5 independent transgenic lines express similarly, however, the expression strength varies. **D)**, **D')**, **H)**, **H')** Expression of HvCLV1 in the SAM displayed by *HvpCLV1:HvCLV1-mVENUS*; 4 independent transgenic lines show similar expression; A) – D) SAMs in Waddington stage I, scale bar 50 µm, E) – H) SAMs in Waddington stage II, scale bar 100 µm; B), C), D), F), G), H) VENUS emission and transmitted light, B'), C'), D'), F'), G'), H') VENUS emission.

4. Discussion

4.1. Tissue-specific expression of *HvSCR* and *HvSHR*

Almost all vascular plants like maize, rice, *Arabidopsis* and barley develop a single-layered endodermis, suggesting a highly conserved mechanism for endodermis formation (Dolan et al., 1993; Kirschner et al., 2017; Hochholdinger et al., 2004b; Rebouillat et al., 2009). In rice and *Arabidopsis*, the endodermis develops from the same CEI as the cortex by first one anticlinal cell division and subsequently one (in *Arabidopsis*) or several (in rice) periclinal divisions of the CEI daughter (Figure 1A, Rebouillat et al., 2009; Dolan et al., 1993). *AtSCR*, *OsSCR1* and *ZmSCR* are all expressed in the endodermis and in one layer of the QC, while *AtSHR* and *OsSHR* are expressed in the stele, but the SHR protein can be detected in stele, QC, CEI and endodermis (Lim et al., 2000; Kamiya et al., 2003a; Sabatini et al., 2003; Helariutta et al., 2000; Du et al., 2001; Cui et al., 2007). In *Arabidopsis*, movement of SHR from the stele to the endodermis, and subsequent sequestration through interaction with SCR determines endodermis fate, and therefore differentiation of the endodermis from the cortex, to where SHR can no longer travel (Helariutta et al., 2000; Du et al., 2001). The SHR homologues from *Brachypodium distachyon* and rice are able to rescue the endodermal cell fate in the *Arabidopsis shr* mutant, and the maize SCR homologue is able to complement radial defects in *Arabidopsis scr* mutant roots, indicating that the SCR homologues not only share a similar expression pattern, but also a conserved function (Wu et al., 2014; Lim et al., 2005). In contrast, the protein movement of the monocot SHRs from the stele to the ground tissue in *Arabidopsis* is not restricted to the endodermis, suggesting that interaction with the *Arabidopsis* SCR is not sufficient to prevent further movement of the monocot SHRs (Wu et al., 2014). Movement of the monocot SHRs to the ground tissue induces the formation of additional ground tissue layers in *Arabidopsis*, indicating a possible mechanism to regulate the cortex cell number in monocots (Wu et al., 2014). In barley seminal roots, the ground tissue consists of a single layer of endodermis and 5 layers of cortex cell layers, similar to other monocots (Kirschner et al., 2017). As reported recently, in barley, cortex and endodermis formation differs from rice and *Arabidopsis* in that the inner cortex and endodermis are derived from the same initial (ICEI), while the outer cortex cells are clonally distinct and originate from the outer cortex initals (OCI) (Figure 1A, Kirschner et al., 2017). In accordance with this classification of two distinct types of CEIs, in this given manuscript it is presented that the *HvSCR* mRNA is restricted to the ICEI, but absent from the OCI (Figure 1B'). Localization of HvSCR-mVENUS in the nucleus indicates furthermore that HvSCR might act as transcription factor (Figure 1I). Moreover, *HvSHR* expression in the stele provides further evidence that, despite the morphological difference between *Arabidopsis* and barley, ground tissue specification could be regulated through the widely conserved SCR-SHR module (Figure 1F'). Additionally to its role in endodermis patterning in *Arabidopsis*, *AtSCR* is also important for QC specification (Sabatini et al., 2003). The size and position of the QC can be determined, on the one hand, by cell division analysis, as the QC cells are less mitotically active than the surrounding

cells (Clowes, 1984; Ni et al., 2014; Dolan et al., 1993; Vanstraelen et al., 2009). On the other hand, established markers for the QC, like WOX5 and SCR are often used to define the presence and position of the QC (Ni et al., 2014; Vanstraelen et al., 2009; Cruz-Ramírez et al., 2013). Studies of the QC development in *scr* mutants of other plants than *Arabidopsis* are still lacking (Slewinski et al., 2012; Sabatini et al., 2003). In barley, however, only occasionally weak *HvSCR* expression could be detected in one layer of the QC (Figure 1B'). The phenotype of the maize *scr* single mutant only partially resembles the *Arabidopsis scr* mutant in respect to the endodermis, suggesting that maize *SCR* genes act redundantly here (Slewinski et al., 2012). A similar redundancy of barley *SCR* genes could also explain the weak *HvSCR* expression in the QC, because close SCR homologues might take over the SCR function in the QC. Candidates for these homologues are AK365059/MLOC_79758 and MLOC AK366346/MLOC_21726, which are closely related to HvSCR based on their phylogeny (Supplementary figure 1). Interestingly, although *SCR* expression is often used as a QC marker (Aida et al., 2004; Ni et al., 2014), *ZmSCR* is expressed in one layer adjacent to the root cap in maize, while the maize QC is proposed to contain 800 – 1200 cells based in their low cell division rate, and therefore comprising more cells than only the *SCR* expressing ones (Jiang et al., 2003; Lim et al., 2000). Likewise, the weak *HvSCR* expression in the barley QC region is detected in only one cell layer, although cell division studies showed that the actual mitotically "quiescent" region in barley comprises more cell layers (Kirschner et al., 2017). The expression patterns of *HvSCR* and *ZmSCR* imply that the mitotically "quiescent" region defined as QC in barley and maize might actually consist of different subgroups of cells, some expressing WOX5, others expressing SCR, depending on their sub-function. Overlap of *AtSCR* and *AtWOX5* expression in the *Arabidopsis* QC could be due to the small size of the *Arabidopsis* root and not necessarily displaying a general concept for other plants.

4.2. A metaxylem-specific role of HvWOX5 in barley

AtWOX5 is expressed in the QC and signals from there to maintain the stemness of the DSCs (Sarkar et al., 2007; Pi et al., 2015). In maize, the *WOX5* homologue *ZmWOX5B* is expressed in the QC and basal provascular strands in the coleoptilar stage embryo (Nardmann et al., 2007). In rice, the WOX5 homologue OsQHB is expressed in the QC and the surrounding region. Additionally, it is expressed in the metaxylem (Kamiya et al., 2003b; Chu et al., 2013; Ni et al., 2014). In barley, the *HvWOX5* mRNA and protein was detected exclusively in the metaxylem of the root meristem, but not in the QC (Figure 2). Thus, although based on protein sequence comparison, HvWOX5 is the closest homologue of the AtWOX5, OsQHB and ZmWOX5 (Supplementary figure 2), HvWOX5 expression pattern differs in barley, only resembling the expression of OsQHB and ZmWOX5B partially. *WOX5* expression is commonly regulated by CLE peptides, for instance, *AtWOX5* is transcriptionally regulated by the peptide AtCLE40, *OsQHB* expression is influenced by the CLE40 homologue OsFCP1 peptide and the closely related OsFCP2 peptide (Stahl et al., 2009; Suzaki et al., 2008; Chu et al., 2013). A role for RAM maintenance has already been shown for the CLE40 homologue

HvCLE402 in barley, and HvWOX5 and HvCLE402 do have overlapping expression patterns in the metaxylem, making a mutual regulation possible (Figure 2, Figure 3, Kirschner et al., 2017). However, *HvWOX5* does not seem to be under transcriptional control of the HvCLE402 peptide, another indication that its role is not homologous to *AtWOX5* when it comes to its role in RAM maintenance (Supplementary figure 3, Stahl et al., 2009). Moreover, exogenous HvCLE402 peptide application has no influence on vasculature development, as it was shown for OsFCP2 in rice (Supplementary figure 3, Chu et al., 2013). Another possibility is that *HvWOX5* and vasculature development are regulated by a different CLE peptide, or by some completely different mechanism.

In *Arabidopsis*, another *WOX* family gene, *WOX4*, is expressed in cambium and procambium and participates in a pathway that maintains the vascular stem cells (Hirakawa et al., 2010). It is regulated by the TRACHEARY ELEMENT DIFFERENTIATION INHIBITORY FACTOR peptide (encoded by CLE41 and CLE44) (Hirakawa et al., 2010). A possible role for the CLE41/44 homologues of barley on *HvWOX5* could therefore be investigated. The fact that HvWOX5 is absent from the QC region and not regulated by the HvCLE402 peptide indicates that another *WOX* gene might have taken over the *WOX* function in the QC. In this case it will be difficult to identify the right WOX candidate, as based on their protein sequence, there is no other WOX protein closely related to HvWOX5 and the other WOX5 homologues (Supplementary figure 2). For AtWOX5 it was shown that it is partially interchangeable with its related protein AtWUS in control of stem cell number in SAM and RAM, therefore indicating that rather promoter specificity than protein function was subject to evolutionary change (Sarkar et al., 2007). Absence of HvWOX5 from the barley QC could also indicate that there is no *WOX* function necessary here. This idea is supported by the finding that, although HvCLE402 peptide application regulates the maintenance of the proximal RAM, the DSCs are not affected as they are in *Arabidopsis* (Kirschner et al., 2017; Stahl et al., 2009). Additionally, although HvCLE402 is expressed in the differentiated columella cells, neither of the putative receptors HvCR4 and HvCLV1 is expressed in the RAM stem cell niche (Figure 3), suggesting a CLE40/WOX5-independent mechanism of DSC regulation in barley.

4.3. The expression patterns of key regulators of shoot meristem size are conserved between barley and *Arabidopsis*

HvCLE402, HvCLV1 and HvCR4 were broadly expressed in the SAM (Figure 4). *AtCLE40* is only expressed at low levels in the *Arabidopsis* SAM, but it is able to activate CLV signalling independently of AtCLV3 (Hobe et al., 2003). In rice, the CLE40 homologue OsFCP1 is required for SAM maintenance as well, and OsFCP1 function primarily depends on the tenth amino acid in the 12 amino acid CLE motif, an isoleucine (Suzaki et al., 2008). The HvCLE402 CLE motif consists of the same amino acids as the one in FCP1, thus at the tenth position, there is an isoleucine (Kirschner et al., 2017). Together with an expression pattern throughout the SAM and in the RAM similar to OsFCP1 and AtCLE40 (Figure 4B', F'), this suggests a similar function for HvCLE402 in the SAM. In the

SAM, HvCLE402 signalling could possibly depend on HvCLV1 and HvCR4, as both are expressed in the same domains (Figure 4D', H'). HvCLV1 is expressed throughout the whole SAM of barley, although in some cases the expression was restricted to the L1 and corpus only, with an exclusion from the layer that corresponds to the L2 in dicots, and in other cases higher expression in the L1 and L2, and lower in the corpus (Figure 4D', H'). Nevertheless, the expression of HvCLV1 in the SAM reflects the expression pattern of CLV1 in *Arabidopsis* and FON1 in rice, suggesting an involvement in the stem cell maintenance pathway. Analysis of the subcellular localization of HvCLV1 revealed that the protein is not exclusively localized at the plasma membrane, but signal of the fluorophore is rather detected in vesicles in the cells (Figure 4D', H'). This might indicate active CLV1 signalling, as Nimchuk and colleagues found for *Arabidopsis* that CLV3 binding to CLV1 activates the CLV1 kinase and CLV1 is internalized from the plasma membrane into lytic vacuoles where it is degraded (Nimchuk et al., 2011). Another kinase that is involved in the shoot development is CRINKLY4 (CR4), that was first identified in maize as receptor-like kinase. The transcript is present in the whole SAM, and the gene is involved in leaf epidermis and endosperm aleurone formation in maize (Becraft et al., 2001). In *Arabidopsis*, the CR4 homologue ACR4 is expressed in the L1 cells in all apical meristems and young organ primordia and necessary for normal cell organisation during L1-derived ovule integument development (Gifford et al., 2003). In barley, the *defective seed 5* (*des5*) mutant, which displays defects in the aleurone cell layer in the seed, was shown to have lower transcript abundance of *HvCR4* (Olsen et al., 2008). HvCR4 is expressed weakly throughout the whole SAM, but at slightly higher levels in the epidermis in the SAM (Figure 4 C'. G'). This expression pattern resembles the expression pattern of maize *CR4* in the whole SAM (Becraft et al., 2001). Together with the observation that in the barley *des5* mutant the defect in the aleurone cell layer goes together with a downregulation of *HvCR4* expression (Olsen et al., 2008), this suggests that downregulation of *HvCR4* expression in the L1 could be the reason for the defect in the aleurone cell layer in the *des5* mutant. In both maize and *Arabidopsis*, localization of the CR4 or ACR4 protein, respectively, was associated with plasmodesmata and hypothesized to control the mobility of a signalling molecule (Tian et al., 2007; Stahl et al., 2013). In the barley SAM, however, no localisation associated with plasmodesmata could be detected (Figure 4C', G'). It will be interesting to study if HvCLE402, or possibly another peptide of the CLE family, is responsible for HvCLV1 or HvCR4 dependent SAM signalling. From the studies in *Arabidopsis* and rice, the presence of a CLV3 homologue in barley would be expected, that takes over a more specific role in stem cell maintenance and would be exclusively expressed in the stem cells (Suzaki et al., 2006; Fletcher et al., 1999). In the available barley genome, however, only *HvCLE402* as *CLV3*/*CLE40* candidate gene could be identified, encoding for a peptide with CLE motif and exhibit the same intron/exon structure (two introns) as AtCLE40, AtCLV3, OsFCP1 and OsFON2 (Mayer et al., 2012; Kirschner et al., 2017). Therefore, there is no obvious candidate for a CLV3 homologue in barley.

5. Supplementary figures

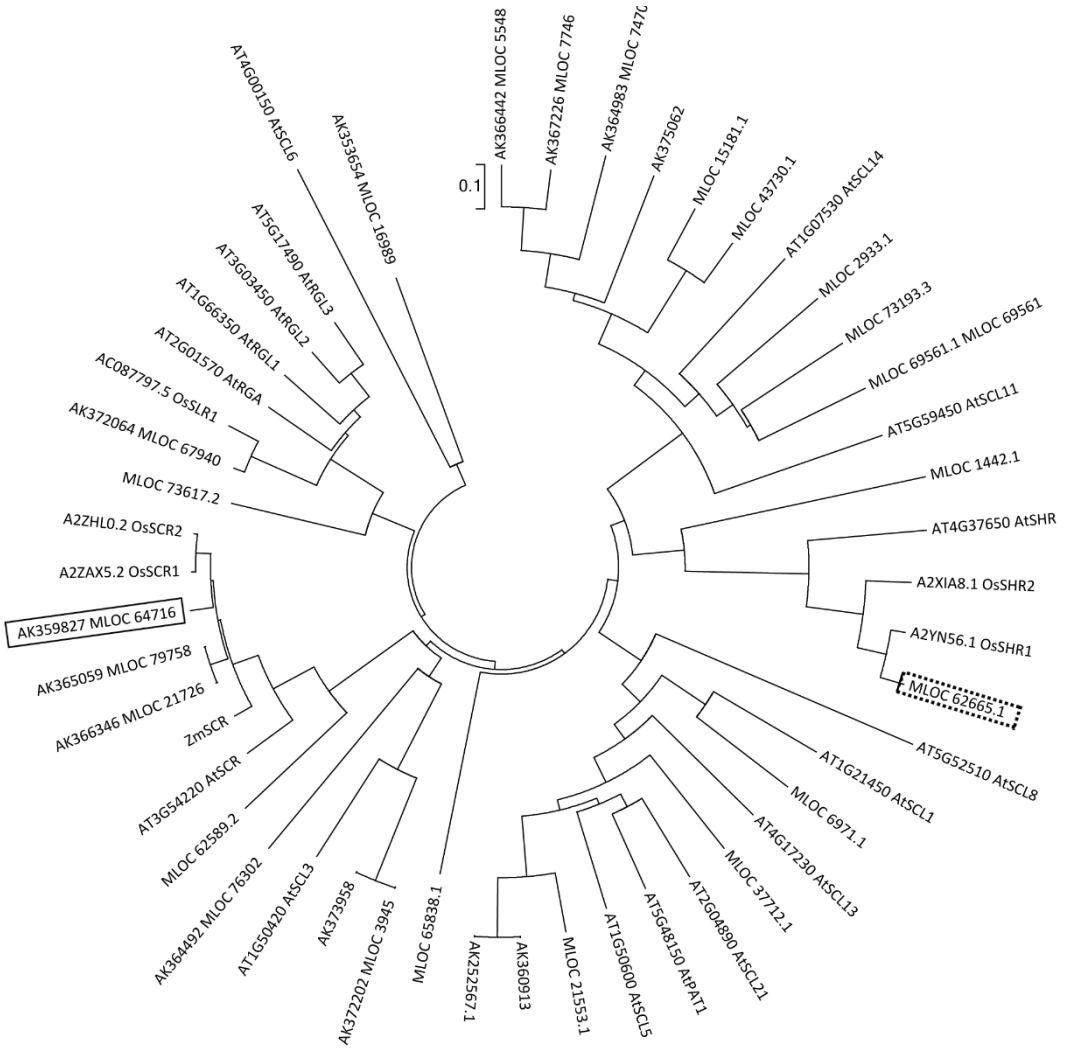

Supplementary figure 1: Phylogenetic tree of representative members of the GRAS family.

Phylogenetic tree of the GRAS family from *Arabidopsis*, rice, maize and barley; sequences from *Arabidopsis* (At) GRAS family members were taken from The *Arabidopsis* Information Resource (TAIR10) and named according to Xu et al., 2015; rice (Os) sequences were taken from Xu et al., 2015; the sequences for maize (Zm) proteins were taken from Lim et al., 2000; for barley homologues, AtSHR and AtSCR were used as template for BLAST-p search on http://webblast.ipk-gatersleben.de/barley_ibsc/ among high confidence genes with an e-value below 5e-33; search among low-confidence genes gave no hits (Mayer et al., 2012); proteins were aligned by MUSCLE alignment in MEGA7; the evolutionary history was inferred using the Neighbor-Joining method. The optimal tree with the sum of branch length = 13.85733761 is shown. The tree is drawn to scale, with branch lengths in the same units as those of the evolutionary distances used to infer the phylogenetic tree. The evolutionary distances were computed using the Poisson correction method and are in the units of the number of amino acid substitutions per site. The analysis involved 49 amino acid sequences. All positions containing gaps and missing data were eliminated. There were a total of 265 positions in the final dataset. Evolutionary analyses were conducted in MEGA7; the frame marks HvSCR, the dashed frame marks HvSHR.

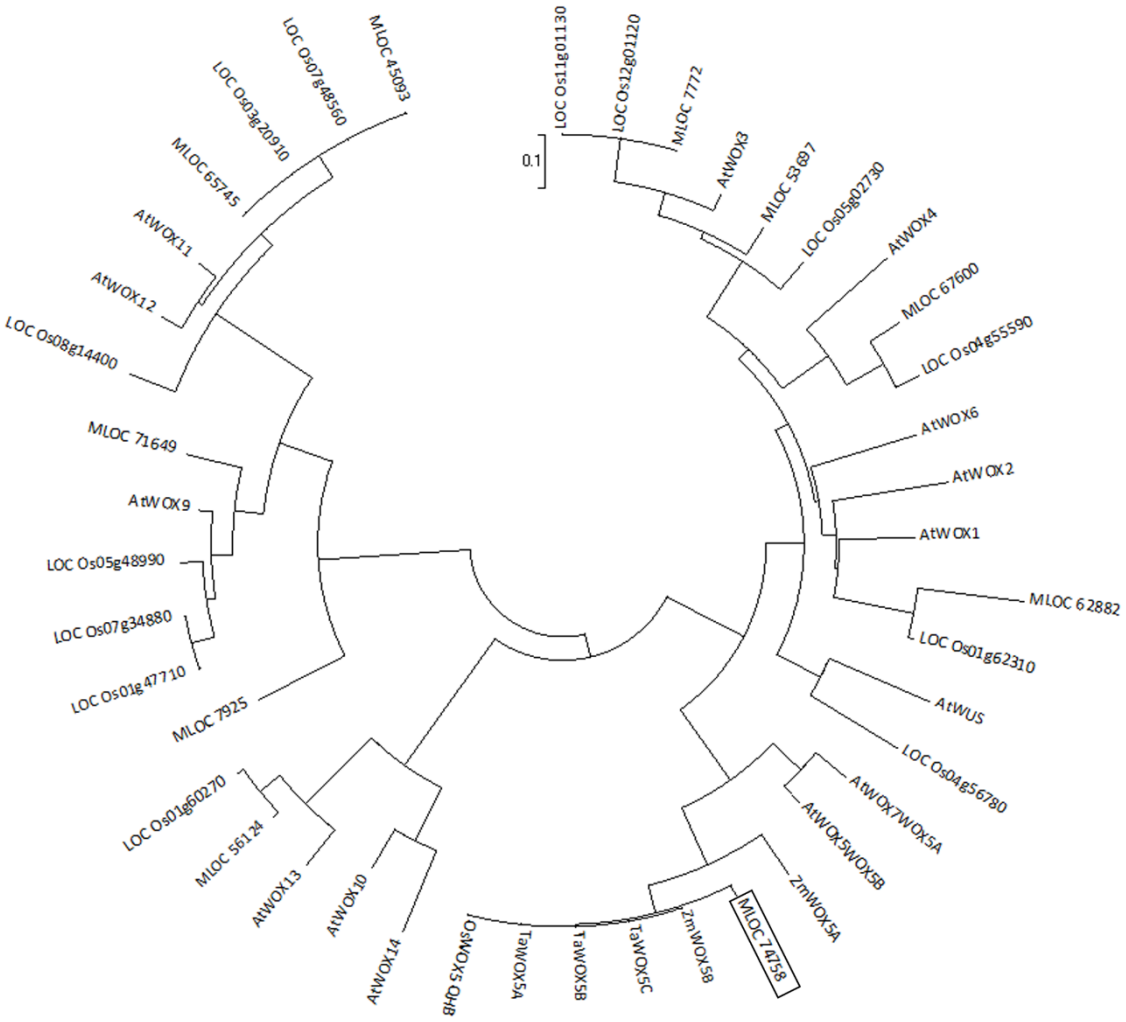

Supplementary figure 2: Phylogenetic tree of WOX family proteins.

Phylogenetic tree of WOX homologues from *Arabidopsis,* rice, wheat, maize and barley; *Arabidopsis* (At) WOX family members were taken from The *Arabidopsis* Information Resource (TAIR10); for barley WOX proteins, AtWOX5, TaWOX5, OsWOX5 and ZmWOX5A protein sequences were used as templates for BLAST-p search on http://webblast.ipk-gatersleben.de/barley_ibsc/ among high- and low-confidence genes with an e-value below 4e-08 (Mayer et al., 2012); for rice WOX homologues, OsQHB (Kamiya et al., 2003b) was used as template for blast-x search at https://phytozome.jgi.doe.gov/pz/portal.html and results with an e-value below3.8e-09 are displayed; selected WOX5 from maize (Zm) and wheat (Ta) homologues were taken from Nardmann et al., 2007 and Zhao et al., 2014; the whole protein sequences were aligned by MUSCLE alignment in MEGA7; the evolutionary history was inferred using the Neighbor-Joining method. The optimal tree with the sum of branch length = 5.64116747 is shown. The tree is drawn to scale, with branch lengths in the same units as those of the evolutionary distances used to infer the phylogenetic tree. The evolutionary distances were computed using the Poisson correction method and are in the units of the number of amino acid substitutions per site. The analysis involved 43 amino acid sequences. All positions containing gaps and missing data were eliminated. There were a total of 37 positions in the final dataset. Evolutionary analyses were conducted in MEGA7; the frame marks HvWOX5.

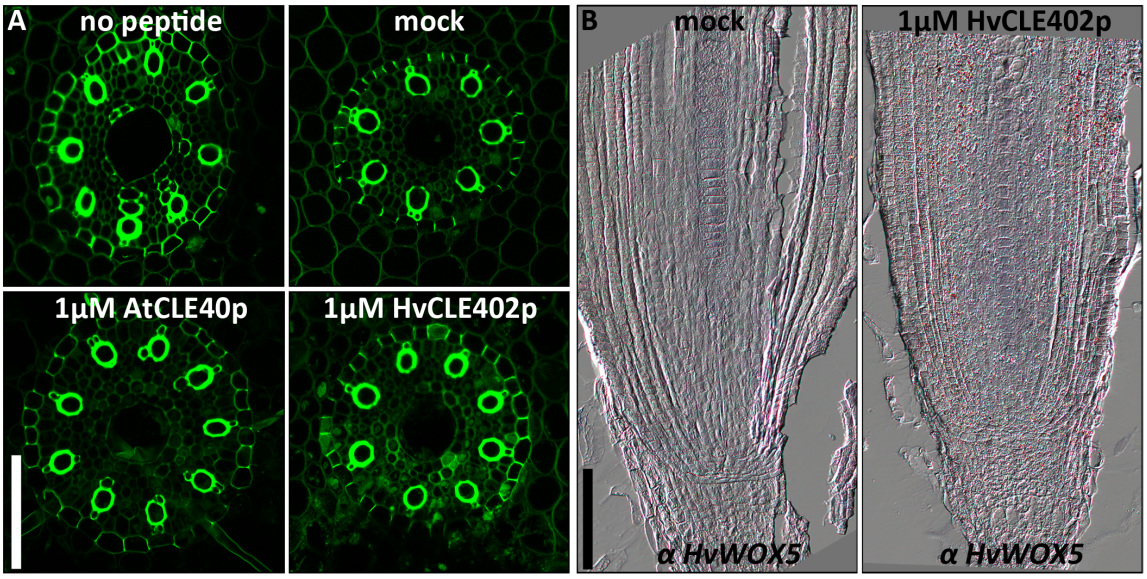

Supplementary figure 3: Effect of CLE40 peptides on the vascular structure and *HvWOX5* expression in the barley cv. Morex.

Application of CLE40 peptides (CLE40p) for 5 DAG does neither influence the structure of the vasculature nor *HvWOX5* expression. **A)** Effect of peptide (as indicated in the captions) on the vasculature; mock = CLE40 consisting of randomized amino acids (Kirschner et al., 2017); roots stained with berberine hemisulfate (green fluorescence of the casparian strip in the endodermis, autofluorescence of the xylem vessels); n = 5 - 6 per treatment, experiment was performed twice. **B)** Effect of HvCLE402 peptide on *HvWOX5* expression; n = 10 per treatment, experiment was performed three times; scale bars 100 µm

Supplementary figure 4: Phylogenetic tree of CLV homologues of barley, *Arabidopsis*, maize and rice.

Selected *Arabidopsis* (At) sequences were taken from The *Arabidopsis* Information Resource (TAIR10); for the barley CLV homologues, AtCLV1 was used as template for BLAST-p search on http://webblast.ipk-gatersleben.de/barley_ibsc/ among high confidence genes with an e-value below 4e-115 and among low-confidence genes with an e-value below 3e-44 (Mayer et al., 2012); sequences for rice FON1 and maize TD1 were taken from Suzaki et al., 2006 and Bommert et al., 2005. MUSCLE alignment of whole protein sequence was performed in MEGA7; the evolutionary history was inferred by using the Maximum Likelihood method based on the JTT matrix-based model. The tree with the highest log likelihood (-119724.7918) is shown. Initial tree(s) for the heuristic search were obtained automatically by applying Neighbor-Join and BioNJ algorithms to a matrix of pairwise distances estimated using a JTT model, and then selecting the topology with superior log likelihood value. The tree is drawn to scale, with branch lengths measured in the number of substitutions per site. The analysis involved 74 amino acid sequences. There were a total of 1888 positions in the final dataset. Evolutionary analyses were conducted in MEGA7; the frame marks HvCLV1.

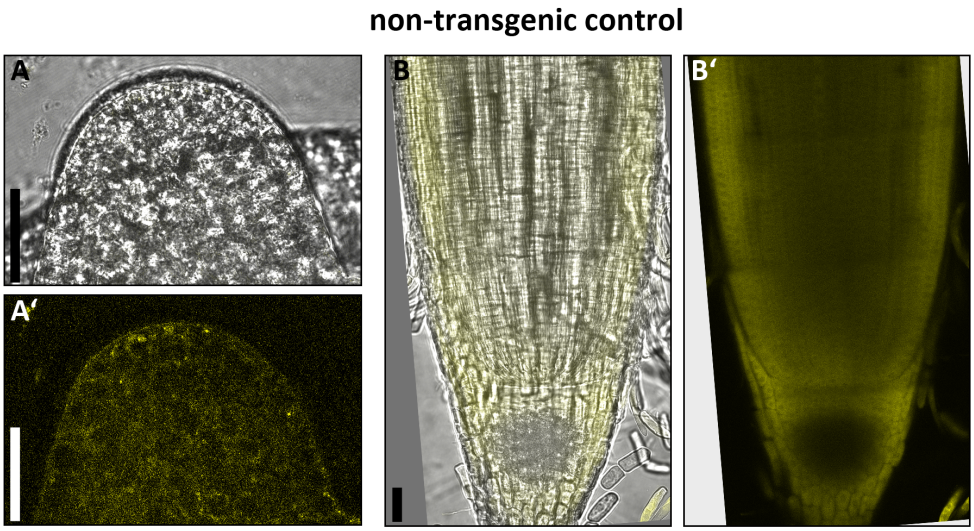

Supplementary figure 5: Non-transgenic control for microscopy (Golden Promise).

A), **A')** SAM in Waddington stage I, settings like Figure 4C), C'). **B)**, **B')** Roots were cleared for one week as described in Material and Methods; settings like in Figure 2 C and C'; A), B) VENUS excitation and transmitted light, A'). B') VENUS excitation; scale bars 50µm.

6. References

Aida, M., Beis, D., Heidstra, R., Willemsen, V., Blilou, I., Galinha, C., Nussaume, L., Noh, Y., Amasino, R., and Scheres, B. (2004). The PLETHORA Genes Mediate Patterning of the Arabidopsis Root Stem Cell Niche. Cell **119**: 109–120.

Becraft, P.W., Kang, S.-H., and Suh, S.-G. (2001). The Maize CRINKLY4 Receptor Kinase Controls a Cell-Autonomous Differentiation Response. Plant Physiol. **127**: 486–496.

van den Berg, C., Willemsen, V., Hendriks, G., Weisbeek, P., and Scheres, B. (1997). Short-range control of cell differentiation in the Arabidopsis root meristem. Nature **390**: 287–289.

Bleckmann, A., Weidtkamp-Peters, S., Seidel, C.A.M., and Simon, R. (2010). Stem Cell Signaling in Arabidopsis Requires CRN to Localize CLV2 to the Plasma Membrane. Plant Physiol. **152**: 166–76.

Bommert, P., Lunde, C., Nardmann, J., Vollbrecht, E., Running, M., Jackson, D., Hake, S., and Werr, W. (2005). thick tassel dwarf1 encodes a putative maize ortholog of the Arabidopsis CLAVATA1 leucine-rich repeat receptor-like kinase. Development **132**: 1235–45.

Brand, U., Fletcher, J.C., Hobe, M., Meyerowitz, E.M., and Simon, R. (2000). Dependence of stem cell fate in Arabidopsis on a feedback loop regulated by CLV3 activity. Science **289**: 617–619.

Carles, C.C. and Fletcher, J.C. (2003). Shoot apical meristem maintenance: the art of a dynamic balance. Trends Plant Sci. **8**: 394–401.

Chu, H., Liang, W., Li, J., Hong, F., Wu, Y., Wang, L., Wang, J., Wu, P., Liu, C., Zhang, Q., Xu, J., and Zhang, D. (2013). A CLE–WOX signalling module regulates root meristem maintenance and vascular tissue development in rice. J. Exp. Bot. **64**: 5359–5369.

Chu, H., Qian, Q., Liang, W., Yin, C., Tan, H., Yao, X., Yuan, Z., Yang, J., Huang, H., Luo, D., Ma, H., and Zhang, D. (2006). The FLORAL ORGAN NUMBER4 Gene Encoding a Putative Ortholog of Arabidopsis CLAVATA3 Regulates Apical Meristem Size in Rice. Plant Physiol. **142**: 1039–1052.

Clark, S.E., Williams, R.W., and Meyerowitz, E.M. (1997). The CLAVATA1 Gene Encodes a Putative Receptor Kinase That Controls Shoot and Floral Meristem Size in Arabidopsis. Cell **89**: 575–585.

Clowes, F.A.L. (1978). Origin of the Quiescent Centre in Zea Mays. New Phytol. **80**: 409–419.

Clowes, F.A.L. (1984). Size And Activity Of Quiescent Centres Of Roots. New Phytol. **96**: 13–21.

Coudert, Y., Périn, C., Courtois, B., Khong, N.G., and Gantet, P. (2010). Genetic control of root development in rice, the model cereal. Trends Plant Sci. **15**: 219–26.

Cruz-Ramírez, A., Díaz-Triviño, S., Wachsman, G., Du, Y., Arteága-Vázquez, M., Zhang, H., Benjamins, R., Blilou, I., Neef, A.B., Chandler, V., and Scheres, B. (2013). A SCARECROW-RETINOBLASTOMA Protein Network Controls Protective Quiescence in the Arabidopsis Root Stem Cell Organizer. PLOS Biol. **11**.

Cui, H., Levesque, M.P., Vernoux, T., Jung, J.W., Paquette, A.J., Gallagher, K.L., Wang, J.Y., Blilou, I., Scheres, B., and Benfey, P.N. (2007). An evolutionarily conserved mechanism delimiting SHR movement defines a single layer of endodermis in plants. Science **316**: 421–5.

Curtis, M.D. and Grossniklaus, U. (2003). A Gateway Cloning Vector Set for High-Throughput Functional Analysis of Genes in Planta. Plant Physiol. **133**: 462–469.

Dolan, L., Janmaat, K., Willemsen, V., Linstead, P., Poethig, S., Roberts, K., and Scheres, B. (1993). Cellular organisation of the Arabidopsis thaliana root. Development **119**: 71–84.

Du, M., Nakajima, K., Sena, G., Nawy, T., and Benfey, P.N. (2001). Intercellular movement of the putative transcription factor SHR in root patterning. Nature **413**: 307–311.

Fiers, M., Golemiec, E., Xu, J., Van Der Geest, L., Heidstra, R., Stiekema, W., and Liu, C. (2005). The 14 – Amino Acid CLV3 , CLE19 , and CLE40 Peptides Trigger Consumption of the Root Meristem in Arabidopsis through a CLAVATA2 -Dependent Pathway. Plant Cell **17**: 2542–2553.

Fletcher, J.C., Brand, U., Running, M.P., Simon, R., and Meyerowitz, E.M. (1999). Signaling of Cell Fate Decisions by CLAVATA3 in Arabidopsis Shoot Meristems. Science **283**: 1911–1914.

Gifford, M.L., Dean, S., and Ingram, G.C. (2003). The Arabidopsis ACR4 gene plays a role in cell layer organisation during ovule integument and sepal margin development. Development **130**: 4249–4258.

Gifford, M.L., Robertson, F.C., Soares, D.C., and Ingram, G.C. (2005). ARABIDOPSIS CRINKLY4 Function , Internalization , and Turnover Are Dependent on the Extracellular Crinkly Repeat Domain. Plant Cell **17**: 1154–1166.

Hardtke, C.S. and Pacheco-Villalobos, D. (2015). The Brachypodium distachyon Root System: A Tractable Model to Investigate Grass Roots. In Genetics and Genomics of Brachypodium.

Hejátko, J., Blilou, I., Brewer, P.B., Friml, J., Scheres, B., and Benková, E. (2006). In situ hybridization technique for mRNA detection in whole mount Arabidopsis samples. Nat. Protoc.

1: 1939–1946.

Helariutta, Y., Fukaki, H., Wysocka-Diller, J., Nakajima, K., Jung, J., Sena, G., Hauser, M.T., and Benfey, P.N. (2000). The SHORT-ROOT gene controls radial patterning of the Arabidopsis root through radial signaling. Cell **101**: 555–567.

Hirakawa, Y., Kondo, Y., and Fukuda, H. (2010). TDIF peptide signaling regulates vascular stem cell proliferation via the WOX4 homeobox gene in Arabidopsis. Plant Cell **22**: 2618–2629.

Hobe, M., Müller, R., Grünewald, M., Brand, U., and Simon, R. (2003). Loss of CLE40, a protein functionally equivalent to the stem cell restricting signal CLV3, enhances root waving in Arabidopsis. Dev. Genes Evol. **213**: 371–381.

Hochholdinger, F., Park, W.J., Sauer, M., and Woll, K. (2004a). From weeds to crops: genetic analysis of root development in cereals. Trends Plant Sci. **9**: 42–48.

Hochholdinger, F., Woll, K., Sauer, M., and Dembinsky, D. (2004b). Genetic dissection of root formation in maize (Zea mays) reveals root-type specific developmental programmes. Ann. Bot. **93**: 359–368.

Imani, J., Li, L., Schäfer, P., and Kogel, K.-H. (2011). STARTS - A stable root transformation system for rapid functional analyses of proteins of the monocot model plant barley. Plant J. **67**: 726–735.

Je, B. Il, Gruel, J., Lee, Y.K., Bommert, P., Arevalo, E.D., Eveland, A.L., Wu, Q., Goldshmidt, A., Meeley, R., Bartlett, M., Komatsu, M., Sakai, H., Jönsson, H., and Jackson, D. (2016). Signaling from maize organ primordial via FASCIATED EAR3 regulates stem cell proliferation and yield traits. Nat. Genet. **48**: 785–791.

Jeong, S., Trotochaud, A.E., and Clark, S.E. (1999). The Arabidopsis CLAVATA2 gene encodes a receptor-like protein required for the stability of the CLAVATA1 receptor-like kinase. Plant Cell **11**: 1925–34.

Jiang, K. and Feldman, L.J. (2005). Regulation of root apical meristem development. Annu. Rev. Cell Dev. Biol. **21**: 485–509.

Jiang, K., Meng, Y.L., and Feldman, L.J. (2003). Quiescent center formation in maize roots is associated with an auxin-regulated oxidizing environment. Development **130**: 1429–1438.

Kamiya, N., Itoh, J.-I., Morikami, A., Nagato, Y., and Matsuoka, M. (2003a). The SCARECROW gene's role in asymmetric cell divisions in rice plants. Plant J. **36**: 45–54.

Kamiya, N., Nagasaki, H., Morikami, A., Sato, Y., and Matsuoka, M. (2003b). Isolation and characterization of a rice WUSCHEL-type homeobox gene that is specifically expressed in the central cells of a quiescent center in the root apical meristem. Plant J. **35**: 429–441.

Kinoshita, A., Nakamura, Y., Sasaki, E., Kyozuka, J., Fukuda, H., and Sawa, S. (2007). Gain-of-function phenotypes of chemically synthetic CLAVATA3/ESR-Related (CLE) peptides in Arabidopsis thaliana and Oryza sativa. Plant Cell Physiol. **48**: 1821–1825.

Kirschner, G.K., Stahl, Y., Von Korff, M., and Simon, R. (2017). Unique and Conserved Features of the Barley Root Meristem. Front. Plant Sci. **8:** 1240.

Koushik, S. V, Chen, H., Thaler, C., Puhl, H.L., and Vogel, S.S. (2006). Cerulean, Venus, and VenusY67C FRET Reference Standards. Biophys. J. **91**: L99–L101.

Lampropoulos, A., Sutikovic, Z., Wenzl, C., Maegele, I., Lohmann, J.U., and Forner, J. (2013). GreenGate - A Novel, Versatile, and Efficient Cloning System for Plant Transgenesis. PLoS One **8**: e83043.

Laufs, P., Grandjean, O., Jonak, C., Kieu, K., and Traas, J. (1998). Cellular Parameters of the Shoot Apical Meristem in Arabidopsis. Plant Cell Online **10**: 1375–1389.

Di Laurenzio, L., Wysocka-Diller, J., Malamy, J.E., Pysh, L., Helariutta, Y., Freshour, G., Hahn, M.G., Feldmann, K. A., and Benfey, P.N. (1996). The SCARECROW gene regulates an asymmetric cell division that is essential for generating the radial organization of the Arabidopsis root. Cell **86**: 423–33.

Laux, T., Mayer, K.F., Berger, J., and Jürgens, G. (1996). The WUSCHEL gene is required for shoot and floral meristem integrity in Arabidopsis. Development **122**: 87–96.

Lim, J., Helariutta, Y., Specht, C.D., Jung, J., Sims, L., Bruce, W.B., Diehn, S., and Benfey, P.N. (2000). Molecular analysis of the SCARECROW gene in maize reveals a common basis for radial patterning in diverse meristems. Plant Cell **12**: 1307–1318.

Lim, J., Jung, J.W., Chae, E.L., Lee, M.H., Bong, J.K., Kim, M., Bruce, W.B., and Benfey, P.N. (2005). Conservation and diversification of SCARECROW in maize. Plant Mol. Biol. **59**: 619–630.

Mayer, K.F., Schoof, H., Haecker, a, Lenhard, M., Jürgens, G., and Laux, T. (1998). Role of WUSCHEL in regulating stem cell fate in the Arabidopsis shoot meristem. Cell **95**: 805–15.

Mayer, K.F.X. et al., The International Barley Genome Sequencing Consortium (2012). A physical, genetic and functional sequence assembly of the barley genome. Nature **491**: 711–716.

Müller, R., Bleckmann, A., and Simon, R. (2008). The receptor kinase CORYNE of Arabidopsis transmits the stem cell-limiting signal CLAVATA3 independently of CLAVATA1. Plant Cell **20**: 934–46.

Nagai, T., Ibata, K., Park, E.S., Kubota, M., Mikoshiba, K., and Miyawaki, A. (2002). A variant of yellow fluorescent protein with fast and efficient maturation for cell-biological applications. Nat. Biotechnol. **20**: 87–90.

Nagasawa, N., Miyoshi, M., Kitano, H., Satoh, H., and Nagato, Y. (1996). Mutations associated with floral organ number in rice. Planta **198**: 627–633.

Nardmann, J. and Werr, W. (2006). The shoot stem cell niche in angiosperms: Expression patterns of WUS orthologues in rice and maize imply major modifications in the course of mono- and dicot evolution. Mol. Biol. Evol. **23**: 2492–2504.

Nardmann, J., Zimmermann, R., Durantini, D., Kranz, E., and Werr, W. (2007). WOX gene phylogeny in Poaceae: a comparative approach addressing leaf and embryo development. Mol. Biol. Evol. **24**: 2474–84.

Ni, J., Shen, Y., Zhang, Y., and Wu, P. (2014). Definition and stabilisation of the quiescent centre in rice roots. Plant Biol. **16**: 1014–1019.

Nimchuk, Z.L., Tarr, P.T., Ohno, C., Qu, X., and Meyerowitz, E.M. (2011). Signaling in the Arabidopsis shoot meristem stem cell niche correlates with ligand-dependent trafficking of the CLV1 receptor kinase. Curr. Biol. **21**: 345–352.

Ogawa, M., Shinohara, H., Sakagami, Y., and Matsubayashi, Y. (2008). Arabidopsis CLV3 peptide directly binds CLV1 ectodomain. Science **319**: 294.

Olsen, L.T., Divon, H.H., Al, R., Fosnes, K., Lid, S.E., and Opsahl-Sorteberg, H.-G. (2008). The defective seed5 (des5) mutant: effects on barley seed development and HvDek1, HvCr4, and HvSal1 gene regulation. J. Exp. Bot. **59**: 3753–65.

Pi, L., Aichinger, E., van der Graaff, E., Llavata-Peris, C.I., Weijers, D., Hennig, L., Groot, E., and Laux, T. (2015). Organizer-Derived WOX5 Signal Maintains Root Columella Stem Cells through Chromatin-Mediated Repression of CDF4 Expression. Dev. Cell **33**: 576–588.

Rebouillat, J., Dievart, A., Verdeil, J.L., Escoute, J., Giese, G., Breitler, J.C., Gantet, P., Espeout, S., Guiderdoni, E., and Périn, C. (2009). Molecular genetics of rice root development. Rice **2**: 15–34.

Sabatini, S., Heidstra, R., Wildwater, M., and Scheres, B. (2003). SCARECROW is involved in

positioning the stem cell niche in the Arabidopsis root meristem. Genes Dev. **17**: 354–8.

Sarkar, A.K., Luijten, M., Miyashima, S., Lenhard, M., Hashimoto, T., Nakajima, K., Scheres, B., Heidstra, R., and Laux, T. (2007). Conserved factors regulate signalling in Arabidopsis thaliana shoot and root stem cell organizers. Nature **446**: 811–814.

Schindelin, J. et al. (2012). Fiji: an open-source platform for biological-image analysis. Nat. Methods **9**: 676–682.

Schoof, H., Lenhard, M., Haecker, A., Mayer, K.F.X., Jürgens, G., and Laux, T. (2000). The Stem Cell Population of Arabidopsis Shoot Meristems Is Maintained by a Regulatory Loop between the CLAVATA and WUSCHEL Genes. Cell **100**: 635–644.

Slewinski, T.L., Anderson, A.A., Zhang, C., and Turgeon, R. (2012). Scarecrow Plays a Role in Establishing Kranz Anatomy in Maize Leaves. Plant Cell Physiol. **53**: 2030–2037.

Stahl, Y., Grabowski, S., Bleckmann, A., Kühnemuth, R., Weidtkamp-Peters, S., Pinto, K.G., Kirschner, G.K., Schmid, J.B., Wink, R.H., Hülsewede, A., Felekyan, S., Seidel, C.A.M., and Simon, R. (2013). Moderation of Arabidopsis Root Stemness by CLAVATA1 and ARABIDOPSIS CRINKLY4 Receptor Kinase Complexes. Curr. Biol. **23**: 1–10.

Stahl, Y. and Simon, R. (2005). Plant stem cell niches. Int. J. Dev. Biol. **49**: 479–89.

Stahl, Y., Wink, R.H., Ingram, G.C., and Simon, R. (2009). A Signaling Module Controlling the Stem Cell Niche in Arabidopsis Root Meristems. Curr. Biol. **19**: 909–914.

Suzaki, T., Sato, M., Ashikari, M., Miyoshi, M., Nagato, Y., and Hirano, H.-Y. (2004). The gene FLORAL ORGAN NUMBER1 regulates floral meristem size in rice and encodes a leucine-rich repeat receptor kinase orthologous to Arabidopsis CLAVATA1. Development **131**: 5649–57.

Suzaki, T., Toriba, T., Fujimoto, M., Tsutsumi, N., Kitano, H., and Hirano, H.-Y. (2006). Conservation and diversification of meristem maintenance mechanism in Oryza sativa: Function of the FLORAL ORGAN NUMBER2 gene. Plant Cell Physiol. **47**: 1591–1602.

Suzaki, T., Yoshida, A., and Hirano, H.-Y. (2008). Functional diversification of CLAVATA3-related CLE proteins in meristem maintenance in rice. Plant Cell **20**: 2049–58.

Taguchi-Shiobara, F., Yuan, Z., Hake, S., and Jackson, D. (2001). The fasciated ear2 gene encodes a leucine-rich repeat receptor-like protein that regulates shoot meristem proliferation in maize. Genes Dev. **15**: 2755–66.

Tian, Q., Olsen, L., Sun, B., Lid, S.E., Brown, R.C., Lemmon, B.E., Fosnes, K., Gruis, D. (Fred),

Opsahl-Sorteberg, H.-G., Otegui, M.S., and Olsen, O.-A. (2007). Subcellular Localization and Functional Domain Studies of DEFECTIVE KERNEL1 in Maize and Arabidopsis Suggest a Model for Aleurone Cell Fate Specification Involving CRINKLY4 and SUPERNUMERARY ALEURONE LAYER1. Plant Cell **19**: 3127–3145.

Vanstraelen, M., Baloban, M., Da Ines, O., Cultrone, A., Lammens, T., Boudolf, V., Brown, S.C., De Veylder, L., Mergaert, P., and Kondorosi, E. (2009). APC/C-CCS52A complexes control meristem maintenance in the Arabidopsis root. PNAS **106**: 11806–11.

Waddington, S.R., Cartwright, P.M., and Wall, P.C. (1983). A quantitative scale of spike initial and pistil development in barley and wheat. Ann. Bot. **51**: 119–130.

Warner, C.A., Biedrzycki, M.L., Jacobs, S.S., Wisser, R.J., Caplan, J.L., and Sherrier, D.J. (2014). An Optical Clearing Technique for Plant Tissues Allowing Deep Imaging and Compatible with Fluorescence Microscopy. Plant Physiol. **166**: 1684–1687.

Wu, S., Lee, C.-M., Hayashi, T., Price, S., Divol, F., Henry, S., Pauluzzi, G., Perin, C., and Gallagher, K.L. (2014). A plausible mechanism, based upon Short-Root movement, for regulating the number of cortex cell layers in roots. Proc. Natl. Acad. Sci. U. S. A. **111**: 16184–9.

Xu, K., Chen, S., Li, T., Ma, X., Liang, X., Ding, X., Liu, H., and Luo, L. (2015). OsGRAS23, a rice GRAS transcription factor gene, is involved in drought stress response through regulating expression of stress-responsive genes. BMC Plant Biol. **15**: 141.

Yadav, R.K., Perales, M., Gruel, J., Girke, T., Jonsson, H., and Reddy, G. V. (2011). WUSCHEL protein movement mediates stem cell homeostasis in the Arabidopsis shoot apex. Genes Dev. **25**: 2025–2030.

Zhao, S., Jiang, Q.-T., Ma, J., Zhang, X.-W., Zhao, Q.-Z., Wang, X.-Y., Wang, C.-S., Cao, X., Lu, Z.-X., Zheng, Y.-L., and Wei, Y.-M. (2014). Characterization and expression analysis of WOX5 genes from wheat and its relatives. Gene **537**: 63–9.

VIII. Summary

In this study, the barley (*Hordeum vulgare*) root apical meristem was analysed in detail in regard to the number and the origin of all occuring cell files. The expression pattern of genes that are known to be important for cell specification, root meristem development and maintenance were examined. Additionally, the expression of genes that are possibly expressed in both root and shoot apical meristem was examined in the shoot apical meristem.

Suberin staining showed that the barley seminal root consists of one layer of epidermis, five cortex cell layers and one endodermal layer surrounding the central cylinder. Cell division studies by EdU staining and RNA *in situ* hybridisation with a probe for *HISTONE H4* demonstrated that the Quiescent Center in barley consists of around 30 cells. Analysis of the cell wall arrangements revealed that endodermis and cortex do not share one common initial like it was observed in *Arabidopsis thaliana* and rice, but that the inner cortex shares a common initial with the endodermis, while the outer cortex is derived from another. Furthermore, the epidermis is derived from a different initial, and independent of the root cap. The among plant species widely conserved CLE40 peptide-dependent signalling pathway to regulate maintenance of the proximal meristem was found to be conserved in barley, the maintenance of the columella stem cells by this signalling pathway, however, seems to be restricted to *Arabidopsis*.

Literature research showed that altogether, the barley root meristem is structured like meristems of other monocots like rice and maize. However, it exhibits small but significant differences, like the origin of cortex and endodermis and the size of the QC. As barley features all root types of other monocots, a primary root, seminal roots and crown roots, and is much more salt-tolerant than other cereal crop plants, it is a valuable model plant for root growth of other monocot plants. There are many examples, in which barley genes were successfully transferred to other plants and increased drought and salinity resistance.

The study about conserved signalling components revealed that many homologue genes exist in barley that might regulate the barley root and shoot meristem homeostasis. *HvSCR* and *HvSHR* expression resembles the expression of their homologues from other plants, indicating a role for endodermis and cortex formation. The *WOX5* homologue *HvWOX5* is expressed in the metaxylem, resembling the expression pattern from other *WOX5* homologues partially, but indicating a role in vascular development. HvCLV1, HvCR4 and *HvCLE402* are expressed throughout the whole shoot meristem, indicating a role for shoot meristem development. Additionally, *HvCLE402* is also expressed in the root meristem, which supports the theory that the root meristem is evolutionarily derived from the shoot meristem.

Summary

Studies on the influence of the phytohormones auxin and cytokinin revealed that both phytohormones have a negative influence on barley root and meristem growth, when applied exogenously to the seedlings. Auxin has a lower influence on root meristem length, therefore the decreased root growth is possibly caused by a lower cell elongation in the whole root. Transgenic barley reporter lines revealed that cytokinin signalling mostly takes place in the stele cells proximal to the QC and in the differentiated root cap cells, but by cytokinin application, expression of the reporter gene can also be induced in the columella stem cells, the QC and epidermis initials, and more proximal in the stele at the transition zone of the meristem. As cytokinin application leads additionally to a reduced meristem size, the phytohormone probably influences the root growth negatively by premature differentiation of the meristem. Analysing signalling targets of auxin revealed that a homologue of AtPLT1, HvPLT1, is expressed in a similar way as AtPLT1 in *Arabidopsis*, in particular in the QC and the surrounding cells. Furthermore, a homologue of the auxin PIN transporters PIN1, HvPIN1, is expressed in the root meristem, its expression is regulated by cytokinin and the intracellular localisation is affected by BFA.

This givens study provides a basis for shoot and root meristem research in barley. Understanding the signalling pathways that regulate meristem development of both shoot and root contributes to the ability to genetically manipulate plant growth and thereby enhance the yield.

IX. Zusammenfassung

In dieser Arbeit wurde das Wurzelapikalmeristem von Gerste (*Hordeum vulgare*) in Bezug auf Anzahl und Entstehung der vorhandenen Zellreihen analysiert. Das Expressionsmuster von Genen wurde untersucht, die an der Zellspezifizierung, Wurzelmeristementwicklung und –aufrechterhaltung beteiligt sind. Zusätzlich wurde die Expression von Genen im Sprossapikalmeristem untersucht, die möglicherweise sowohl im Wurzel- als auch im Sprossapikalmeristem exprimiert sind.

Suberinfärbung zeigte, dass die Seminal-Wurzeln von Gerste aus einer Schicht Epidermiszellen, fünf Cortex-Zellreihen und einer Schicht Endodermis bestehen, die den Zentralzylinder umgeben. Zellteilungsstudien mit EdU-Färbung und RNA *in situ*-Hybridisierung mit einer Sonde gegen *HISTONE H4* zeigten, dass das Ruhende Zentrum (QC) in Gerste aus ungefähr 30 Zellen besteht. Analysen der Zellwand-Anordnung ergaben, dass Endodermis und Cortex nicht wie in *Arabidopsis* und Reis aus einer gemeinsamen Initial-Zelle hervorgehen, sondern dass die inneren Cortexzellschichten und Endodermis eine gemeinsame Initialzelle teilen, während die äußeren Cortexzellschichten aus einer separaten Initialzelle hervorgehen. Außerdem geht die Epidermis aus einer anderen Initialzelle hervor, die unabhängig von der Wurzelhaube ist. Der zwischen Pflanzenspezies weitgehend konservierte CLE40-peptidabhängige Signalweg zur Aufrechterhaltung des proximalen Meristems ist auch in Gerste konserviert, die Aufrechterhaltung der Columella-Stammzellen durch diesen Signalweg scheint jedoch auf *Arabidopsis* beschränkt zu sein

Literaturrecherchen ergaben, dass das Wurzelmeristem von Gerste weitgehend genauso strukturiert ist wie das von anderen einkeimblättrigen Pflanzen wie Reis und Mais. Jedoch weist es kleine, aber signifikante Unterschiede auf, wie etwa den Ursprung von Cortex und Endodermis und die Größe des QCs. Da Gerste alle Wurzeltypen besitzt, die auch andere einkeimblättrige Pflanzen aufweisen, nämlich eine Primärwurzel, Seminalwurzeln und Kronwurzeln, und Gerste salztoleranter ist als andere Getreide-Erntepflanzen, kann sie als wertvolle Modellpflanze für Wurzelentwicklung in anderen einkeimblättrigen Pflanzen dienen. Es gibt viele Beispiele, in denen Gene aus Gerste schon erfolgreich in andere Pflanzen übertragen, und damit die Trockenstress- und Salz-Toleranz erhöht wurde.

Die Analyse der konservierten Signalkomponenten ergab, dass in Gerste viele homologe Gene existieren, die potentiell Wurzel- und Sprossmeristemhomöostase regulieren könnten. Das *HvSCR*- und *HvSHR*-Expressionsmuster gleicht dabei der Expression der homologen Gene aus anderen Pflanzen, sodass eine Rolle in Endodermis- und Cortexentstehung möglich wäre. Das *WOX5*-Homolog *HvWOX5* ist im Metaxylem exprimiert, was nur zum Teil der Expression von anderen *WOX5*-Homologen entspricht, aber eine Rolle für die vaskuläre Entwicklung impliziert. HvCLV1, HvCR4 und *HvCLE402* sind im ganzen Sprossapikalmeristem exprimiert und dadurch möglicherweise an der Sprossmeristem-Entwicklung beteiligt. Zusätzlich ist *HvCLE402* auch im Wurzelmeristem

exprimiert, was die Theorie unterstützt, dass das Wurzelmeristem entwicklungsgeschichtlich vom Sprossapikalmeristem abstammt.

Analyse der Einwirkung von Auxin und Cytokinin zeigten, dass beide Phytohormone einen negativen Einfluss auf das Wachstum von Gerstenwurzeln und dem Wurzelmeristem haben, wenn die Pflanzen exogen damit behandelt werden. Auxin hat einen geringeren Einfluss auf die Wurzelmeristemlänge, deswegen ist es möglich, dass das verringerte Wurzelwachstum durch eine geringere Zell-Elongation in der ganzen Wurzel ausgelöst wird. Transgene Reporterlinien deckten auf, dass Cytokinin-Signalwege hauptsächlich in den Stele-Zellen proximal vom QC und in der differenzierten Wurzelhaube aktiv sind, die Expression der Reporterlinien aber durch exogene Behandlung mit Cytokinin auch in den Columella-Stammzellen, dem QC und den Epidermis-Initialen aktiviert werden kann, und darüberhinaus auch in der Stele auf Höhe der Transitionszone. Da Cytokininbehandlung zusätzlich zu einer reduzierten Meristemlänge führt, ist es wahrscheinlich, dass das Phytohormon das Wurzelwachstum durch eine vorzeitige Differenzierung des Meristems negativ beeinflusst. Analysen der Zielgene des Auxin-Signalwegs zeigten, dass das Homolog von AtPLT1, HvPLT1, in einem ähnlichen Muster exprimiert ist wie AtPLT1 in *Arabidopsis*, nämlich im QC und den umliegenden Stammzellen. Außerdem ist auch ein Homolog des Auxin-Transporters PIN1, HvPIN1, auch im Wurzelmeristem exprimiert, seine Expression wird von Cytokinin reguliert und die intrazelluläre Lokalisation wird von BFA beeinflusst.

Die vorliegende Arbeit stellt die Basis für Wurzel- und Sprossmeristem-Forschung in Gerste dar. Die Signalwege zu verstehen, die die Meristementwicklung von Spross und Wurzel regulieren, leistet einen wichtigen Beitrag zur genetischen Manipulation von Pflanzenwachstum, hin zu einem höheren Ertrag.

X. Appendix

1. Abbreviations

2,4D	2,4-dichlorophenoxyacetic acid
6-BA	6-benzylaminopurine
ABA	abscisic acid
ACR4	ARABIDOPSIS CRINKYL4
AIL	AINTEGUMENTA-like
AHK	ARABIDOPSIS HISTIDINE KINASE
AHP	ARABIDOPSIS HISTIDINE PHOSPHOTRANSFER PROTEIN
AP2/EREBP	APETALA2/ethylene-responsive element binding protein
ARF	AUXIN RESPONSE FACTOR
ARF-GEF	GDP/GTP exchange factor for small G proteins of the ADP-ribosylation factor
ARR	ARABIDOPSIS RESPONSE REGULATOR
Aux/IAA	AUXIN/ INDOLE-3-ACETIC ACID
AuxRe	auxin responsive element
bp	base pairs
BCIP	5-bromo-4-chloro-3'-indolyphosphate p-toluidine salt
BFA	Brefeldin-A
bGLU	*β-glucosidase* promoter
CBL	calcineurin B-like
cDNA	complementary DNA
CIPK	CBL-interacting protein kinase
CKX	CYTOKININ OXIDASE/DEHYDROGENASE
CLE40	CLV3/ ENDOSPERM SURROUNDING REGION40
CLV1	CLAVATA1
CLV2	CLAVATA2
CLV3	CLAVATA3
cMX	central metaxylem

CRN	CORYNE
cv.	cultivar
DAG	days after germination
DSC	distal stem cell
EtOH	Ethanol
FCP1	FON2-LIKE CLE PROTEIN1
FEA2	FASCIATED EAR2
FON1	FLORAL ORGAN NUMBER1
FON2	FLORAL ORGAN NUMBER2
gDNA	genomic DNA
H2B	HISTONE H2B
IBA	indole-3-butyric acid
IAA	indole-3-acetic acid
ICEI	inner cortex endodermis initial
IPT	ISOPENTENYLTRANSFERASE
mPS-PI	modified pseudo-Schiff propidium iodide
NAA	1-naphthalene acetic acid
NBT	nitro-blue tetrazolium chloride
NPA	1-N-Naphthylphthalamic acid
OC	organizing center
OCI	outer cortex initial
PBS	phosphate buffered saline
PIN	PINFORMED
PLT	PLETHORA
pMX	peripheral metaxylem
QHB	QUIESCENT-CENTER-SPECIFIC HOMEOBOX
QC	quiescent center
QTL	quantitative trait locus

RAM	root apical meristem
SAM	shoot apical meristem
SCR	SCARECROW
SHR	SHORTROOT
SHY2	SHORT HYPOCOTYL2
TCS	Two Component signalling Sensor
TD1	THICK TASSEL DWARF
TIR1/AFB	TRANSPORT INHIBITOR RESPONSE 1/AUXIN SIGNALING F-BOX
t-Z	*trans*-zeatin
WOX5	WUSCHEL-RLEATED HOMEOBOX5
WUS	WUSCHEL

2. List of genes, promoter length and identifiers

Gene name	identifier	Morex_ contig	annotation	Length of used promoter [bp upstream of start codon]	Length of CDS, genomic DNA [bp from start to stop codon]
HvWOX5	MLOC_74758.1	66485	WUSCHEL-related homeobox 5	5228	758
HvCLV1	MLOC_66232.2	51275	Receptor protein kinase-like protein	2826	3573
HvPLT1	MLOC_76811.2	73008	AP2-like ethylene-responsive transcription factor	1929	3433
HvCR4	AK374415	146323	Kinase family protein	1266	2694
HvSCR	AK359827	49323	Scarecrow transcription factor family protein	2539	2362
HvPIN1	AK357068 MLOC-64867	49437	Auxin efflux carrier	3453	2402
HvCLE402	MLOC_3686.1	132695	CLE family OsCLE402 protein	2034	318
HvSHR	MLOC_62665.1	46826	GRAS family transcription factor	Not used	1791
HvHISTONE H4	AK362824	2450454	Histone H4	Not used	309

Table 1: List of cloned genes
Information taken from http://webblast.ipk-gatersleben.de/barley_ibsc/ (Mayer et al 2012).

3. List of transgenic lines

#	Construct name	Basis vector	Available lines	Expressing lines	Expression in T2 confirmed?
125	*HvpWOX5:HvWOX5-mV*	pAB134	1, 2, 3, 4, 5	2, 3, 4	not yet
126	*HvpSCR:HvSCR-mV*	pAB134	1, 2, 4	4	not yet
127	*HvpCR4:HvCR4-mV*	pAB134	4, 5, 6, 7, 8, 9, 11, 12, 14, 16, 18, 19, 24, 33	9, 11, 12, 18, 24	not yet
128	*HvpCLV1:HvCLV1-mV*	pAB134	1, 2, 3, 4	1, 2, 3, 4	yes
129	*DR5::GFP*	Gift from Benková lab	1, 2, 3, 4, 5, 6, 7, 10, 11, 12, 14, 15, 16, 17, 18, 19, 20, 21, 22, 23, 24, 27, 28, 29, 30, 31, 33, 34, 35, 36	-	-
138	*HvpCLE40:VENUS-H2B*	pAB146	1, 2, 3, 4, 5-2, 5, 7, 8, 9, 10, 11, 13, 14, 15, 16, 17, 18, 19, 20, 22, 23, 24, 25, 26, 27, 28, 29, 30, 31, 32, 33, 34, 35, 36, 37, 39	5, 5-2, 13, 16, 18, 23, 29, 30, 31, 32	not yet
139	*TCSn:Venus-H2B*	pAB146	1, 2, 3, 4, 6, 7, 8, 9, 10, 11, 12, 12, 15, 16, 17, 18, 19, 21, 22, 25, 26, 27, 28, 29, 30, 31, 32, 33, 35, 36, 37, 38, 39, 40, 43, 45, 46	1, 4, 6, 7, 9, 10, 21	yes
140	*HvpPLT1:HvPLT1-mV*	pAB134	1, 2, 3, 4 (2x), 10, 11, 12, 13, 14, 16, 17, 19, 21, 22, 23, 24, 25, 26, 27, 28, 29, 30, 31, 32, 33, 34, 35, 36, 37, 38, 39, 40, 41, 42	1, 2, 3, 10, 17, 25	yes
141	*HvpPIN1:HvPIN1-mV*	pAB134	1, 2, 3, 6, 7, 8, 9, 12, 13, 15, 16, 17, 18, 20, 23, 26, 27, 29, 30, 31, 32, 33, 34, 35, 36, 37, 38, 39, 40, 41	9, 12, 20, 27, 40	not yet
143	*DR5v2-Venus-H2B*	pAB146	3, 4, 5, 7, 8, 9, 10, 12, 13, 15, 16, 18, 19, 20, 21, 22, 23, 24, 25, 26, 27, 28, 29, 30, 31, 32, 33, 34, 35, 36, 37, 38, 39, 40	18, 25, 36, 37	-

Table 2: List of available transgenic lines.

4. Plasmid maps

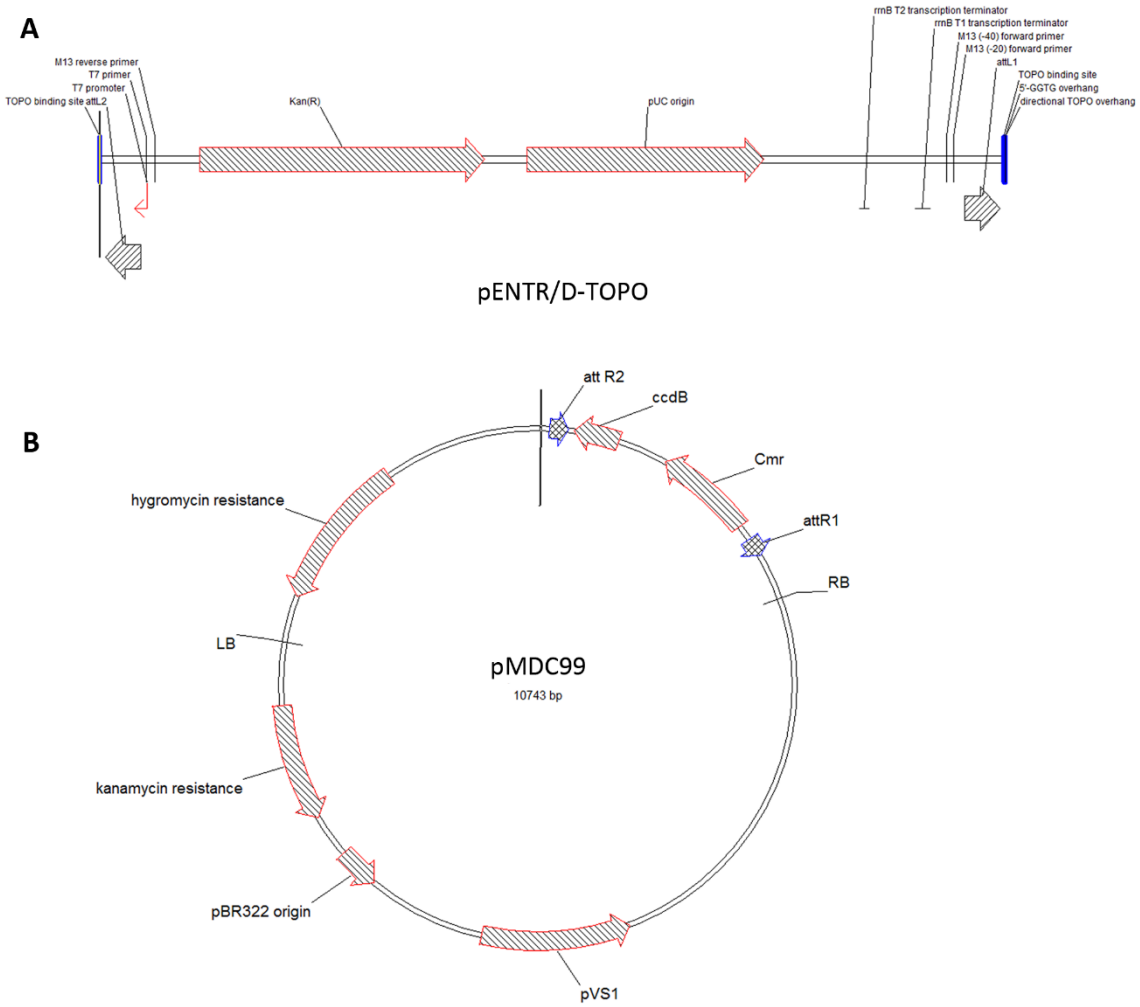

Figure 1: Exemplary maps of entry and destination vectors.

A) Plasmid map of pENTR/D-TOPO entry vector (Invitrogen) without insert; attL1, attL2 = Gateway recombination sites; Kan(R) = kanamycin resistance. **B)** Plasmid map for pMDC99 used as backbone for destination vectors; LB = left border, RB = right border, attR1, attR2 = Gateway recombination sites; ccdB = cytotoxic protein for bacterial selection; Cmr = chloramphenicol resistance; pVS1 = minimal replicon for replication in gram negative bacteria; pBR322 = replication starting point.

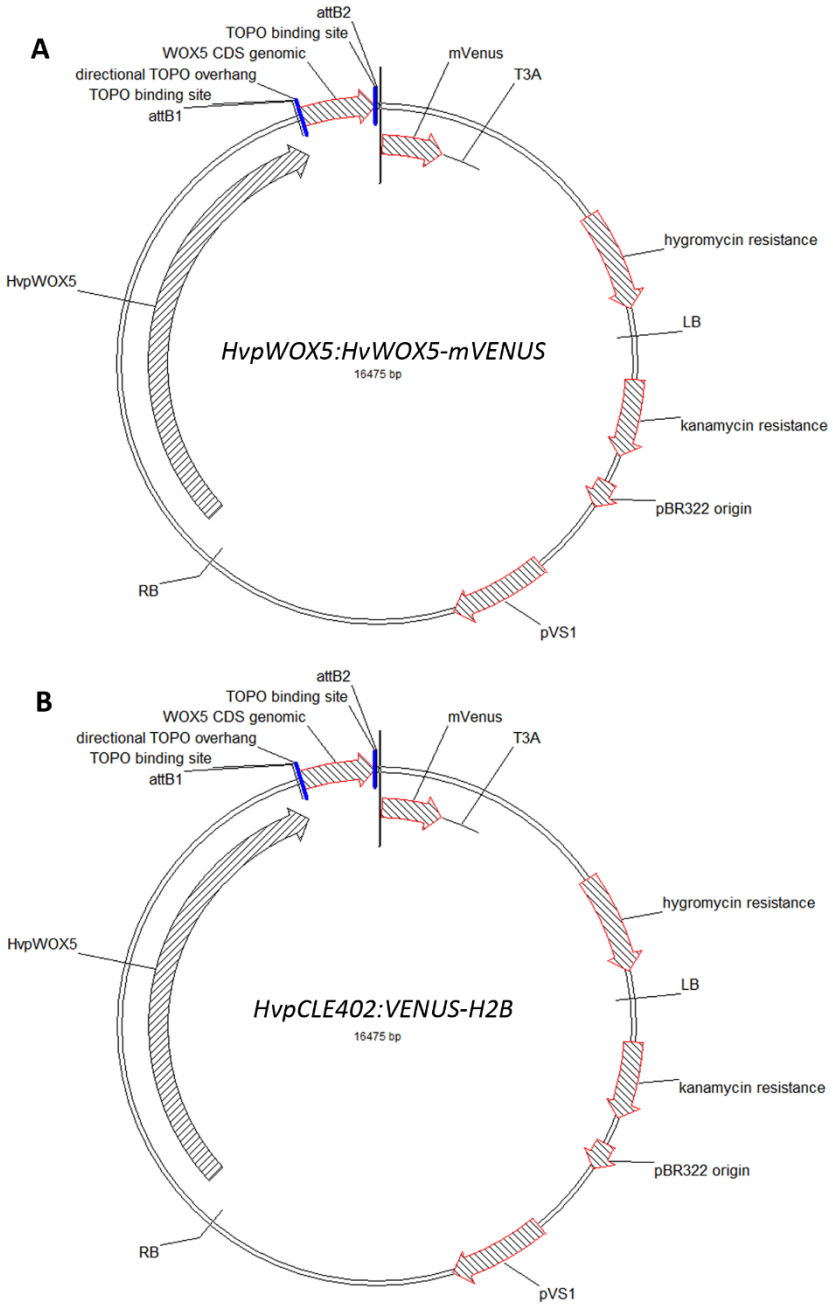

Figure 2: Exemplary maps of expression vectors.

A) Exemplary plasmid map for translational reporter lines (*HvpWOX5:HvWOX5-mVENUS*), expressing the gene and *mVENUS* under the respective endogenous promoter. **B)** Exemplary plasmid map for transcriptional reporter lines (*HvpCLE402:VENUS-H2B*), expressing *VENUS* fused to *H2B* under the respective promoter. LB = left border, RB = right border; attB1, attB2 = Gateway recombination sites; T3A = transcriptional terminator; pVS1 = minimal replicon for replication in gram negative bacteria; pBR322 = replication starting point.

5. Primers

Experiment		Primer name	sequence (5'-3')
transgenic lines			
HvpWOX5:HvWOX5-mV	amplifying CDS	GK-HvWOX5-fw+CACC	CACCATGGAGGCGCTGAGCGG
		GK-HvWOX5-rv-stop	GACTAGATACCGATCGAAGCTGCAGAGCCT
	amplifying promoter	GK-HvpWOX5-fw-AscI	AAAGGCGCGCCTCCATAAATTTCCCCACTGTTGTTT
		GK-HvpWOX5-rv-AscI	AAAGGCGCGCCTGACACTATGCTAGCTCGATTGAGC
HvpSCR:HvSCR-mV	amplifying CDS	GK-HvSCR-fw+CACC	CACCATGGTCCGAA GCGCCC
		GK-HvSCR-rv-stop	GCGACCAGAGGTGGTGTGCATGG
	amplifying promoter	GK-HvpSCR-fw-AscI	AAAGGCGCGCCGCTTCGTAATTCTCTCCGATCTA
		GK-HvpSCR-rv	GGCGGCGAGTTCTTGGTGGTC
		GK-HvpSCR-rv-AscI	AAAGGCGCGCCGGCGGCGGCGAGTTCTT
HvpCR4:HvCR4-mV	amplifying CDS	GK-HvCR4-fw+CACC	CACCATGGGCAGTGTTCTAGCTCTCTCTC
		GK-HvCR4-rv-stop	GAAGTTGTGCTGCAAGTACAGGTTCTCCT
	amplifying promoter	GK-HvpCR4-fw	TGCATGCATGCATGGTAGAGAGATG
		GK-HvpCR4-fw-AscI	AAAGGCGCGCCTGCATGCATGCATGGTA
		GK-HvpCR4-rv	TCCTTGAAGCTCGGAGCTAATGCC
		GK-HvpCR4-rv-AscI	AAAGGCGCGCCTCCTTGAAGCTCGGA
HvpCLV1:HvCLV1-mV	amplifying CDS	GK-HvCLV1-fw+CACC	CACCATGCCGCCACCTCACCTGC
		GK-HvCLV1-rv-stop2	GAAGGAGAGGATGAGGTCGTCGTCGG
	amplifying promoter	GK-HvpCLV1-fw-AscI	AAAGGCGCGCCGTTTATTTATTGAAGTATTAATCA
		GK-HvpCLV1-rv3	GCAGGTGAGGTGGCGGCATTGTG

		GK-HvpCLV1-rv-AscI	AAAGGCGCGCCTGTGGCGGGC
DR5v2-Venus-H2B	amplifying *DR5* sequence	GK-DR5v2-fw	CACCAACCCAACTCCATACTGGAATTC
		GK-DR5v2-rv	CCTGTAATTGTAATTGTAAATAGT
HvpCLE40:VENUS-H2B	amplifying promoter	GK-HvpCLE402-fw+CACC	CACCCATGCGACGTTCCCCAACAGCCT
		GK-HvpCLE402-rv	CCAATCCGGCCTTGGCCCTAGCG
HvpPLT1:HvPLT1-mV	amplifying CDS	GK-HvPLT1-fw+CACC	CACCATGGAGGAGGAGGAGCGGG
		GK-HvPLT1-rv-stop	TTCCATTCCAAAGATCGGCGTCTGAAAGGCT
	amplifying promoter	GK-HvpPLT1-fw-AscI	AAAGGCGCGCCTTGGTCGTTGCAATCAAT
		GK-HvpPLT1-rv	CTCGCCTGCACATGCATACACACACATACAT
		GK-HvpPLT1-rv-AscI	AAAGGCGCGCCCTCGCCTGCACAT
HvpPIN1:HvPIN1-mV	amplifying CDS	GK-HvPIN1-fw+CACCv2	CACCATGATCACGGGCACGGACTTC
		GK-HvPIN1-rv-v2	TCACAGGCCGAGCAGGATGTAGTAGA
	insert mVENUS	GK-mVenus+SmaI-fw	AAACCCGGGATGGTGAGCAAGGGCGAG
		GK-mVenus+SmaI-rv-stop	AAACCCGGGCTTGTACAGCTCGTCCA
	amplifying promoter	GK-HvpPIN1-fw-v2	GTGCATGAACCGTTGCTTCAAGTTC
		GK-HvpPIN1-fw-AscI-v2	AAAGGCGCGCCGTGCATGAACCGTTGCT
		GK-HvpPIN1-rv-v2	CTTGCCCTGTGTTTCCTTGCTCCTC
		GK-HvpPIN1-rv-AscI-v2	AAAGGCGCGCCCTTGCCCTGTGTTTCCTT

RNA *in situ* hybridisations

	HvWOX5	GK-HvWOX5-fw-GG-Entry-Exon1	AAAGGTCTCAGGCTTAATGGAGGGCGCTGAGCGG
		GK-HvWOX5-rv-GG-Entry-Exon2	AAAGGTCTCTCTGAGACTAGATACCGATCGA

HvSCR	GK-HvSCR-fw-GG-Entry-Exon1	AAAGGTCTCAGGCTTAATGGTCCGCAAGCGCCC
	GK-HvSCR-rv-GG-Entry-Exon2	AAAGGTCTCTCTGAGCGACCAGAGGTGGTGTG
	GK-HvSCR-fw-GG-Entry-VHIID	AAAGGTCTCAGGCTTAGCTGCTGCTGCAGTGCGC
	GK-HvSCR-rv-GG-Entry-VHIID	AAAGGTCTCTCTGACCACTGGAGCCCCTGCATGA
HvSHR	GK-HvSHR-fw-GG-Entry-Anfang	AAAGGTCTCAGGCTTAATGGATACGCTGTTTAGGTTG
	GK-HvSHR-rv-GG-Entry-Anfang	AAAGGTCTCTCTGACAGCCGTGGACGATGTGGAGAGC
HvPLT1	GK-HvPLT1-fw-GG-Entry	AAAGGTCTCAGGCTTAATGGAGGAGGAGGAGC
	GK-HvPLT1-rv-GG-Entry	AAAGGTCTCTCTGATTCCATTCCAAAGATCGGC
HvH4	GK-HvH4-fw-GG-Entry-Anfang	AAAGGTCTCAGGCTTAATGTCGGGGCGCGGCAAGGGCGGCAA
	GK-HvH4-rv-GG-Entry-Anfang	AAAGGTCTCTCTGAGCCTCCGAAGCCGTAGAGGGTGCGTC

XI. List of Figures

XII. List of Supplementary figures

Role of Auxin and Cytokinin in Barley Root Growth and Root Meristem Maintenance

Conserved Pathways in the Barley Root and Shoot Apical Meristem

XIII. List of tables

XIV. Acknowledgements

First, and obviously, I want to thank Rüdiger for the opportunity to do my PhD in his group, and for not getting too annoyed about the misunderstandings we sometimes had. Thanks to Maria for co-supervising my doctoral studies and providing an insight into the science of plant breeding genetics which turned out to be a little different from developmental genetics.

Thanks Yvonne, for supervising my master and doctoral thesis (and bachelor, actually – such a long time has gone by) and organising my abroad stays in Drøbak, Oslo, Edinburgh and Wageningen.

Thanks to Marc, Maike, Mari, Barbara, Ikram and Yvonne for proof-reading and discussing my thesis.

(Häufig ist ja gar nix kaputt, man ist nur zu blöd)

Thanks to the Center of Advanced Imaging (the CAi), our technicians Cornelia, Silke and Carin, and Monika and Mehmet for creating an efficient and comfortable working atmosphere (and funny lunch times).

Thanks to the AG Simon for a really nice atmosphere, Jenia, Patrick, Maike, Greg, Barbara, Nozomi, Ksenia, Mehdi, and the former members René, Fred, Adrian, Stephan, Julia, Laura. Thanks Abdullah for being vollkommen okay.

Thanks to all the other CEPLAS young researchers who made all the numerous CEPLAS events bearable and much more fun.

Thanks to the Schuberts, for the lab meetings in former times, and the Kleins for having some nice group activities together.

Thanks Helge and Marcel for the Metal, Whiskey and Scottish experiences.

Thanks Petra for the cooking at lunch times, the coffee meetings, the foundation of the pancake Fridays and for being such a close friend.

Thanks Nadja, for being so kind and open-minded about everything.

Thanks Karine, Stephanie, Kim, Madlen, Tobi and Jahan for all the nice city trips.

Thanks to our Norwegian friends Mari and Vilde, to bring the warm Norwegian atmosphere to our lab and inviting me so kindly to Norway.

Thanks Avantika, to give me an understanding of the Indian way of thinking (it still seems weird to me, though), and Rebecca for sharing (or rather enduring) the Indian “experience” with me.

Thanks Micol, and Sandra, for getting to know you and spend time with the horses here and there.

Acknowledgements

Thanks Otho, for thinking in a non-standard way, for all the coffee and for convincing me about the advantages of open-source (although you hardly ever mentioned that).

Thanks Steffi, for the coffee breaks and the chats about music.

And importantly, thanks Marc for everything! The music, the concerts, the city trips, the parties… for always being interested no matter what I was complaining about, and for the help in the lab. I still doubt that I could have done this PhD without your support!

And, at last, what kept me motivated during this time:

♫ ♪ "ALLES ERTRÄGLICH, ES MUSS NUR IMMER MUSIK DA SEIN" ♪ ♫

Broilers, „33rpm"

The End